

Lecture Notes in Physics 924

Jian-Xin Zhu

Bogoliubov- de Gennes Method and Its Applications

 Springer

Lecture Notes in Physics

Volume 924

Founding Editors

W. Beiglböck
J. Ehlers
K. Hepp
H. Weidenmüller

Editorial Board

M. Bartelmann, Heidelberg, Germany
B.-G. Englert, Singapore, Singapore
P. Hänggi, Augsburg, Germany
M. Hjorth-Jensen, Oslo, Norway
R.A.L. Jones, Sheffield, UK
M. Lewenstein, Barcelona, Spain
H. von Löhneysen, Karlsruhe, Germany
J.-M. Raimond, Paris, France
A. Rubio, Donostia, San Sebastian, Spain
M. Salmhofer, Heidelberg, Germany
S. Theisen, Potsdam, Germany
D. Vollhardt, Augsburg, Germany
J.D. Wells, Ann Arbor, USA
G.P. Zank, Huntsville, USA

The Lecture Notes in Physics

The series Lecture Notes in Physics (LNP), founded in 1969, reports new developments in physics research and teaching—quickly and informally, but with a high quality and the explicit aim to summarize and communicate current knowledge in an accessible way. Books published in this series are conceived as bridging material between advanced graduate textbooks and the forefront of research and to serve three purposes:

- to be a compact and modern up-to-date source of reference on a well-defined topic
- to serve as an accessible introduction to the field to postgraduate students and nonspecialist researchers from related areas
- to be a source of advanced teaching material for specialized seminars, courses and schools

Both monographs and multi-author volumes will be considered for publication. Edited volumes should, however, consist of a very limited number of contributions only. Proceedings will not be considered for LNP.

Volumes published in LNP are disseminated both in print and in electronic formats, the electronic archive being available at springerlink.com. The series content is indexed, abstracted and referenced by many abstracting and information services, bibliographic networks, subscription agencies, library networks, and consortia.

Proposals should be sent to a member of the Editorial Board, or directly to the managing editor at Springer:

Christian Caron
Springer Heidelberg
Physics Editorial Department I
Tiergartenstrasse 17
69121 Heidelberg/Germany
christian.caron@springer.com

More information about this series at <http://www.springer.com/series/5304>

Jian-Xin Zhu

Bogoliubov-de Gennes Method and Its Applications

 Springer

Jian-Xin Zhu
Theoretical Division, MS B262
Los Alamos National Laboratory
Los Alamos
New Mexico, USA

ISSN 0075-8450

ISSN 1616-6361 (electronic)

Lecture Notes in Physics

ISBN 978-3-319-31312-2

ISBN 978-3-319-31314-6 (eBook)

DOI 10.1007/978-3-319-31314-6

Library of Congress Control Number: 2016940969

© Springer International Publishing Switzerland 2016

This work is subject to copyright. All rights are reserved by the Publisher, whether the whole or part of the material is concerned, specifically the rights of translation, reprinting, reuse of illustrations, recitation, broadcasting, reproduction on microfilms or in any other physical way, and transmission or information storage and retrieval, electronic adaptation, computer software, or by similar or dissimilar methodology now known or hereafter developed.

The use of general descriptive names, registered names, trademarks, service marks, etc. in this publication does not imply, even in the absence of a specific statement, that such names are exempt from the relevant protective laws and regulations and therefore free for general use.

The publisher, the authors and the editors are safe to assume that the advice and information in this book are believed to be true and accurate at the date of publication. Neither the publisher nor the authors or the editors give a warranty, express or implied, with respect to the material contained herein or for any errors or omissions that may have been made.

Printed on acid-free paper

This Springer imprint is published by Springer Nature
The registered company is Springer International Publishing AG Switzerland

Preface

This is a book discussing the Bogoliubov-de Gennes (BdG) method and its major applications to superconductors. It was originally formulated by De Gennes in his book *Superconductivity of Metals and Alloys* and is based on the BCS theory of superconductivity, i.e., Cooper pair formation due to an effective pairing interaction around the Fermi energy. It consists essentially of a coupled set of Schrödinger equations, enabling a description of superconductivity with much information on both quasiparticle and superconducting order parameter properties. The method becomes particularly useful by providing insight into quasiparticle properties down to the atomic scale, which can be detected by such local probes as scanning tunneling microscopy. The understanding of quasiparticle properties is important in uncovering the mechanism for superconductivity. Therefore, the BdG formalism serves as a complementary approach to the Ginzburg–Landau theory, which is a choice to describe the spatial variations of superconducting order parameter slowly varying at a larger length scale.

The BdG theory was initially applied to understand the variation of superconducting order parameter in layered structures and quasiparticle states around a single vortex core in conventional *s*-wave superconductors. At that time, the BdG equations were solved analytically for some special cases. With significant advance in computer power, the BdG method is now widely used to address the local electronic structure in superconductors in much more complicated situations. Its application has recently been expanded to unconventional superconductors like high-temperature cuprates and topological superconductors. Due to its simplicity, the BdG formalism can be easily accessed by undergraduate and graduate students with the knowledge of quantum mechanics, who want to learn some interesting superconducting phenomena by solving a generalized set of Schrödinger equations through computer simulations. Throughout the book, we use the synonyms, BdG method, BdG formalism, and BdG theory, interchangeably with the same meaning.

The book is organized into two parts. The first part is on the formalism itself and consists of two chapters. The second part of the book, Chaps. 3–7, covers important applications of the BdG method. Chapter 1 is on the derivation of the BdG equations in the continuum model. Chapter 2 gives an alternative derivation of the equations in

the tight-binding model, based on which a more realistic description of the normal-state band structure can be incorporated. The structure of the equations and its connection with the Abrikosov–Gorkov Green function method, as well as solutions in the uniform case, are discussed in these first two chapters. Chapter 3 deals with the local electronic structure around a single impurity in a superconductor. The Yu-Shiba-Rusinov state around a magnetic impurity and Majorana mode from a coupling to a spin chain in *s*-wave superconductors and impurity resonance states in *d*-wave superconductors are discussed. Chapter 4 treats the influence on macroscopic properties by disorder effects in both *s*-wave and *d*-wave superconductors. The localization of impurity-induced resonance states in a *d*-wave superconductor is also discussed by using the one-parameter scaling analysis within the BdG formalism. Chapter 5 deals with the magnetic field effects on the local electronic structure of superconductors. The quasiparticle states around a single vortex core and in the mixed-state of conventional and unconventional superconductors are considered. The effect from a competing order on the quasiparticle states in a *d*-wave vortex core is explored. In addition, the Fulde–Ferrell–Larkin–Ovchinnikov state due to the spin Zeeman interaction of a magnetic field is also considered. In Chap. 6, I discuss the transport properties of junctions formed with a superconductor. The Andreev reflection on the differential conductance and its response to spin polarization and topological superconductivity are explored. Chapter 7 covers the topological effects with a focus on the periodicity of supercurrent in multiply connected geometries at mesoscale and quantum size effects on the superconducting properties in nanoscale superconductors. I would like to comment that the topics chosen in the chapters on the applications of the BdG equations have a direct relevance to the present frontiers of research in such emerging fields as iron-based superconductors, topological superconductors, and cold atoms.

The author would like to thank C.-D. Gong and Z.D. Wang for introducing him into the area of strongly correlated electron physics and superconductivity in his undergraduate and graduate student ages, C.S. Ting for exposing him to the phenomenology of high-temperature cuprate superconductors, and A.V. Balatsky and A.R. Bishop for the help with nurturing new ideas in local electronic structure and competing orders in strongly correlated electronic systems. The author wants to thank C.-R. Hu, T.K. Lee, B. Friedman, I. Martin, I. Vekhter, M.J. Graf, D.N. Sheng, Z.-Y. Weng, and Y. Chen for stimulating discussions and collaborations, on various topics of superconductivity. The author is also indebted to excellent colleagues, postdocs, and students in Los Alamos National Laboratory and Texas Center for Superconductivity at the University of Houston for making his exploration of superconductivity a great pleasure. I also want to thank Ms. Liesbeth Mol, editorial director for the physical sciences at Springer, for her steadfast support and enthusiasm, which made this project possible. The manuscript also benefited greatly from valuable comments from the Series Editor and the skillful editing of Christian Caron. Last but not least, I am enormously grateful to my wife Jian Xu for her love, understanding, and support.

Contents

Part I Bogoliubov-de Gennes Theory: Method

1 Bogliubov-de Gennes Equations for Superconductors in the Continuum Model	3
1.1 Introduction	3
1.2 Quantum Many-Body Hamiltonian	4
1.3 Second Quantization	9
1.4 Basic Properties of Superconductors	13
1.5 Derivation of the BdG Equations in the Continuum Model	14
1.5.1 Derivation	15
1.5.2 Local Density of States	21
1.5.3 Gauge Invariance	22
1.6 Structure of a General Gap Matrix	22
1.7 Solution to the BdG Equations in Homogeneous Systems	25
1.8 Relation to the Abrikosov-Gor'kov Equations	31
References	35
2 BdG Equations in Tight-Binding Model	37
2.1 Derivation of BdG Equations in a Tight-Bind Model	37
2.1.1 Local Density of States and Bond Current in the Lattice Model	44
2.1.2 Optical Conductivity and Superfluid Density in the Lattice Model	45
2.2 Solution to the BdG Equations in the Lattice Model for a Uniform Superconductor	56
2.3 Abrikosov-Gorkov Equations in the Lattice Model	60
References	64

Part II Bogoliubov-de Gennes Theory: Applications

3 Local Electronic Structure Around a Single Impurity in Superconductors	69
3.1 Introduction	69
3.2 Yu-Shiba-Rusinov Impurity States in an <i>s</i> -Wave Superconductor	69
3.3 Majorana Fermion in an <i>s</i> -Wave Superconductor with a Chain of Localized Spins.....	77
3.4 Impurity Resonance State in a <i>d</i> -Wave Superconductor	82
References	87
4 Disorder Effects on Electronic and Transport Properties in Superconductors	89
4.1 Anderson Theorem for Disordered <i>s</i> -Wave Superconductor.....	89
4.2 Suppression of Superconductivity in a Disordered <i>d</i> -Wave Superconductor	94
4.3 Quasiparticle Localization in a Disordered <i>d</i> -Wave Superconductor.....	100
References	109
5 Local Electronic Structure in Superconductors Under a Magnetic Field	111
5.1 Effect of the Magnetic Field	111
5.2 Vortex Core State in an <i>s</i> -Wave Superconductor	114
5.2.1 Single Isolated Vortex	114
5.2.2 High Field Limit	123
5.3 Vortex Core States in a <i>d</i> -Wave Superconductor	124
5.3.1 Single Isolated Vortex	125
5.3.2 Quasiparticle States in a Mixed-State of <i>d</i> -Wave Superconductors	127
5.4 Fulde-Ferrell-Larkin-Ovchinnikov State due to a Zeeman Magnetic Field	134
References	138
6 Transport Across Normal-Metal/Superconductor Junctions	141
6.1 Blonder-Tinkham-Klapwijk Scattering Formalism.....	141
6.2 Tunneling Conductance Through a Normal-Metal/Superconductor Junction	146
6.3 Suppression of Andreev Reflection in a Ferromagnet/ <i>s</i> -Wave Superconductor Junction	155
6.4 Transport Properties Through a Topological-Insulator/Superconductor Junction	158
References	166

- 7 Topological and Quantum Size Effects in Superconductors at Reduced Length Scale** 169
 - 7.1 Persistent Current in a Mesoscopic *s*-Wave Superconducting Ring 169
 - 7.2 Persistent Current in Multiply Connected Mesoscopic *d*-Wave Superconducting Geometries 176
 - 7.2.1 Cylindrical Geometry 176
 - 7.2.2 Square Loop Geometry 178
 - 7.3 Quantum Size Effects in Nanoscale Superconductors 181
 - References 184

- Additional Reading** 187

List of Acronyms

AB	Aharonov-Bohm
BCS	Bardeen-Cooper-Schrieffer
BdG	Bogoliubov-de Gennes
DFT	Density functional theory
GGA	Generalized gradient approximation
LDA	Local density approximation

Part I
Bogoliubov-de Gennes Theory: Method

Chapter 1

Bogoliubov-de Gennes Equations for Superconductors in the Continuum Model

Abstract In this chapter, a general introduction to the correlated electronic materials as well as a brief account of superconductor discovery is given. The Bogoliubov-de Gennes equations for superconductors are derived in the continuum. The symmetry of the equations is discussed. Finally, a connection of the BdG equations to the Green's function method is made.

1.1 Introduction

In daily life, one is frequently encountered with the states of classical matter, and transformation among these states or so called phases. For example, water can exist in the forms of ice, liquid, and vapor. The transition between these forms can be realized by varying temperature and pressure. These classical phenomena are the outcomes of the collective motion of atoms and molecules, the understanding of which constitutes the main subject of classical statistical physics.

In solid-state electronic materials, electrons are the major players. Since each of them possesses charge $-e$ ($e > 0$) and spin (an intrinsic degree of freedom), the electronic states exhibit insulating, metallic, and even superconducting and magnetic behaviors. The Mott-Hubbard-type insulating state occurs when the Coulomb repulsion among valence electrons are too large as compared with their kinetic energy (i.e., narrow electron energy band) in a pristine crystal [1, 2]. Therefore, these electrons have no nearby empty sites for them to hop to and they are trapped around ions. In an Anderson insulator, the electrons are localized due to the random distributed impurities in an impure metal, in which one can think of these electrons as waves and these waves cannot propagate beyond the localization length due to the wave-like interference effect [3–5]. Ideally, no conductivity exists in both types of insulators. In the metallic state, they can sneak by all ions in the presence of an electric field and conduct electricity. The difference between metallic and insulating states is striking in real materials. For example, the resistivity in copper is about $1.7 \times 10^{-8} \Omega \text{ m}$ while the resistivity in undoped $\text{Sm}_2\text{CuO}_{4+y}$ is as large as $\sim 1 \Omega \text{ m}$ at low temperatures [6]. In the magnetic state, electronic spins can be aligned into parallel, antiparallel, or other patterns.

More interestingly, in the superconducting state, electrons move throughout the whole system with zero resistance. These unique properties have formed the basis

for operating electronic devices. Some of them have already been used in nowadays power plants, computers, and wind turbines, to list a few. Therefore, a microscopic understanding of the origin of these electronic states as well as how to control them has significant implications to technological applications. For superconductivity, it is now well accepted that the superconducting current arises from the formation of Cooper pairs [7] mediated by some kind of bosons such as phonons, which is originally proposed by Bardeen, Cooper, and Schrieffer (BCS) [8]. The single-particle excitations in the superconducting state can not only provide insight into the fundamental properties of superconductivity itself such as pairing nature but also serve as new entities of significant technology implications as a response to defects or magnetic field etc. The Bogoliubov-de Gennes (BdG) [9] approach, which is the main focus of this text, is now a very powerful method to describe these single-particle approximations in inhomogeneous superconductors. Before we proceed to bring out the BdG mathematical formalism, it should be helpful for the readers to be exposed with a quantum many-body framework in a more broad area of strongly correlated electronic systems.

1.2 Quantum Many-Body Hamiltonian

A typical solid consists of the order of 10^{23} atoms. Each atom has the atomic number of electrons. In addition to interacting with nuclei, these electrons are interacting among themselves. In principle, one can start with a Hamiltonian to describe the motions of both electrons and nuclei:

$$\mathcal{H} = \sum_i \frac{\mathbf{p}_i^2}{2m_e} - \sum_{i,l} \frac{Z_l e^2}{|\mathbf{r}_i - \mathbf{R}_l|} + \frac{1}{2} \sum_{i,j} \frac{e^2}{|\mathbf{r}_i - \mathbf{r}_j|} + \sum_l \frac{\mathbf{P}_l^2}{2M_l} + \frac{1}{2} \sum_{l,j} \frac{Z_l Z_j e^2}{|\mathbf{R}_l - \mathbf{R}_j|}. \quad (1.1)$$

Here the first and the fourth terms are the kinetic energy of the electrons and nuclei while the second, third, fifth terms represent the potential energy due to the Coulomb interaction between electrons and nuclei and among the electronic and nuclear degrees of freedom themselves. The variables \mathbf{p}_i and \mathbf{P}_l denote the momentum of each individual electron and nucleus, while the coordinates \mathbf{r}_i and \mathbf{R}_l are the variables conjugate to \mathbf{p}_i and \mathbf{P}_l . The quantities m_e , M_l , and Z_l are the mass of electron and nucleus, and the atomic number, respectively. Note that each electron carries a negative charge $-e$ ($e > 0$) and each nucleus carries a positive charge $Z_l e$. Therefore, the interaction between electrons and nuclei is attractive while that among electrons or nuclei themselves is repulsive. A schematic drawing of this many-particle problem for a frozen lattice of nuclei is shown in Fig. 1.1. Classically,

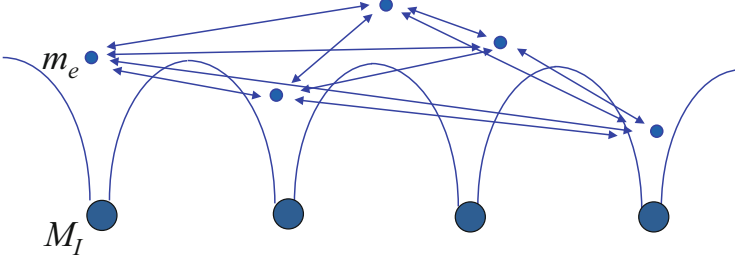


Fig. 1.1 Many-particle Hamiltonian of a solid consisting of electrons in a frozen lattice of nuclei

the equations of motion of the whole system are given by the Hamilton's equations

$$\dot{r}_{i,\alpha} = \frac{\partial \mathcal{H}}{\partial p_{i,\alpha}}, \quad \dot{p}_{i,\alpha} = -\frac{\partial \mathcal{H}}{\partial r_{i,\alpha}}, \quad (1.2)$$

for the electronic degrees of freedom, and

$$\dot{R}_{I,\alpha} = \frac{\partial \mathcal{H}}{\partial P_{I,\alpha}}, \quad \dot{P}_{I,\alpha} = -\frac{\partial \mathcal{H}}{\partial R_{I,\alpha}}, \quad (1.3)$$

for the nuclear degrees of freedom. These equations are precisely equivalent to the Newton's laws of motion. Here α ($= x, y, z$) denotes the three components of a vector in the cartesian coordinate system. Unfortunately, many important physical properties of electronic phenomena in solids cannot be captured by the classical mechanics and require a description within the quantum mechanics. There the coordinates and momenta no longer commute with each other. Instead they should follow the Heisenberg uncertainty principles as represented by the commutators:

$$[r_{i,\alpha}, p_{j,\beta}]_- = i\hbar \delta_{ij} \delta_{\alpha\beta} \quad \text{and} \quad [R_{I,\alpha}, P_{J,\beta}]_- = i\hbar \delta_{IJ} \delta_{\alpha\beta}. \quad (1.4)$$

Here \hbar is the reduced Planck's constant. The commutators by Eq. (1.4) indicate the coordinates and momenta are now quantum mechanical operators. In the coordinate representation, the momentum operator can be written as

$$\mathbf{p}_i = \frac{\hbar}{i} \nabla_i \quad \text{and} \quad \mathbf{P}_I = \frac{\hbar}{i} \nabla_I. \quad (1.5)$$

Correspondingly, the operator form of the Hamiltonian (1.1) becomes

$$\begin{aligned} \mathcal{H} = & -\sum_i \frac{\hbar^2}{2m_e} \nabla_i^2 - \sum_{i,I} \frac{Z_I e^2}{|\mathbf{r}_i - \mathbf{R}_I|} + \frac{1}{2} \sum_{i,j} \frac{e^2}{|\mathbf{r}_i - \mathbf{r}_j|} \\ & - \sum_I \frac{\hbar^2}{2M_I} \nabla_I^2 + \frac{1}{2} \sum_{I,J} \frac{Z_I Z_J e^2}{|\mathbf{R}_I - \mathbf{R}_J|}. \end{aligned} \quad (1.6)$$

As such, the evolution of a state of the whole system is described by a quantum many-body wave-function, described by the Schrödinger equation¹:

$$i\hbar \frac{\partial \Psi}{\partial t} = \mathcal{H} \Psi , \quad (1.7)$$

where the many-body wave-function is the function of the variables $(\{\mathbf{r}_i\}, \{\mathbf{R}_I\}; t)$. When there are no external potentials or when they are time independent, the wave function can take the form

$$\Psi(\{\mathbf{r}_i\}, \{\mathbf{R}_I\}; t) = \Phi(\{\mathbf{r}_i\}, \{\mathbf{R}_I\}) e^{-iEt/\hbar} , \quad (1.8)$$

with the $\Phi(\{\mathbf{r}_i\}, \{\mathbf{R}_I\})$ satisfying the steady-state Schrödinger equation:

$$\mathcal{H} \Phi(\{\mathbf{r}_i\}, \{\mathbf{R}_I\}) = E \Phi(\{\mathbf{r}_i\}, \{\mathbf{R}_I\}) . \quad (1.9)$$

Here E is the total energy of the many-particle system. Theoretically, the wave-functions $\Phi(\{\mathbf{r}_i\}, \{\mathbf{R}_I\})$ contain all information needed to describe every property of the system. In practice, a direct solution of Eq. (1.9) is prohibitively difficult and a hierarchy of theoretical approximations are in order. Notice that the only small term in Eq. (1.6) is the kinetic energy of nuclear motion, which is smaller than that of electronic motion by a factor of m_e/M_I . Therefore, within the Born-Oppenheimer approximation [10], the wave function for the entire system can be written as

$$\Phi_{an}(\{\mathbf{r}_i\}, \{\mathbf{R}_I\}) = \Psi_\alpha(\{\mathbf{r}_i\} : \{\mathbf{R}_I\}) u_{n\alpha}(\{\mathbf{R}_I\}) . \quad (1.10)$$

Here $\Psi_\alpha(\{\mathbf{r}_i\} : \{\mathbf{R}_I\})$ are the wave-functions for the electrons with the nuclei positions $\{\mathbf{R}_I\}$ as a fixed set of parameters and satisfying the equation

$$\begin{aligned} & \left[- \sum_i \frac{\hbar^2}{2m_e} \nabla_i^2 - \sum_{i,I} \frac{Z_I e^2}{|\mathbf{r}_i - \mathbf{R}_I|} + \frac{1}{2} \sum_{ij} \frac{e^2}{|\mathbf{r}_i - \mathbf{r}_j|} + \frac{1}{2} \sum_{I,J} \frac{Z_I Z_J e^2}{|\mathbf{R}_I - \mathbf{R}_J|} \right] \Psi_\alpha(\{\mathbf{r}_i\} : \{\mathbf{R}_I\}) \\ & = W_\alpha(\{\mathbf{R}_I\}) \Psi_\alpha(\{\mathbf{r}_i\} : \{\mathbf{R}_I\}) , \end{aligned} \quad (1.11)$$

while $u_{n\alpha}(\{\mathbf{R}_I\})$ are the wave-functions for the nuclear motion, and they satisfy the equation

$$\left[- \sum_I \frac{\hbar^2}{2M_I} \nabla_I^2 + W_\alpha(\{\mathbf{R}_I\}) - E \right] u_{n\alpha}(\{\mathbf{R}_I\}) = 0 , \quad (1.12)$$

¹For simplicity, the discussion is restricted to the non-relativistic limit. For a fully relativistic description, the kinetic energy at least for the electronic degrees of freedom should be replaced by the Dirac Hamiltonian.

within the so-called “frozen phonon” approximation. By going beyond the Born-Oppenheimer approximation, a perturbation theory can be developed for the electron-phonon interactions, which are responsible for the inelastic scattering of electrons in metals, polaron formation in ionic crystals, and pairing of electrons in some metals and compounds. As such, it is important to focus on the electronic dynamics as described by Eq. (1.11) with the nuclear positions $\{\mathbf{R}_I\}$ as parameters. It has no effect whether we solve for W including nucleus-nucleus repulsive interaction or solve the following equation

$$\left[-\sum_i \frac{\hbar^2}{2m_e} \nabla_i^2 - \sum_{i,I} \frac{Z_I e^2}{|\mathbf{r}_i - \mathbf{R}_I|} + \frac{1}{2} \sum_{ij} \frac{e^2}{|\mathbf{r}_i - \mathbf{r}_j|} \right] \Psi_\alpha(\{\mathbf{r}_i\} : \{\mathbf{R}_I\}) = E_\alpha(\{\mathbf{R}_I\}) \Psi_\alpha(\{\mathbf{r}_i\} : \{\mathbf{R}_I\}), \quad (1.13)$$

and add the nucleus-nucleus repulsive interaction afterwards. Equation (1.13) must be solved with the appropriate boundary conditions for the wave-functions. For example, $\Psi_\alpha(\{\mathbf{r}_i\} : \{\mathbf{R}_I\})$ must be vanishing when the electrons are infinitely far away from an isolated atom or molecule, or must be satisfying the periodic boundary condition for crystalline solids. Also since electrons are spin- $\frac{1}{2}$ fermions, the wave-functions Ψ_α must be antisymmetric with the interexchange of two electrons. Even so, due to the inter-electron Coulomb repulsion, Eq. (1.13) cannot be solved directly except for problems with few number of electrons. The difficulty in solving it numerically grows exponentially with the increase in the number of correlated electrons. This exponential problem will not be overcome for the cases involving many correlated electrons, which are typical in solids, regardless of the fact that the computational power is continuing to grow rapidly.

To approach this problem, two strategies are mostly taken. One is to directly deal with Eq. (1.13) and map it onto a single-particle Hamiltonian while the other is to dramatically reduce Eq. (1.13) to an effective quantum many-body Hamiltonian so that electronic correlation effects can be qualitatively understood. The former is borne out within density functional theory (DFT) [11], in which the problem is made equivalent to solving the single-particle Kohn-Sham equations [12]:

$$\left[-\frac{\hbar^2}{2m_e} \nabla^2 + V_{\text{KS},s}(\mathbf{r}) \right] \psi_{s,\alpha}(\mathbf{r}) = E_{s,\alpha} \psi_{s,\alpha}(\mathbf{r}), \quad (1.14)$$

with

$$V_{\text{KS},s}(\mathbf{r}) = -\sum_I \frac{Z_I e^2}{|\mathbf{r} - \mathbf{R}_I|} + \int d^3 r' \frac{e^2 n(\mathbf{r}')}{|\mathbf{r} - \mathbf{r}'|} + V_{\text{xc},s}(\mathbf{r}). \quad (1.15)$$

In Eq. (1.14), $\psi_{s,\alpha}$ and $E_{s,\alpha}$ are the Kohn-Sham eigenfunctions and the corresponding eigenvalues for spin projection s . In the DFT framework, the electronic correlation

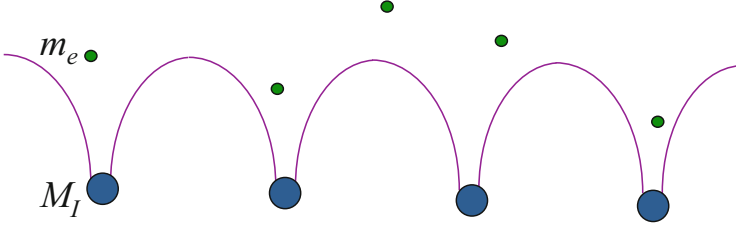


Fig. 1.2 Single-particle Hamiltonian of a solid consisting of electrons in a frozen lattice of nuclei

effects are encoded in the exchange-correlation potential $V_{xc,s}(\mathbf{r})$.² A schematic drawing of this single-particle problem is shown in Fig. 1.2. Since the single-particle Kohn-Sham potential $V_{KS,s}$ is in turn determined by the Kohn-Sham eigenfunctions via the local electron density $n(\mathbf{r}) = \sum_s \sum_{\alpha=1}^{N_s} |\psi_{s,\alpha}(\mathbf{r})|^2$ with the total number of $N_e = N_{\uparrow} + N_{\downarrow}$ electrons occupying N_e lowest-lying spin-orbitals, the Kohn-Sham equations (1.14) should be solved self-consistently. Although the mapping from Eq.(1.13) to Eq.(1.14) is exact under the Hohenberg-Kohn theorem [13] for the ground state, the construction of the functional itself is nontrivial. So far the local density approximation (LDA) and its variants like generalized-gradient approximation (GGA) are the most often used. The LDA- or GGA-based DFT theory has been very successful in describing many materials for both ground-state energies and band structures, suggesting weak electronic correlations in these materials. However, the LDA-based DFT is not successful in describing other important classes of materials with open d - and f -shell orbitals (i.e., with partially occupied valence electrons occupying these orbitals). For example, LDA-based DFT predicts such transition metal oxides as La_2CuO_4 , MnO , and NiO to be metals but they are insulators in reality. Similarly, for intermetallic f -electron systems like lanthanides and actinides, the LDA-based DFT usually gives effective mass of quasiparticles around the Fermi energy one or two orders of magnitude smaller than the experimental values. This failure demonstrates that the LDA-based DFT does not adequately address the electronic correlations in these materials, where the electrons experience very strong Coulomb repulsion when they occupy these narrow orbitals. The construction of more powerful exchange-correlation functionals for these narrow band materials remains a challenge in the DFT community [14].

Instead in the latter strategic approach, the electronic correlations are addressed directly by treating the competition between electron kinetic energy and inter-electron potential energy in a quantum many-body manner but within a much simplified low-energy model Hamiltonian [15, 16]. Some representative low-energy models will be presented after we introduce the second quantization in the next section.

²A spin index is introduced to allow for possible magnetic states. However, for simplicity of the discussion, the spin-orbit coupling effect is neglected.

1.3 Second Quantization

The direct treatment of the quantum many-body systems through the Schrödinger wave-function method is cumbersome and is not practical. It is convenient to use the second quantization to discuss the many identical interacting particles. As we recall, in the first quantization, the physical observables become quantum mechanical operators and the total energy is the expectation value of the Hamiltonian operator against the many-particle wave-function, which is the summation of the contributions for the single-particle kinetic energy and two-particle potential energy. In the second quantization, the wave-function itself becomes field operators, which can be expressed in the particle occupation number representation. In this representation, the many-particle state can be described by the occupation of identical particles in each single-particle state and the statistics symmetry regarding the particle being of Bose or Fermi character is protected in each step. This field quantization method is not only essential for the description of particle creation and destruction in the relativistic quantum field theory, but also powerful to describe the strongly correlated electronic systems.

For the correlated electrons as described by the Schrödinger equation (1.13), the Hamiltonian can be rewritten as

$$\mathcal{H}_e = \sum_i h(\mathbf{r}_i) + \frac{1}{2} \sum_{ij} v_{ee}(|\mathbf{r}_i - \mathbf{r}_j|), \quad (1.16)$$

where the single-particle operator

$$h(\mathbf{r}_i) = -\frac{\hbar^2}{2m_e} \nabla_i^2 - \sum_l \frac{Z_l e^2}{|\mathbf{r}_i - \mathbf{R}_l|}, \quad (1.17)$$

and the two particle operator

$$v_{ee}(|\mathbf{r}_i - \mathbf{r}_j|) = \frac{e^2}{|\mathbf{r}_i - \mathbf{r}_j|}. \quad (1.18)$$

Since electrons are fermions, the Hamiltonian (1.16) in the second quantized form is given by Fetter and Walecka [17], Mahan [18]

$$\hat{\mathcal{H}}_e = \int d\mathbf{x} \hat{\psi}^\dagger(\mathbf{x}) h(\mathbf{x}) \hat{\psi}(\mathbf{x}) + \frac{1}{2} \int \int d\mathbf{x} d\mathbf{x}' \hat{\psi}^\dagger(\mathbf{x}) \hat{\psi}^\dagger(\mathbf{x}') v_{ee}(\mathbf{x}, \mathbf{x}') \hat{\psi}(\mathbf{x}') \hat{\psi}(\mathbf{x}). \quad (1.19)$$

The first term on the right-hand side describes the non-interacting (also called single-particle) part of electrons while the second term the electron-electron interaction. Here the variable \mathbf{x} denotes both the real-space coordinates \mathbf{r} and the spin projection (usually along the z -axis) s , that is, $\mathbf{x} \equiv (\mathbf{r}, s)$. Different from the continuous variable \mathbf{r} , the spin projection can only take the discretized values,

$s = \pm\hbar/2$.³ Therefore, a summation is implied in the integral over the spin index in \mathbf{x} . In Eq. (1.19), the field operator $\hat{\psi}^\dagger(\mathbf{x})$ ($\hat{\psi}(\mathbf{x})$) creates (annihilates) an electron at a coordinate \mathbf{x} , and they satisfy the anticommutation rules as

$$\{\hat{\psi}(\mathbf{x}), \hat{\psi}(\mathbf{x}')\} = 0, \quad (1.20a)$$

$$\{\hat{\psi}^\dagger(\mathbf{x}), \hat{\psi}^\dagger(\mathbf{x}')\} = 0, \quad (1.20b)$$

$$\{\hat{\psi}(\mathbf{x}), \hat{\psi}^\dagger(\mathbf{x}')\} = \delta(\mathbf{x} - \mathbf{x}'). \quad (1.20c)$$

We note that the field operator $\hat{\psi}^\dagger(\mathbf{x})$ is the hermitian conjugate of $\hat{\psi}(\mathbf{x})$. Here the curly brackets represent the anticommutator, i.e., for two operators \hat{A} and \hat{B} ,

$$\{\hat{A}, \hat{B}\} = \hat{A}\hat{B} + \hat{B}\hat{A}. \quad (1.21)$$

The δ -function is understood as Dirac-type for the continuous spatial coordinates while as Kronecker-type for the discrete variables, that is,

$$\delta(\mathbf{x} - \mathbf{x}') = \delta(\mathbf{r} - \mathbf{r}')\delta_{ss'}. \quad (1.22)$$

More generally, if the single-particle Hamiltonian is non-local in the \mathbf{x} coordinate space, which is especially true when the spin-orbit coupling due to the relativistic effect is included, the single-particle Hamiltonian takes the form of $h(\mathbf{x}, \mathbf{x}')$. The system Hamiltonian of correlated electrons is then written as

$$\begin{aligned} \hat{\mathcal{H}}_e &= \int \int d\mathbf{x}d\mathbf{x}' \hat{\psi}^\dagger(\mathbf{x})h(\mathbf{x}, \mathbf{x}')\hat{\psi}(\mathbf{x}') \\ &+ \frac{1}{2} \int \int d\mathbf{x}d\mathbf{x}' \hat{\psi}^\dagger(\mathbf{x})\hat{\psi}^\dagger(\mathbf{x}')v_{ee}(\mathbf{x}, \mathbf{x}')\hat{\psi}(\mathbf{x}')\hat{\psi}(\mathbf{x}). \end{aligned} \quad (1.23)$$

Similarly, for any single-particle operator having

$$\mathcal{O} = \sum_i O(\mathbf{r}_i), \quad (1.24)$$

in the first quantization, its second quantized form is given by

$$\mathcal{O} = \int d\mathbf{x}\hat{\psi}^\dagger(\mathbf{x})O(\mathbf{x})\hat{\psi}(\mathbf{x}). \quad (1.25)$$

³Later on, we will also interchangeably use the symbol $\sigma = \pm 1$ for the spin variables, $s = (\hbar/2)\sigma$.

or

$$\mathcal{O} = \int \int d\mathbf{x} d\mathbf{x}' \hat{\psi}^\dagger(\mathbf{x}) O(\mathbf{x}, \mathbf{x}') \hat{\psi}(\mathbf{x}') . \quad (1.26)$$

for the non-local case. In addition, although the original electron-electron interaction v_{ee} is repulsive, the second quantized Hamiltonian for the low-energy modeling remains to have the similar form even if inter-particle interaction is attractive.

Depending on the specific form of the Hamiltonian to be studied, the field operators can be expanded in terms of a complete set of basis functions, which are usually the eigenstates of the single-particle part of the Hamiltonian.

In the jellium model, where an interacting electron gas is placed in a background of the uniformly distributed positive charges, it is convenient to write the field operators as a linear combination of creation and annihilation operators corresponding to plane waves

$$\psi_\sigma(\mathbf{r}) = \frac{1}{\sqrt{\mathcal{V}}} \sum_{\mathbf{k}} e^{i\mathbf{k}\cdot\mathbf{r}} c_{\mathbf{k}\sigma} , \quad (1.27a)$$

$$\psi_\sigma^\dagger(\mathbf{r}) = \frac{1}{\sqrt{\mathcal{V}}} \sum_{\mathbf{k}} e^{-i\mathbf{k}\cdot\mathbf{r}} c_{\mathbf{k}\sigma}^\dagger , \quad (1.27b)$$

where \mathcal{V} denotes the volume of the gas, and the annihilation and creation operators $c_{i\sigma}$ and $c_{i\sigma}^\dagger$ satisfy the anticommutation relation for fermions

$$\{c_{\mathbf{k}\sigma}, c_{\mathbf{k}'\sigma'}^\dagger\} = \delta_{\mathbf{k}\mathbf{k}'} \delta_{\sigma\sigma'} , \quad (1.28a)$$

$$\{c_{\mathbf{k}\sigma}, c_{\mathbf{k}'\sigma'}\} = \{c_{\mathbf{k}\sigma}^\dagger, c_{\mathbf{k}'\sigma'}^\dagger\} = 0 . \quad (1.28b)$$

Accordingly, the second quantized Hamiltonian for the interacting electron gas is given by

$$\mathcal{H} = \sum_{\mathbf{k}\sigma} \varepsilon_{\mathbf{k}} c_{\mathbf{k}\sigma}^\dagger c_{\mathbf{k}\sigma} + \frac{1}{2\mathcal{V}} \sum_{\mathbf{q} \neq 0} \sum_{\mathbf{k}\mathbf{k}'} \sum_{\sigma\sigma'} v_{ee}(\mathbf{q}) c_{\mathbf{k}+\mathbf{q},\sigma}^\dagger c_{\mathbf{k}'-\mathbf{q},\sigma'}^\dagger c_{\mathbf{k}'\sigma'} c_{\mathbf{k}\sigma} , \quad (1.29)$$

where

$$\varepsilon_{\mathbf{k}} = \frac{\hbar^2 k^2}{2m_e} , \quad (1.30)$$

is the single-particle energy dispersion and

$$v_{ee}(\mathbf{q}) = \frac{4\pi e^2}{q^2} , \quad (1.31)$$

is the Fourier transform of the long-ranged Coulomb repulsion.

For the narrow band materials, the electronic correlations are significant. It is convenient to represent the field operators in terms of local orbitals. Representative examples of these local orbitals are Wannier orbitals or local atomic orbitals within the tight-binding approximation (TBA) to the systems with large atomic distances. If we consider only a single narrow band to be partially filled in a solid, the field operators can be represented as

$$\psi_{\sigma}(\mathbf{r}) = \sum_i \phi(\mathbf{r} - \mathbf{R}_i) c_{i\sigma}, \quad (1.32a)$$

$$\psi_{\sigma}^{\dagger}(\mathbf{r}) = \sum_i \phi^*(\mathbf{r} - \mathbf{R}_i) c_{i\sigma}^{\dagger}, \quad (1.32b)$$

where $\phi(\mathbf{r} - \mathbf{R}_i)$ is the localized orbital at atomic site \mathbf{R}_i , and the annihilation and creation operators $c_{i\sigma}$ and $c_{i\sigma}^{\dagger}$ satisfy the anticommutation relation for fermions

$$\{c_{i\sigma}, c_{j\sigma'}^{\dagger}\} = \delta_{ij} \delta_{\sigma\sigma'}, \quad (1.33a)$$

$$\{c_{i\sigma}, c_{j\sigma'}\} = \{c_{i\sigma}^{\dagger}, c_{j\sigma'}^{\dagger}\} = 0. \quad (1.33b)$$

The Hamiltonian for the single-orbital Hubbard model is given by Hubbard [1]

$$\mathcal{H} = - \sum_{ij} t_{ij} c_{i\sigma}^{\dagger} c_{j\sigma} + \frac{U}{2} \sum_{i\sigma} n_{i\sigma} n_{i\bar{\sigma}}, \quad (1.34)$$

where $\bar{\sigma} = -\sigma$ with $\sigma = +1$ or \uparrow for spin up and $\sigma = -1$ or \downarrow for spin down,

$$t_{ij} = - \int d\mathbf{r} \phi^*(\mathbf{r} - \mathbf{R}_i) h(\mathbf{r}) \phi(\mathbf{r} - \mathbf{R}_j), \quad (1.35)$$

is the hopping integral between two atomic sites,

$$U = e^2 \int \int d\mathbf{r} d\mathbf{r}' \frac{|\phi(\mathbf{r} - \mathbf{R}_i)|^2 |\phi(\mathbf{r}' - \mathbf{R}_i)|^2}{|\mathbf{r} - \mathbf{r}'|}. \quad (1.36)$$

To derive this Hubbard model, the multi-center integral for the Coulomb interaction has been neglected.

Similarly, within the TBA, the Anderson lattice model is defined as [19]

$$\begin{aligned} \mathcal{H} = & - \sum_{ij,\sigma} t_{ij} c_{i\sigma}^{\dagger} c_{j\sigma} + \sum_{ij,\sigma\alpha} (V_{i\sigma,j\alpha} c_{i\sigma}^{\dagger} f_{j\alpha} + \text{H.c.}) \\ & + \sum_{i,\alpha} \epsilon_i^f f_{i\alpha}^{\dagger} f_{i\alpha} + \frac{U_f}{2} \sum_i n_{i\alpha}^f n_{i\bar{\alpha}}^f. \end{aligned} \quad (1.37)$$

Here the localized f -orbitals with energy level ε_i^f is hybridized with the conduction band while the electrons within the localized f -orbital electrons experience Hubbard- U repulsion. The quantity $V_{i\sigma,j\alpha}$ is the hybridization strength and the index α represents a two-component quantum state of the f -orbital.

These minimal models have been intensively used for understanding such emergent phenomena as localization-delocalization, heavy fermion, magnetism and superconductivity in transition metal oxides and intermetallic f -electron systems in condensed matter physics community. The creation and annihilation operators in the second quantization are also the central elements in the definition of Green's functions, which are used in quantum many-body theory. In particular, the Green's functions have been used as convenient quantities to evaluate the dynamic self-energies within the dynamical mean-field theory (DMFT) [20] for strongly correlated electronic systems, which maps the quantum lattice many-body problem to an effective quantum impurity one (still strongly correlated!). Recently, the LDA+DMFT approach [21–23] has been developed to investigate strongly correlated electronic materials. The approach incorporates the merits from both LDA and DMFT, and has been successful in giving a unified description of electronic states from weak to strong coupling limits, on the aspects of quasiparticle renormalization and magnetism. As for the phenomenology of superconductivity and related ordering states, the above quantum many-body approaches also lay down the foundations for the effective modeling description covered in the following chapters.

1.4 Basic Properties of Superconductors

Superconductivity was discovered by H. Kamerlingh Onnes in 1911 on mercury. Thereafter, it has also been discovered in other elemental solids like lead and niobium, and other simple compounds. The highest temperature superconductor has been Nb_3Sn until the year of 1986, when the high temperature superconductivity was discovered in copper-based oxides. In the copper-family of superconductors, the highest temperature superconductor is the ceramic $\text{HgBa}_2\text{Cu}_2\text{Cu}_3\text{O}_{8+\delta}$ with a transition temperature $T_c \sim 130$ degrees of Kelvin. In 2008, the iron-based superconductors was discovered with a highest transition temperature of 55 K obtained in $\text{SmO}_{1-x}\text{F}_x\text{FeAs}$. A chronicle for the discovery of superconductors is shown in Fig. 1.3. The hallmarks of the superconductors are the zero resistivity and perfect diamagnetism as they are cooled below a critical temperature T_c . For all the superconductors discovered so far, the flux quantization experiments have provided strong evidence that the superconductivity arises from the formation of Cooper pairs [7] by electrons. However, the mechanism for glueing the electrons can be very different from materials to materials. The Cooper pairs are mediated by phonons, that is, lattice vibrational modes, in conventional superconductors while they are via a more exotic process (e.g., the fluctuations of the electron spins) in

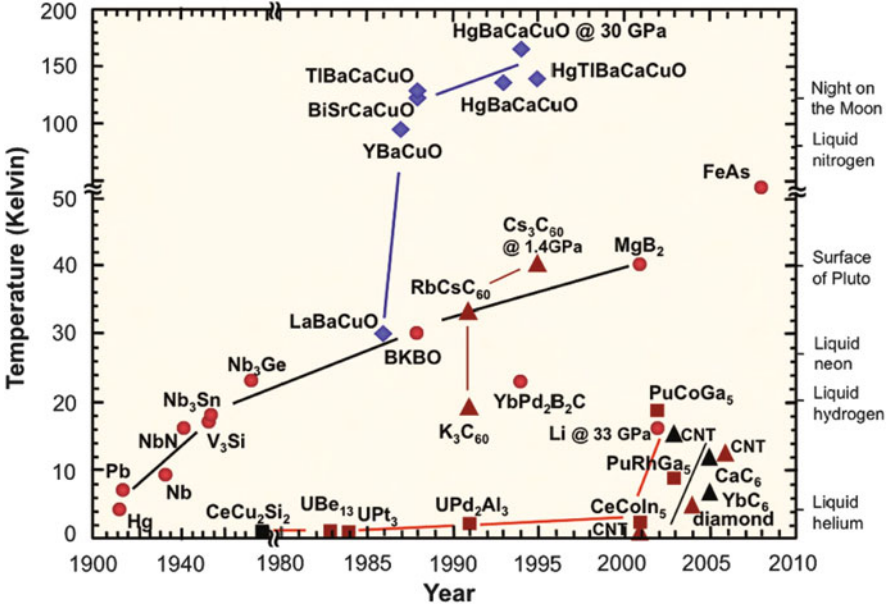


Fig. 1.3 Timeline of the superconductor discovery. Image courtesy of U.S. DOE Office of Basic Energy Sciences

unconventional superconductors. Accordingly, the pairing symmetry that describes the relative orbital motion of the paired electrons can be different. An s -wave pairing symmetry is commonly observed in conventional superconductors, while other unconventional pairing symmetry like p -, d -, f - and s_{\pm} -wave can occur in unconventional superconductors. The latter includes Sr_2RuO_4 , ^3He , high-temperature cuprates, heavy fermion inter-metallic compounds, and recently discovered iron-based superconductors. On the one hand, the unconventional superconductors are accompanied with multiple electronic phases, a typical feature of strongly correlated electronic materials. On the other hand, although the BCS [8] theory, invoking the electron-phonon coupling as a pairing mechanism, is originally developed for the conventional superconductors, it seems that the quasiparticle properties in the superconducting state can be described by the BCS theory for the unconventional superconductors. This is the underlying basic assumption for the BdG [9] approach.

1.5 Derivation of the BdG Equations in the Continuum Model

The BdG [9] approach relies on the assumption that there exist well-defined quasiparticles in the superconductor. It has the advantage of providing information about the one-particle excitations of the system. The quasiparticle excitation spectrum

can be obtained, together with the corresponding quasiparticle amplitudes. The BdG formalism is essentially correct in the weak-coupling regime, but also yields qualitative results in situations of very strong coupling, as was pointed out by Bishop et al. [24]. The interest in microscopic electronic structure calculations of this type was revived by low-temperature scanning-tunneling-microscopy (STM) experiments which provided extremely detailed, spatially resolved, excitation spectra around a single impurity, near the interface/surface, and around a vortex core in the presence of an Abrikosov flux lattice. An explanation of these results requires the knowledge of the one-particle local density of states of the system, which is best described in the framework of the BdG theory.

1.5.1 Derivation

We start with the second-quantized Hamiltonian for electrons experiencing an effective two-particle attractive interaction:

$$\mathcal{H} = \int d\mathbf{r} \psi_\alpha^\dagger(\mathbf{r}) h_\alpha(\mathbf{r}) \psi_\alpha(\mathbf{r}) - \frac{1}{2} \int \int d\mathbf{r} d\mathbf{r}' V_{\text{eff}}(\mathbf{r}, \mathbf{r}') \psi_\alpha^\dagger(\mathbf{r}) \psi_\beta^\dagger(\mathbf{r}') \psi_\beta(\mathbf{r}') \psi_\alpha(\mathbf{r}) . \quad (1.38)$$

Here $\psi_\alpha^\dagger(\mathbf{r})$ and $\psi_\alpha(\mathbf{r})$ are creation and annihilation field operators of an electron with spin α at position \mathbf{r} . They obey the anti-commutation relation

$$\{\psi_\alpha(\mathbf{r}), \psi_\beta^\dagger(\mathbf{r}')\} = \delta(\mathbf{r} - \mathbf{r}') \delta_{\alpha\beta} , \quad (1.39)$$

$$\{\psi_\alpha(\mathbf{r}), \psi_\beta(\mathbf{r}')\} = \{\psi_\alpha^\dagger(\mathbf{r}), \psi_\beta^\dagger(\mathbf{r}')\} = 0 . \quad (1.40)$$

The single particle Hamiltonian is given by

$$h_\alpha(\mathbf{r}) = \frac{[\frac{\hbar}{i} \nabla_{\mathbf{r}} + \frac{e}{c} \mathbf{A}(\mathbf{r})]^2}{2m_e} - e\phi(\mathbf{r}) + \alpha \mu_B H(\mathbf{r}) - E_F , \quad (1.41)$$

with $\mathbf{A}(\mathbf{r})$ and $\phi(\mathbf{r})$ the vector and scalar potentials. The magnetic field $H(\mathbf{r})$ has assumed to be along the z direction. The single particle energy is measured relative to the Fermi energy E_F . We have also chosen $V_{\text{eff}}(\mathbf{r}, \mathbf{r}')$ to be positive while introduced a prefactor “ $-$ ” to denote the attractive interaction in the second term of Eq. (1.38). Of course, the symmetry relation $V_{\text{eff}}(\mathbf{r}', \mathbf{r}) = V_{\text{eff}}(\mathbf{r}, \mathbf{r}')$ still holds. The repeated spin index means the summation. Since we are most interested in the electron pairing in a superconductor, we can perform a Hartree-Fock-like mean-field approximation to the second term of Eq. (1.38) but in the particle-particle

pairing channel.⁴ A caution should be taken that this assumption is reasonable at low temperatures when the system is deep into the superconducting state, and the superconducting phase fluctuation, which is important near the transition temperature, is neglected. The mean-field Hamiltonian can then be written as follows⁵:

$$\begin{aligned} \mathcal{H}_{\text{eff}} = & \int d\mathbf{r} \psi_{\alpha}^{\dagger}(\mathbf{r}) h_{\alpha}(\mathbf{r}) \psi_{\alpha}(\mathbf{r}) + \int \int d\mathbf{r} d\mathbf{r}' [\Delta(\mathbf{r}, \mathbf{r}') \psi_{\uparrow}^{\dagger}(\mathbf{r}) \psi_{\downarrow}^{\dagger}(\mathbf{r}') + \text{H.c.}] \\ & + \int \int d\mathbf{r} d\mathbf{r}' |\Delta(\mathbf{r}, \mathbf{r}')|^2 / V_{\text{eff}}(\mathbf{r}, \mathbf{r}'), \end{aligned} \quad (1.42)$$

where the pair potential is given by

$$\Delta(\mathbf{r}, \mathbf{r}') = -V_{\text{eff}}(\mathbf{r} - \mathbf{r}') \langle \psi_{\downarrow}(\mathbf{r}') \psi_{\uparrow}(\mathbf{r}) \rangle = V_{\text{eff}}(\mathbf{r} - \mathbf{r}') \langle \psi_{\uparrow}(\mathbf{r}) \psi_{\downarrow}(\mathbf{r}') \rangle, \quad (1.43)$$

$$\Delta^*(\mathbf{r}, \mathbf{r}') = -V_{\text{eff}}(\mathbf{r} - \mathbf{r}') \langle \psi_{\uparrow}^{\dagger}(\mathbf{r}) \psi_{\downarrow}^{\dagger}(\mathbf{r}') \rangle = V_{\text{eff}}(\mathbf{r} - \mathbf{r}') \langle \psi_{\downarrow}^{\dagger}(\mathbf{r}') \psi_{\uparrow}^{\dagger}(\mathbf{r}) \rangle. \quad (1.44)$$

The effective Hamiltonian equation (1.42) is in a bi-linear form and can be diagonalized exactly. By using the commutation relation for fermionic operators $\hat{A}, \hat{B}, \hat{C}$

$$[A, BC]_{-} = \{A, B\}C - B\{A, C\}, \quad (1.45)$$

and the function property

$$\int dx' f(x') \frac{d\delta(x-x')}{dx'} = -\frac{df(x)}{dx}, \quad (1.46)$$

we obtain the following relations

$$[\psi_{\uparrow}(\mathbf{r}), \mathcal{H}_{\text{eff}}]_{-} = h_{\uparrow}(\mathbf{r}) \psi_{\uparrow}(\mathbf{r}) + \int d\mathbf{r}' \Delta(\mathbf{r}, \mathbf{r}') \psi_{\downarrow}^{\dagger}(\mathbf{r}'), \quad (1.47a)$$

$$[\psi_{\uparrow}^{\dagger}(\mathbf{r}), \mathcal{H}_{\text{eff}}]_{-} = -h_{\uparrow}^*(\mathbf{r}) \psi_{\uparrow}^{\dagger}(\mathbf{r}) - \int d\mathbf{r}' \Delta^*(\mathbf{r}, \mathbf{r}') \psi_{\downarrow}(\mathbf{r}'), \quad (1.47b)$$

$$[\psi_{\downarrow}(\mathbf{r}), \mathcal{H}_{\text{eff}}]_{-} = h_{\downarrow}(\mathbf{r}) \psi_{\downarrow}(\mathbf{r}) - \int d\mathbf{r}' \Delta(\mathbf{r}', \mathbf{r}) \psi_{\uparrow}^{\dagger}(\mathbf{r}'), \quad (1.47c)$$

$$[\psi_{\downarrow}^{\dagger}(\mathbf{r}), \mathcal{H}_{\text{eff}}]_{-} = -h_{\downarrow}^*(\mathbf{r}) \psi_{\downarrow}^{\dagger}(\mathbf{r}) + \int d\mathbf{r}' \Delta^*(\mathbf{r}', \mathbf{r}) \psi_{\uparrow}(\mathbf{r}'). \quad (1.47d)$$

⁴We notice that the normal-state Hartree-Fock term can be absorbed into the chemical potential, which will not modify the results qualitatively.

⁵Here we only consider the spin-singlet pairing, in which a spin-up electron is paired with a spin-down electron. The spin-triplet pairing, in which electrons are paired with equal spin, can be discussed similarly.

Note that $h^*(\mathbf{r}) \neq h(\mathbf{r})$. Equations (1.47)(a)–(d) show that the electron field operator can be expressed as a linear combination of electron- and hole-like quasiparticle excitations, which enables us to perform a Bogoliubov canonical transformation [25, 26]:

$$\psi_\sigma(\mathbf{r}) = \sum_n [u_{n\sigma}(\mathbf{r})\gamma_n - \sigma v_{n\sigma}^*(\mathbf{r})\gamma_n^\dagger]. \quad (1.48)$$

Be reminded the summation is over the excitation states with positive energy. In the expanded form for each individual spin projection, the transformation becomes

$$\psi_\uparrow(\mathbf{r}) = \sum_n [u_\uparrow^n(\mathbf{r})\gamma_n - v_\uparrow^{n*}(\mathbf{r})\gamma_n^\dagger], \quad \psi_\uparrow^\dagger(\mathbf{r}) = \sum_n [u_\uparrow^{n*}(\mathbf{r})\gamma_n^\dagger - v_\uparrow^n(\mathbf{r})\gamma_n], \quad (1.49)$$

$$\psi_\downarrow(\mathbf{r}) = \sum_n [u_\downarrow^n(\mathbf{r})\gamma_n + v_\downarrow^{n*}(\mathbf{r})\gamma_n^\dagger], \quad \psi_\downarrow^\dagger(\mathbf{r}) = \sum_n [u_\downarrow^{n*}(\mathbf{r})\gamma_n^\dagger + v_\downarrow^n(\mathbf{r})\gamma_n]. \quad (1.50)$$

In the above transformation, the quasiparticle operators γ_n and γ_n^\dagger are also fermionic operators obeying the anti-commutation relation

$$\{\gamma_n, \gamma_m^\dagger\} = \delta_{nm}, \quad (1.51)$$

$$\{\gamma_n, \gamma_m\} = \{\gamma_n^\dagger, \gamma_m^\dagger\} = 0. \quad (1.52)$$

The anti-communication relation between the quasiparticle operators also ensures the anti-communication relation for the original electron field operators given in Eqs. (1.39) and (1.40).

The remaining task is to establish the eigen-equation for the quasiparticle wave functions $(u_\sigma(\mathbf{r}), v_\sigma(\mathbf{r}))^{\text{Transpose}}$. Assume the diagonalized Hamiltonian to be

$$\mathcal{H}_{\text{eff}} = E_g + \sum_n E_n \gamma_n^\dagger \gamma_n, \quad (1.53)$$

where the excitation energy is positive and E_g is the ground state energy. We first observe the following commutation relations

$$[\gamma_n^\dagger, \mathcal{H}_{\text{eff}}]_- = -E_n \gamma_n^\dagger, \quad (1.54)$$

$$[\gamma_n, \mathcal{H}_{\text{eff}}]_- = E_n \gamma_n. \quad (1.55)$$

Upon the substitution of Eqs. (1.49) and (1.50), and with the aid of Eqs. (1.54) and (1.55), we can compare the coefficients of these terms with γ_n and γ_n^\dagger and arrive at

the following set of equations:

$$\begin{cases} h_{\uparrow}(\mathbf{r})u_{\uparrow}^n(\mathbf{r}) + \int d\mathbf{r}' \Delta(\mathbf{r}, \mathbf{r}')v_{\downarrow}^n(\mathbf{r}') = E_n u_{\uparrow}^n(\mathbf{r}), \\ h_{\downarrow}(\mathbf{r})u_{\downarrow}^n(\mathbf{r}) + \int d\mathbf{r}' \Delta(\mathbf{r}', \mathbf{r})v_{\uparrow}^n(\mathbf{r}') = E_n u_{\downarrow}^n(\mathbf{r}), \\ \int d\mathbf{r}' \Delta^*(\mathbf{r}, \mathbf{r}')u_{\downarrow}^n(\mathbf{r}') - h_{\uparrow}^*(\mathbf{r})v_{\uparrow}^n(\mathbf{r}) = E_n v_{\uparrow}^n(\mathbf{r}), \\ \int d\mathbf{r}' \Delta^*(\mathbf{r}', \mathbf{r})u_{\uparrow}^n(\mathbf{r}') - h_{\downarrow}^*(\mathbf{r})v_{\downarrow}^n(\mathbf{r}) = E_n v_{\downarrow}^n(\mathbf{r}). \end{cases} \quad (1.56)$$

To see the structure of the above set of equations more clearly, we can write it into a compact matrix form:

$$\int d\mathbf{r}' \hat{M}(\mathbf{r}, \mathbf{r}') \hat{\phi}(\mathbf{r}') = E_n \hat{\phi}(\mathbf{r}), \quad (1.57)$$

where

$$\hat{M}(\mathbf{r}, \mathbf{r}') = \begin{bmatrix} h_{\uparrow}(\mathbf{r})\delta(\mathbf{r} - \mathbf{r}') & 0 & 0 & \Delta(\mathbf{r}, \mathbf{r}') \\ 0 & h_{\downarrow}(\mathbf{r})\delta(\mathbf{r} - \mathbf{r}') & \Delta(\mathbf{r}', \mathbf{r}) & 0 \\ 0 & \Delta^*(\mathbf{r}, \mathbf{r}') & -h_{\uparrow}^*(\mathbf{r})\delta(\mathbf{r} - \mathbf{r}') & 0 \\ \Delta^*(\mathbf{r}', \mathbf{r}) & 0 & 0 & -h_{\downarrow}^*(\mathbf{r})\delta(\mathbf{r} - \mathbf{r}') \end{bmatrix} \quad (1.58)$$

and

$$\hat{\phi}(\mathbf{r}') = \begin{pmatrix} u_{\uparrow}^n(\mathbf{r}') \\ u_{\downarrow}^n(\mathbf{r}') \\ v_{\uparrow}^n(\mathbf{r}') \\ v_{\downarrow}^n(\mathbf{r}') \end{pmatrix}. \quad (1.59)$$

From Eq. (1.58), we can see that in the absence of spin-orbit coupling and other spin-flip scattering interactions, the set of equations as given by Eq. (1.58) is blocked diagonalized into two subsets of equations:

$$\begin{cases} h_{\uparrow}(\mathbf{r})u_{\uparrow}^{\tilde{n}1}(\mathbf{r}) + \int d\mathbf{r}' \Delta(\mathbf{r}, \mathbf{r}')v_{\downarrow}^{\tilde{n}1}(\mathbf{r}') = E_{\tilde{n}1} u_{\uparrow}^{\tilde{n}1}(\mathbf{r}), \\ \int d\mathbf{r}' \Delta^*(\mathbf{r}', \mathbf{r})u_{\uparrow}^{\tilde{n}1}(\mathbf{r}') - h_{\downarrow}^*(\mathbf{r})v_{\downarrow}^{\tilde{n}1}(\mathbf{r}) = E_{\tilde{n}1} v_{\downarrow}^{\tilde{n}1}(\mathbf{r}), \end{cases} \quad (1.60)$$

and

$$\begin{cases} h_{\downarrow}(\mathbf{r})u_{\downarrow}^{\tilde{n}2}(\mathbf{r}) + \int d\mathbf{r}' \Delta(\mathbf{r}', \mathbf{r})v_{\uparrow}^{\tilde{n}2}(\mathbf{r}') = E_{\tilde{n}2} u_{\downarrow}^{\tilde{n}2}(\mathbf{r}), \\ \int d\mathbf{r}' \Delta^*(\mathbf{r}, \mathbf{r}')u_{\downarrow}^{\tilde{n}2}(\mathbf{r}') - h_{\uparrow}^*(\mathbf{r})v_{\uparrow}^{\tilde{n}2}(\mathbf{r}) = E_{\tilde{n}2} v_{\uparrow}^{\tilde{n}2}(\mathbf{r}). \end{cases} \quad (1.61)$$

That is, the spin-up electron-like component of wave function $u_{\uparrow}(\mathbf{r})$ is coupled only to the spin-down hole-like component of wave function $v_{\downarrow}(\mathbf{r})$ while the spin-down

electron-like component of wave function $u_{\downarrow}(\mathbf{r})$ is coupled only to the spin-up hole-like component of wave function $v_{\uparrow}(\mathbf{r})$. Each of these two subsets of equations are now a 2 by 2 matrix equation in the Nambu space. By breaking the $U(1)$ gauge symmetry, this unusual space allows the emergence of superconducting pairing state. The mathematical structure of these equations looks similar to those describing the coupling between particles in conduction band and holes in the valence band in semiconductor physics. However, we should be cautioned that the origin of these equations in superconductors is really due to an *effective* electron-electron pairing. To be clear, we have redefined the number of eigenstate index. If the original set of eigen-equations as given in Eq.(1.56) has N number of eigenvalues, each subset of eigen-equations will have $N/2$ number of eigenvalues. In this decoupling, the diagonalized Hamiltonian as given in Eq.(1.53) can be written as:

$$\mathcal{H}_{\text{eff}} = E_g + \sum_{\tilde{n}\mu} E_{\tilde{n}\mu} \gamma_{\tilde{n}\mu}^{\dagger} \gamma_{\tilde{n}\mu}, \quad (1.62)$$

with $\mu = 1, 2$. Correspondingly, the canonical transform can also be re-written as:

$$\psi_{\uparrow}(\mathbf{r}) = \sum_{\tilde{n}} [u_{\uparrow}^{\tilde{n}1}(\mathbf{r})\gamma_{\tilde{n}1} - v_{\uparrow}^{\tilde{n}2*}(\mathbf{r})\gamma_{\tilde{n}2}^{\dagger}], \quad \psi_{\uparrow}^{\dagger}(\mathbf{r}) = \sum_{\tilde{n}} [u_{\uparrow}^{\tilde{n}1*}(\mathbf{r})\gamma_{\tilde{n}1}^{\dagger} - v_{\uparrow}^{\tilde{n}2}(\mathbf{r})\gamma_{\tilde{n}2}], \quad (1.63)$$

$$\psi_{\downarrow}(\mathbf{r}) = \sum_{\tilde{n}} [u_{\downarrow}^{\tilde{n}2}(\mathbf{r})\gamma_{\tilde{n}2} + v_{\downarrow}^{\tilde{n}1*}(\mathbf{r})\gamma_{\tilde{n}1}^{\dagger}], \quad \psi_{\downarrow}^{\dagger}(\mathbf{r}) = \sum_{\tilde{n}} [u_{\downarrow}^{\tilde{n}2*}(\mathbf{r})\gamma_{\tilde{n}2}^{\dagger} + v_{\downarrow}^{\tilde{n}1}(\mathbf{r})\gamma_{\tilde{n}1}]. \quad (1.64)$$

We now prove that the set of equations given by Eqs. (1.60) and (1.61) has the following symmetry property: *If $(u_{\uparrow}^{\tilde{n}1}, v_{\downarrow}^{\tilde{n}1})^{\text{Transpose}}$ is the eigenfunction of Eq. (1.60) with eigenvalue $E_{\tilde{n}1}$, then $(v_{\downarrow}^{\tilde{n}1*}, -u_{\uparrow}^{\tilde{n}1*})^{\text{Transpose}}$ is also the eigensolution to Eq. (1.61) with eigenvalue $-E_{\tilde{n}1}$.* We take the complex conjugation to Eq.(1.60), which yields to

$$\begin{cases} h_{\uparrow}^*(\mathbf{r})u_{\uparrow}^{\tilde{n}1*}(\mathbf{r}) + \int d\mathbf{r}' \Delta^*(\mathbf{r}, \mathbf{r}')v_{\downarrow}^{\tilde{n}1*}(\mathbf{r}') = E_{\tilde{n}1}u_{\uparrow}^{\tilde{n}1*}(\mathbf{r}), \\ \int d\mathbf{r}' \Delta(\mathbf{r}', \mathbf{r})u_{\uparrow}^{\tilde{n}1*}(\mathbf{r}') - h_{\downarrow}(\mathbf{r})v_{\downarrow}^{\tilde{n}1*}(\mathbf{r}) = E_{\tilde{n}1}v_{\downarrow}^{\tilde{n}1*}(\mathbf{r}). \end{cases} \quad (1.65)$$

Multiplying the second expression in the above set of equations by a minus sign on both sides, we re-arrange the whole set of equations into

$$\begin{cases} h_{\downarrow}(\mathbf{r})v_{\downarrow}^{\tilde{n}1*}(\mathbf{r}) + \int d\mathbf{r}' \Delta(\mathbf{r}', \mathbf{r})(-u_{\uparrow}^{\tilde{n}1*}(\mathbf{r}')) = -E_{\tilde{n}1}v_{\downarrow}^{\tilde{n}1*}(\mathbf{r}), \\ \int d\mathbf{r}' \Delta^*(\mathbf{r}, \mathbf{r}')v_{\downarrow}^{\tilde{n}1*}(\mathbf{r}') - h_{\uparrow}^*(\mathbf{r})(-u_{\uparrow}^{\tilde{n}1*}(\mathbf{r})) = -E_{\tilde{n}1}(-u_{\uparrow}^{\tilde{n}1*}(\mathbf{r})). \end{cases} \quad (1.66)$$

Equation (1.66) is just identical to Eq. (1.61) with the equivalence:

$$\begin{pmatrix} u_{\downarrow}^{\tilde{n}2}(\mathbf{r}) \\ v_{\uparrow}^{\tilde{n}2}(\mathbf{r}) \end{pmatrix} \equiv \begin{pmatrix} v_{\downarrow}^{\tilde{n}1*}(\mathbf{r}) \\ -u_{\uparrow}^{\tilde{n}1}(\mathbf{r}) \end{pmatrix}, \quad (1.67)$$

and $E_{\tilde{n}2} \equiv -E_{\tilde{n}1}$. This property has a significant consequence. It suggests that we merely need to solve one set of equations, e.g., Eq. (1.60), instead of both Eqs. (1.60) and (1.61), and obtain all information essential for the measurable. It saves the computational time significantly, which is desirable for the real-space inhomogeneous or disordered problems, even in a collinear spin-polarization. Note again here that this simplification exists in the absence of the spin-orbit coupling and other spin-flip scattering terms in the Hamiltonian. However, a more general symmetry property, as will be shown in the next chapter, can be derived even in the presence of these terms. We note that Eqs. (1.60) and (1.61) involve the pair potential $\Delta(\mathbf{r}, \mathbf{r}')$. Substituting Eqs. (1.49) and (1.50) into Eq. (1.43), we arrive at

$$\begin{aligned} \Delta(\mathbf{r}, \mathbf{r}') &= V(\mathbf{r} - \mathbf{r}') \langle \psi_{\uparrow}(\mathbf{r}) \psi_{\downarrow}(\mathbf{r}') \rangle \\ &= V(\mathbf{r} - \mathbf{r}') \sum_{\tilde{n}}^{\prime} [u_{\uparrow}^{\tilde{n}1}(\mathbf{r}) v_{\downarrow}^{\tilde{n}1*}(\mathbf{r}') f(-E_{\tilde{n}1}) - v_{\uparrow}^{\tilde{n}2*}(\mathbf{r}) u_{\downarrow}^{\tilde{n}2}(\mathbf{r}') f(E_{\tilde{n}2})] \\ &= V(\mathbf{r} - \mathbf{r}') \sum_{\tilde{n}}^{\prime} u_{\uparrow}^{\tilde{n}1}(\mathbf{r}) v_{\downarrow}^{\tilde{n}1*}(\mathbf{r}') f(-E_{\tilde{n}1}). \end{aligned} \quad (1.68)$$

On the other hand,

$$\begin{aligned} \Delta(\mathbf{r}, \mathbf{r}') &= -V(\mathbf{r} - \mathbf{r}') \langle \psi_{\downarrow}(\mathbf{r}') \psi_{\uparrow}(\mathbf{r}) \rangle \\ &= -V(\mathbf{r} - \mathbf{r}') \sum_{\tilde{n}}^{\prime} [-u_{\downarrow}^{\tilde{n}2}(\mathbf{r}') v_{\uparrow}^{\tilde{n}2*}(\mathbf{r}) f(-E_{\tilde{n}2}) + v_{\downarrow}^{\tilde{n}1*}(\mathbf{r}') u_{\uparrow}^{\tilde{n}1}(\mathbf{r}) f(E_{\tilde{n}1})] \\ &= -V(\mathbf{r} - \mathbf{r}') \sum_{\tilde{n}}^{\prime} u_{\uparrow}^{\tilde{n}1}(\mathbf{r}) v_{\downarrow}^{\tilde{n}1*}(\mathbf{r}') f(E_{\tilde{n}1}). \end{aligned} \quad (1.69)$$

Here we have used the symmetry property in the derivation, and the statistical average

$$\langle \gamma_{\tilde{n}\mu}^{\dagger} \gamma_{\tilde{m}\nu} \rangle = \delta_{\tilde{n}\tilde{m}} \delta_{\mu\nu} f(E_{\tilde{n}\mu}), \quad (1.70)$$

and

$$\langle \gamma_{\tilde{n}\mu} \gamma_{\tilde{m}\nu} \rangle = \langle \gamma_{\tilde{n}\mu}^{\dagger} \gamma_{\tilde{m}\nu}^{\dagger} \rangle = 0, \quad (1.71)$$

where the Fermi distribution function

$$f(E_{\tilde{n}\mu}) = \frac{1}{\exp(E_{\tilde{n}\mu}/k_B T) + 1}, \quad (1.72)$$

with k_B the Boltzmann constant and T the temperature. Notice the disappearance of “ r ” above the summation symbol, meaning the summation is over both positive and negative eigenvalues. Combination of Eqs. (1.68) and (1.69) gives

$$\Delta(\mathbf{r}, \mathbf{r}') = \frac{V(\mathbf{r} - \mathbf{r}')}{2} \sum_{\tilde{n}} u_{\uparrow}^{\tilde{n}1}(\mathbf{r}) v_{\downarrow}^{\tilde{n}1*}(\mathbf{r}') \tanh\left(\frac{E_{\tilde{n}1}}{2k_B T}\right). \quad (1.73)$$

For spin-singlet pairing, $\Delta(\mathbf{r}, \mathbf{r}') = \Delta(\mathbf{r}', \mathbf{r})$, and we can have a more symmetric form of the expression

$$\Delta(\mathbf{r}, \mathbf{r}') = \frac{V(\mathbf{r} - \mathbf{r}')}{4} \sum_{\tilde{n}} [u_{\uparrow}^{\tilde{n}1}(\mathbf{r}) v_{\downarrow}^{\tilde{n}1*}(\mathbf{r}') + u_{\uparrow}^{\tilde{n}1}(\mathbf{r}') v_{\downarrow}^{\tilde{n}1*}(\mathbf{r})] \tanh\left(\frac{E_{\tilde{n}1}}{2k_B T}\right). \quad (1.74)$$

When there is no spin-polarization effect, Eqs. (1.60) and (1.61) are identical and they recover the original formalism proposed by de-Gennes [9] for an s -wave superconductor and that for an anisotropic superconductor [27]. Since a Bogoliubov canonical transformation is involved in the development of the formalism, these sets of equations are called the Bogoliubov-de Gennes equations.

1.5.2 Local Density of States

Once the solution to the BdG equations is obtained, the local density of states can be evaluated according to

$$\rho(\mathbf{r}, E) = \sum_{n,\sigma} \left\{ |u_{\sigma}^n(\mathbf{r})|^2 \delta(E - E_n) + |v_{\sigma}^n(\mathbf{r})|^2 \delta(E + E_n) \right\}, \quad (1.75)$$

where $\delta(x)$ is the Dirac delta function and can be approximated numerically as

$$\delta(x) = \frac{1}{\pi} \frac{\Gamma}{x^2 + \Gamma^2}, \quad (1.76)$$

with Γ a lifetime broadening parameter. In the absence of the spin-orbit coupling and spin-flip scattering, Eq. (1.75) becomes

$$\rho(\mathbf{r}, E) = \sum_n \left\{ |u_{\uparrow}^n(\mathbf{r})|^2 \delta(E - E_n) + |v_{\downarrow}^n(\mathbf{r})|^2 \delta(E + E_n) \right\}. \quad (1.77)$$

Equivalently, the thermalized local density of states can be written as

$$\rho(\mathbf{r}, E) = \sum_n \left\{ |u_{\uparrow}^n(\mathbf{r})|^2 \left(-\frac{\partial f(E - E_n)}{\partial E} \right) + |v_{\downarrow}^n(\mathbf{r})|^2 \left(-\frac{\partial f(E + E_n)}{\partial E} \right) \right\}. \quad (1.78)$$

The local density of states is proportional to the local tunneling conductance as measured by the scanning tunneling microscopy.

In the following discussion, unless specified otherwise the BdG equation (1.60) will be mainly used. We will drop the spin subscript to u and v , and the quasiparticle branch index, as well as the symbol tilde on the eigenstate index. We keep only the spin index for the single-particle Hamiltonian itself.

1.5.3 Gauge Invariance

The choice of the vector potential \mathbf{A} is not unique, since $\mathbf{A}'(\mathbf{r}) = \mathbf{A}(\mathbf{r}) + \nabla\chi(\mathbf{r})$, with χ an arbitrary function, will give the same magnetic field as that determined from \mathbf{A} , that is, $\nabla \times \mathbf{A}'(\mathbf{r}) = \nabla \times \mathbf{A}(\mathbf{r}) = \mathbf{H}(\mathbf{r})$. Thus \mathbf{A} and \mathbf{A}' are equally acceptable to describe the field $\mathbf{H}(\mathbf{r})$. All physically measurable quantities will have the same expectation values when calculated with \mathbf{A} and \mathbf{A}' .

Suppose that the eigenfunctions (u, v) of the BdG equation with the vector potential \mathbf{A} are known. It can be easily proved that the eigenfunctions (u', v') with the vector potential $\mathbf{A}' = \mathbf{A} + \nabla\chi(\mathbf{r})$ differs from (u, v) as

$$\begin{pmatrix} u'(\mathbf{r}) \\ v'(\mathbf{r}) \end{pmatrix} = \begin{pmatrix} e^{-ie\chi(\mathbf{r})/\hbar c} & 0 \\ 0 & e^{ie\chi(\mathbf{r})/\hbar c} \end{pmatrix} \begin{pmatrix} u(\mathbf{r}) \\ v(\mathbf{r}) \end{pmatrix}, \quad (1.79)$$

while the pair potential is modified as

$$\Delta'(\mathbf{r}, \mathbf{r}') = \Delta(\mathbf{r}, \mathbf{r}') e^{-ie[\chi(\mathbf{r}) + \chi(\mathbf{r}')]/\hbar c}. \quad (1.80)$$

1.6 Structure of a General Gap Matrix

The spin wavefunction of a singlet state is antisymmetric upon an interchange of the particles (spin indices). It enables us to write the order parameter as

$$\hat{\Delta}(\mathbf{k}) = d_0(\mathbf{k}) \begin{pmatrix} 0 & 1 \\ -1 & 0 \end{pmatrix} = d_0(\mathbf{k}) i\hat{\sigma}_2 = d_0(\mathbf{k}) \hat{\chi}_0. \quad (1.81)$$

In terms of the spin up (\uparrow) and spin down (\downarrow) wavefunctions of individual electrons, the quantity

$$\hat{\chi}_0 = i\hat{\sigma}_2 = \begin{pmatrix} 0 & 1 \\ -1 & 0 \end{pmatrix}, \quad (1.82)$$

corresponds to the singlet wave function $\frac{1}{\sqrt{2}}[|\uparrow\rangle|\downarrow\rangle - |\downarrow\rangle|\uparrow\rangle]$. The factor $\hat{\chi}_0$ is antisymmetric upon interchanging spin variables of the order parameter while $d_0(\mathbf{k})$ is symmetric upon interchanging orbital variables of the order parameter, that is, $d_0(-\mathbf{k}) = d_0(\mathbf{k})$. The singlet pairing symmetry has been discovered in most of the conventional superconductors [28], high-temperature cuprates [29], iron-based superconductors [30], and Ce-115 [31] and Pu-115 [32, 33] heavy fermion superconductors.

For the triplet pairing state, the total spin is $S = 1$ for the two paired electrons and accordingly there are three spin wavefunctions. Therefore, the pairing amplitude for each of these spin states can be different and \mathbf{k} -dependent. The order parameter may then be written in the form:

$$\hat{\Delta}(\mathbf{k}) = \mathbf{d}(\mathbf{k}) \cdot \hat{\boldsymbol{\sigma}} i\hat{\sigma}_2 = \mathbf{d}(\mathbf{k}) \cdot \hat{\boldsymbol{\chi}}, \quad (1.83)$$

where the vector \mathbf{d} measures the amplitude of the order parameter and the matrices

$$\hat{\chi}_1 = i\hat{\sigma}_1\hat{\sigma}_2 = \begin{pmatrix} -1 & 0 \\ 0 & 1 \end{pmatrix}, \quad (1.84)$$

$$\hat{\chi}_2 = i\hat{\sigma}_2\hat{\sigma}_2 = \begin{pmatrix} i & 0 \\ 0 & i \end{pmatrix}, \quad (1.85)$$

and

$$\hat{\chi}_3 = i\hat{\sigma}_3\hat{\sigma}_2 = \begin{pmatrix} 0 & 1 \\ 1 & 0 \end{pmatrix}. \quad (1.86)$$

They correspond to the spin wavefunctions

$$\hat{\chi}_1 \rightarrow \frac{-1}{\sqrt{2}}[|\uparrow\rangle|\uparrow\rangle - |\downarrow\rangle|\downarrow\rangle] \quad (1.87)$$

$$\hat{\chi}_2 \rightarrow \frac{i}{\sqrt{2}}[|\uparrow\rangle|\uparrow\rangle + |\downarrow\rangle|\downarrow\rangle], \quad (1.88)$$

and

$$\hat{\chi}_3 \rightarrow \frac{1}{\sqrt{2}}[|\uparrow\rangle|\downarrow\rangle + |\downarrow\rangle|\uparrow\rangle]. \quad (1.89)$$

Now all three of these wavefunctions are symmetric upon interchanging the spin indices. In an expanded form, the triplet order parameter is written as:

$$\hat{\Delta}(\mathbf{k}) = \begin{pmatrix} -d_x(\mathbf{k}) + id_y(\mathbf{k}) & d_z(\mathbf{k}) \\ d_z(\mathbf{k}) & d_x(\mathbf{k}) + id_y(\mathbf{k}) \end{pmatrix}. \quad (1.90)$$

Recall that $\hat{\Delta}$ must satisfy the Pauli antisymmetric property $\hat{\Delta}_{\beta\alpha}(-\mathbf{k}) = -\hat{\Delta}_{\alpha\beta}(\mathbf{k})$, so we have $\mathbf{d}(-\mathbf{k}) = -\mathbf{d}(\mathbf{k})$. Also notice that the parity of spherical harmonics is $(-1)^{-l}$, the above behavior is in accord with our intuition for p -wave ($l = 1$) (or more generally, odd angular momentum) pairing.

If the vector $\mathbf{d}(\mathbf{k})$ has the form $\mathbf{d}(\mathbf{k}) = a(\mathbf{k})\hat{\mathbf{n}}(\mathbf{k})$, where $a(\mathbf{k})$ is a complex number and $\hat{\mathbf{n}}(\mathbf{k})$ is a real unit vector, we then have the property

$$\mathbf{d}(\mathbf{k}) \times \mathbf{d}^*(\mathbf{k}) = 0. \quad (1.91)$$

This property leads to the constraint

$$\begin{aligned} \hat{\Delta}^\dagger(\mathbf{k})\hat{\Delta}(\mathbf{k}) &= |\mathbf{d}|^2\hat{\mathbf{1}} + i\hat{\sigma} \cdot [\mathbf{d}(\mathbf{k}) \times \mathbf{d}^*(\mathbf{k})] \\ &= |\mathbf{d}|^2\hat{\mathbf{1}}. \end{aligned} \quad (1.92)$$

We refer to a state where \mathbf{d} has the property as given by Eq. (1.91) as the unitary state because $\hat{\Delta}^\dagger\hat{\Delta}$ is then proportional to the unit matrix. A rigorous classification of the symmetry properties of triplet superconductors was given by Blount [34], and Ueda and Rice [35] based on the group theory.

For the p -wave pairing state, the most general gap structure would involve a sum over all possible spin-orbital wavefunction products, each with its own complex amplitude, which we may write as

$$\hat{\Delta} = \sum_{i,\alpha} D_{\alpha i} \hat{\chi}_\alpha \hat{k}_i. \quad (1.93)$$

Here the indices α and i denotes the three component in spin and orbitals spaces with $\hat{k}_x = \sin\theta \cos\phi$, $\hat{k}_y = \sin\theta \sin\phi$, and $\hat{k}_z = \cos\theta$ while χ_α already given above. The matrix $D_{\alpha i}$ allows nine complex (equivalently, 18 real) coefficients and suggests the possibility of 18 types of pairing states. So far, the spin triplet pairing states has been discovered in ${}^3\text{He}$ superfluid [36] and possibly in Sr_2RuO_4 [37] and heavy-fermion UPt_3 and UBe_{13} [38–40] superconductors. In superfluid ${}^3\text{He}$, two phases are stabilized at zero magnetic field and very low temperatures, depending

on pressure [41]. They can be represented by the $D_{\alpha i}$ matrices:

$$\text{(B phase): } \hat{D} = \Delta_0 \begin{pmatrix} 1 & 0 & 0 \\ 0 & 1 & 0 \\ 0 & 0 & 1 \end{pmatrix}, \quad (1.94)$$

$$\text{(A phase): } \hat{D} = \Delta_0 \begin{pmatrix} 0 & 0 & 0 \\ 0 & 0 & 0 \\ 1 & i & 0 \end{pmatrix}. \quad (1.95)$$

The corresponding gap matrices are:

$$\text{(B phase): } \hat{\Delta} = \Delta_0 \begin{pmatrix} -\hat{k}_x + i\hat{k}_y & \hat{k}_z \\ \hat{k}_z & \hat{k}_x + i\hat{k}_y \end{pmatrix}, \quad (1.96)$$

$$\text{(A phase for } \mathbf{d} \parallel \hat{\mathbf{z}}): \hat{\Delta} = \Delta_0 \begin{pmatrix} 0 & \hat{k}_x + i\hat{k}_y \\ \hat{k}_x + i\hat{k}_y & 0 \end{pmatrix}. \quad (1.97)$$

The B-phase is also called the BW phase proposed by Balian and Werthamer [42]. In this phase, the single particle spectrum and the energy gap are isotropic; the total spin and orbital angular momenta are each equal to 1; the spin susceptibility is finite at zero temperature. The A-phase is also called the ABM-phase proposed by Anderson, Brinkman, and Morel [43]. In this phase, the S_z channel is completely suppressed and the spin susceptibility is very similar to that in the normal state.

1.7 Solution to the BdG Equations in Homogeneous Systems

Let us start with the non-spin-polarization situation. In homogeneous systems, there exists the translational symmetry. In the limit of homogeneous electron gas, the translation symmetry itself is continuous. Therefore, it would be convenient to expand the BdG wave function in terms of plane waves:

$$\begin{pmatrix} u(\mathbf{r}) \\ v(\mathbf{r}) \end{pmatrix} = \frac{1}{\sqrt{\Omega}} \begin{pmatrix} u_{\mathbf{k}} \\ v_{\mathbf{k}} \end{pmatrix} e^{i\mathbf{k}\cdot\mathbf{r}}, \quad (1.98)$$

where Ω is the volume of the entire system. Substitution of Eq. (1.98) into Eq. (1.60) leads to

$$\xi_{\mathbf{k}} u_{\mathbf{k}} + \Delta_{\mathbf{k}} v_{\mathbf{k}} = E_{\mathbf{k}} u_{\mathbf{k}}, \quad (1.99a)$$

$$\Delta_{\mathbf{k}}^* u_{\mathbf{k}} - \xi_{\mathbf{k}} v_{\mathbf{k}} = E_{\mathbf{k}} u_{\mathbf{k}}, \quad (1.99b)$$

where

$$\xi_{\mathbf{k}} = \frac{\hbar k^2}{2m_e} - E_F, \quad (1.100)$$

is the single-particle energy dispersion, while

$$\Delta_{\mathbf{k}} = \int d\mathbf{r}' \Delta(\mathbf{r}, \mathbf{r}') e^{-i\mathbf{k} \cdot (\mathbf{r} - \mathbf{r}')}, \quad (1.101)$$

is the Fourier transform of the real-space superconducting pair potential. Using the definition of the pair potential $\Delta(\mathbf{r}, \mathbf{r}')$ given by Eq. (1.74) into Eq. (1.101), we obtain

$$\Delta_{\mathbf{k}} = \frac{1}{2\Omega} \sum_{\mathbf{k}'} V_{\mathbf{k}\mathbf{k}'} u_{\mathbf{k}} v_{\mathbf{k}'}^* \tanh\left(\frac{E_{\mathbf{k}'}}{2k_B T}\right) \quad (1.102)$$

with the term

$$V_{\mathbf{k}\mathbf{k}'} = \int d\mathbf{r}' V(\mathbf{r}, \mathbf{r}') e^{-i\mathbf{k} \cdot (\mathbf{r} - \mathbf{r}')} \cos(\mathbf{k} \cdot (\mathbf{r} - \mathbf{r}')). \quad (1.103)$$

retaining only the pairing interaction of allowed orbital harmonics. For an isotropic s -wave pairing symmetry, we use the ansatz

$$V_{\mathbf{k}\mathbf{k}'} = V_s, \quad (1.104)$$

and correspondingly

$$\Delta_{\mathbf{k}} = \Delta_s, \quad (1.105)$$

which has no momentum dependence. For a d -wave pairing symmetry in a two-dimensional system, we have the ansatz

$$V_{\mathbf{k}\mathbf{k}'} = V_d \cos(2\phi_{\mathbf{k}}) \cos(2\phi_{\mathbf{k}'}), \quad (1.106)$$

and correspondingly

$$\Delta_{\mathbf{k}} = \Delta_d \cos(2\phi_{\mathbf{k}}), \quad (1.107)$$

with $\phi_{\mathbf{k}}$ being the azimuthal angle of \mathbf{k} around the Fermi energy. We note that in the summation on the right-hand-side of Eq. (1.102), both positive and negative energy eigenvalues are still taken into account. The profile of the energy gap around the Fermi surface for these two types of pairing symmetry is depicted in Fig. 1.4. For the isotropic s -wave superconductors, the quasiparticle gap is uniform along the Fermi

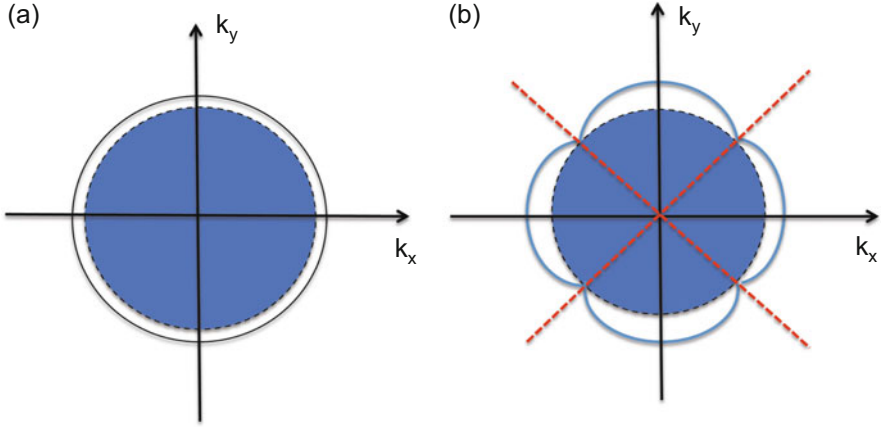


Fig. 1.4 A schematic drawing of quasiparticle excitation gap for an s -wave (a) and a $d_{x^2-y^2}$ -wave pairing superconductor (b)

surface. For the $d_{x^2-y^2}$ -wave superconductors, the quasiparticle gap is closed at some special momentum directions $\varphi = \frac{\pi}{4}, \frac{3\pi}{4}, \frac{5\pi}{4}, \frac{7\pi}{4}$. These gapless quasiparticles are called nodal quasiparticles.

A little algebra yields the eigensolutions

$$\begin{pmatrix} u_{\mathbf{k}} \\ v_{\mathbf{k}} \end{pmatrix} = \begin{pmatrix} u_{\mathbf{k}}^{(0)} e^{i\varphi_{\mathbf{k}}} \\ v_{\mathbf{k}}^{(0)} \end{pmatrix} \quad (1.108)$$

corresponding to the eigenvalue

$$E_{\mathbf{k}} = \sqrt{\xi_{\mathbf{k}}^2 + |\Delta_{\mathbf{k}}|^2}. \quad (1.109)$$

and

$$\begin{pmatrix} u_{\mathbf{k}} \\ v_{\mathbf{k}} \end{pmatrix} = \begin{pmatrix} -v_{\mathbf{k}}^{(0)} e^{i\varphi_{\mathbf{k}}} \\ u_{\mathbf{k}}^{(0)} \end{pmatrix} \quad (1.110)$$

corresponding to the eigenvalue $-E_{\mathbf{k}}$. Here the BdG wave function amplitude is given by

$$\begin{pmatrix} u_{\mathbf{k}}^{(0)} \\ v_{\mathbf{k}}^{(0)} \end{pmatrix} = \begin{pmatrix} \sqrt{\frac{1}{2} \left(1 + \frac{\xi_{\mathbf{k}}}{E_{\mathbf{k}}} \right)} \\ \sqrt{\frac{1}{2} \left(1 - \frac{\xi_{\mathbf{k}}}{E_{\mathbf{k}}} \right)} \end{pmatrix}, \quad (1.111)$$

and $\varphi_{\mathbf{k}}$ is the phase angle of $\Delta_{\mathbf{k}}$. Therefore, we obtain the self-consistency equation for the pair potential

$$\Delta_s = \frac{1}{(2\pi)^3} \int d\mathbf{k} V_s \frac{\Delta_s}{2E_{\mathbf{k}}} \tanh\left(\frac{E_{\mathbf{k}}}{2k_B T}\right), \quad (1.112)$$

for a three-dimensional s -wave superconductor with the quasiparticle excitation energy $E_{\mathbf{k}} = \sqrt{\xi_{\mathbf{k}}^2 + \Delta_s^2}$; and

$$\Delta_d = \frac{1}{(2\pi)^2} \int d\mathbf{k} V_d \cos^2(2\varphi) \frac{\Delta_d}{2E_{\mathbf{k}}} \tanh\left(\frac{E_{\mathbf{k}}}{2k_B T}\right), \quad (1.113)$$

for a two-dimensional $d_{x^2-y^2}$ -wave superconductor with the quasiparticle excitation energy $E_{\mathbf{k}} = \sqrt{\xi_{\mathbf{k}}^2 + (\Delta_d \cos(2\varphi))^2}$.

We can convert the three-dimensional integral into

$$\int d\mathbf{k} \rightarrow \int_0^{2\pi} d\phi \int_0^\pi \sin\theta d\theta \int_0^\infty k^2 dk \rightarrow 4\pi \int_0^\infty k^2 dk,$$

when the integrand has the spherical symmetry; while we can convert the two-dimensional integral into

$$\int d\mathbf{k} \rightarrow \int_0^{2\pi} d\phi \int_0^\infty k dk \rightarrow 2\pi \int_0^\infty k dk,$$

when the integrand has the cylindrical symmetry. Therefore, for a parabolic normal-state single-particle energy dispersion, $\xi_{\mathbf{k}} = \frac{\hbar^2 k^2}{2m_e} - E_F$, the integral over momentum amplitude k can be changed to the integral over the energy as

$$\frac{1}{(2\pi)^D} \int d\mathbf{k} \rightarrow \int g(\epsilon) d\epsilon, \quad (1.114)$$

where $D = 2$ and 3 and $g(\epsilon)$ denotes the density of states for electrons of one spin orientation, and is given by

$$g(\epsilon) = \frac{1}{4\pi^2} \left(\frac{2m_e}{\hbar^2}\right)^{3/2} \epsilon^{1/2}, \quad (1.115)$$

for the three-dimensional system, while

$$g(\epsilon) = \frac{m_e}{2\pi\hbar^2} \epsilon, \quad (1.116)$$

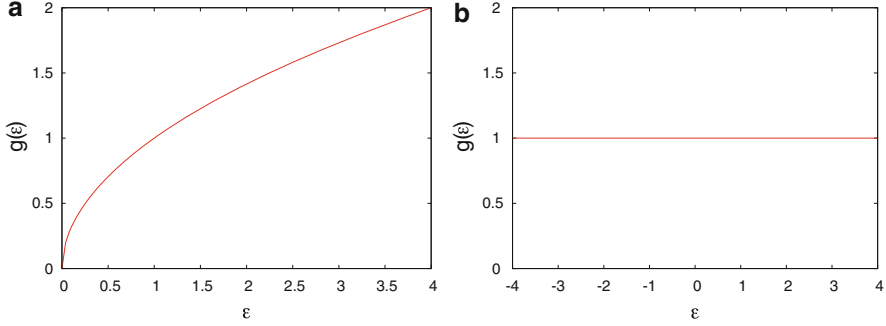


Fig. 1.5 Density of states for a three-dimensional (a) and a two-dimensional (b) electron gas

for the two-dimensional system. These expressions of density of states are shown in Fig. 1.5. In the BCS-type weak-coupling theory for superconductivity, the pairing interaction is limited to a range of $[-\hbar\omega_c, \hbar\omega_c]$ around the Fermi surface. The cutoff ω_c is the Debye frequency of phonons in conventional superconductors. In most strongly correlated superconductors, ω_c is the energy scale characterizing spin, charge, or orbital fluctuations and is approximated by the width of a renormalized narrow band. One should be cautioned that for the strongly correlated superconductivity, the description of retardation effect is beyond the scope of BCS-based BdG theory.

Now the self-consistency equations (1.112) and (1.113), for the non-trivial $\Delta_s \neq 0$ and $\Delta_d \neq 0$, become

$$\begin{aligned}
 1 &= \int_{-\hbar\omega_c}^{\hbar\omega_c} d\epsilon g(\epsilon) V_s \frac{1}{2E} \tanh\left(\frac{E}{2k_B T}\right) \\
 &\approx g(0) V_s \int_0^{\hbar\omega_c} d\epsilon \frac{1}{E} \tanh\left(\frac{E}{2k_B T}\right), \quad (1.117)
 \end{aligned}$$

for the s -wave superconductivity; and

$$\begin{aligned}
 1 &= \frac{1}{2\pi} \int_{-\hbar\omega_c}^{\hbar\omega_c} \int_0^{2\pi} d\epsilon d\varphi g(\epsilon) V_d \cos^2(2\varphi) \frac{1}{2E} \tanh\left(\frac{E}{2k_B T}\right) \\
 &= \frac{g(0) V_d}{2\pi} \int_0^{\hbar\omega_c} \int_0^{2\pi} d\epsilon d\varphi \cos^2(2\varphi) \frac{1}{E} \tanh\left(\frac{E}{2k_B T}\right), \quad (1.118)
 \end{aligned}$$

for the d -wave superconductivity. To derive the second line in each of the above two equations, we use the assumption that the density of states changes slightly in the range of $[-\hbar\omega_c, \hbar\omega_c]$ around the Fermi surface and can be approximated by that at the Fermi energy, i.e., $g(0)$. For the temperature $T = 0$ K, an analytical expression

for the s -wave superconductors can be obtained

$$\Delta_s(T = 0) = \hbar\omega_c \sinh^{-1} \left[\frac{1}{g(0)V_s} \right] \approx 2\hbar\omega_c \exp \left[-\frac{1}{g(0)V_s} \right], \quad (1.119)$$

for $g(0)V_s \ll 1$; while for the d -wave superconductivity, the following numerical solution needs to be found

$$1 = \frac{g(0)V_d}{2\pi} \int_0^{\hbar\omega_c} \int_0^{2\pi} d\epsilon d\varphi \frac{\cos^2(2\varphi)}{\sqrt{\epsilon^2 + \Delta_d^2(T = 0) \cos^2(2\varphi)}}. \quad (1.120)$$

The condition for the superconducting transition temperature is $\Delta_s = 0$ for s -wave superconductors while $\Delta_d = 0$ for the d -wave superconductors, which leads to

$$1 = g(0)V_s \int_0^{\hbar\omega_c} d\epsilon \frac{1}{\epsilon} \tanh \left(\frac{\epsilon}{2k_B T} \right), \quad (1.121)$$

and

$$1 = \frac{g(0)V_d}{2} \int_0^{\hbar\omega_c} d\epsilon \frac{1}{\epsilon} \tanh \left(\frac{\epsilon}{2k_B T} \right). \quad (1.122)$$

In the condition of $\hbar\omega_c/k_B T_c \gg 1$, we have

$$\begin{aligned} T_c &= \frac{2e^\gamma}{k_B \pi} \hbar\omega_c \exp \left[-\frac{1}{g(0)V_s} \right] \\ &= 1.13 \hbar\omega_c \exp \left[-\frac{1}{g(0)V_s} \right], \end{aligned} \quad (1.123)$$

and

$$\begin{aligned} T_c &= \frac{2e^\gamma}{k_B \pi} \hbar\omega_c \exp \left[-\frac{1}{2g(0)V_d} \right] \\ &= 1.13 \hbar\omega_c \exp \left[-\frac{1}{2g(0)V_d} \right]. \end{aligned} \quad (1.124)$$

Here the Euler constant $\gamma \approx 0.5772$ is used.

With the BdG solutions as given by Eqs. (1.108) and (1.110), we can find the bulk density of states

$$\frac{\rho_s(E)}{g(0)} = \begin{cases} \frac{E}{\sqrt{E^2 - \Delta_s^2}}, & E > \Delta_s \\ 0, & E < \Delta_s \end{cases} \quad (1.125)$$

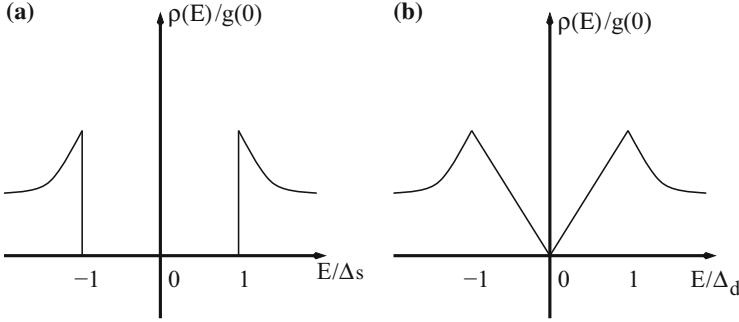


Fig. 1.6 Quasiparticle density of states for a uniform three-dimensional *s*-wave (a) and a uniform two-dimensional *d*-wave (b) superconductor

for the uniform *s*-wave superconductors, and

$$\frac{\rho_d(E)}{g(0)} = \begin{cases} \int_0^{2\pi} \frac{d\varphi}{2\pi} \frac{E}{\sqrt{E^2 - \Delta_d^2 \cos^2(2\varphi)}}, & E > |\Delta_d \cos(2\varphi)| \\ 0, & E < |\Delta_d \cos(2\varphi)| \end{cases} \quad (1.126)$$

for the uniform *d*-wave superconductors. A schematic density of states for both *s*-wave and *d*-wave superconductors is shown in Fig. 1.6. For the *s*-wave superconductors, a sharp gap feature is seen with vanishing density of states inside the energy range of $[-\Delta_s, \Delta_s]$, while for the *d*-wave superconductors, the density of states is linear in energy inside $[-\Delta_d, \Delta_d]$, due to the existence of nodal quasiparticles.

All the above discussions demonstrate that, in the homogeneous superconductors, the BdG equations can reproduce all the known results obtained through the Bogoliubov-Valatin canonical transformation. However, as will be demonstrated in later chapters, the BdG equations are more convenient to study the properties of inhomogeneous superconductors.

1.8 Relation to the Abrikosov-Gor'kov Equations

We should also be aware that the Hamiltonian (1.42) can also be solved via the Green's function technique. We first define a two-component field operator in the Nambu space [44, 45]:

$$\hat{\Psi}(\mathbf{r}, \tau) = \begin{pmatrix} \psi_{\uparrow}(\mathbf{r}, \tau) \\ \psi_{\downarrow}(\mathbf{r}, \tau) \end{pmatrix}, \quad (1.127)$$

where

$$\psi_{\sigma}(\mathbf{r}, \tau) = e^{\mathcal{H}_{\text{eff}}\tau/\hbar} \psi_{\sigma}(\mathbf{r}) e^{-\mathcal{H}_{\text{eff}}\tau/\hbar}, \quad (1.128)$$

$$\psi_{\sigma}^{\dagger}(\mathbf{r}, \tau) = e^{\mathcal{H}_{\text{eff}}\tau/\hbar} \psi_{\sigma}^{\dagger}(\mathbf{r}) e^{-\mathcal{H}_{\text{eff}}\tau/\hbar}. \quad (1.129)$$

are the field operators defined in the Heisenberg picture. Note that $\psi_{\sigma}^{\dagger}(\mathbf{r}, \tau) \neq [\psi_{\sigma}(\mathbf{r}, \tau)]^{\dagger}$. We can then introduce the Green's function

$$\begin{aligned} \mathcal{G}(\mathbf{r}\tau; \mathbf{r}'\tau') &= -\langle T_{\tau}[\hat{\Psi}(\mathbf{r}, \tau) \otimes \hat{\Psi}^{\dagger}(\mathbf{r}', \tau')] \rangle \\ &= -\theta(\tau - \tau') \langle \hat{\Psi}(\mathbf{r}, \tau) \otimes \hat{\Psi}^{\dagger}(\mathbf{r}', \tau') \rangle \\ &\quad + \theta(\tau' - \tau) \langle \hat{\Psi}^{\dagger}(\mathbf{r}', \tau') \otimes \hat{\Psi}(\mathbf{r}, \tau) \rangle. \end{aligned} \quad (1.130)$$

Here \otimes means the direct product of two vector fields. The bracket $\langle \dots \rangle$ means the statistic average

$$\langle \hat{O} \rangle = \text{Tr}[e^{-\beta(\mathcal{H}_{\text{eff}} - \Omega)} \hat{O}], \quad (1.131)$$

with the thermodynamic potential Ω given by

$$e^{-\beta\Omega} = \text{Tr}[e^{-\beta\mathcal{H}_{\text{eff}}}] . \quad (1.132)$$

The factor T_{τ} is a τ -ordering operator, which arranges operators with earliest time τ to the right. The subscript τ is affixed to T to distinguish T_{τ} from the temperature. In expanded form, the Green's function becomes

$$\mathcal{G}(\mathbf{r}\tau; \mathbf{r}'\tau') = \begin{pmatrix} -\langle T_{\tau}[\psi_{\uparrow}(\mathbf{r}, \tau) \psi_{\uparrow}^{\dagger}(\mathbf{r}', \tau')] \rangle - \langle T_{\tau}[\psi_{\uparrow}(\mathbf{r}, \tau) \psi_{\downarrow}(\mathbf{r}', \tau')] \rangle \\ -\langle T_{\tau}[\psi_{\downarrow}^{\dagger}(\mathbf{r}, \tau) \psi_{\uparrow}^{\dagger}(\mathbf{r}', \tau')] \rangle - \langle T_{\tau}[\psi_{\downarrow}^{\dagger}(\mathbf{r}, \tau) \psi_{\downarrow}(\mathbf{r}', \tau')] \rangle \end{pmatrix}, \quad (1.133)$$

Since the trace is unchanged upon a cyclic variation of operators, we can easily prove that the Green's function is a function of the difference $\tau - \tau'$, that is,

$$\mathcal{G}(\mathbf{r}\tau; \mathbf{r}'\tau') = \mathcal{G}(\mathbf{r}, \mathbf{r}'; \tau - \tau'), \quad (1.134)$$

with $\tau - \tau'$ restricted in the range of $[-\beta, \beta]$ and the factor $\beta = 1/k_B T$. Therefore, the Fourier transform is given by

$$\mathcal{G}(\mathbf{r}, \mathbf{r}'; i\omega_n) = \int_0^{\beta\hbar} d\tau e^{i\omega_n\tau} \mathcal{G}(\mathbf{r}, \mathbf{r}'; \tau), \quad (1.135)$$

$$\mathcal{G}(\mathbf{r}, \mathbf{r}'; \tau) = \frac{1}{\beta} \sum_n e^{-i\omega_n\tau} \mathcal{G}(\mathbf{r}, \mathbf{r}'; i\omega_n), \quad (1.136)$$

where the Matsubara frequency $\omega_n = (2n + 1)\pi k_B T / \hbar$ with $n = -\infty, \dots, -1, 0, 1, \dots, \infty$.

Using the equation of motion for $\psi_\sigma(\mathbf{r}, \tau)$ and $\psi_\sigma^\dagger(\mathbf{r}, \tau)$:

$$-\hbar \frac{\partial \psi_\sigma(\mathbf{r}, \tau)}{\partial \tau} = [\psi_\sigma(\mathbf{r}, \tau), \mathcal{H}_{\text{eff}}]_-, \quad (1.137)$$

$$-\hbar \frac{\partial \psi_\sigma^\dagger(\mathbf{r}, \tau)}{\partial \tau} = [\psi_\sigma^\dagger(\mathbf{r}, \tau), \mathcal{H}_{\text{eff}}]_-, \quad (1.138)$$

and Eq. (1.47), we can obtain the equation of motion for the Green's function

$$\int d\mathbf{r}'' \hat{M}(\mathbf{r}, \mathbf{r}''; \tau) \mathcal{G}(\mathbf{r}'' \tau; \mathbf{r}' \tau') = \delta(\mathbf{r} - \mathbf{r}') \delta(\tau - \tau') \hat{1}, \quad (1.139)$$

with

$$\hat{M}(\mathbf{r}, \mathbf{r}', \tau) = \begin{pmatrix} (-\frac{\partial}{\partial \tau} - h_\uparrow(\mathbf{r}))\delta(\mathbf{r} - \mathbf{r}') & -\Delta(\mathbf{r}, \mathbf{r}') \\ -\Delta^*(\mathbf{r}', \mathbf{r}) & (-\frac{\partial}{\partial \tau} + h_\downarrow^*(\mathbf{r}))\delta_{ij} \end{pmatrix}. \quad (1.140)$$

for the spin-single pairing case, and subject to the self-consistency condition:

$$\Delta(\mathbf{r}, \mathbf{r}') = -V(\mathbf{r}, \mathbf{r}') \mathcal{G}_{12}(\mathbf{r} \tau \rightarrow \tau' + 0^+, \mathbf{r}' \tau'), \quad (1.141)$$

$$\Delta^*(\mathbf{r}, \mathbf{r}') = -V(\mathbf{r}, \mathbf{r}') \mathcal{G}_{21}(\mathbf{r}' \tau \rightarrow \tau' + 0^+, \mathbf{r} \tau'). \quad (1.142)$$

Equation (1.139) is the famous Abrikosov-Gorkov equations [46] for superconductivity in the continuum model. This set of equations is also the starting point for the derivation of Ginzburg-Landau theory. When the order parameter varies slowly in space, the approximate Ginzburg-Landau theory is simpler to solve than the original Abrikosov-Gorkov theory.

The Abrikosov-Gorkov theory is closely related to the BdG theory. With the time dependence of the quasiparticle operators:

$$\gamma_n(\tau) = \gamma_n e^{-E_n \tau / \hbar}, \quad (1.143)$$

$$\gamma_n^\dagger(\tau) = \gamma_n^\dagger e^{E_n \tau / \hbar}. \quad (1.144)$$

and the canonical transformation, we can obtain for example:

$$\begin{aligned} \mathcal{G}_{11}(\mathbf{r}, \mathbf{r}'; \tau) &= -\theta(\tau) \sum_{\tilde{n}} [u_{\uparrow}^{\tilde{n}1}(\mathbf{r}) u_{\uparrow}^{\tilde{n}1*}(\mathbf{r}') f(-E_{\tilde{n}1}) e^{-E_{\tilde{n}1} \tau / \hbar} + v_{\uparrow}^{\tilde{n}2*}(\mathbf{r}) v_{\uparrow}^{\tilde{n}2}(\mathbf{r}') f(E_{\tilde{n}2}) e^{E_{\tilde{n}2} \tau / \hbar}] \\ &\quad + \theta(-\tau) \sum_{\tilde{n}} [u_{\uparrow}^{\tilde{n}1*}(\mathbf{r}') u_{\uparrow}^{\tilde{n}1}(\mathbf{r}) f(E_{\tilde{n}1}) e^{-E_{\tilde{n}1} \tau / \hbar} + v_{\uparrow}^{\tilde{n}2*}(\mathbf{r}') v_{\uparrow}^{\tilde{n}2}(\mathbf{r}) f(-E_{\tilde{n}2}) e^{E_{\tilde{n}2} \tau / \hbar}], \end{aligned} \quad (1.145)$$

and

$$\begin{aligned} \mathcal{G}_{22}(\mathbf{r}, \mathbf{r}'; \tau) = & -\theta(\tau) \sum_{\tilde{n}} [u_{\downarrow}^{\tilde{n}2*}(\mathbf{r}) u_{\downarrow}^{\tilde{n}2}(\mathbf{r}') f(E_{\tilde{n}2}) e^{E_{\tilde{n}2}\tau/\hbar} + v_{\downarrow}^{\tilde{n}1}(\mathbf{r}) v_{\downarrow}^{\tilde{n}1*}(\mathbf{r}') f(-E_{\tilde{n}1}) e^{-E_{\tilde{n}1}\tau/\hbar}] \\ & + \theta(-\tau) \sum_n [u_{\downarrow}^{\tilde{n}2}(\mathbf{r}') u_{\downarrow}^{\tilde{n}2*}(\mathbf{r}) f(-E_{\tilde{n}2}) e^{E_{\tilde{n}2}\tau/\hbar} + v_{\downarrow}^{\tilde{n}1*}(\mathbf{r}') v_{\downarrow}^{\tilde{n}1}(\mathbf{r}) f(E_{\tilde{n}1}) e^{-E_{\tilde{n}1}\tau/\hbar}]. \end{aligned} \quad (1.146)$$

It is straightforward to obtain the Green's function in the frequency domain

$$\begin{aligned} \mathcal{G}_{11}(\mathbf{r}, \mathbf{r}'; i\omega_n) &= \int_0^{\beta\hbar} d\tau e^{i\omega_n\tau} \mathcal{G}_{11}(\mathbf{r}, \mathbf{r}'; \tau) \\ &= - \sum'_{\tilde{n}} [u_{\uparrow}^{\tilde{n}1}(\mathbf{r}) u_{\uparrow}^{\tilde{n}1*}(\mathbf{r}') f(-E_{\tilde{n}1}) \int_0^{\beta\hbar} d\tau e^{(i\omega_n - E_{\tilde{n}1}/\hbar)\tau} \\ &\quad + v_{\uparrow}^{\tilde{n}2*}(\mathbf{r}) v_{\uparrow}^{\tilde{n}2}(\mathbf{r}') f(E_{\tilde{n}2}) \int_0^{\beta\hbar} d\tau e^{(i\omega_n + E_{\tilde{n}2}/\hbar)\tau}] \\ &= - \sum'_{\tilde{n}} \left\{ \frac{u_{\uparrow}^{\tilde{n}1}(\mathbf{r}) u_{\uparrow}^{\tilde{n}1*}(\mathbf{r}')}{i\omega_n - E_{\tilde{n}1}/\hbar} f(-E_{\tilde{n}1}) (e^{\beta\hbar(i\omega_n - E_{\tilde{n}1}/\hbar)} - 1) \right. \\ &\quad \left. + \frac{v_{\uparrow}^{\tilde{n}2*}(\mathbf{r}) v_{\uparrow}^{\tilde{n}2}(\mathbf{r}')}{i\omega_n + E_{\tilde{n}2}/\hbar} f(E_{\tilde{n}2}) (e^{\beta\hbar(i\omega_n + E_{\tilde{n}2}/\hbar)} - 1) \right\} \\ &= \sum'_{\tilde{n}} \left[\frac{u_{\uparrow}^{\tilde{n}1}(\mathbf{r}) u_{\uparrow}^{\tilde{n}1*}(\mathbf{r}')}{i\omega_n - E_{\tilde{n}1}/\hbar} + \frac{v_{\uparrow}^{\tilde{n}2*}(\mathbf{r}) v_{\uparrow}^{\tilde{n}2}(\mathbf{r}')}{i\omega_n + E_{\tilde{n}2}/\hbar} \right], \end{aligned} \quad (1.147)$$

and

$$\begin{aligned} \mathcal{G}_{22}(\mathbf{r}, \mathbf{r}'; i\omega_n) &= \int_0^{\beta\hbar} d\tau e^{i\omega_n\tau} \mathcal{G}_{22}(\mathbf{r}, \mathbf{r}'; \tau) \\ &= - \sum'_{\tilde{n}} [u_{\downarrow}^{\tilde{n}2*}(\mathbf{r}) u_{\downarrow}^{\tilde{n}2}(\mathbf{r}') f(E_{\tilde{n}2}) \int_0^{\beta\hbar} d\tau e^{(i\omega_n + E_{\tilde{n}2}/\hbar)\tau} \\ &\quad + v_{\downarrow}^{\tilde{n}1}(\mathbf{r}) v_{\downarrow}^{\tilde{n}1*}(\mathbf{r}') f(-E_{\tilde{n}1}) \int_0^{\beta\hbar} d\tau e^{(i\omega_n + E_{\tilde{n}1}/\hbar)\tau}] \\ &= - \sum'_{\tilde{n}} \left\{ \frac{u_{\downarrow}^{\tilde{n}2*}(\mathbf{r}) u_{\downarrow}^{\tilde{n}2}(\mathbf{r}')}{i\omega_n + E_{\tilde{n}2}/\hbar} f(E_{\tilde{n}2}) (e^{\beta\hbar(i\omega_n + E_{\tilde{n}2}/\hbar)} - 1) \right. \end{aligned}$$

$$\begin{aligned}
& + \frac{v_{\downarrow}^{\tilde{n}1}(\mathbf{r})v_{\downarrow}^{\tilde{n}1*}(\mathbf{r}')}{i\omega_n - E_{\tilde{n}1}/\hbar} f(E_{\tilde{n}1}) (e^{\beta\hbar(i\omega_n - E_{\tilde{n}1}/\hbar)} - 1) \Big\} \\
& = \sum'_{\tilde{n}} \left[\frac{u_{\downarrow}^{\tilde{n}2*}(\mathbf{r})u_{\downarrow}^{\tilde{n}2}(\mathbf{r}')}{i\omega_n + E_{\tilde{n}2}/\hbar} + \frac{v_{\downarrow}^{\tilde{n}1}(\mathbf{r})v_{\downarrow}^{\tilde{n}1*}(\mathbf{r}')}{i\omega_n - E_{\tilde{n}1}/\hbar} \right]. \quad (1.148)
\end{aligned}$$

Here we have used the fact that

$$e^{i\omega_n\beta\hbar} = -1. \quad (1.149)$$

In addition, if we know the solution to the Abrikosov-Gorkov equations of motion for the Green's functions, the local density of states can be calculated as

$$\begin{aligned}
\rho_{\uparrow}(\mathbf{r}, E) &= -\frac{1}{\hbar\pi} \text{Im}[\mathcal{G}_{11}(\mathbf{r}, \mathbf{r}; i\omega_n \rightarrow E/\hbar + i0^+)] \\
&= \sum'_{\tilde{n}} [|u_{\uparrow}^{\tilde{n}1}(\mathbf{r})|^2 \delta(E - E_{\tilde{n}1}) + |v_{\uparrow}^{\tilde{n}2}(\mathbf{r})|^2 \delta(E + E_{\tilde{n}2})], \quad (1.150)
\end{aligned}$$

and

$$\begin{aligned}
\rho_{\downarrow}(\mathbf{r}, E) &= \frac{1}{\hbar\pi} \text{Im}[\mathcal{G}_{22}(\mathbf{r}, \mathbf{r}; -i\omega_n \rightarrow -(E/\hbar + i0^+))] \\
&= \sum'_{\tilde{n}} [|u_{\downarrow}^{\tilde{n}2}(\mathbf{r})|^2 \delta(E - E_{\tilde{n}2}) + |v_{\downarrow}^{\tilde{n}1}(\mathbf{r})|^2 \delta(E + E_{\tilde{n}2})]. \quad (1.151)
\end{aligned}$$

Here we have used the following identity for the real frequency ω

$$\frac{1}{\omega \pm i0^+} = \mathcal{P} \frac{1}{\omega} \mp i\pi\delta(\omega), \quad (1.152)$$

with \mathcal{P} denotes a Cauchy principal value. Therefore, we have demonstrated an exact relation between the BdG theory and the Abrikosov-Gorkov theory.

References

1. J. Hubbard, Proc. R. Soc. (Lond.) **A276**, 238 (1963)
2. F. Gebhard, *The Mott Metal-Insulator Transition: Models and Methods* (Springer, Berlin, 1997)
3. E. Abrahams, P.W. Anderson, D.C. Licciardello, T.V. Ramakrishnan. Phys. Rev. Lett. **42**, 673 (1979)
4. B.L. Altshuler, P.A. Lee, R.A. Webb (eds.), *Mesoscopic Phenomena in Solids* (Elsevier, Amsterdam, 1991)
5. E. Abrahams, *50 Years of Anderson Localization* (World Scientific, Singapore, 2010)

6. A. Tsukada et al., *Solid State Commun.* **133**, 427 (2005)
7. L.N. Cooper, *Phys. Rev.* **104**, 1189 (1956)
8. J. Bardeen, L.N. Cooper, J.R. Schrieffer, *Phys. Rev.* **108**, 1175 (1957)
9. P.G. de Gennes, *Superconductivity of Metals and Alloys* (W.A. Benjamin, New York, 1966)
10. M. Born, J.R. Oppenheimer, *Ann. Phys.* **84**, 457 (1927)
11. R.M. Martin, *Electronic Structure: Basic Theory and Practical Methods* (Cambridge University Press, Cambridge, 2004)
12. W. Kohn, L.J. Sham, *Phys. Rev.* **137**, A1441 (1965)
13. P. Hohenberg, W. Kohn, *Phys. Rev.* **136**, B864 (1964)
14. J.P. Perdew, *MRS Bull.* **38**, 743 (2013)
15. E. Fradkin, *Field Theories of Condensed Matter Systems* (Addison-Wesley, Redwood City, 1991)
16. A. Auerbach, *Interacting Electrons and Quantum Magnetism* (Springer, Berlin, 1994)
17. A.L. Fetter, J.D. Walecka, *Quantum Theory of Many-Particle Systems* (McGraw-Hill, New York, 1971)
18. G.D. Mahan, *Many-Particle Physics*, 3rd edn. (Kluwer Academic/Plenum, New York, 2000)
19. A. Hewson, *The Kondo Problem to Heavy Fermions* (Cambridge University Press, Cambridge, 1993)
20. A. Georges, G. Kotliar, W. Krauth, M. Rozenberg, *Rev. Mod. Phys.* **68**, 13 (1996)
21. G. Kotliar, S. Savrasov, V. Oudovenko, O. Parcolet, C. Marianetti, *Rev. Mod. Phys.* **78**, 865 (2006)
22. K. Held, *Adv. Phys.* **56**, 829 (2007)
23. V. Anisimov, Y. Izyumov, *Electronic Structure of Strongly Correlated Materials* (Springer, Berlin, 2010)
24. A.R. Bishop, P.S. Lomdahl, J.R. Schrieffer, S.A. Trugman, *Phys. Rev. Lett.* **61**, 2709 (1988)
25. N.N. Bogoliubov, *Sov. Phys. -JETP* **7**, 41 (1958)
26. J.G. Valatin, *Nuovo Cimento* **7**, 843 (1958)
27. C. Bruder, *Phys. Rev. B* **41**, 4017 (1990)
28. R.D. Parks, *Superconductivity* (Dekker, New York, 1969)
29. P.A. Lee, N. Nagaosa, X.-G. Wen, *Rev. Mod. Phys.* **78**, 17 (2006)
30. P.J. Hirschfeld, M.M. Korshunov, I.I. Mazin, *Rep. Prog. Phys.* **74**, 124508 (2011)
31. J.D. Thompson, Z. Fisk, *J. Phys. Soc. Jpn.* **81**, 011002 (2012)
32. J. L. Sarrao et al., *Nature* **420**, 297 (2002)
33. N.J. Curro et al., *Nature* **434**, 622 (2005)
34. E.I. Bount, *Phys. Rev. B* **32**, 2935 (1985)
35. K. Ueda, T.M. Rice, *Phys. Rev. B* **31**, 7114 (1985)
36. P.W. Anderson, W.F. Brinkman, in *The Physics of Liquid and Solid Helium*, ed. by K.H. Bennemann, J.B. Ketterson (Wiley, New York, 1978)
37. K. Ishida et al., *Nature* **396**, 658 (1998)
38. C.M. Varma, in *Moment Formation in Solids*, ed. by W. J. L. Buyers (Plenum, New York, 1984)
39. H.R. Ott et al., *Phys. Rev. Lett.* **52**, 1915 (1984)
40. P.W. Anderson, *Phys. Rev. B* **30**, 1549 (1984)
41. D. Vollhardt, P. Wölfle, *The Superfluid Phases of Helium 3* (Taylor and Francis, London, 1990)
42. R. Balian, N.R. Werthamer, *Phys. Rev.* **131**, 1553 (1963)
43. P.W. Anderson, P. Morel, *Phys. Rev.* **123**, 1911 (1961)
44. Y. Nambu, *Phys. Rev.* **117**, 648 (1960)
45. J.R. Schrieffer, *The Theory of Superconductivity* (Benjamin, New York, 1964)
46. A.A. Abrikosov, L.P. Gorkov, I.E. Dzyaloshinski, *Methods of Quantum Field Theory in Statistical Physics* (Dover Publications, New York, 1963)

Chapter 2

BdG Equations in Tight-Binding Model

Abstract In this chapter, I give an alternative derivation of the Bogoliubov-de Gennes equations for superconductors. It is based on a tight-binding model. A general symmetry of the equations is discussed. A few physically measurable quantities are derived in terms of the BdG eigenfunctions. The solutions to the BdG equations in the uniform case are provided. Finally, I also make its connection to the lattice Abrikosov-Gorkov equations.

2.1 Derivation of BdG Equations in a Tight-Bind Model

In the previous chapter, we have derived the BdG equations in the continuum model. The continuum model is reasonable to describe weak-coupling superconductors, especially when they have a wide-band metallic normal state. For the superconductors like high-temperature cuprates, the electronic band is quite narrow. Therefore, as we are encountered in solid state physics [1], the tight-binding model, either constructed from atomic orbitals or from Wannier orbitals, is appropriate to be used for studying narrow band behaviors arising from electronic correlation effects.

We generalize the second-quantized Hamiltonian given by Eq. (1.38) to include the spin-orbit coupling and spin-flip scattering interactions, in addition to the regular potential scattering. The single-particle part of the Hamiltonian is of the form:

$$H_0 = \int \int d\mathbf{r}d\mathbf{r}' \psi_\alpha^\dagger(\mathbf{r})h_{\alpha\beta}(\mathbf{r}, \mathbf{r}')\psi_\beta(\mathbf{r}') \quad (2.1)$$

where $h_{\alpha\beta}(\mathbf{r}, \mathbf{r}')$ is general enough to include the non-local and spin-flip effects. The field operators are now expressed in the localized-state basis as

$$\psi_\alpha(\mathbf{r}) = \sum_i w(\mathbf{r} - \mathbf{R}_i)c_{i\alpha} \quad (2.2a)$$

$$\psi_\alpha^\dagger(\mathbf{r}) = \sum_i w^*(\mathbf{r} - \mathbf{R}_i)c_{i\alpha}^\dagger \quad (2.2b)$$

where $c_{i\alpha}^\dagger$ ($c_{i\alpha}$) creates (annihilates) an electron of spin α at site i , and $w(\mathbf{r} - \mathbf{R}_i)$ is a localized orbital around the atomic site \mathbf{R}_i . The atomic orbitals or maximally localized Wannier orbitals are most amenable to have a physical interpretation. Substitution of these expressions into Eq. (2.1) gives

$$\begin{aligned} H_0 &= \sum_{ij, \sigma\sigma'} c_{i\sigma}^\dagger h_{i\sigma, j\sigma'} c_{j\sigma} \\ &= - \sum_{i \neq j, \sigma\sigma'} t_{i\sigma, j\sigma'} c_{i\sigma}^\dagger c_{j\sigma'} + \sum_{i\sigma} \epsilon_i c_{i\sigma}^\dagger c_{i\sigma} + \sum_{i, \sigma\sigma'} \Omega_{i, \sigma\sigma'} c_{i\sigma}^\dagger c_{i\sigma'}. \end{aligned} \quad (2.3)$$

Here the summation over the site indices ij in the kinetic energy (and also the nearest-neighbor interaction in Eq. 2.4 below) excludes those term with $i = j$. In the kinetic energy, the spin-orbit term has also been included by identifying the spin flip when an electron hops from one site to its nearest neighbor. The on-site single particle energy is introduced to consider the disorder or such inhomogeneity problems as those with a (non-magnetic) single impurity; while the third term accounts for the magnetic impurity effects (with the internal dynamics of the magnetic impurity neglected here).

We then follow the same ansatz for the extended Hubbard model [2], and write down an effective model Hamiltonian for superconductivity:

$$\begin{aligned} \mathcal{H} &= H_0 - \mu \sum_{i\sigma} c_{i\sigma}^\dagger c_{i\sigma} + U \sum_i \left(n_{i\uparrow} - \frac{1}{2} \right) \left(n_{i\downarrow} - \frac{1}{2} \right) - \frac{V}{2} \sum_{i \neq j} n_i n_j \\ &= \sum_{ij, \sigma\sigma'} c_{i\sigma}^\dagger \left[h_{i\sigma, j\sigma'} - \left(\mu + \frac{U}{2} \right) \delta_{ij} \delta_{\sigma\sigma'} \right] c_{j\sigma'} + U \sum_i n_{i\uparrow} n_{i\downarrow} - \frac{V}{2} \sum_{i \neq j} n_i n_j. \end{aligned} \quad (2.4)$$

Here $n_i = \sum_{\sigma} n_{i\sigma}$ with $n_{i\sigma} = c_{i\sigma}^\dagger c_{i\sigma}$ is the particle number operator on site i . The on-site and nearest-neighbor electron-electron interaction strengths are, respectively, U and V . Positive values of U and negative values of V represent the repulsive interaction while negative values of U and positive values of V represent the attractive interaction since we have assigned a minus sign before the nearest-neighbor interaction term. Note that the single particle energy is measured with respect to the chemical potential μ .

The derivation of the BdG equations for the on-site and nearest-neighbor pairing interaction is similar to that for the continuum model in Chap. 1. To be distinct, the above extended Hubbard model enables a description of possible competing orders. We show one example here by considering on-site repulsion ($U > 0$), which drives magnetic instability, and nearest-neighbor attraction ($V > 0$) for the d -wave pairing superconductivity. Therefore, we retain the standard Hartree-Fock term for the onsite repulsion and the anomalous Hartree-Fock terms for nearest-neighbor attraction. The inclusion of an onsite repulsion in the mean-field approximation

helps stabilize the d -wave pairing state, which comes from the nearest-neighbor pairing interaction. The effective mean-field Hamiltonian with a singlet pairing symmetry is now given by:

$$\mathcal{H}_{eff} = \sum_{ij, \sigma\sigma'} c_{i\sigma}^\dagger \tilde{h}_{i\sigma, j\sigma'} c_{j\sigma'} + \sum_{ij} [\Delta_{ij} c_{i\uparrow}^\dagger c_{j\downarrow}^\dagger + \Delta_{ij}^* c_{j\downarrow} c_{i\uparrow}] + E_{const}. \quad (2.5)$$

Here the effective single-particle Hamiltonian is given by

$$\tilde{h}_{i\sigma, j\sigma'} = h_{i\sigma, j\sigma'} - \left(\mu + \frac{U}{2} - U \langle n_{i\bar{\sigma}} \rangle \right) \delta_{ij} \delta_{\sigma\sigma'}, \quad (2.6)$$

the singlet-pairing potential

$$\Delta_{ij} = \frac{V}{2} \left(\langle c_{i\uparrow} c_{j\downarrow} \rangle - \langle c_{i\downarrow} c_{j\uparrow} \rangle \right), \quad (2.7)$$

$$\Delta_{ij}^* = \frac{V}{2} \left(\langle c_{j\downarrow}^\dagger c_{i\uparrow}^\dagger \rangle - \langle c_{j\uparrow}^\dagger c_{i\downarrow}^\dagger \rangle \right), \quad (2.8)$$

and the constant energy term is given by

$$E_{const} = -U \langle n_{i\uparrow} \rangle \langle n_{i\downarrow} \rangle + \sum_{ij} \frac{|\Delta_{ij}|^2}{V}. \quad (2.9)$$

It is evident that the singlet pairing potential satisfies the symmetry properties: $\Delta_{ji} = \Delta_{ij}$. Also we note again that the single particle energy is measured with respect to the chemical potential μ .

We then obtain the following commutation relations:

$$[c_{i\uparrow}, \mathcal{H}_{eff}]_- = \sum_{j\sigma'} \tilde{h}_{i\uparrow, j\sigma'} c_{j\sigma'} + \sum_j \Delta_{ij} c_{j\downarrow}^\dagger, \quad (2.10a)$$

$$[c_{i\uparrow}^\dagger, \mathcal{H}_{eff}]_- = - \sum_{j\sigma'} \tilde{h}_{j\sigma', i\uparrow} c_{j\sigma'}^\dagger - \sum_j \Delta_{ij}^* c_{j\downarrow}, \quad (2.10b)$$

$$[c_{i\downarrow}, \mathcal{H}_{eff}]_- = \sum_{j\sigma'} \tilde{h}_{i\downarrow, j\sigma'} c_{j\sigma'} - \sum_j \Delta_{ji} c_{j\uparrow}^\dagger, \quad (2.10c)$$

$$[c_{i\downarrow}^\dagger, \mathcal{H}_{eff}]_- = - \sum_{j\sigma'} \tilde{h}_{j\sigma', i\downarrow} c_{j\sigma'}^\dagger + \sum_j \Delta_{ji}^* c_{j\uparrow}. \quad (2.10d)$$

Equations (2.10)(a)–(d) show that the electron field operator can be expressed as a linear combination of electron- and hole-like quasiparticle excitations, which

enables us to perform a Bogoliubov canonical transformation:

$$c_{i\sigma} = \sum_n' (u_{i\sigma}^n \gamma_n - \sigma v_{i\sigma}^{n*} \gamma_n^\dagger), \quad c_{i\sigma}^\dagger = \sum_n' (u_{i\sigma}^{n*} \gamma_n^\dagger - \sigma v_{i\sigma}^n \gamma_n), \quad (2.11)$$

where $\sigma = \pm 1$ denotes the up and down spin orientations. The operators γ_n^\dagger (γ_n) create (annihilate) a Bogoliubov quasiparticle at state n . The prime sign above the summation in the transformation means only those states with positive energy are counted. The quasiparticle operators satisfy the anti-commutation relations:

$$\{\gamma_n, \gamma_m^\dagger\} = \delta_{nm}, \quad (2.12)$$

$$\{\gamma_n, \gamma_m\} = \{\gamma_n^\dagger, \gamma_m^\dagger\} = 0. \quad (2.13)$$

These relations also guarantee the anti-commutation relations among the original electronic field operators.

With the above canonical transformation, the Hamiltonian is diagonalized in the following form:

$$H_{eff} = \sum_n E_n \gamma_n^\dagger \gamma_n + E'_{const}, \quad (2.14)$$

where the index n also includes the pseudo-spin state index. Upon substitution of Eq. (2.11) into Eq. (2.10), and with the aid of the following commutation relations,

$$[\gamma_n^\dagger, H_{eff}]_- = -E_n \gamma_n^\dagger, \quad (2.15)$$

$$[\gamma_n, H_{eff}]_- = E_n \gamma_n, \quad (2.16)$$

we compare the coefficients of the terms with γ_n and γ_n^\dagger and arrive at

$$E_n u_{i\uparrow}^n = \sum_{j\sigma'} \tilde{h}_{i\uparrow, j\sigma'} u_{j\sigma'} + \sum_j \Delta_{ij} v_{j\downarrow}^n, \quad (2.17)$$

$$E_n u_{i\downarrow}^n = \sum_{j\sigma'} \tilde{h}_{i\downarrow, j\sigma'} u_{j\sigma'} + \sum_j \Delta_{ji} v_{j\uparrow}^n, \quad (2.18)$$

$$E_n v_{i\uparrow}^n = -\sum_{j\sigma'} \sigma' \tilde{h}_{i\uparrow, j\sigma'}^* v_{j\sigma'} + \sum_j \Delta_{ij}^* u_{j\downarrow}^n, \quad (2.19)$$

$$E_n v_{i\downarrow}^n = \sum_{j\sigma'} \sigma' \tilde{h}_{i\downarrow, j\sigma'}^* v_{j\sigma'} + \sum_j \Delta_{ji}^* u_{j\uparrow}^n. \quad (2.20)$$

This set of BdG equations can be cast into a matrix form:

$$\sum_j \hat{M}_{ij} \hat{\phi}_j = E_n \hat{\phi}_i, \quad (2.21)$$

where

$$\hat{M}_{ij} = \begin{bmatrix} \tilde{h}_{i\uparrow j\uparrow} & \tilde{h}_{i\uparrow j\downarrow} & 0 & \Delta_{ij} \\ \tilde{h}_{i\downarrow j\uparrow} & \tilde{h}_{i\downarrow j\downarrow} & \Delta_{ji} & 0 \\ 0 & \Delta_{ij}^* & -\tilde{h}_{i\uparrow j\uparrow}^* & \tilde{h}_{i\uparrow j\downarrow}^* \\ \Delta_{ji}^* & 0 & \tilde{h}_{i\downarrow j\uparrow}^* & -\tilde{h}_{i\downarrow j\downarrow}^* \end{bmatrix}, \quad (2.22)$$

and

$$\hat{\phi}_i = \begin{pmatrix} u_{i\uparrow} \\ u_{i\downarrow} \\ v_{i\uparrow} \\ v_{i\downarrow} \end{pmatrix}. \quad (2.23)$$

This set of BdG equations is subjected to the self-consistency conditions:

$$n_{i\uparrow} = \sum_n' [|u_{i\uparrow}^n|^2 f(E_n) + |v_{i\uparrow}^n|^2 f(-E_n)], \quad (2.24)$$

$$n_{i\downarrow} = \sum_n' [|u_{i\downarrow}^n|^2 f(E_n) + |v_{i\downarrow}^n|^2 f(-E_n)], \quad (2.25)$$

and

$$\Delta_{ij} = \frac{V}{4} \sum_n' [(u_{i\uparrow}^n v_{j\downarrow}^{n*} + u_{j\downarrow}^n v_{i\uparrow}^{n*}) + (u_{i\downarrow}^n v_{j\uparrow}^{n*} + u_{j\uparrow}^n v_{i\downarrow}^{n*})] \tanh\left(\frac{E_n}{2k_B T}\right), \quad (2.26)$$

where $f(E)$ is the Fermi-Dirac distribution function defined in Eq. (1.72).

From Eqs. (2.17)–(2.20), it is not difficult to prove the following theorem: If $(u_{i\uparrow}^n, v_{i\downarrow}^n, u_{i\downarrow}^n, v_{i\uparrow}^n)$ is the solution to the BdG equations with eigenvalue E_n , then $(-v_{i\uparrow}^{n*}, u_{i\downarrow}^{n*}, v_{i\downarrow}^{n*}, -u_{i\uparrow}^{n*})$ is the solution to the same equations with eigenvalue $-E_n$. Using this symmetry property, we can also rewrite Eqs. (2.24)–(2.26) as

$$n_{i\uparrow} = \sum_n |u_{i\uparrow}^n|^2 f(E_n), \quad (2.27)$$

$$n_{i\downarrow} = \sum_n |v_{i\downarrow}^n|^2 f(-E_n), \quad (2.28)$$

and

$$\Delta_{ij} = \frac{V}{4} \sum_n [u_{i\uparrow}^n v_{j\downarrow}^{n*} + u_{j\uparrow}^n v_{i\downarrow}^{n*}] \tanh\left(\frac{E_n}{2k_B T}\right). \quad (2.29)$$

In the absence of spin-orbit coupling and other spin-flip scattering terms, that is $\tilde{h}_{i\uparrow,j\downarrow} = \tilde{h}_{i\downarrow,j\uparrow} = 0$, the BdG equations become block-diagonalized into two sets of equations:

$$\begin{cases} E_{\tilde{n}1} u_{i\uparrow}^{\tilde{n}1} = \sum_j \tilde{h}_{i\uparrow,j\uparrow} u_{j\uparrow}^{\tilde{n}1} + \sum_j \Delta_{ij} v_{j\downarrow}^{\tilde{n}1}, \\ E_{\tilde{n}1} v_{i\downarrow}^{\tilde{n}1} = -\sum_j \tilde{h}_{i\downarrow,j\downarrow}^* v_{j\downarrow}^{\tilde{n}1} + \sum_j \Delta_{ji}^* u_{j\uparrow}^{\tilde{n}1}, \end{cases} \quad (2.30)$$

and

$$\begin{cases} E_{\tilde{n}2} u_{i\downarrow}^{\tilde{n}2} = \sum_j \tilde{h}_{i\downarrow,j\downarrow} u_{j\downarrow}^{\tilde{n}2} + \sum_j \Delta_{ji} v_{j\uparrow}^{\tilde{n}2}, \\ E_{\tilde{n}2} v_{i\uparrow}^{\tilde{n}2} = -\sum_j \tilde{h}_{i\uparrow,j\uparrow}^* v_{j\uparrow}^{\tilde{n}2} + \sum_j \Delta_{ij}^* u_{j\downarrow}^{\tilde{n}2}. \end{cases} \quad (2.31)$$

This block-diagonalization structure leads to a distinct nature of the canonical transformation:

$$c_{i\uparrow} = \sum_{\tilde{n}} (u_{i\uparrow}^{\tilde{n}1} \gamma_{\tilde{n}1} - v_{i\uparrow}^{\tilde{n}2*} \gamma_{\tilde{n}2}^\dagger), \quad c_{i\uparrow}^\dagger = \sum_{\tilde{n}} (u_{i\uparrow}^{\tilde{n}1*} \gamma_{\tilde{n}1}^\dagger - v_{i\uparrow}^{\tilde{n}2} \gamma_{\tilde{n}2}), \quad (2.32)$$

$$c_{i\downarrow} = \sum_{\tilde{n}} (u_{i\downarrow}^{\tilde{n}2} \gamma_{\tilde{n}2} + v_{i\downarrow}^{\tilde{n}1*} \gamma_{\tilde{n}1}^\dagger), \quad c_{i\downarrow}^\dagger = \sum_{\tilde{n}} (u_{i\downarrow}^{\tilde{n}2*} \gamma_{\tilde{n}2}^\dagger + v_{i\downarrow}^{\tilde{n}1} \gamma_{\tilde{n}1}). \quad (2.33)$$

The block diagonalization and the symmetry property suggest that we merely need to solve Eq. (2.30) subject to the self-consistency condition:

$$n_{i\uparrow} = \sum_{\tilde{n}} |u_{i\uparrow}^{\tilde{n}1}|^2 f(E_{\tilde{n}1}), \quad (2.34)$$

$$n_{i\downarrow} = \sum_{\tilde{n}} |v_{i\downarrow}^{\tilde{n}1}|^2 f(-E_{\tilde{n}1}), \quad (2.35)$$

and

$$\Delta_{ij} = \frac{V}{4} \sum_{\tilde{n}} [u_{i\uparrow}^{\tilde{n}1} v_{j\downarrow}^{\tilde{n}1*} + u_{j\uparrow}^{\tilde{n}1} v_{i\downarrow}^{\tilde{n}1*}] \tanh\left(\frac{E_{\tilde{n}1}}{2k_B T}\right). \quad (2.36)$$

Therefore, by reducing the diagonalization of a $4N$ by $4N$ matrix down to that of a $2N$ by $2N$ matrix, the computational efficiency is improved significantly. Here N would be $N_x N_y$ for a two-dimensional lattice while $N_x N_y N_z$ for a three-dimensional lattice with N_x , N_y , and N_z being the linear dimension of the system. When it is obvious that no spin-flip effect occurs, the reduced set of BdG equations, Eq. (2.30), will be used with the hat symbol on the energy eigenvalue index and the set index dropped. It will be encountered frequently in the later discussions.

It is straightforward for us to obtain the BdG equations for an s -wave superconductor in the lattice model. There we first replace U by $-U$ ($U > 0$) so that the Hamiltonian becomes

$$\mathcal{H} = \sum_{ij,\sigma\sigma'} c_{i\sigma}^\dagger \left[h_{i\sigma,j\sigma'} - \mu \delta_{ij} \delta_{\sigma\sigma'} \right] c_{j\sigma'} - U \sum_i n_{i\uparrow} n_{i\downarrow}, \quad (2.37)$$

which leads to the BdG equations:

$$E_n u_{i\uparrow}^n = \sum_{j\sigma'} \tilde{h}_{i\uparrow,j\sigma'} u_{j\sigma'}^n + \Delta_{ii} v_{i\downarrow}^n, \quad (2.38)$$

$$E_n u_{i\downarrow}^n = \sum_{j\sigma'} \tilde{h}_{i\downarrow,j\sigma'} u_{j\sigma'}^n + \Delta_{ii} v_{i\uparrow}^n, \quad (2.39)$$

$$E_n v_{i\uparrow}^n = - \sum_{j\sigma'} \sigma' \tilde{h}_{i\uparrow,j\sigma'}^* v_{j\sigma'}^n + \Delta_{ii}^* u_{j\downarrow}^n, \quad (2.40)$$

$$E_n v_{i\downarrow}^n = \sum_{j\sigma'} \sigma' \tilde{h}_{i\downarrow,j\sigma'}^* v_{j\sigma'}^n + \Delta_{ii}^* u_{i\uparrow}^n. \quad (2.41)$$

Here

$$\tilde{h}_{i\sigma,j\sigma'} = h_{i\sigma,j\sigma'} - \mu \delta_{ij} \delta_{\sigma\sigma'}, \quad (2.42)$$

and the self-consistency condition

$$\Delta_{ii} = \frac{U}{2} \sum_n' [u_{i\uparrow}^n v_{i\downarrow}^{n*} + u_{i\downarrow}^n v_{i\uparrow}^{n*}] \tanh\left(\frac{E_n}{2k_B T}\right). \quad (2.43)$$

In the absence of spin-orbit coupling and spin-flip scattering, the BdG equations become

$$\begin{cases} E_{\tilde{n}1} u_{i\uparrow}^{\tilde{n}1} = \sum_j \tilde{h}_{i\uparrow,j\uparrow} u_{j\uparrow}^{\tilde{n}1} + \Delta_{ii} v_{i\downarrow}^{\tilde{n}1}, \\ E_{\tilde{n}1} v_{i\downarrow}^{\tilde{n}1} = - \sum_j \tilde{h}_{i\downarrow,j\downarrow}^* v_{j\downarrow}^{\tilde{n}1} + \Delta_{ii}^* u_{i\uparrow}^{\tilde{n}1}, \end{cases} \quad (2.44)$$

and

$$\begin{cases} E_{\tilde{n}2} u_{i\downarrow}^{\tilde{n}2} = \sum_j \tilde{h}_{i\downarrow,j\downarrow} u_{j\downarrow}^{\tilde{n}2} + \Delta_{ii} v_{i\uparrow}^{\tilde{n}2}, \\ E_{\tilde{n}2} v_{i\uparrow}^{\tilde{n}2} = - \sum_j \tilde{h}_{i\uparrow,j\uparrow}^* v_{j\uparrow}^{\tilde{n}2} + \Delta_{ii}^* u_{i\downarrow}^{\tilde{n}2}. \end{cases} \quad (2.45)$$

with

$$\Delta_{ii} = \frac{U}{2} \sum_{\tilde{n}} u_{i\uparrow}^{\tilde{n}1} v_{i\downarrow}^{\tilde{n}1*} \tanh\left(\frac{E_{\tilde{n}1}}{2k_B T}\right). \quad (2.46)$$

Unless explicitly specified, we will focus on Eq. (2.44) with the tilde on the eigen-energy index and set index dropped.

The tight-binding model, from which the BdG equations are derived, has the origin from such strongly correlated models as the t - J model [3] for high-temperature cuprates. The derived BdG equations in the tight-binding model have been used not only for unconventional superconductors with narrow electron band [4–9] but also for s -wave superconductors [10]. The calculated quantities range from the local density states to the superfluid density, which will be discussed in more details in later chapters.

2.1.1 Local Density of States and Bond Current in the Lattice Model

From Eqs. (2.24), (2.25), we extract the expression for the local density of states:

$$\rho_{i\sigma}(E) = \sum_n' [|u_{i\sigma}^n|^2 \delta(E_n - E) + |v_{i\sigma}|^2 \delta(E_n + E)] . \quad (2.47)$$

and the corresponding thermalized density of states

$$\rho_{i\sigma}(E) = - \sum_n' [|u_{i\sigma}^n|^2 f'(E_n - E) + |v_{i\sigma}|^2 f'(E_n + E)] . \quad (2.48)$$

The bond current can be derived in the following way. The Heisenberg equation of motion for $\langle n_i \rangle = \langle n_{i\uparrow} \rangle + \langle n_{i\downarrow} \rangle$ is:

$$\begin{aligned} i\hbar \frac{\partial \langle n_i \rangle}{\partial t} &= \langle [n_i, H]_- \rangle \\ &= \langle \{ - \sum_{j \neq i, \sigma, \sigma'} [-t(j\sigma', i\sigma) c_{j\sigma'}^\dagger c_{i\sigma} + t(i\sigma, j\sigma') c_{i\sigma}^\dagger c_{j\sigma'}] \} \rangle , \end{aligned} \quad (2.49)$$

where H is the system Hamiltonian given by Eq. (2.4). The electrical current operator from site j to site i is then found to be:

$$\hat{J}_{ij} = \frac{e}{i\hbar} \sum_{\sigma, \sigma'} [t(i\sigma, j\sigma') c_{i\sigma}^\dagger c_{j\sigma'} - t(j\sigma', i\sigma) c_{j\sigma'}^\dagger c_{i\sigma}] , \quad (2.50)$$

and the average bond current is given by:

$$J_{ij} = \frac{e}{i\hbar} \sum_{\sigma, \sigma'} \sum_n^l \{t(i\sigma, j\sigma') [u_{i\sigma}^{n*} u_{j\sigma'}^n f(E_n) + \sigma\sigma' v_{i\sigma}^n v_{j\sigma'}^{n*} (1 - f(E_n))] - \text{c.c.}\} . \quad (2.51)$$

Using the symmetry property of the BdG equations, we can also write the physical quantities in the following form:

$$n_{i\sigma} = \sum_n |u_{i\sigma}^n|^2 f(E_n) = \sum_n |v_{i\sigma}^n|^2 [1 - f(E_n)] , \quad (2.52)$$

$$\begin{aligned} J_{ij} &= \frac{e}{i\hbar} \sum_{\sigma, \sigma'} \sum_n \{t(i\sigma, j\sigma') u_{i\sigma}^{n*} u_{j\sigma'}^n f(E_n) - \text{c.c.}\} \\ &= \frac{e}{i\hbar} \sum_{\sigma, \sigma'} \sum_n \{t(i\sigma, j\sigma') \sigma\sigma' v_{i\sigma}^n v_{j\sigma'}^{n*} (1 - f(E_n)) - \text{c.c.}\} , \end{aligned} \quad (2.53)$$

and

$$\rho_{i\sigma}(E) = - \sum_n |u_{i\sigma}^n|^2 f'(E_n - E) = - \sum_n |v_{i\sigma}^n|^2 f'(E_n + E) . \quad (2.54)$$

These new formulations are especially useful when we study the ferromagnetic impurity or Zeeman effect because the wavefunction of quasiparticles can be solved in a 2×2 spin space.

2.1.2 Optical Conductivity and Superfluid Density in the Lattice Model

The BdG solutions can not only describe the local density of states, which is a direct measure of single particle properties, but also the eigenfunctions can be used to study the two-particle correlations. In particular, the optical superconductivity reveals the information about the coherent peak [11], while the superfluid stiffness [12] and its temperature dependence set a criterion for superconductivity. Both quantities are directly measurable in experiments. Theoretically, the formulae for these quantities, as derived from the BdG method, are also valid for inhomogeneous superconductors.

The formula of the superfluid density in a lattice model was first derived by Scalapino et al. [12, 13] in a Hubbard model. It was then used for calculations in other models. In the following, we give the derivation for the model with the Hamiltonian defined by Eq.(2.4) in the absence of spin-orbit coupling and other spin-flip scattering, that is,

$$\mathcal{H} = \sum_{ij, \sigma} c_{i\sigma}^\dagger \left[-t_{ij} - \left(\mu + \frac{U}{2} - U_i^{\text{imp}} \right) \delta_{ij} \right] c_{j\sigma} + U \sum_i n_{i\uparrow} n_{i\downarrow} - \frac{V}{2} \sum_{i \neq j} n_i n_j .$$

$$(2.55)$$

Here the impurity potential is represented by U_i^{imp} .

In the presence of an electric field pointing to the x -direction,

$$E_x(\mathbf{r}_i, t) = \mathcal{E}_x e^{i(\mathbf{q}\cdot\mathbf{r}_i - \omega t)} . \quad (2.56)$$

The current density along the x -direction is defined as

$$J_x(\mathbf{r}_i, t) = \sigma_{xx}(\mathbf{r}_i, \omega) E_x(\mathbf{r}_i, t) , \quad (2.57)$$

where $\sigma_{xx}(\mathbf{r}_i, \omega)$ is the local conductivity. In the Coulomb gauge, which dictates $\nabla \cdot \mathbf{A} = 0$ and the scalar potential $\phi = 0$, the electric field can be expressed in terms of a vector potential

$$A_x(\mathbf{r}_i, t) = -\frac{i}{\omega} E_x(\mathbf{r}_i, t) . \quad (2.58)$$

Therefore, the total Hamiltonian becomes

$$H_t = -\sum_{ij,\sigma} \tilde{t}_{ij} c_{i\sigma}^\dagger c_{j\sigma} + \sum_{i\sigma} (U_i^{\text{imp}} - \frac{U}{2} - \mu) c_{i\sigma}^\dagger c_{i\sigma} + U \sum_i n_{i\uparrow} n_{i\downarrow} - \frac{V}{2} \sum_{ij} n_i n_j . \quad (2.59)$$

where

$$\tilde{t}_{ij} = t_{ij} e^{i\phi_{ij}(t)} , \quad (2.60)$$

with the gauge phase $\phi_{ij}(t) = eA_{ij} = eA_x(\mathbf{r}_i, t)(x_i - x_j)$. Hereafter the charge e for electrons includes the sign. In the linear response limit, we expand this hopping term up to the second order of $A_x(\mathbf{r}_i, t)$:

$$\tilde{t}_{ij} \approx t[1 + i\phi_{ij} + \frac{1}{2!}(i\phi_{ij})^2] . \quad (2.61)$$

The total Hamiltonian can then be rewritten as:

$$H_t = H - i \sum_{ij,\sigma} \phi_{ij}(t) t_{ij} c_{i\sigma}^\dagger c_{j\sigma} + \frac{1}{2} \sum_{ij,\sigma} \phi_{ij}^2(t) t_{ij} c_{i\sigma}^\dagger c_{j\sigma} . \quad (2.62)$$

If we limit the hopping integral only between the nearest neighbors, we have

$$\begin{aligned} H_t = H - iea \sum_{i,\sigma} [-A_x(\mathbf{r}_i, t) t_{i,i+\hat{x}} c_{i\sigma}^\dagger c_{i+\hat{x},\sigma} + A_x(\mathbf{r}_{i+\hat{x}}, t) t_{i+\hat{x},i} c_{i+\hat{x},\sigma}^\dagger c_{i\sigma}] \\ + \frac{e^2 a^2}{2} \sum_{i,\sigma} [A_x^2(\mathbf{r}_i, t) t_{i,i+\hat{x}} c_{i\sigma}^\dagger c_{i+\hat{x},\sigma} + A_x^2(\mathbf{r}_{i+\hat{x}}, t) t_{i+\hat{x},i} c_{i+\hat{x},\sigma}^\dagger c_{i\sigma}] \end{aligned}$$

$$\begin{aligned}
&\approx H - iea \sum_{i,\sigma} A_x(\mathbf{r}_i, t) [-t_{i,i+\hat{x}} c_{i\sigma}^\dagger c_{i+\hat{x},\sigma} + t_{i+\hat{x},i} c_{i+\hat{x},\sigma}^\dagger c_{i\sigma}] \\
&\quad + \frac{e^2 a^2}{2} \sum_{i,\sigma} A_x^2(\mathbf{r}_i, t) [t_{i,i+\hat{x}} c_{i\sigma}^\dagger c_{i+\hat{x},\sigma} + t_{i+\hat{x},i} c_{i+\hat{x},\sigma}^\dagger c_{i\sigma}] \\
&\approx H - ea \sum_i A_x(\mathbf{r}_i, t) J_x^P(\mathbf{r}_i) - \frac{e^2 a^2}{2} \sum_i A_x^2(\mathbf{r}_i, t) K_x(\mathbf{r}_i) \\
&= H + H'(t) , \tag{2.63}
\end{aligned}$$

where the particle current and the local kinetic energy associated with the x -oriented links are defined as

$$\begin{aligned}
J_x^P(\mathbf{r}_i) &= i \sum_{\sigma} [t_{i+\hat{x},i} c_{i+\hat{x},\sigma}^\dagger c_{i\sigma} - t_{i,i+\hat{x}} c_{i\sigma}^\dagger c_{i+\hat{x},\sigma}] \\
&= it \sum_{\sigma} [c_{i+\hat{x},\sigma}^\dagger c_{i\sigma} - c_{i\sigma}^\dagger c_{i+\hat{x},\sigma}] , \tag{2.64}
\end{aligned}$$

and

$$\begin{aligned}
K_x(\mathbf{r}_i) &= - \sum_{\sigma} [t_{i,i+\hat{x}} c_{i\sigma}^\dagger c_{i+\hat{x},\sigma} + t_{i+\hat{x},i} c_{i+\hat{x},\sigma}^\dagger c_{i\sigma}] \\
&= -t \sum_{\sigma} [c_{i\sigma}^\dagger c_{i+\hat{x},\sigma} + c_{i+\hat{x},\sigma}^\dagger c_{i\sigma}] . \tag{2.65}
\end{aligned}$$

The x -oriented current density operator is then found to be

$$J_x^Q(\mathbf{r}_i) = - \frac{\delta H'(t)}{\delta A_x(\mathbf{r}_i, t)} = e J_x^P(\mathbf{r}_i) + e^2 K_x(\mathbf{r}_i) A_x(\mathbf{r}_i, t) . \tag{2.66}$$

Here we have set the lattice constant $a = 1$.

An alternative derivation of the current density operator is to start with the electric polarization operator:

$$\mathbf{P} = e \sum_i \mathbf{r}_i n_i \tag{2.67}$$

with its x -component

$$P_x = e \sum_i x_i n_i . \tag{2.68}$$

The time-derivative is

$$\begin{aligned}
J_x^Q(\mathbf{r}_i) &= i[H_t, P_x] \\
&= ie \sum_{ij,\sigma} x_i [\tilde{t}_{ij} c_{i\sigma}^\dagger c_{j\sigma} - \tilde{t}_{ji} c_{j\sigma}^\dagger c_{i\sigma}] \\
&= ie \sum_{ij,\sigma} (x_i - x_j) \tilde{t}_{ij} c_{i\sigma}^\dagger c_{j\sigma} \\
&= ie \sum_{ij,\sigma} (x_i - x_j) t_{ij} (1 + i\phi_{ij}) c_{i\sigma}^\dagger c_{j\sigma} \\
&= eJ_x^P(\mathbf{r}_i) + e^2 K_x(\mathbf{r}_i) A_x(\mathbf{r}_i, t) .
\end{aligned} \tag{2.69}$$

Now let us calculate the expectation value of the current density operator. In the linear response theory, the statistical operator in the interaction picture is given by:

$$\hat{\rho}_I(t) = \hat{\rho}_I(-\infty) - \frac{i}{\hbar} \int_{-\infty}^t [H'_I(t'), \hat{\rho}_I(-\infty)]_- dt' . \tag{2.70}$$

The expectation of a physical variable is found to be:

$$\langle \hat{O} \rangle = \text{Tr}[\hat{\rho}_I(-\infty) \hat{O}_I] - \frac{i}{\hbar} \int_{-\infty}^t \text{Tr}\{\hat{\rho}_I(-\infty) [\hat{O}_I(t), H'_I(t')]_-\} dt' \tag{2.71}$$

$$= \langle \hat{O}_I \rangle_0 - \frac{i}{\hbar} \int_{-\infty}^t \langle [\hat{O}_I(t), H'_I(t')]_- \rangle_0 dt' , \tag{2.72}$$

where

$$\hat{O}_I = e^{iHt} \hat{O} e^{-iHt} , \tag{2.73}$$

and

$$H'_I(t) = e^{iHt} H'(t) e^{-iHt} . \tag{2.74}$$

with the term proportional to $A^2(t)$ in $H'(t)$ neglected. The particle current density is then given by

$$\langle J_x^P(\mathbf{r}_i) \rangle = -i \int_{-\infty}^t \langle [J_x^P(\mathbf{r}_i, t), H'_I(t)] \rangle , \tag{2.75}$$

where the particle operator and the perturbation term in the Heisenberg picture with respect to the unperturbed Hamiltonian H are given by, respectively,

$$J_x^P(\mathbf{r}_i, t) = e^{iHt} J_x^P(\mathbf{r}_i) e^{-iHt} . \tag{2.76}$$

We notice that the first term in $H'(t)$ can be rewritten as

$$-e \sum_{i,\sigma} A_x(\mathbf{r}_i, t) J_x^P(\mathbf{r}_i) = \frac{ie}{\omega} J_x^P(-\mathbf{q}) E_x e^{-i\omega t}, \quad (2.77)$$

where the Fourier transform of the particle density operator is given by

$$J_x^P(\mathbf{q}) = \sum_i e^{-i\mathbf{q}\cdot\mathbf{r}_i} J_x^P(\mathbf{r}_i). \quad (2.78)$$

We then obtain

$$\langle J_x^P(\mathbf{r}_i) \rangle = \frac{e}{\omega} E_x(\mathbf{r}_i, t) e^{-i\mathbf{q}\cdot\mathbf{r}_i} \int_{-\infty}^t dt' e^{i\omega(t-t')} \langle [J_x^P(\mathbf{r}_i, t), J_x^P(-\mathbf{q}, t')] \rangle. \quad (2.79)$$

Finally, the current density is found to be

$$\begin{aligned} \langle J_x^Q(\mathbf{r}_i) \rangle &= \frac{e^2}{\omega} E_x(\mathbf{r}_i, t) e^{-i\mathbf{q}\cdot\mathbf{r}_i} \int_{-\infty}^t dt' e^{i\omega(t-t')} \langle [J_x^P(\mathbf{r}_i, t), J_x^P(-\mathbf{q}, t')] \rangle \\ &\quad - \frac{ie^2}{\omega} \langle K_x(\mathbf{r}_i) \rangle E_x(\mathbf{r}_i, t). \end{aligned} \quad (2.80)$$

The local conductivity is then given by

$$\begin{aligned} \sigma_{xx}(\mathbf{r}_i, \omega) &= \frac{\langle J_x^Q(\mathbf{r}_i) \rangle}{E_x(\mathbf{r}_i, t)} \\ &= \frac{e^2}{\omega} e^{-i\mathbf{q}\cdot\mathbf{r}_i} \int_{-\infty}^t dt' e^{i\omega(t-t')} \langle [J_x^P(\mathbf{r}_i, t), J_x^P(-\mathbf{q}, t')] \rangle \\ &\quad - \frac{ie^2}{\omega} \langle K_x(\mathbf{r}_i) \rangle. \end{aligned} \quad (2.81)$$

To eliminate the atomic fluctuations, we take an average over the spatial variable \mathbf{r}_i and obtain the conductivity

$$\sigma_{xx}(\mathbf{q}, \omega) = \frac{e^2}{N\omega} \int_{-\infty}^t dt' e^{i\omega(t-t')} \langle [J_x^P(\mathbf{q}, t), J_x^P(-\mathbf{q}, t')] \rangle - \frac{ie^2}{\omega} \langle K_x \rangle.$$

where

$$\langle K_x \rangle = \frac{1}{N} \sum_i \langle K_x(\mathbf{r}_i) \rangle. \quad (2.82)$$

Since the correlation function in Eq. (2.82) is only a function of the time difference $t - t'$, we can express the conductivity as

$$\begin{aligned}\sigma_{xx}(\mathbf{q}, \omega) &= \frac{e^2}{N\omega} \int_0^\infty dt e^{i\omega t} \langle [J_x^P(\mathbf{q}, t), J_x^P(-\mathbf{q}, 0)] \rangle - \frac{ie^2}{\omega} \langle K_x \rangle \\ &= \frac{e^2}{i\omega} \left[\frac{i}{N} \int_{-\infty}^\infty dt \theta(t) e^{i\omega t} \langle [J_x^P(\mathbf{q}, t), J_x^P(-\mathbf{q}, 0)] \rangle + \langle K_x \rangle \right] \\ &= \frac{e^2}{i\omega} [-\Pi_{xx}(\mathbf{q}, \omega) + \langle K_x \rangle],\end{aligned}\quad (2.83)$$

where we define the retarded correlation function of the particle current operator as

$$\Pi_{xx}(\mathbf{q}, t) = -\frac{i}{N} \theta(t) \langle [J_x^P(\mathbf{q}, t), J_x^P(-\mathbf{q}, 0)] \rangle, \quad (2.84)$$

with its Fourier transform

$$\Pi_{xx}(\mathbf{q}, \omega) = \int_{-\infty}^\infty dt e^{i\omega t} \Pi_{xx}(\mathbf{q}, t). \quad (2.85)$$

The frequency-dependent, uniform electrical conductivity is given by taking the limit $\mathbf{q} \rightarrow 0$:

$$\sigma_{xx}(\omega) = \frac{e^2}{i\omega} [-\Pi_{xx}(\mathbf{q} = 0, \omega) + \langle K_x \rangle]. \quad (2.86)$$

The dc conductivity is obtained by taking first the limit $\mathbf{q} \rightarrow 0$ and then the limit $\omega \rightarrow 0$.

$$\sigma_{xx} = -\lim_{\omega \rightarrow 0} \frac{e^2}{i\omega} [-\Pi_{xx}(\mathbf{q} = 0, \omega) + \langle K_x \rangle]. \quad (2.87)$$

Be reminded that the order of these limits cannot be reversed.

Similarly the transverse conductivity can also be derived as:

$$\sigma_{xy}(\mathbf{q}, \omega) = \frac{e^2}{i\omega} [-\Pi_{xy}(\mathbf{q}, \omega)]. \quad (2.88)$$

It is convenient to calculate the retarded correlation function in the Matsubara formalism. First define the equivalent current-current correlation function in the Matsubara formalism:

$$\Pi_{xx}(\mathbf{q}, \tau) = -\frac{1}{N} \langle T_\tau [J_x^P(\mathbf{q}, \tau) J_x^P(-\mathbf{q}, 0)] \rangle, \quad (2.89)$$

$$\Pi_{xx}(\mathbf{q}, i\omega_n) = \int_0^\beta d\tau e^{i\omega_n \tau} \Pi_{xx}(\mathbf{q}, \tau), \quad (2.90)$$

where $\omega_n = 2n\pi T$ since the current density operator is regarded as a bosonic operator acting as a composite particle. The Matsubara function is evaluated as best one can. Then the desired retarded function is obtained by performing the analytical continuation $i\omega_n \rightarrow \omega + i\delta$:

$$\Pi_{xx}(\mathbf{q}, \omega) = \Pi_{xx}(\mathbf{q}, i\omega_n \rightarrow \omega + i\delta) . \quad (2.91)$$

Technically, we always write the conductivity formula as:

$$\sigma_{xx}(\mathbf{q}, \omega) = \frac{e^2}{i(\omega + i\delta)} [-\Pi_{xx}(\mathbf{q}, \omega) + \langle K_x \rangle] , \quad (2.92)$$

and its uniform counterpart

$$\sigma_{xx}(\omega) = \frac{e^2}{i(\omega + i\delta)} [-\Pi_{xx}(\mathbf{q} = 0, \omega) + \langle K_x \rangle] . \quad (2.93)$$

If the numerator approaches a finite limit as $\omega \rightarrow 0$, the real part of $\sigma_{xx}(\omega)$ will contain a delta function contribution $D\delta(\omega)$ with the ‘‘Drude weight’’ given by

$$\frac{D}{\pi e^2} \equiv \frac{\rho^*}{4\pi} = -\langle K_x \rangle + \Pi_{xx}(\mathbf{q} = 0, \omega \rightarrow 0) , \quad (2.94)$$

with ρ^* an effective density of the mobile charge carriers in units of their mass. This implies a zero resistance state.

In a superconductor, the Meissner effect is the current response to a static, i.e., $\omega = 0$ and transverse gauge potential $\mathbf{q} \cdot \mathbf{A}(\mathbf{q}, \omega = 0) = 0$. In this case, the electric field $\mathbf{E} = 0$. When we only apply a transverse electric field along the x -direction, we should have $q_x A_x(\mathbf{q}, \omega = 0) = 0$, which requires $q_x = 0$. Following the same procedure as before, we can find the expectation value of the electrical current operator

$$\begin{aligned} \langle J_x^Q(\mathbf{r}_i) \rangle &= ie^2 A_x(\mathbf{r}_i) e^{-i\mathbf{q}\cdot\mathbf{r}_i} \int_{-\infty}^t dt' \langle [J_x^P(\mathbf{r}_i, t), J_x^P(-\mathbf{q}, t')] \rangle \\ &\quad + e^2 \langle K_x(\mathbf{r}_i) \rangle A_x(\mathbf{r}_i) . \end{aligned} \quad (2.95)$$

We then have

$$\frac{\langle J_x^Q(\mathbf{r}_i) \rangle}{e^2 A_x(\mathbf{r}_i)} = ie^{-i\mathbf{q}\cdot\mathbf{r}_i} \int_{-\infty}^t dt' \langle [J_x^P(\mathbf{r}_i, t), J_x^P(-\mathbf{q}, t')] \rangle + \langle K_x(\mathbf{r}_i) \rangle . \quad (2.96)$$

By performing an average over the spatial variable \mathbf{r}_i to eliminate the atomic fluctuations, we define an effective ‘‘Drude weight’’ as

$$\frac{D_s}{\pi e^2} = \frac{\rho_s^*}{4\pi} = -\langle K_x \rangle + \Pi_{xx}(q_x = 0, q_y \rightarrow 0, \omega = 0). \quad (2.97)$$

The quantity D_s measures the superfluid density in units of the mass. The crucial difference between ρ^* and ρ_s^* is the order in which the momentum and frequency approach zero.

For a superconductor, we perform the BdG transformation:

$$c_{i\sigma} = \sum_{n(E_n \geq 0)} (u_{i\sigma}^n \gamma_n - \sigma v_{i\sigma}^{n*} \gamma_n^\dagger). \quad (2.98)$$

The kinetic energy can be found readily:

$$\langle K_x \rangle = -\frac{t}{N} \sum_{i,n,\sigma} \{f(E_n)[u_{i+x,\sigma}^{n*} u_{i\sigma}^n + \text{c.c.}] + (1-f(E_n))[v_{i+x,\sigma}^{n*} v_{i\sigma}^n + \text{c.c.}]\}. \quad (2.99)$$

However, the re-expression of the current-current correlation function is much more tedious. In the expansion form, the commutator:

$$[J_x^P(\mathbf{q}, t), J_x^P(-\mathbf{q}, 0)] = (it)^2 \sum_{i\sigma} \sum_{i'\sigma'} e^{-i\mathbf{q}\cdot(\mathbf{r}_i - \mathbf{r}_{i'})} [\hat{A} + \hat{B} + \hat{C} + \hat{D}], \quad (2.100)$$

where

$$\hat{A} = [c_{i+\hat{x},\sigma}^\dagger(t) c_{i\sigma}(t), c_{i'+\hat{x},\sigma'}^\dagger c_{i'\sigma'}], \quad (2.101)$$

$$\hat{B} = -[c_{i+\hat{x},\sigma}^\dagger(t) c_{i\sigma}(t), c_{i'+\hat{x},\sigma'}^\dagger c_{i'+\hat{x},\sigma'}], \quad (2.102)$$

$$\hat{C} = -[c_{i\sigma}^\dagger(t) c_{i+\hat{x},\sigma}(t), c_{i'+\hat{x},\sigma'}^\dagger c_{i'\sigma'}], \quad (2.103)$$

$$\hat{D} = [c_{i\sigma}^\dagger(t) c_{i+\hat{x},\sigma}(t), c_{i'\sigma'}^\dagger c_{i'+\hat{x},\sigma'}], \quad (2.104)$$

with

$$\begin{aligned} c_{i+\hat{x},\sigma}^\dagger(t) c_{i\sigma}(t) &= \sum_{n_1, n_2} [(u_{i+\hat{x},\sigma}^{n_1*} \gamma_{n_1}^\dagger(t) - \sigma v_{i+\hat{x},\sigma}^{n_1} \gamma_{n_1}(t)) (u_{i\sigma}^{n_2} \gamma_{n_2}(t) - \sigma v_{i\sigma}^{n_2*} \gamma_{n_2}^\dagger(t))] \\ &= \sum_{n_1, n_2} [u_{i+\hat{x},\sigma}^{n_1*} u_{i\sigma}^{n_2} e^{i(E_{n_1} - E_{n_2})t} \gamma_{n_1}^\dagger \gamma_{n_2} - \sigma u_{i+\hat{x},\sigma}^{n_1*} v_{i\sigma}^{n_2*} e^{i(E_{n_1} + E_{n_2})t} \gamma_{n_1}^\dagger \gamma_{n_2}^\dagger \\ &\quad - \sigma v_{i+\hat{x},\sigma}^{n_1} u_{i\sigma}^{n_2} e^{-i(E_{n_1} + E_{n_2})t} \gamma_{n_1} \gamma_{n_2} + v_{i+\hat{x},\sigma}^{n_1} v_{i\sigma}^{n_2*} e^{-i(E_{n_1} - E_{n_2})t} \gamma_{n_1} \gamma_{n_2}^\dagger], \end{aligned} \quad (2.105)$$

and

$$\begin{aligned}
c_{i\sigma}^\dagger(t)c_{i+\hat{x},\sigma}(t) &= \sum_{n_1, n_2} [(u_{i\sigma}^{n_1*} \gamma_{n_1}^\dagger(t) - \sigma v_{i\sigma}^{n_1} \gamma_{n_1}(t))(u_{i+\hat{x},\sigma}^{n_2} \gamma_{n_2}(t) - \sigma v_{i+\hat{x},\sigma}^{n_2*} \gamma_{n_2}^\dagger(t))] \\
&= \sum_{n_1, n_2} [u_{i\sigma}^{n_1*} u_{i+\hat{x},\sigma}^{n_2} e^{i(E_{n_1}-E_{n_2})t} \gamma_{n_1}^\dagger \gamma_{n_2} - \sigma u_{i\sigma}^{n_1*} v_{i+\hat{x},\sigma}^{n_2*} e^{i(E_{n_1}+E_{n_2})t} \gamma_{n_1}^\dagger \gamma_{n_2}^\dagger \\
&\quad - \sigma v_{i\sigma}^{n_1} u_{i+\hat{x},\sigma}^{n_2} e^{-i(E_{n_1}+E_{n_2})t} \gamma_{n_1} \gamma_{n_2} + v_{i\sigma}^{n_1} v_{i+\hat{x},\sigma}^{n_2*} e^{-i(E_{n_1}-E_{n_2})t} \gamma_{n_1} \gamma_{n_2}^\dagger].
\end{aligned} \tag{2.106}$$

Using the following relations

$$\langle [\gamma_{n_1}^\dagger \gamma_{n_2}, \gamma_{n_3}^\dagger \gamma_{n_4}] \rangle = (\langle \gamma_{n_1}^\dagger \gamma_{n_1} \rangle - \langle \gamma_{n_2}^\dagger \gamma_{n_2} \rangle) \delta_{n_1 n_4} \delta_{n_2 n_3}, \tag{2.107}$$

$$\langle [\gamma_{n_1}^\dagger \gamma_{n_2}, \gamma_{n_3} \gamma_{n_4}^\dagger] \rangle = -(\langle \gamma_{n_1}^\dagger \gamma_{n_1} \rangle - \langle \gamma_{n_2}^\dagger \gamma_{n_2} \rangle) \delta_{n_1 n_3} \delta_{n_2 n_4}, \tag{2.108}$$

$$\langle [\gamma_{n_1}^\dagger \gamma_{n_2}, \gamma_{n_3} \gamma_{n_4}] \rangle = (\delta_{n_1 n_4} \delta_{n_2 n_3} - \delta_{n_1 n_3} \delta_{n_2 n_4}) (\langle \gamma_{n_1}^\dagger \gamma_{n_1} \rangle - \langle \gamma_{n_2} \gamma_{n_2}^\dagger \rangle), \tag{2.109}$$

$$\langle [\gamma_{n_1} \gamma_{n_2}, \gamma_{n_3}^\dagger \gamma_{n_4}^\dagger] \rangle = (\delta_{n_1 n_4} \delta_{n_2 n_3} - \delta_{n_1 n_3} \delta_{n_2 n_4}) (\langle \gamma_{n_1} \gamma_{n_1}^\dagger \rangle - \langle \gamma_{n_2}^\dagger \gamma_{n_2} \rangle), \tag{2.110}$$

$$\langle [\gamma_{n_1} \gamma_{n_2}, \gamma_{n_3}^\dagger \gamma_{n_4}] \rangle = -(\langle \gamma_{n_1} \gamma_{n_1}^\dagger \rangle - \langle \gamma_{n_2} \gamma_{n_2}^\dagger \rangle) \delta_{n_1 n_3} \delta_{n_2 n_4}, \tag{2.111}$$

$$\langle [\gamma_{n_1} \gamma_{n_2}, \gamma_{n_3} \gamma_{n_4}^\dagger] \rangle = (\langle \gamma_{n_1} \gamma_{n_1}^\dagger \rangle - \langle \gamma_{n_2} \gamma_{n_2}^\dagger \rangle) \delta_{n_1 n_4} \delta_{n_2 n_3}, \tag{2.112}$$

we obtain

$$\begin{aligned}
\langle \hat{A} \rangle &= \sum_{n_1, n_2} [u_{i+\hat{x},\sigma}^{n_1*} u_{i\sigma}^{n_2} e^{i(E_{n_1}-E_{n_2})t} u_{i'+\hat{x},\sigma}^{n_2*} u_{i'\sigma'}^{n_1} (\langle \gamma_{n_1}^\dagger \gamma_{n_1} \rangle - \langle \gamma_{n_2}^\dagger \gamma_{n_2} \rangle) \\
&\quad - u_{i+\hat{x},\sigma}^{n_1*} u_{i\sigma}^{n_2} e^{i(E_{n_1}-E_{n_2})t} v_{i'+\hat{x},\sigma'}^{n_1} v_{i'\sigma'}^{n_2*} (\langle \gamma_{n_1}^\dagger \gamma_{n_1} \rangle - \langle \gamma_{n_2}^\dagger \gamma_{n_2} \rangle) \\
&\quad + \sigma \sigma' u_{i+\hat{x},\sigma}^{n_1*} v_{i\sigma}^{n_2*} e^{i(E_{n_1}+E_{n_2})t} v_{i'+\hat{x},\sigma'}^{n_2} u_{i'\sigma'}^{n_1} (\langle \gamma_{n_1}^\dagger \gamma_{n_1} \rangle - \langle \gamma_{n_2} \gamma_{n_2}^\dagger \rangle) \\
&\quad - \sigma \sigma' u_{i+\hat{x},\sigma}^{n_1*} v_{i\sigma}^{n_2*} e^{i(E_{n_1}+E_{n_2})t} v_{i'+\hat{x},\sigma'}^{n_1} u_{i'\sigma'}^{n_2} (\langle \gamma_{n_1}^\dagger \gamma_{n_1} \rangle - \langle \gamma_{n_2} \gamma_{n_2}^\dagger \rangle) \\
&\quad + \sigma \sigma' v_{i+\hat{x},\sigma}^{n_1} u_{i\sigma}^{n_2} e^{-i(E_{n_1}+E_{n_2})t} u_{i'+\hat{x},\sigma'}^{n_2*} v_{i'\sigma'}^{n_1*} (\langle \gamma_{n_1} \gamma_{n_1}^\dagger \rangle - \langle \gamma_{n_2}^\dagger \gamma_{n_2} \rangle) \\
&\quad - \sigma \sigma' v_{i+\hat{x},\sigma}^{n_1} u_{i\sigma}^{n_2} e^{-i(E_{n_1}+E_{n_2})t} u_{i'+\hat{x},\sigma'}^{n_1*} v_{i'\sigma'}^{n_2*} (\langle \gamma_{n_1} \gamma_{n_1}^\dagger \rangle - \langle \gamma_{n_2}^\dagger \gamma_{n_2} \rangle) \\
&\quad - v_{i+\hat{x},\sigma}^{n_1} v_{i\sigma}^{n_2*} e^{-i(E_{n_1}-E_{n_2})t} u_{i'+\hat{x},\sigma'}^{n_1*} u_{i'\sigma'}^{n_2} (\langle \gamma_{n_1} \gamma_{n_1}^\dagger \rangle - \langle \gamma_{n_2} \gamma_{n_2}^\dagger \rangle) \\
&\quad + v_{i+\hat{x},\sigma}^{n_1} v_{i\sigma}^{n_2*} e^{-i(E_{n_1}-E_{n_2})t} v_{i'+\hat{x},\sigma'}^{n_2} v_{i'\sigma'}^{n_1*} (\langle \gamma_{n_1} \gamma_{n_1}^\dagger \rangle - \langle \gamma_{n_2} \gamma_{n_2}^\dagger \rangle)]. \tag{2.113}
\end{aligned}$$

$$\begin{aligned}
& -v_{i\sigma}^{n_1} v_{i+\hat{x},\sigma}^{n_2*} e^{-i(E_{n_1}-E_{n_2})t} u_{i'\sigma}^{n_1*} u_{i'+\hat{x},\sigma'}^{n_2} (\langle \gamma_{n_1} \gamma_{n_1}^\dagger \rangle - \langle \gamma_{n_2} \gamma_{n_2}^\dagger \rangle) \\
& + v_{i\sigma}^{n_1} v_{i+\hat{x},\sigma}^{n_2*} e^{-i(E_{n_1}-E_{n_2})t} v_{i'\sigma'}^{n_2} v_{i'+\hat{x},\sigma'}^{n_1*} (\langle \gamma_{n_1} \gamma_{n_1}^\dagger \rangle - \langle \gamma_{n_2} \gamma_{n_2}^\dagger \rangle). \quad (2.116)
\end{aligned}$$

By defining

$$A_{n_1, n_2}(\mathbf{q}) = \sum_{i\sigma} e^{-i\mathbf{q}\cdot\mathbf{r}_i} [u_{i+\hat{x},\sigma}^{n_1*} u_{i\sigma}^{n_2} - u_{i\sigma}^{n_1*} u_{i+\hat{x},\sigma}^{n_2}], \quad (2.117)$$

$$B_{n_1, n_2}(\mathbf{q}) = \sum_{i\sigma} \sigma e^{-i\mathbf{q}\cdot\mathbf{r}_i} [u_{i+\hat{x},\sigma}^{n_1*} v_{i\sigma}^{n_2*} - u_{i\sigma}^{n_1*} v_{i+\hat{x},\sigma}^{n_2*}], \quad (2.118)$$

$$C_{n_1, n_2}(\mathbf{q}) = \sum_{i\sigma} \sigma e^{-i\mathbf{q}\cdot\mathbf{r}_i} [v_{i+\hat{x},\sigma}^{n_1} u_{i\sigma}^{n_2} - v_{i\sigma}^{n_1} u_{i+\hat{x},\sigma}^{n_2}], \quad (2.119)$$

$$D_{n_1, n_2}(\mathbf{q}) = \sum_{i\sigma} e^{-i\mathbf{q}\cdot\mathbf{r}_i} [v_{i+\hat{x},\sigma}^{n_1} v_{i\sigma}^{n_2*} - v_{i\sigma}^{n_1} v_{i+\hat{x},\sigma}^{n_2*}], \quad (2.120)$$

we find the current-current correlation function

$$\begin{aligned}
\Pi_{xx}(\mathbf{q}, \omega) &= -\frac{1}{N} \sum_{n_1, n_2} \left\{ \frac{A_{n_1, n_2}(\mathbf{q}) [-A_{n_1, n_2}^*(\mathbf{q}) - D_{n_1, n_2}(-\mathbf{q})]}{\omega + (E_{n_1} - E_{n_2}) + i\delta} (\langle \gamma_{n_1}^\dagger \gamma_{n_1} \rangle - \langle \gamma_{n_2}^\dagger \gamma_{n_2} \rangle) \right. \\
&+ \frac{B_{n_1, n_2}(\mathbf{q}) [-B_{n_1, n_2}^*(\mathbf{q}) - C_{n_1, n_2}(-\mathbf{q})]}{\omega + (E_{n_1} + E_{n_2}) + i\delta} (\langle \gamma_{n_1}^\dagger \gamma_{n_1} \rangle - \langle \gamma_{n_2} \gamma_{n_2}^\dagger \rangle) \\
&+ \frac{C_{n_1, n_2}(\mathbf{q}) [-C_{n_1, n_2}^*(\mathbf{q}) - B_{n_1, n_2}(-\mathbf{q})]}{\omega - (E_{n_1} + E_{n_2}) + i\delta} (\langle \gamma_{n_1} \gamma_{n_1}^\dagger \rangle - \langle \gamma_{n_2}^\dagger \gamma_{n_2} \rangle) \\
&+ \left. \frac{D_{n_1, n_2}(\mathbf{q}) [-D_{n_1, n_2}^*(\mathbf{q}) - A_{n_1, n_2}(-\mathbf{q})]}{\omega - (E_{n_1} - E_{n_2}) + i\delta} (\langle \gamma_{n_1} \gamma_{n_1}^\dagger \rangle - \langle \gamma_{n_2} \gamma_{n_2}^\dagger \rangle) \right\} \\
&= \frac{1}{N} \sum_{n_1, n_2} \left\{ \frac{A_{n_1, n_2}(\mathbf{q}) [A_{n_1, n_2}^*(\mathbf{q}) + D_{n_1, n_2}(-\mathbf{q})]}{\omega + (E_{n_1} - E_{n_2}) + i\delta} [f(E_{n_1}) - f(E_{n_2})] \right. \\
&+ \frac{B_{n_1, n_2}(\mathbf{q}) [B_{n_1, n_2}^*(\mathbf{q}) + C_{n_1, n_2}(-\mathbf{q})]}{\omega + (E_{n_1} + E_{n_2}) + i\delta} [f(E_{n_1}) - f(-E_{n_2})] \\
&+ \frac{C_{n_1, n_2}(\mathbf{q}) [C_{n_1, n_2}^*(\mathbf{q}) + B_{n_1, n_2}(-\mathbf{q})]}{\omega - (E_{n_1} + E_{n_2}) + i\delta} [f(-E_{n_1}) - f(E_{n_2})] \\
&+ \left. \frac{D_{n_1, n_2}(\mathbf{q}) [D_{n_1, n_2}^*(\mathbf{q}) + A_{n_1, n_2}(-\mathbf{q})]}{\omega - (E_{n_1} - E_{n_2}) + i\delta} [f(-E_{n_1}) - f(-E_{n_2})] \right\}. \quad (2.121)
\end{aligned}$$

Using the symmetry relation of eigenstates for positive and negative eigenvalues in the BdG equation, we can write the Π_{xx} in a simplified form:

$$\Pi_{xx}(\mathbf{q}, \omega) = \frac{1}{N} \sum_{n_1, n_2} \left\{ \frac{A_{n_1, n_2}(\mathbf{q}) [A_{n_1, n_2}^*(\mathbf{q}) + D_{n_1, n_2}(-\mathbf{q})]}{\omega + (E_{n_1} - E_{n_2}) + i\delta} [f(E_{n_1}) - f(E_{n_2})] \right\}, \quad (2.122)$$

where E_n cover all eigenvalues from the BdG equation.

For the optical conductivity and charge stiffness, we set $\mathbf{q} = 0$ and obtain:

$$\Pi_{xx}(\omega) = \frac{1}{N} \sum_{n_1, n_2} \left\{ \frac{A_{n_1, n_2} [A_{n_1, n_2}^* + D_{n_1, n_2}]}{\omega + (E_{n_1} - E_{n_2}) + i\delta} [f(E_{n_1}) - f(E_{n_2})] \right\}, \quad (2.123)$$

where $A = A(\mathbf{q} = 0)$ and $D = D(\mathbf{q} = 0)$.

For the superfluid density, we first set $\omega = 0$ and obtain

$$\begin{aligned} \Pi_{xx}(\mathbf{q} \rightarrow 0) &= \frac{1}{N} \sum_{n_1, n_2} \left\{ \frac{A_{n_1, n_2}(\mathbf{q} \rightarrow 0) [A_{n_1, n_2}^*(\mathbf{q} \rightarrow 0) + D_{n_1, n_2}(-\mathbf{q} \rightarrow 0)]}{E_{n_1} - E_{n_2}} \right. \\ &\quad \left. \times [f(E_{n_1}) - f(E_{n_2})] \right\}. \end{aligned} \quad (2.124)$$

An alternative derivation of the optical conductivity and superfluid can be carried out within the Green function method, which is left for the readers to explore as an exercise. The above formulae for optical conductivity and superfluid density are particularly useful for the study of inhomogeneous superconductors.

2.2 Solution to the BdG Equations in the Lattice Model for a Uniform Superconductor

We consider the case in the absence of spin-orbit coupling and other spin-flip scattering effect, and assume only a superconducting order is present in the system. In the nearest-neighbor hopping approximation for the tight-binding model of a cubic system, the normal-state single-particle energy dispersion is given by

$$\epsilon_{\mathbf{k}} = -2t(\cos k_x a + \cos k_y a + \cos k_z a), \quad (2.125)$$

for a three-dimensional cubic lattice, while

$$\epsilon_{\mathbf{k}} = -2t(\cos k_x a + \cos k_y a), \quad (2.126)$$

for a two-dimensional square lattice. Here a is the lattice constant and t is the nearest-neighbor hopping integral. From these dispersions, the normal-state density

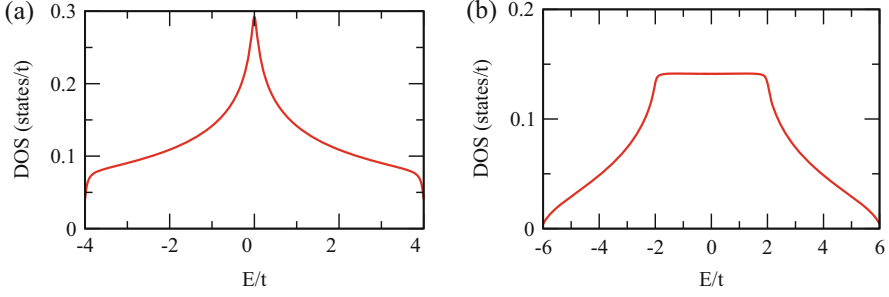


Fig. 2.1 Normal-state single-particle density of states for a two-dimensional (a) and three-dimensional (b) system. Lattice size is chosen to be 400×400 for the 2D system and $200 \times 200 \times 200$ for the 3D system. The intrinsic lifetime broadening $\Gamma = 0.05$ is used for the calculation

of states can be numerically evaluated. The results of normal-state density of states are shown in Fig. 2.1. As one can see, for the 2D system, the DOS exhibits the van Hove singularity. The strong energy dependence of this DOS will influence the magnitude of the superconducting order parameter. For high-temperature cuprate superconductors, the electrons are mostly confined into a two-dimensional Cu square lattice and the energy dispersion for the low-energy Cu-3d electrons usually includes the next-nearest-neighbor hopping

$$\epsilon_{\mathbf{k}} = -2t(\cos k_x a + \cos k_y a) - 4t' \cos k_x a \cos k_y a . \quad (2.127)$$

We consider a pristine 2D superconductor with an s -wave or $d_{x^2-y^2}$ -wave pairing symmetry. In this case, the system is invariant under a translation with a lattice constant a of the square lattice, and the BdG wave functions take the Bloch wavelike:

$$u_i = \frac{1}{\sqrt{N_L}} u_{\mathbf{k}} e^{i\mathbf{k} \cdot \mathbf{r}_i} , \quad (2.128)$$

$$v_i = \frac{1}{\sqrt{N_L}} v_{\mathbf{k}} e^{i\mathbf{k} \cdot \mathbf{r}_i} , \quad (2.129)$$

which gives rise to

$$E_{\mathbf{k}} u_{\mathbf{k}} = \xi_{\mathbf{k}} u_{\mathbf{k}} + \Delta_{\mathbf{k}} v_{\mathbf{k}} , \quad (2.130a)$$

$$E_{\mathbf{k}} v_{\mathbf{k}} = -\xi_{\mathbf{k}} v_{\mathbf{k}} + \Delta_{\mathbf{k}}^* u_{\mathbf{k}} . \quad (2.130b)$$

Here

$$\xi_{\mathbf{k}} = \epsilon_{\mathbf{k}} - \mu \quad (2.131)$$

and

$$\Delta_{\mathbf{k}} = \Delta_s \quad (2.132)$$

for the s -wave pairing symmetry while

$$\Delta_{\mathbf{k}} = (\Delta_d/2)(\cos k_x a - \cos k_y a) \quad (2.133)$$

for the d -wave pairing symmetry.

A little algebra yields to the eigensolutions

$$\begin{pmatrix} u_{\mathbf{k}} \\ v_{\mathbf{k}} \end{pmatrix} = \begin{pmatrix} u_{\mathbf{k}}^{(0)} e^{i\varphi_{\mathbf{k}}} \\ v_{\mathbf{k}}^{(0)} \end{pmatrix} \quad (2.134)$$

corresponding to the eigenvalue

$$E_{\mathbf{k}} = \sqrt{\xi_{\mathbf{k}}^2 + |\Delta_{\mathbf{k}}|^2}. \quad (2.135)$$

and

$$\begin{pmatrix} u_{\mathbf{k}} \\ v_{\mathbf{k}} \end{pmatrix} = \begin{pmatrix} -v_{\mathbf{k}}^{(0)} e^{i\varphi_{\mathbf{k}}} \\ u_{\mathbf{k}}^{(0)} \end{pmatrix} \quad (2.136)$$

corresponding to the eigenvalue $-E_{\mathbf{k}}$. Here the BdG wave function amplitude is given by

$$\begin{pmatrix} u_{\mathbf{k}}^{(0)} \\ v_{\mathbf{k}}^{(0)} \end{pmatrix} = \begin{pmatrix} \sqrt{\frac{1}{2} \left(1 + \frac{\xi_{\mathbf{k}}}{E_{\mathbf{k}}}\right)} \\ \sqrt{\frac{1}{2} \left(1 - \frac{\xi_{\mathbf{k}}}{E_{\mathbf{k}}}\right)} \end{pmatrix}, \quad (2.137)$$

and $\varphi_{\mathbf{k}}$ is the phase angle of $\Delta_{\mathbf{k}}$. Therefore, we obtain the self-consistency equation for the pair potential

$$\Delta_s = \frac{1}{N_L} \sum_{\mathbf{k}} V_s \frac{\Delta_s}{2E_{\mathbf{k}}} \tanh\left(\frac{E_{\mathbf{k}}}{2k_B T}\right), \quad (2.138)$$

for a three-dimensional s -wave superconductor with the quasiparticle excitation energy $E_{\mathbf{k}} = \sqrt{\xi_{\mathbf{k}}^2 + \Delta_s^2}$; and

$$\Delta_d = \frac{1}{N_L} \sum_{\mathbf{k}} V_d (\cos k_x a - \cos k_y a)^2 \frac{\Delta_d}{2E_{\mathbf{k}}} \tanh\left(\frac{E_{\mathbf{k}}}{2k_B T}\right), \quad (2.139)$$

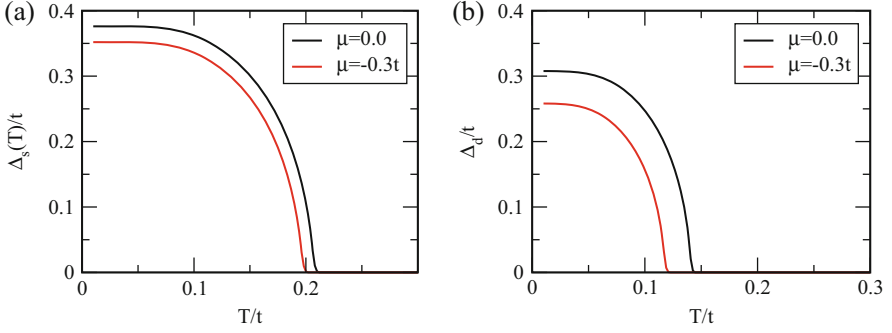


Fig. 2.2 Temperature dependence of the superconducting order parameter for an s -wave (a) and $d_{x^2-y^2}$ -wave (b) pairing symmetry for various values of chemical potential in a 2D tight-binding lattice model with nearest-neighbor hopping. Lattice size is chosen to be 400×400 for the calculations. The energy and temperature ($k_B T$ and k_B is set to 1) are measured in units of t

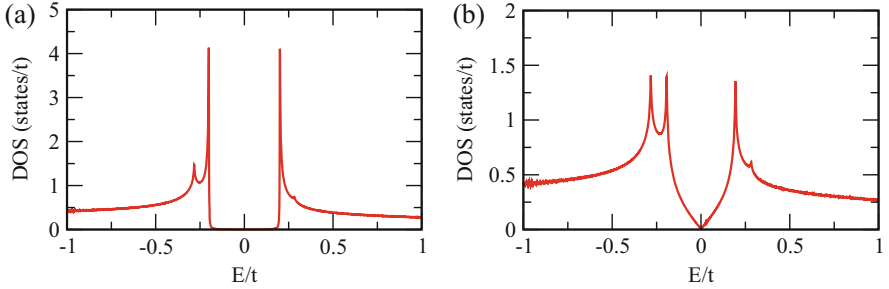


Fig. 2.3 Density of states for a pristine 2D superconductor with s -wave (a) and $d_{x^2-y^2}$ -wave (b) pairing symmetry. A square-lattice tight-binding model with normal-state single-particle energy dispersion given by Eq. (2.127) is used. The parameter $t' = -0.3t$ and $\mu = -t$, and $\Delta_s = \Delta_d = 0.2t$ are taken. Lattice size is chosen to be 4096×4096 and $\Gamma = 0.001t$ is used for the calculations

for a two-dimensional $d_{x^2-y^2}$ -wave superconductor with the quasiparticle excitation energy $E_{\mathbf{k}} = \sqrt{\xi_{\mathbf{k}}^2 + [\frac{\Delta_d}{2}(\cos k_x a - \cos k_y a)]^2}$. In Fig. 2.2, the temperature dependence of superconducting order parameter for various values of chemical potential is shown. The results show that the zero-temperature superconducting pair potential and transition temperature are dependent on the location of the chemical potential, at which the intensity of density of states is tuned. In the 2D tight-binding model with nearest-neighbor hopping, the van Hove singularity occurs at the normal state energy $\epsilon = 0$. In Fig. 2.3, we show the typical feature of density of states for a 2D superconductor described by a square-lattice tight-binding model. The normal-state single-particle energy dispersion given by Eq. (2.127) with $t' = -0.3t$ and a chemical potential $\mu = -t$ are considered. For the s -wave pairing symmetry, a well-shape characteristic as marked by the superconducting coherent peaks around the Fermi energy at $E = 0$ is exhibited in the density of states. Instead, for

the $d_{x^2-y^2}$ -wave pairing symmetry, a V-shape characteristic is exhibited in the density of states around the Fermi energy, which arises from the gapless nodal quasiparticles. In addition, the normal-state van Hove singularity peak is shifted by the superconducting gap opening.

2.3 Abrikosov-Gorkov Equations in the Lattice Model

Similar to the continuum model, we can also establish the Abrikosov-Gorkov theory in the lattice model. Here we generalize it to include the effects of spin-orbit coupling and spin-flip scattering. We first define a 4-component spinor field operator in the Nambu space

$$\hat{\Psi}_i(\tau) = \begin{pmatrix} c_{i\uparrow}(\tau) \\ c_{i\downarrow}(\tau) \\ c_{i\uparrow}^\dagger(\tau) \\ c_{i\downarrow}^\dagger(\tau) \end{pmatrix}, \quad (2.140)$$

and

$$\hat{\Psi}_i^\dagger(\tau) = \left(c_{i\uparrow}^\dagger(\tau) \ c_{i\downarrow}^\dagger(\tau) \ c_{i\uparrow}(\tau) \ c_{i\downarrow}(\tau) \right), \quad (2.141)$$

where the electronic operators

$$c_{i\sigma}(\tau) = e^{\mathcal{H}_{\text{eff}}\tau/\hbar} c_{i\sigma} e^{-\mathcal{H}_{\text{eff}}\tau/\hbar}, \quad (2.142)$$

$$c_{i\sigma}^\dagger(\tau) = e^{\mathcal{H}_{\text{eff}}\tau/\hbar} c_{i\sigma}^\dagger e^{-\mathcal{H}_{\text{eff}}\tau/\hbar}, \quad (2.143)$$

are defined in the imaginary-time space and \mathcal{H}_{eff} is given by Eq. (2.5). Note that $c_{i\sigma}^\dagger(\tau) \neq [c_{i\sigma}(\tau)]^\dagger$. We then introduce the real-space Green's function in the lattice model as

$$\begin{aligned} \mathcal{G}(i\tau; j\tau') &= -\langle T_\tau (\hat{\Psi}_i(\tau) \otimes \hat{\Psi}_j^\dagger(\tau')) \rangle, \\ &= -\theta(\tau - \tau') \langle \hat{\Psi}_i(\tau) \otimes \hat{\Psi}_j^\dagger(\tau') \rangle + \theta(\tau' - \tau) \langle \hat{\Psi}_j^\dagger(\tau') \otimes \hat{\Psi}_i(\tau) \rangle. \end{aligned} \quad (2.144)$$

Therefore, in an expanded form, it becomes

$$\begin{aligned} &\mathcal{G}(i\tau; j\tau') \\ &= \begin{pmatrix} -\langle T_\tau (c_{i\uparrow}(\tau) c_{j\uparrow}^\dagger(\tau')) \rangle & -\langle T_\tau (c_{i\uparrow}(\tau) c_{j\downarrow}^\dagger(\tau')) \rangle & -\langle T_\tau (c_{i\uparrow}(\tau) c_{j\uparrow}(\tau')) \rangle & -\langle T_\tau (c_{i\uparrow}(\tau) c_{j\downarrow}(\tau')) \rangle \\ -\langle T_\tau (c_{i\downarrow}(\tau) c_{j\uparrow}^\dagger(\tau')) \rangle & -\langle T_\tau (c_{i\downarrow}(\tau) c_{j\downarrow}^\dagger(\tau')) \rangle & -\langle T_\tau (c_{i\downarrow}(\tau) c_{j\uparrow}(\tau')) \rangle & -\langle T_\tau (c_{i\downarrow}(\tau) c_{j\downarrow}(\tau')) \rangle \\ -\langle T_\tau (c_{i\uparrow}^\dagger(\tau) c_{j\uparrow}^\dagger(\tau')) \rangle & -\langle T_\tau (c_{i\uparrow}^\dagger(\tau) c_{j\downarrow}^\dagger(\tau')) \rangle & -\langle T_\tau (c_{i\uparrow}^\dagger(\tau) c_{j\uparrow}(\tau')) \rangle & -\langle T_\tau (c_{i\uparrow}^\dagger(\tau) c_{j\downarrow}(\tau')) \rangle \\ -\langle T_\tau (c_{i\downarrow}^\dagger(\tau) c_{j\uparrow}^\dagger(\tau')) \rangle & -\langle T_\tau (c_{i\downarrow}^\dagger(\tau) c_{j\downarrow}^\dagger(\tau')) \rangle & -\langle T_\tau (c_{i\downarrow}^\dagger(\tau) c_{j\uparrow}(\tau')) \rangle & -\langle T_\tau (c_{i\downarrow}^\dagger(\tau) c_{j\downarrow}(\tau')) \rangle \end{pmatrix}. \end{aligned} \quad (2.145)$$

Since the trace is unchanged upon a cyclic variation of operators, we can easily prove that the Green's function is a function of the difference $\tau - \tau'$, that is,

$$\mathcal{G}(i\tau; j\tau') = \mathcal{G}(i, j; \tau - \tau') , \quad (2.146)$$

with $\tau - \tau'$ restricted in the range of $[-\beta, \beta]$ and the factor $\beta = 1/k_B T$. Therefore, the Fourier transform is given by

$$\mathcal{G}(i, j; i\omega_n) = \int_0^\beta d\tau e^{i\omega_n \tau} \mathcal{G}(i, j; \tau) , \quad (2.147)$$

$$\mathcal{G}(i, j; \tau) = \frac{1}{\beta} \sum_n e^{-i\omega_n \tau} \mathcal{G}(i, j; i\omega_n) , \quad (2.148)$$

where the Matsubara frequency $\omega_n = (2n + 1)\pi k_B T / \hbar$ with $n = -\infty, \dots, -1, 0, 1, \dots, \infty$.

Using the equation of motion for $c_{i\sigma}(\tau)$ and $c_{i\sigma}^\dagger(\tau)$:

$$-\hbar \frac{\partial c_{i\sigma}(\tau)}{\partial \tau} = [c_{i\sigma}(\tau), \mathcal{H}_{eff}]_- , \quad (2.149)$$

$$-\hbar \frac{\partial c_{i\sigma}^\dagger(\tau)}{\partial \tau} = [c_{i\sigma}^\dagger(\tau), \mathcal{H}_{eff}]_- , \quad (2.150)$$

and Eq. (2.10), we can obtain the equation of motion for the Green's function

$$\sum_{j'} \hat{M}_{ij'}(\tau) \mathcal{G}(j'\tau; j\tau') = \delta_{ij} \delta(\tau - \tau') \hat{1} , \quad (2.151)$$

with

$$\hat{M}_{ij}(\tau) = \begin{pmatrix} -\frac{\partial}{\partial \tau} \delta_{ij} - \tilde{h}_{i\uparrow j\uparrow} & -\tilde{h}_{i\uparrow j\downarrow} & 0 & -\Delta_{ij} \\ -\tilde{h}_{i\downarrow j\uparrow} & -\frac{\partial}{\partial \tau} \delta_{ij} - \tilde{h}_{i\downarrow j\downarrow} & -\Delta_{ji} & 0 \\ 0 & -\Delta_{ij}^* & -\frac{\partial}{\partial \tau} \delta_{ij} + \tilde{h}_{i\uparrow j\uparrow}^* & -\tilde{h}_{i\uparrow j\downarrow}^* \\ -\Delta_{ji}^* & 0 & -\tilde{h}_{i\uparrow j\downarrow}^* & -\frac{\partial}{\partial \tau} \delta_{ij} + \tilde{h}_{i\downarrow j\downarrow}^* \end{pmatrix} . \quad (2.152)$$

for the spin-singlet pairing case, and subject to the self-consistency condition:

$$\Delta_{ij} = -\frac{V}{2} [\mathcal{G}_{14}(i\tau \rightarrow \tau' + 0^+, j\tau') - \mathcal{G}_{23}(i\tau \rightarrow \tau' + 0^+, j\tau')] , \quad (2.153)$$

$$\Delta_{ij}^* = -\frac{V}{2} [\mathcal{G}_{41}(i\tau \rightarrow \tau' + 0^+, j\tau') - \mathcal{G}_{32}(i\tau \rightarrow \tau' + 0^+, j\tau')] . \quad (2.154)$$

In the absence of the spin-orbit coupling and spin-flip scattering, we can decouple the equation of motion for the Green's function into two sets:

$$\sum_{j'} \begin{pmatrix} -\frac{\partial}{\partial \tau} \delta_{ij'} - \tilde{h}_{i\uparrow j'\uparrow} & -\Delta_{ij'} \\ -\Delta_{j'i}^* & -\frac{\partial}{\partial \tau} \delta_{ij'} + \tilde{h}_{i\downarrow j'\downarrow}^* \end{pmatrix} \begin{pmatrix} \mathcal{G}_{11}(j'\tau; j\tau') & \mathcal{G}_{14}(j'\tau; j\tau') \\ \mathcal{G}_{41}(j'\tau; j\tau') & \mathcal{G}_{44}(j'\tau; j\tau') \end{pmatrix} \\ = \delta_{ij} \delta(\tau - \tau') \hat{1}, \quad (2.155)$$

and

$$\sum_{j'} \begin{pmatrix} -\frac{\partial}{\partial \tau} \delta_{ij'} - \tilde{h}_{i\downarrow j'\downarrow} & -\Delta_{j'i} \\ -\Delta_{ij'}^* & -\frac{\partial}{\partial \tau} \delta_{ij'} + \tilde{h}_{i\uparrow j'\uparrow}^* \end{pmatrix} \begin{pmatrix} \mathcal{G}_{22}(j'\tau; j\tau') & \mathcal{G}_{23}(j'\tau; j\tau') \\ \mathcal{G}_{32}(j'\tau; j\tau') & \mathcal{G}_{33}(j'\tau; j\tau') \end{pmatrix} \\ = \delta_{ij} \delta(\tau - \tau') \hat{1}. \quad (2.156)$$

In this case, either one of the above two sets of equations of motion is sufficient to solve the whole problem. More interestingly, there exists a close relation between the Green's function and the BdG eigenfunctions. Specifically, with the time dependence of the quasiparticle operators:

$$\gamma_n(\tau) = \gamma_n e^{-E_n \tau / \hbar}, \quad (2.157)$$

$$\gamma_n^\dagger(\tau) = \gamma_n^\dagger e^{E_n \tau / \hbar}. \quad (2.158)$$

and the canonical transformation, we can obtain for the most general case the following matrix elements of the Green's function

$$\mathcal{G}_{11}(i, j; \tau) = -\theta(\tau) \sum_n [u_{i\uparrow}^n u_{j\uparrow}^{n*} f(-E_n) e^{-E_n \tau / \hbar} + v_{i\uparrow}^{n*} v_{j\uparrow}^n f(E_n) e^{E_n \tau / \hbar}] \\ + \theta(-\tau) \sum_n [u_{j\uparrow}^{n*} u_{i\uparrow}^n f(E_n) e^{-E_n \tau / \hbar} + v_{j\uparrow}^n v_{i\uparrow}^{n*} f(-E_n) e^{E_n \tau / \hbar}], \quad (2.159)$$

and

$$\mathcal{G}_{44}(i, j; \tau) = -\theta(\tau) \sum_n [u_{i\downarrow}^{n*} u_{j\downarrow}^n f(E_n) e^{E_n \tau / \hbar} + v_{i\downarrow}^n v_{j\downarrow}^{n*} f(-E_n) e^{-E_n \tau / \hbar}] \\ + \theta(-\tau) \sum_n [u_{j\downarrow}^n u_{i\downarrow}^{n*} f(-E_n) e^{E_n \tau / \hbar} + v_{j\downarrow}^{n*} v_{i\downarrow}^n f(E_n) e^{-E_n \tau / \hbar}]. \quad (2.160)$$

It is straightforward to obtain the Green's function in the frequency domain

$$\begin{aligned}
\mathcal{G}_{11}(i, j; i\omega_n) &= \int_0^{\beta\hbar} d\tau e^{i\omega_n\tau} \mathcal{G}_{11}(i, j; \tau) \\
&= - \sum'_n [u_{i\uparrow}^n u_{j\uparrow}^{n*} f(-E_n) \int_0^{\beta\hbar} d\tau e^{(i\omega_n - E_n/\hbar)\tau} \\
&\quad + v_{i\uparrow}^{n*} v_{j\uparrow}^n f(E_n) \int_0^{\beta\hbar} d\tau e^{(i\omega_n + E_n/\hbar)\tau}] \\
&= - \sum'_n \left\{ \frac{u_{i\uparrow}^n u_{j\uparrow}^{n*}}{i\omega_n - E_n/\hbar} f(-E_n) (e^{\beta\hbar(i\omega_n - E_n/\hbar)} - 1) \right. \\
&\quad \left. + \frac{v_{i\uparrow}^{n*} v_{j\uparrow}^n}{i\omega_n + E_n/\hbar} f(E_n) (e^{\beta\hbar(i\omega_n + E_n/\hbar)} - 1) \right\} \\
&= \sum'_n \left[\frac{u_{i\uparrow}^n u_{j\uparrow}^{n*}}{i\omega_n - E_n/\hbar} + \frac{v_{i\uparrow}^{n*} v_{j\uparrow}^n}{i\omega_n + E_n/\hbar} \right], \tag{2.161}
\end{aligned}$$

and

$$\begin{aligned}
\mathcal{G}_{44}(i, j; i\omega_n) &= \int_0^{\beta\hbar} d\tau e^{i\omega_n\tau} \mathcal{G}_{44}(i, j; \tau) \\
&= - \sum'_n [u_{i\downarrow}^{n*} u_{j\downarrow}^n f(E_n) \int_0^{\beta\hbar} d\tau e^{(i\omega_n + E_n/\hbar)\tau} \\
&\quad + v_{i\downarrow}^n v_{j\downarrow}^{n*} f(-E_n) \int_0^{\beta\hbar} d\tau e^{(i\omega_n + E_n/\hbar)\tau}] \\
&= - \sum'_n \left\{ \frac{u_{i\downarrow}^{n*} u_{j\downarrow}^n}{i\omega_n + E_n/\hbar} f(E_n) (e^{\beta\hbar(i\omega_n + E_n/\hbar)} - 1) \right. \\
&\quad \left. + \frac{v_{i\downarrow}^n v_{j\downarrow}^{n*}}{i\omega_n - E_n/\hbar} f(-E_n) (e^{\beta\hbar(i\omega_n - E_n/\hbar)} - 1) \right\} \\
&= \sum'_n \left[\frac{u_{i\downarrow}^{n*} u_{j\downarrow}^n}{i\omega_n + E_n/\hbar} + \frac{v_{i\downarrow}^n v_{j\downarrow}^{n*}}{i\omega_n - E_n/\hbar} \right]. \tag{2.162}
\end{aligned}$$

Other matrix elements of the Green's function can be evaluated in the same way, which are left for exercise.

In the absence of the spin-orbit coupling and spin-flip scattering, we can rewrite the Green's matrix elements as

$$\mathcal{G}_{11}(i, j; i\omega_n) = \sum_{\tilde{n}}' \left[\frac{u_{i\uparrow}^{\tilde{n}1} u_{j\uparrow}^{\tilde{n}1*}}{i\omega_n - E_{\tilde{n}1}/\hbar} + \frac{v_{i\uparrow}^{\tilde{n}2*} v_{j\uparrow}^{\tilde{n}2}}{i\omega_n + E_{\tilde{n}2}/\hbar} \right], \quad (2.163)$$

and

$$\mathcal{G}_{44}(i, j; i\omega_n) = \sum_{\tilde{n}}' \left[\frac{u_{i\downarrow}^{\tilde{n}2*} u_{j\downarrow}^{\tilde{n}2}}{i\omega_n + E_{\tilde{n}2}/\hbar} + \frac{v_{i\downarrow}^{\tilde{n}1} v_{j\downarrow}^{\tilde{n}1*}}{i\omega_n - E_{\tilde{n}1}/\hbar} \right]. \quad (2.164)$$

In summary, we have demonstrated that once we know the eigensolution of the BdG equations, the Abrikosov-Gorkov Green's function can be expressed rigorously. Conversely, if we know the solution to the Abrikosov-Gorkov equations of motion for the Green's functions, the local density of states can be calculated as

$$\begin{aligned} \rho_{i,\uparrow}(E) &= -\frac{1}{\hbar\pi} \text{Im}[\mathcal{G}_{11}(i, i; i\omega_n \rightarrow E/\hbar + i0^+)] \\ &= \sum_{\tilde{n}}' [|u_{i\uparrow}^{\tilde{n}1}|^2 \delta(E - E_{\tilde{n}1}) + |v_{i\uparrow}^{\tilde{n}2}|^2 \delta(E + E_{\tilde{n}2})], \end{aligned} \quad (2.165)$$

and

$$\begin{aligned} \rho_{i,\downarrow}(E) &= \frac{1}{\hbar\pi} \text{Im}[\mathcal{G}_{44}(i, i; -i\omega_n \rightarrow -(E/\hbar + i0^+))] \\ &= \sum_{\tilde{n}}' [|u_{i\downarrow}^{\tilde{n}2}|^2 \delta(E - E_{\tilde{n}2}) + |v_{i\downarrow}^{\tilde{n}1}|^2 \delta(E + E_{\tilde{n}2})]. \end{aligned} \quad (2.166)$$

The above expressions for the local density of states are the same as those given in terms of the eigensolution to the BdG equations (2.47). As we will show in later chapters, the Green's function technique is very useful and convenient for some situations.

References

1. N.W. Ashcroft, N.D. Mermin, *Solid State Physics* (Saunders College, Philadelphia, 1976)
2. R. Micnas, J. Ranninger, S. Robaszkiewicz, *Rev. Mod. Phys.* **62**, 113 (1990)
3. G. Kotliar, J. Liu, *Phys. Rev. B* **38**, 5142(R) (1988)
4. T. Xiang, J.M. Wheatley, *Phys. Rev. B* **51**, 11721 (1995)
5. Y. Wang, A.H. MacDonald, *Phys. Rev. B* **52**, 3876 (1995)
6. M. Franz, C. Kallin, A.J. Berlinsky, *Phys. Rev. B* **54**, R6897 (1996)
7. M. Franz, C. Kallin, A.J. Berlinsky, M.I. Salkola, *Phys. Rev. B* **56**, 7882 (1997)

8. M. Takigawa, M. Ichioka, K. Machida, Phys. Rev. Lett. **83**, 3057 (1999)
9. J.-X. Zhu, T.K. Lee, C.S. Ting, C.-R. Hu, Phys. Rev. B **61**, 8667 (2000)
10. A. Ghosal, M. Randeria, N. Trivedi, Phys. Rev. B **65**, 014501 (2001)
11. S. Takahashi, A. Shoyama, M. Tachiki, Physica C **185–189**, 1677 (1991)
12. D.J. Scalapino, S.R. White, S.C. Zhang, Phys. Rev. Lett. **68**, 2830 (1992)
13. D.J. Scalapino, S.R. White, S.C. Zhang, Phys. Rev. B **47**, 7995 (1993)

Part II
Bogoliubov-de Gennes Theory:
Applications

Chapter 3

Local Electronic Structure Around a Single Impurity in Superconductors

Abstract In this chapter, I am going to discuss the local electronic structure around a single impurity. Both the nonmagnetic and magnetic impurity scattering in conventional s -wave and unconventional d -wave superconductors will be considered. The local electron density of states and the existence of impurity bound or virtual bound states will be explored. The possible realization of Majorana zero-energy modes is discussed for the case of electrons coupled to a spin chain in an s -wave superconductor. These results have a direct relevance to the STM measurements. The results will also be compared with the T -matrix method.

3.1 Introduction

The local electronic structure around a single impurity in a superconductor can provide unique information about the superconducting pairing symmetry [1]. The obtained local density of states can be directly measured by the scanning tunneling microscopy (STM) nowadays. The STM technique has made a significant stride in understanding the pairing symmetry of unconventional superconductors. Theoretically, the study of local electronic structure around a single impurity is also a very important step toward understanding the disorder effect on the bulk superconductivity. The impurity scattering can be either static, which we usually treat as the potential scattering, or dynamic like magnetic impurity or electronic scattering off a local vibrational mode, both of which has internal degrees of freedom. The dynamic scatters cause the inelastic scattering effect of electrons. Here we limit the discussions on the elastic scattering off potential scatters and without loss of generality, consider two-dimensional superconductors, which are described by a tight-binding model on a square lattice.

3.2 Yu-Shiba-Rusinov Impurity States in an s -Wave Superconductor

The condition for the existence of bound state and the spatial oscillations of order parameter and electron density was first studied by Fetter [2] around a spherical impurity in an s -wave superconductor. The existence of bound states due

to resonance scattering in an s -wave superconductor was also considered in an Anderson impurity model by Machida and Shibata [3], Shiba [4], and Machida [5]. For these cases of nonmagnetic impurity scattering, because the product of the bulk superconducting order parameter and the density of states at the Fermi energy is too small (of the order of 10^{-3}), the bound state energy is essentially located near the gap edge. However, the situation becomes very different in the presence of a single magnetic impurity. The quasiparticle scattering off a classical spin was first studied by Yu [6], Shiba [7], and Rusinov [8, 9], who predicted the existence of in-gap bound states, with the energy depending on the exchange coupling between the classical spin and conduction electrons.

The Hamiltonian for an s -wave superconductor with a single-site impurity can be written as

$$\mathcal{H} = \sum_{ij,\sigma} [-t_{ij} - \mu\delta_{ij}] c_{i\sigma}^\dagger c_{j\sigma} + \sum_i [\Delta_i c_{i\uparrow}^\dagger c_{i\downarrow}^\dagger + \text{H.c.}] + \sum_\sigma (\epsilon_I + J\sigma) c_{0\sigma}^\dagger c_{0\sigma}. \quad (3.1)$$

In principle, as we discussed in earlier chapters, the pair potential Δ_i should be determined self-consistently. However, at this moment, we neglect this self-consistency and approximate this pair potential by that for the pristine system. As such,

$$\begin{aligned} \mathcal{H}_0 &= \sum_{ij,\sigma} [-t_{ij} - \mu\delta_{ij}] c_{i\sigma}^\dagger c_{j\sigma} + \sum_i [\Delta_i c_{i\uparrow}^\dagger c_{i\downarrow}^\dagger + \text{H.c.}] \\ &= \sum_{\mathbf{k}\sigma} \xi_{\mathbf{k}} c_{\mathbf{k}\sigma}^\dagger c_{\mathbf{k}\sigma} + \Delta_s \sum_{\mathbf{k}} [c_{\mathbf{k}\uparrow}^\dagger c_{-\mathbf{k}\downarrow}^\dagger + \text{H.c.}], \end{aligned} \quad (3.2)$$

and

$$\mathcal{H}_{\text{imp}} = \sum_\sigma (\epsilon_I + J\sigma) c_{0\sigma}^\dagger c_{0\sigma}. \quad (3.3)$$

Here ϵ_I and J are the strength of the nonmagnetic and ferromagnetic impurity scattering, respectively. Figure 3.1 shows the relative strength of potential in spin up and down channels. In this case, it is particularly convenient to solve the problem in the T -matrix method. By following procedure given in the previous chapter, the

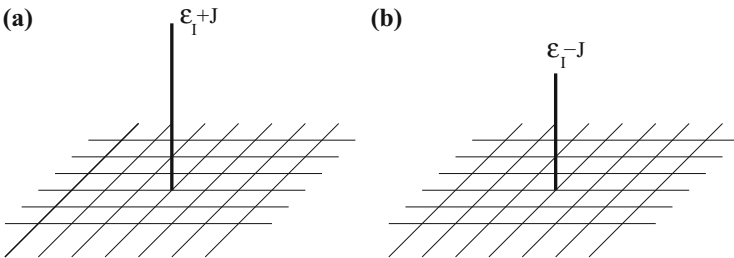


Fig. 3.1 Relative strength of the impurity potential in spin up (a) and spin down (b) channels

Abrikosov-Gorkov equations of motion for the Green's function corresponding to the Hamiltonian equation (3.1) is found to be:

$$\sum_{j'} [i\omega_n \delta_{ij'} \hat{\sigma}_0 - \hat{h}_{ij'}] \mathcal{G}(j', j; i\omega_n) = \delta_{ij} \hat{\sigma}_0 + \hat{V}_{imp} \delta_{i0} \mathcal{G}(0, j; i\omega_n), \quad (3.4)$$

Because of the non-spin-flip scattering considered here, the Green's function has been re-defined from Eq. (2.155) as

$$\mathcal{G}(i, j; \tau) = \begin{pmatrix} -\langle T_\tau(c_{i\uparrow}(\tau)c_{j\uparrow}^\dagger) \rangle - \langle T_\tau(c_{i\uparrow}(\tau)c_{j\downarrow}) \rangle \\ -\langle T_\tau(c_{i\downarrow}^\dagger(\tau)c_{i\uparrow}^\dagger) \rangle - \langle T_\tau(c_{i\downarrow}^\dagger(\tau)c_{j\downarrow}) \rangle \end{pmatrix}, \quad (3.5)$$

which is a 2×2 matrix in the Nambu space. In Eq. (3.4), the impurity scattering matrix is written as

$$\hat{V}_{imp} = \epsilon_I \hat{\sigma}_3 + J \hat{\sigma}_0, \quad (3.6)$$

with the identify matrix

$$\hat{\sigma}_0 = \begin{pmatrix} 1 & 0 \\ 0 & 1 \end{pmatrix}, \quad (3.7)$$

and the third component of the Pauli matrix

$$\hat{\sigma}_3 = \begin{pmatrix} 1 & 0 \\ 0 & -1 \end{pmatrix}. \quad (3.8)$$

The single particle Hamiltonian is also a 2×2 matrix

$$\hat{h}_{ij} = \begin{pmatrix} -t_{ij} - \mu \delta_{ij} & \Delta_s \\ \Delta_s & t_{ij} + \mu \delta_{ij} \end{pmatrix}. \quad (3.9)$$

On the other hand, we can also have the Abrikosov-Gorkov equations of motion for the Green's function corresponding to the Hamiltonian equation (3.2):

$$\sum_{j'} [i\omega_n \delta_{ij'} \hat{\sigma}_0 - \hat{h}_{ij'}] \mathcal{G}_0(j', j; i\omega_n) = \delta_{ij} \hat{\sigma}_0, \quad (3.10)$$

where $\mathcal{G}_0(i, j'; i\omega_n)$ is the Fourier transform of

$$\mathcal{G}_0(i, j; \tau) = \begin{pmatrix} -\langle T_\tau(c_{i\uparrow}(\tau)c_{j\uparrow}^\dagger) \rangle_0 - \langle T_\tau(c_{i\uparrow}(\tau)c_{j\downarrow}) \rangle_0 \\ -\langle T_\tau(c_{i\downarrow}^\dagger(\tau)c_{i\uparrow}^\dagger) \rangle_0 - \langle T_\tau(c_{i\downarrow}^\dagger(\tau)c_{j\downarrow}) \rangle_0 \end{pmatrix}, \quad (3.11)$$

with subscript “0” for the statistical average and Heisenberg field operator $c_{i\sigma}(\tau)$ with respect to Eq. (3.2). Since the Hamiltonian equation (3.2) holds the spatial translational invariance, we can find

$$\mathcal{G}_0(i, j; i\omega_n) = \frac{1}{N_L} \sum_{\mathbf{k}} \mathcal{G}_0(\mathbf{k}; i\omega_n) e^{i\mathbf{k} \cdot (\mathbf{r}_i - \mathbf{r}_j)} , \quad (3.12)$$

with

$$\begin{aligned} \mathcal{G}_0(\mathbf{k}; i\omega_n) &= \left[\begin{array}{cc} i\omega_n - \xi_{\mathbf{k}} & -\Delta_s \\ -\Delta_s & i\omega_n + \xi_{\mathbf{k}} \end{array} \right]^{-1} \\ &= \frac{1}{(i\omega_n - \xi_{\mathbf{k}})(i\omega_n + \xi_{\mathbf{k}}) - \Delta_s^2} \begin{pmatrix} i\omega_n + \xi_{\mathbf{k}} & \Delta_s \\ \Delta_s & i\omega_n - \xi_{\mathbf{k}} \end{pmatrix} . \end{aligned} \quad (3.13)$$

In a tight-binding model up to the next-nearest-neighbor hopping, the single particle energy dispersion is given by Eq. (2.127) and

$$\xi_{\mathbf{k}} = \epsilon_{\mathbf{k}} - \mu . \quad (3.14)$$

The wave vector in the square lattice is given by $\mathbf{k} = k_x \mathbf{e}_x + k_y \mathbf{e}_y$ with $k_{x,y} = \frac{2\pi}{N_L} n_{x,y}$ and $n_{x,y}$ running from $-N_{x,y}/2$ to $N_{x,y}/2 - 1$, the lattice vector in the direct space is given by $\mathbf{r}_i = i_x \mathbf{a}_{e_x} + i_y \mathbf{a}_{e_y}$ with the integers $i_{x,y}$ running from $-N_{x,y}/2$ to $N_{x,y}/2 - 1$. The unit vectors $\mathbf{e}_{x,y}$ are along the bond direction of the square lattice and the $N_L = N_x N_y$.

From Eqs. (3.4) and (3.10), we can obtain the recursion relation:

$$\begin{aligned} \mathcal{G}(i, j; i\omega_n) &= \mathcal{G}_0(i, j; i\omega_n) + \sum_{j'} \mathcal{G}_0(i, j'; i\omega_n) \hat{V}_{imp} \delta_{j'0} \mathcal{G}(j', j; i\omega_n) \\ &= \mathcal{G}_0(i, j; i\omega_n) + \mathcal{G}_0(i, 0; i\omega_n) \hat{V}_{imp} \mathcal{G}(0, j; i\omega_n) . \end{aligned} \quad (3.15)$$

From Eq. (3.15), we can evaluate the Green's function with site i at the impurity site

$$\mathcal{G}(0, j; i\omega_n) = \mathcal{G}_0(0, j; i\omega_n) + \mathcal{G}_0(0, 0; i\omega_n) \hat{V}_{imp} \mathcal{G}(0, j; i\omega_n) , \quad (3.16)$$

which leads to

$$\mathcal{G}(0, j; i\omega_n) = [\hat{\sigma}_0 - \mathcal{G}_0(0, 0; i\omega_n) \hat{V}_{imp}] \mathcal{G}_0(0, j; i\omega_n) . \quad (3.17)$$

We then substitute Eq. (3.17) into Eq. (3.15) and arrive at

$$\mathcal{G}(i, j; i\omega_n) = \mathcal{G}_0(i, j; i\omega_n) + \mathcal{G}_0(i, 0; i\omega_n) \hat{T}_{imp}(i\omega_n) \mathcal{G}_0(0, j; i\omega_n) , \quad (3.18)$$

where the T -matrix is given by

$$\hat{T}_{imp}^{-1}(i\omega_n) = [\hat{V}_{imp}^{-1} - \mathcal{G}_0(0, 0; i\omega_n)]^{-1}. \quad (3.19)$$

With the matrix \hat{V}_{imp} given by Eq. (3.6), we can determine the T -matrix to be

$$\hat{T}_{imp}(i\omega_n) = \frac{1}{\Pi(i\omega_n)} \begin{pmatrix} \frac{1}{-\epsilon_I + J} - \mathcal{G}_{22}^0(i\omega_n) & \mathcal{G}_{12}^0(i\omega_n) \\ \mathcal{G}_{21}^0(i\omega_n) & \frac{1}{\epsilon_I + J} - \mathcal{G}_{11}^0(i\omega_n) \end{pmatrix}, \quad (3.20)$$

where

$$\Pi(i\omega_n) = \left(\frac{1}{\epsilon_I + J} - \mathcal{G}_{11}^0(i\omega_n) \right) \left(\frac{1}{-\epsilon_I + J} - \mathcal{G}_{22}^0(i\omega_n) \right) - \mathcal{G}_{12}^0(i\omega_n) \mathcal{G}_{21}^0(i\omega_n). \quad (3.21)$$

Here we have abbreviated the Green's function $\mathcal{G}_0(0, 0; i\omega_n)$ as $\mathcal{G}^0(i\omega_n)$. The pole of the T -matrix with

$$\Pi(i\omega_n \rightarrow \omega_c) = 0, \quad (3.22)$$

determines a true or virtual bound state induced by the impurity scattering. Physically, the most direct measure of the possible existence of this kind of states is through the calculation of local density of states (LDOS):

$$\begin{aligned} \rho_i(E) &= \rho_{i\uparrow}(E) + \rho_{i\downarrow}(E) \\ &= -\frac{1}{\pi} \text{Im}[\mathcal{G}_{11}(i, i; i\omega_n \rightarrow E + i0^+) - \mathcal{G}_{22}(i, i; -i\omega_n \rightarrow -(E + i0^+))], \end{aligned} \quad (3.23)$$

which follows from the discussion in Chap. 2.

In Fig. 3.2, we show the energy dependence of LDOS around a single zero-ranged potential scatter in an s -wave superconductor defined on a two-dimensional lattice. The results are obtained within the T -matrix theory, where the self-consistency on the superconducting pair potential is neglected. The lattice is described by a tight-binding model with the hopping parameter included up to the next-nearest-neighbors. As is shown, the shape of LDOS for the nonmagnetic impurity remains similar to that for the pristine case (i.e., no impurity scattering). Its intensity on the impurity site (see Fig. 3.2a) suppressed significantly while the LDOS intensity on the nearest-neighboring site to the impurity shows almost no change compared to the pristine case. However, in the presence of a ferromagnetic potential scatter, in-gap quasiparticle states are induced. They are revealed as peaks in the LDOS inside the superconducting gap (see Fig. 3.2b). The location of these in-gap states is dependent on the exchange coupling strength. It first moves toward the Fermi energy with the increased coupling strength and then crosses the Fermi energy when the coupling

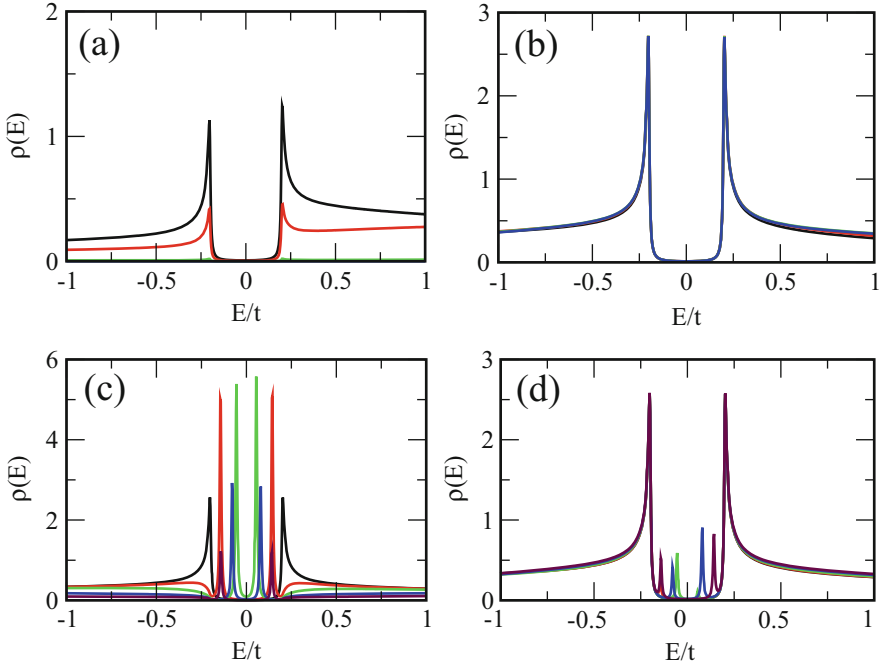


Fig. 3.2 Local density of states around a zero-ranged nonmagnetic ((a)–(b)) and magnetic ((c)–(d)) potential scatter in an s -wave superconductor defined on a two-dimensional square lattice. The *left column* is for the LDOS calculated at the impurity site while the *right column* is for the LDOS calculated at a site nearest-neighbor to the impurity site. For the nonmagnetic potential scatter ((a)–(b)), we take $\varepsilon_I = 1t$ (black), $2t$ (red), $10t$ (green), and $100t$ (blue) with J fixed at 0. For the magnetic potential scatter ((c)–(d)), we take $J = 0.01t$ (black), $0.5t$ (red), $1t$ (green), $2t$ (blue), and $3t$ (maroon) with ε_I fixed at 0. Here we have used a tight-binding model up to next-nearest neighbor hopping with $t' = -0.2t$ and $\mu = -0.8t$. The pair potential is taken as $\Delta_0 = 0.2t$. The broadening parameter is $\gamma = 0.005t$

strength is further increased. In addition, the spectral weight of the particle and hole in-gap states on the impurity site is nearly symmetric while noticeably asymmetric on the nearest-neighbor sites.

As we have shown above, the T -matrix theory is quite convenient for the study of local quasiparticle properties around a single-site impurity in a uniform background of superconducting order parameter. Rigorously, the superconducting order parameter can be modified near the impurity. In this case, one needs to solve the BdG equations self-consistently. Since a single-site impurity breaks the translational invariance in space, a very large system size should be considered at a first glance, which presents the computational challenge for diagonalization of the system Hamiltonian. In practice, since the superconducting order parameter around a single impurity varies at a length scale of the superconducting coherence

length ξ , which is inversely proportional to the superconducting energy gap, we can consider a finite area around the impurity. However, this is not generically true for the quasiparticle states, which can be extended into a region further away from the impurity site. To accommodate these conditions, one can use a supercell technique. We now consider the single impurity problem as an example of how to use the technique. Consider the supercell containing a single impurity located at the center on a two-dimensional lattice. The cell size is $N_x \times N_y$. Therefore, the entire system now consists of a repeated stacking of these supercells. When the supercell size is sufficiently large that the quasiparticle states induced by the single impurity do not overlap between two nearest-neighbor supercells, the physics from this superlattice should mimic the problem of a single impurity in an otherwise pristine system. For the superlattice, we can apply Bloch theorem to write the BdG wavefunction as

$$\begin{cases} u_{i\sigma} = \frac{1}{\sqrt{M}} \tilde{u}_{i\sigma} e^{i\mathbf{K} \cdot (\mathbf{R} + \mathbf{r}_i)} , \\ v_{i\sigma} = \frac{1}{\sqrt{M}} \tilde{v}_{i\sigma} e^{i\mathbf{K} \cdot (\mathbf{R} + \mathbf{r}_i)} , \end{cases} \quad (3.24)$$

Here $M = M_x \times M_y$ with $M_x N_x$ and $M_y N_y$ the linear dimension of the entire system. The symbol \tilde{i} labels the sites in a given unit cell. The Bravais lattice $\mathbf{R} = I_x N_x \mathbf{e}_x + I_y N_y \mathbf{e}_y$ with $I_{x(y)}$ integers and $\mathbf{e}_{x(y)}$ unit vectors along the x and y -bond directions. To simplify the discussion, we have taken the unit length $a = 1$. Subjecting the above Bloch wave function to the periodic boundary condition leads to the wave vectors corresponding to the supercell

$$\mathbf{K} = K_x \mathbf{e}_x + K_y \mathbf{e}_y , \quad (3.25)$$

where $K_x = 2\pi n_x / M_x N_x$ and $K_y = 2\pi n_y / M_y N_y$ with $n_x = -M_x/2, -M_x/2 + 1, \dots, M_x/2 - 2, M_x/2 - 1$ and $n_y = -M_y/2, -M_y/2 + 1, \dots, M_y/2 - 2, M_y/2 - 1$ for M_x and M_y even integers. Upon substitution of Eq. (3.24) into Eq. (2.44), we obtain the BdG equations in a tight-binding model with hopping integrals up to the next-nearest neighbors:

$$E_n(\mathbf{K}) u_{i\uparrow}^n(\mathbf{K}) = \sum_{\delta} \tilde{h}_{i\uparrow, i+\delta\uparrow} e^{i\mathbf{K} \cdot \mathbf{r}_{\delta}} u_{i+\delta\uparrow}^n(\mathbf{K}) + \Delta_{\tilde{i}\tilde{i}} v_{i\downarrow}^n(\mathbf{K}) , \quad (3.26)$$

$$E_n(\mathbf{K}) v_{i\downarrow}^n(\mathbf{K}) = - \sum_{\delta} \tilde{h}_{i\downarrow, i+\delta\downarrow}^* e^{i\mathbf{K} \cdot \mathbf{r}_{\delta}} v_{i+\delta\downarrow}^n(\mathbf{K}) + \Delta_{\tilde{i}\tilde{i}}^* u_{i\uparrow}^n(\mathbf{K}) , \quad (3.27)$$

subject to the self-consistency condition:

$$\Delta_{\tilde{i}\tilde{i}} = \frac{U}{2M} \sum_{\mathbf{K}, n} u_{i\uparrow}^n(\mathbf{K}) v_{i\downarrow}^{n*}(\mathbf{K}) \tanh\left(\frac{E_n(\mathbf{K})}{2k_B T}\right) . \quad (3.28)$$

Once the self-consistent solution is obtained, the local density of states in a given supercell is then evaluated according to

$$\rho_{\bar{i}}(E) = \frac{1}{M} \sum_{\mathbf{K},n} [|u_{\bar{i}\uparrow}^n(\mathbf{K})|^2 \delta(E - E_n(\mathbf{K})) + |v_{\bar{i}\downarrow}^n(\mathbf{K})|^2 \delta(E + E_n(\mathbf{K}))]. \quad (3.29)$$

Figure 3.3 shows the self-consistent solution of a single impurity in an s -wave superconductor. As we can see, in the presence of a unitary non-magnetic impurity, the superconducting order parameter is indeed strongly suppressed at the impurity site. However, no impurity bound states exist. Instead, in the presence of a ferromagnetic impurity, the superconducting order parameter is suppressed even with an intermediate exchange coupling. In this case, the quasiparticle peaks with energies inside the gap are exhibited in the local density of states. The results are qualitatively consistent with those obtained within the T -matrix theory, suggesting the in-gap states are of Yu-Shiba-Rusinov origin. Therefore, this example demonstrates that the

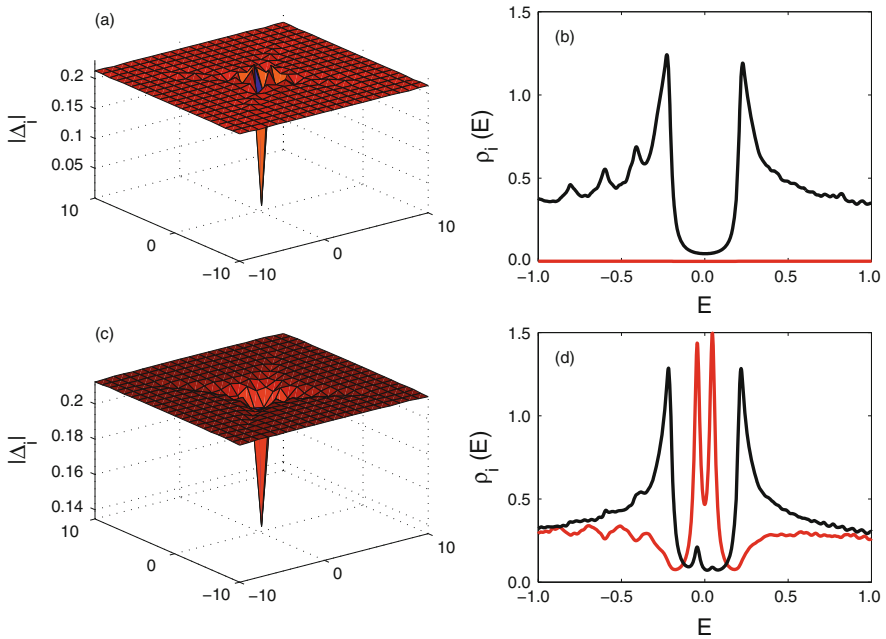


Fig. 3.3 Self-consistent solution to a single impurity in an s -wave superconductor. The *top row* displays the results of the spatial variation of the superconducting order parameter and the local density of states for a nonmagnetic impurity. The *bottom row* displays those for a ferromagnetic impurity. For the local density of states, only the results on the impurity site (*red line*) and on the site nearest neighbor to the impurity site (*black line*) are plotted. The calculations are carried out for an s -wave superconductor defined on a two-dimensional square lattice. The pairing interaction is taken to be $U = 1.5t$ and the temperature $T = 0.01t$. The supercell size has the dimension of 21 by 21. The nonmagnetic impurity potential strength $\epsilon_I = 100t$ while the ferromagnetic impurity potential $J = 1t$. Here we have used a tight-binding model up to next-nearest neighbor hopping with $t' = -0.2t$ and $\mu = -0.8t$. The broadening parameter is $\gamma = 0.01t$

fully self-consistent BdG approach can provide more insight into the local electronic structure of a superconductor.

3.3 Majorana Fermion in an s -Wave Superconductor with a Chain of Localized Spins

As we know, the conventional fermions come with a pair of the creation and annihilation operators, (c^\dagger, c) , satisfying the Fermi-Dirac anti-commutation relations $\{c, c^\dagger\} = 1$. The operators c and c^\dagger are not self-adjoint but they are the adjoint of each other. In contrast to these complex fermions, Majorana fermions are real-valued fermions, that is, they are their own anti-particles and self-adjoint with the property of $c^\dagger = c$. Although these particles may or may not exist in nature as elementary particles, there is intensive interest in their realization in solid state systems [10–13]. In particular, it is proposed that the Majorana fermions can perform better than the complex fermions in keeping the quantum coherence and are proposed as basic building units for quantum computation [14]. For the realization of Majorana fermions in superconductors, a natural strategy is to use the zero-energy or midgap Bogoliubov excitation modes. This observation follows from the particle-hole symmetry of Bogoliubov quasiparticles as evident from the BdG equations: The quasiparticle operators $\gamma(E)$ and $\gamma^\dagger(E)$ are related by

$$\gamma(E) = \gamma^\dagger(-E). \quad (3.30)$$

When the quasiparticle excitation energy is zero, we obtain $\gamma = \gamma^\dagger$, suggesting that the particle is its own antiparticle. The search of midgap excitations with the character of Majorana fermions has been made in chiral p -wave superconductors in early years [15, 16] and more recently revived with new proposals [17]. A specific system of interest is that a chain of magnetic atoms on surface of a conventional s -wave superconductor. It has been shown [18–20] that when the magnetic atoms in the chain form a spiral with the correct pitch, the Yu-Shiba-Rusinov states discussed in previous section can give rise to an effective one-dimensional topological superconductor with Majorana fermions bound to its ends. A schematic setup is shown in Fig. 3.4. The model Hamiltonian is given by

$$\begin{aligned} \mathcal{H} = & \sum_{ij\sigma} (-t_{ij} - \delta_{ij}\mu) c_{i\sigma}^\dagger c_{j\sigma} + J \sum_{i \in I} \mathbf{S}_i \cdot (c_{i\sigma}^\dagger \boldsymbol{\sigma}_{\sigma\sigma'} c_{i\sigma'}) \\ & + \sum_i [\Delta_i c_{i\uparrow}^\dagger c_{i\downarrow}^\dagger + \text{H.c.}]. \end{aligned} \quad (3.31)$$

Here the s -wave superconducting pair potential is defined in the BCS mean-field approximation

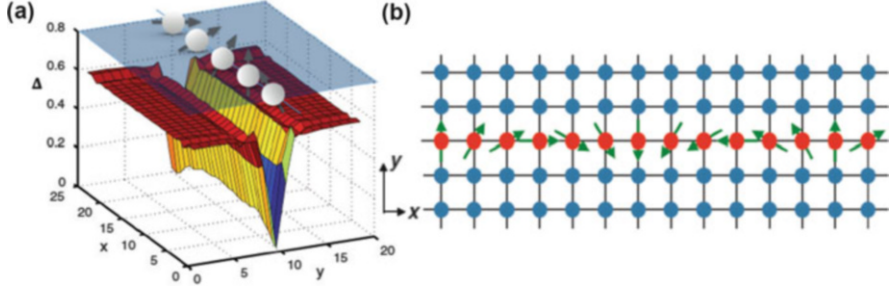


Fig. 3.4 (a) Schematic picture of a chain of magnetic impurities adsorbed on the surface of an s -wave superconductor. Suppression of the superconducting order parameter Δ_i from the self-consistent BdG solution is also shown. (b) The tight-binding lattice with a row of magnetic atoms. From [21]

$$\Delta_i = U \langle c_{i\uparrow} c_{i\downarrow} \rangle, \quad (3.32)$$

where U is an effective pairing interaction. The third term in the Hamiltonian describes the exchange coupling with strength J of a chain of magnetic spins with the superconducting electrons. We consider a two-dimensional lattice of the dimension $N_L = N_x \times N_y$ for the s -wave superconductor, which lies in the xy -plane, and choose the chain of the magnetic atoms aligned along the x -direction. For the case that the magnetic moments form a coplanar spiral at wave vector G , the classical spin can be written as

$$\mathbf{S}_i = S(\cos Gx_i, -\sin Gx_i, 0), \quad (3.33)$$

where (x_i, y_i) are the coordinate of site i . It represents the spin rotating in the x - y plane. With a periodic condition along the x -direction, it is convenient to perform a spin-dependent gauge transformation to superconducting electron operators:

$$c_{i\sigma} \rightarrow \tilde{c}_{i\sigma} = \tilde{c}_{i\sigma} \exp\left[\frac{i}{2}\sigma Gx_i\right], \quad (3.34)$$

which effectively aligns the local spin quantization axis for the conduction electrons along the classical spin \mathbf{S}_i and leads to the Hamiltonian

$$\begin{aligned} \mathcal{H} = & \sum_{ij\sigma} (-t_{ij} e^{-\frac{i}{2}\sigma G(x_i - x_j)} - \delta_{ij}\mu) \tilde{c}_{i\sigma}^\dagger \tilde{c}_{j\sigma} + JS \sum_{i \in I} \tilde{c}_{i\sigma}^\dagger \sigma_{\sigma\sigma'}^x \tilde{c}_{i\sigma'} \\ & + \sum_i [\Delta_i \tilde{c}_{i\uparrow}^\dagger \tilde{c}_{i\downarrow}^\dagger + \text{H.c.}] - \frac{1}{U} \sum_i |\Delta_i|^2. \end{aligned} \quad (3.35)$$

In the spin reference frame with spin quantized along the x -direction, the effective hopping term becomes spin-dependent $-t_{ij} e^{-\frac{i}{2}\sigma G(x_i - x_j)}$ and can be interpreted as the

hopping with an effective spin-orbit coupling; while the last term in the first line of the above Hamiltonian represents a uniform Zeeman field of the strength JS .

In the one-dimensional limit $N_y = 1$, the entire system is translationally invariant and the pair potential Δ is a constant. We can perform a canonical transformation

$$\tilde{c}_{i\sigma} = \frac{1}{\sqrt{N_L}} \sum_k \tilde{c}_{k\sigma} e^{ikx_i}, \quad (3.36)$$

into the Block representation, where k is the wave vector in the first Brillouin zone of the one-dimensional system. The Hamiltonian is then found as

$$\begin{aligned} \mathcal{H} = & \sum_{k\sigma} \xi_{k\sigma} \tilde{c}_{k\sigma}^\dagger \tilde{c}_{k\sigma} + JS \sum_{k\sigma\sigma'} \tilde{c}_{k\sigma}^\dagger \sigma_{\sigma\sigma'}^x \tilde{c}_{k\sigma'} \\ & + \sum_k [\Delta \tilde{c}_{k\uparrow}^\dagger \tilde{c}_{-k\downarrow}^\dagger + \text{H.c.}] - \frac{N_x}{U} \Delta^2, \end{aligned} \quad (3.37)$$

where the spin-dependent energy dispersion in nearest-neighbor hopping model is given by

$$\xi_{k\sigma} = -2t \cos[(k + \sigma G/2)a] - \mu \quad (3.38)$$

with a being the lattice constant. In the normal state ($\Delta = 0$), the single-particle energy dispersion of the system becomes

$$E_k = \xi_{k,+} \pm \sqrt{\xi_{k,-}^2 + J^2 S^2}, \quad (3.39)$$

where

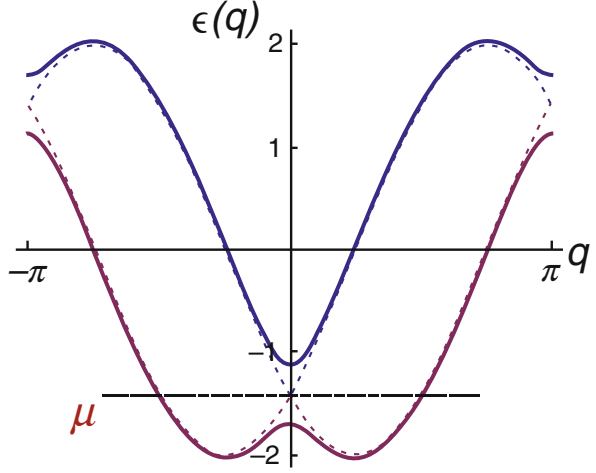
$$\xi_{k,\pm} = \frac{1}{2} [\xi_{k\uparrow} \pm \xi_{k\downarrow}]. \quad (3.40)$$

For $k = 0, \pi$ so that $\xi_{k,-} = 0$, the quasiparticle has an excitation gap of JS , as shown in Fig. 3.5. It implies that when the chemical potential lies inside the gap by satisfying the condition

$$|\mu + 2t \cos(Ga/2)| \leq JS, \quad (3.41)$$

there exists a single non-degenerate Fermi point in the right half of the Brillouin zone. The Kitaev criterion [22] then tells that the system is a one-dimensional topological superconductor upon turning on the small superconducting pair potential ($\Delta \neq 0$). It turns out [23–25] that in the one-dimensional system, for an optimized spin spiral pitch G , which minimizes the ground-state energy, the condition Eq. (3.41) is always satisfied.

Fig. 3.5 Normal-state energy dispersion in the one-dimensional electron system coupled to the one-dimensional spin chain. From [21]



For the two-dimensional superconductor, the translation invariance is broken along the y -direction, that is, perpendicular to the spin chain, we can only rely on the numerical simulations to solve the BdG equations

$$\sum_j \tilde{H}_{ij} \Psi_j^n = E_n \Psi_i^n, \quad (3.42)$$

where the matrix

$$\tilde{H}_{ij} = \begin{bmatrix} \tilde{h}_{i\uparrow,j\uparrow} & \tilde{h}_{i\uparrow,j\downarrow} & 0 & \delta_{ij}\Delta_i \\ \tilde{h}_{i\downarrow,j\uparrow} & \tilde{h}_{i\downarrow,j\downarrow} & \delta_{ij}\Delta_i & 0 \\ 0 & \delta_{ij}\Delta_i^* & -\tilde{h}_{i\uparrow,j\uparrow}^* & \tilde{h}_{i\uparrow,j\downarrow}^* \\ \delta_{ij}\Delta_i^* & 0 & \tilde{h}_{i\downarrow,j\uparrow}^* & -\tilde{h}_{i\downarrow,j\downarrow}^* \end{bmatrix}, \quad (3.43)$$

and the eigenvector $\Psi_i^n = (u_{i\uparrow}^n, u_{i\downarrow}^n, v_{i\uparrow}^n, v_{i\downarrow}^n)^{\text{Transpose}}$. Here the matrix normal-state single-particle Hamiltonian matrix is given by

$$\tilde{h}_{ij} = \begin{pmatrix} -t_{ij}e^{-\frac{i}{2}G(x_i-x_j)} - \delta_{ij}\mu & JS\delta_{ij} \\ JS\delta_{ij} & -t_{ij}e^{\frac{i}{2}G(x_i-x_j)} - \delta_{ij}\mu \end{pmatrix}. \quad (3.44)$$

For the bulk system, the closed boundary condition is applicable and the system is still translationally invariant along the x -direction, which allows us to introduce a mixed representation through the transformation

$$\Psi_i^n = \frac{1}{\sqrt{N_x}} \sum_{k_x} \Psi_{i_y}^n(k_x) e^{ik_x i_x a}. \quad (3.45)$$

The BdG equations can be block-diagonalized as

$$\sum_{j_y} \begin{bmatrix} \tilde{h}_{i_y \uparrow j_y \uparrow}(k_x) & \tilde{h}_{i_y \uparrow j_y \downarrow}(k_x) & 0 & \delta_{i_y j_y} \Delta_{i_y} \\ \tilde{h}_{i_y \downarrow j_y \uparrow}(k_x) & \tilde{h}_{i_y \downarrow j_y \downarrow}(k_x) & \delta_{i_y j_y} \Delta_{i_y} & 0 \\ 0 & \delta_{i_y j_y} \Delta_{i_y}^* & -\tilde{h}_{i_y \uparrow j_y \uparrow}^*(k_x) & \tilde{h}_{i_y \uparrow j_y \downarrow}^*(k_x) \\ \delta_{i_y j_y} \Delta_{i_y}^* & 0 & \tilde{h}_{i_y \downarrow j_y \uparrow}^*(k_x) & -\tilde{h}_{i_y \downarrow j_y \downarrow}^*(k_x) \end{bmatrix} \begin{pmatrix} u_{j_y \uparrow}^{\tilde{n}} \\ u_{j_y \downarrow}^{\tilde{n}} \\ v_{j_y \uparrow}^{\tilde{n}} \\ v_{j_y \downarrow}^{\tilde{n}} \end{pmatrix} = E_n \begin{pmatrix} u_{i_y \uparrow}^{\tilde{n}} \\ u_{i_y \downarrow}^{\tilde{n}} \\ v_{i_y \uparrow}^{\tilde{n}} \\ v_{i_y \downarrow}^{\tilde{n}} \end{pmatrix} \quad (3.46)$$

with

$$\tilde{h}_{i_y j_y}(k_x) = \begin{pmatrix} -t_{i_y j_y} + (-2t \cos[(k_x + G/2)a] - \mu) \delta_{i_y j_y} & JS \delta_{i_y j_y} \\ JS \delta_{i_y j_y} & -t_{i_y j_y} + (-2t \cos[(k_x - G/2)a] - \mu) \delta_{i_y j_y} \end{pmatrix}. \quad (3.47)$$

With the aid of these eigensolutions, the ground-state energy can be calculated as a function of the free-parameter G , that is $E_g(G)$, for a given chemical potential, from which the spin spiral pitch G^* can be determined. The typical results are shown in Fig. 3.6 [21]. The strong suppression of the s -wave superconducting order parameter

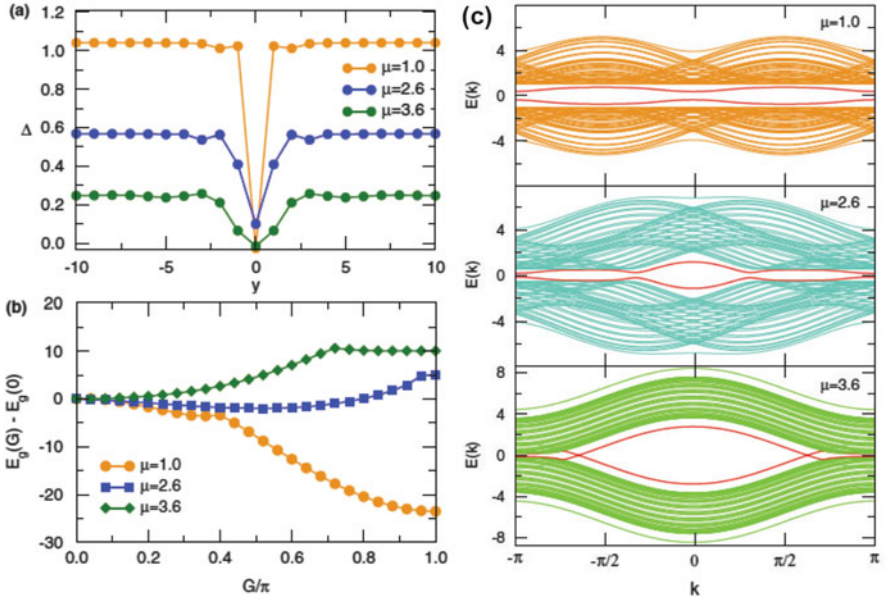


Fig. 3.6 Spatial variation of the superconducting order parameter Δ_{i_y} obtained through the self-consistent solution to the BdG equations (3.42) (a), the dependence of the ground-state energy on the spiral pitch (b), and band structure on the longitudinal wave vector k_x (c) for various values of the chemical potential $\mu = 1.0, 2.6, 3.6$. The system size is taken to be $N_L = N_x \times N_y = 100 \times 20$. The other parameter values are chosen as $U = 3.6, JS = 2$. The energies are measured in units of nearest neighbor hopping parameter $t = 1$. From [21]

(see Fig. 3.6a) is seen along the spin chain. This superconducting potential quantum well can trap low-energy quasiparticle states. For the chosen chemical potential values, the optimized spiral pitch G_* has the values of π , 0 and in between (see Fig. 3.6c), corresponding to the antiferromagnetic, ferromagnetic, and topological spiral phases. In all these phases, distinctive Shiba states are obtained (see Fig. 3.6c). These are described by the effective one-dimensional model and the Majorana zero-energy edge modes can be induced in the system with open boundaries (i.e., at the both ends of the spin chain).

3.4 Impurity Resonance State in a d -Wave Superconductor

The d -wave pairing symmetry, especially, $d_{x^2-y^2}$ -wave pairing symmetry, has been observed in high-temperature cuprate superconductors [26, 27]. As we have discussed above, the s -wave superconductivity is not so sensitive to non-magnetic impurity potential scattering, by showing no existence of in-gap states. However, for a d -wave pairing symmetry, the local electronic structure can be quite distinct in the immediate vicinity of an isolated non magnetic impurity [28–40]. It has been theoretically predicted by Balatsky, Salkola and co-workers [31, 32] that, in a d -wave superconductor, a single nonmagnetic impurity can generate quasiparticle resonance states at subgap energies. This prediction has been confirmed by scanning tunneling microscopy experiments [41].

To demonstrate this local properties, we can again employ the T -matrix theory as explained in Sect. 4.2 except that the pair potential is now of the form

$$\Delta_{\mathbf{k}} = \frac{\Delta_0}{2}(\cos k_x - \cos k_y), \quad (3.48)$$

defined in a tight-binding model for a square lattice.

In Fig. 3.7, we show the energy dependence of LDOS around a single zero-ranged potential scatter in a $d_{x^2-y^2}$ -wave superconductor defined on a two-dimensional lattice. The results are obtained within the T -matrix theory, where the self-consistency on the superconducting pair potential is neglected. The lattice is described by a tight-binding model with the hopping parameter included up to the next-nearest-neighbors. As is shown, the shape of LDOS for the nonmagnetic impurity can change dramatically with the strength of the scattering potential. In particular, due to the locally breaking of the particle-hole symmetry of the electronic states, the spectral weight for the electron and hole component of quasiparticle resonance peaks is biased. For the repulsive potential scatter, the LDOS resonance state has a dominant hole component on the impurity site (see Fig. 3.7a) while a dominant electron component on the nearest-neighboring site to the impurity (see Fig. 3.7b). In contrast, for the attractive potential scatter, the LDOS resonance has a dominant electron component on the impurity site (Fig. 3.7c) but a dominant hole contribution on the nearest-neighboring sites (Fig. 3.7d).

To take into account the full self-consistency of the superconducting order parameter, we use the supercell technique as discussed in Sect. 4.2. Now for

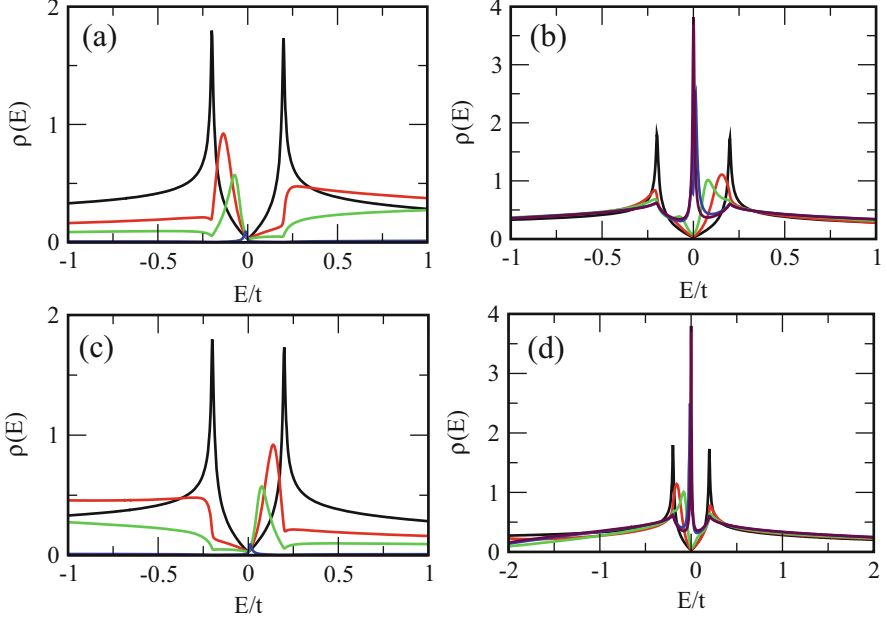


Fig. 3.7 Local density of states around a zero-ranged nonmagnetic potential scatter in a d -wave superconductor defined on a two-dimensional square lattice. The *left column* is for the LDOS calculated at the impurity site while the *right column* is for the LDOS calculated at a site nearest-neighbor to the impurity site. For the repulsive potential scatter ((a)–(b)), we take $\varepsilon_I = 1t$ (red), $2t$ (green), $10t$ (blue), and $100t$ (maroon). For the attractive potential scatter ((c)–(d)), we take $\varepsilon_I = -1t$ (red), $-2t$ (green), $-10t$ (blue), $-100t$ (maroon). The DOS for the pristine system ($\varepsilon_I = 0$ with black lines) is also shown. Here we have used a tight-binding model up to next-nearest neighbor hopping with $t' = -0.2t$ and $\mu = -0.8t$. The pair potential is taken as $\Delta_0 = 0.2t$. The broadening parameter is $\gamma = 0.005t$

the d -wave superconducting order parameter, the pairing interaction should be of nearest-neighbor type on a square lattice. In the supercell technique, the BdG equations [c.f. Eq. (2.30)] become:

$$E_n(\mathbf{K})u_{i\uparrow}^n(\mathbf{K}) = \sum_{\delta} e^{i\mathbf{K}\cdot\mathbf{r}_{\delta}} [\tilde{h}_{i\uparrow, i+\delta\uparrow}^n u_{i+\delta\uparrow}^n(\mathbf{K}) + \Delta_{i\bar{i}+\delta} v_{i+\delta\downarrow}^n(\mathbf{K})], \quad (3.49)$$

$$E_n(\mathbf{K})v_{i\downarrow}^n(\mathbf{K}) = \sum_{\delta} e^{i\mathbf{K}\cdot\mathbf{r}_{\delta}} [-\tilde{h}_{i\downarrow, i+\delta\downarrow}^n v_{i+\delta\uparrow}^n(\mathbf{K}) + \Delta_{i+\delta, i}^* u_{i+\delta\uparrow}^n(\mathbf{K})], \quad (3.50)$$

subject to the self-consistency condition:

$$\Delta_{i\bar{i}+\delta} = \frac{V}{4M} \sum_{\mathbf{K}, n} [u_{i\uparrow}^n(\mathbf{K})v_{i+\delta\downarrow}^{n*}(\mathbf{K})e^{-i\mathbf{K}\cdot\mathbf{r}_{\delta}} + u_{i+\delta, \uparrow}^n(\mathbf{K})v_{i\downarrow}^{n*}(\mathbf{K})e^{i\mathbf{K}\cdot\mathbf{r}_{\delta}}] \tanh\left(\frac{E_n(\mathbf{K})}{2k_B T}\right). \quad (3.51)$$

The d -wave and the induced extended- s -wave OP components are then defined as

$$\Delta_d(\mathbf{i}) = \frac{1}{4}[\Delta_{\hat{x}}(\mathbf{i}) + \Delta_{-\hat{x}}(\mathbf{i}) - \Delta_{\hat{y}}(\mathbf{i}) - \Delta_{-\hat{y}}(\mathbf{i})], \quad (3.52)$$

$$\Delta_s(\mathbf{i}) = \frac{1}{4}[\Delta_{\hat{x}}(\mathbf{i}) + \Delta_{-\hat{x}}(\mathbf{i}) + \Delta_{\hat{y}}(\mathbf{i}) + \Delta_{-\hat{y}}(\mathbf{i})]. \quad (3.53)$$

Here \hat{x} and \hat{y} are the unit vectors along x - and y -bond direction of the square lattice. We note that the expression for the LDOS is still the same as that given by Eq. (3.29). In Fig. 3.8, the typical results are shown for a repulsive impurity with the scattering strength in the unitary limit. The d -wave superconducting order parameter is strongly suppressed near the impurity site while a subdominant (extended) s -wave superconducting order parameter is induced around the impurity. In addition, the LDOS near the impurity site exhibits a resonance peak close to the Fermi energy and the spatial dependence of the LDOS at this resonance energy shows tails along the

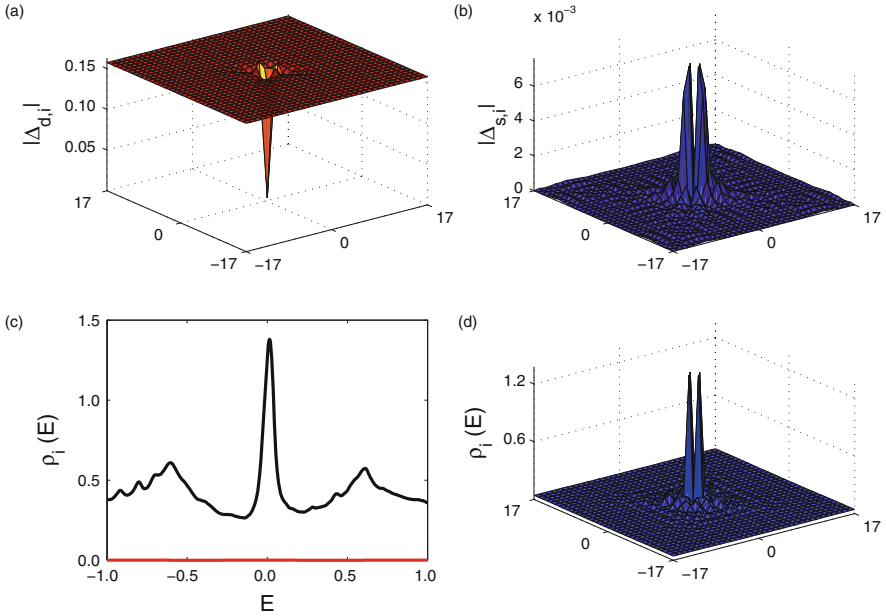


Fig. 3.8 Self-consistent solution to the BdG equations for a single impurity in a d -wave superconductor. The *top row* displays the spatial variation of the d -wave (a) and induced s -wave (b) components of the superconducting order parameter. The *bottom row* displays the local density of states on the site nearest neighbor to the impurity site (c) and the spatial dependence of the LDOS at the resonance energy $E_r = 0.014t$ (d). The calculations are carried out for the $d_{x^2-y^2}$ -wave superconductor defined on a two-dimensional square lattice. The pairing interaction is taken to be $V = 1.5t$ and the temperature $T = 0.01t$. The supercell size has the dimension of 35 by 35. The nonmagnetic impurity potential strength $\epsilon_I = 100t$. Here we have used a tight-binding model up to next-nearest neighbor hopping with $t' = -0.2t$ and $\mu = -0.8t$. The broadening parameter is $\gamma = 0.02t$

nodal direction of the $d_{x^2-y^2}$ -wave order parameter. These results are fully consistent with those obtained from the T -matrix theory.

Before closing this chapter, one remark is in order. All of the BdG equations presented so far are derived within an effective BCS theory, which is believed to describe reasonably well the quasiparticles in the superconducting dome even for high-temperature cuprates. Actually, the phase diagram of high-temperature cuprate superconductors is much more complicated with an antiferromagnetic Neel order in its parent compound. These features are mostly discussed in the t - J model, which is a low-energy model derived from the one-band Hubbard model in the localized moment limit. Therefore, it should be appropriate to discuss the superconducting phase within this model. The t - J model Hamiltonian defined on a two-dimensional square lattice can be written as:

$$\begin{aligned} \mathcal{H} = & - \sum_{\langle ij \rangle \sigma} t_{ij} c_{i\sigma}^\dagger c_{j\sigma} + \sum_{i \in I} \varepsilon_i n_i - \mu \sum_i n_i \\ & + \frac{J}{2} \sum_{\langle ij \rangle} [\mathbf{S}_i \cdot \mathbf{S}_j - \frac{1}{4} n_i n_j] + \frac{W}{2} \sum_{\langle ij \rangle} n_i n_j. \end{aligned} \quad (3.54)$$

Here the electrons are subjected to single occupancy constraint with \mathbf{S}_i the spin- $\frac{1}{2}$ operator on site i . The quantity $n_i = \sum_{\sigma} c_{i\sigma}^\dagger c_{i\sigma}$ is the electron number operator on site i and ε_i is the on-site single-particle potential introduced to describe the impurity scattering or more generally disorder effect. The superexchange interaction $J > 0$ ensures an antiferromagnetic state at zero doping. We have also included a direct nearest-neighbor interaction term so that $W = 0$ and $J/4$ correspond to two versions of the standard t - J model. This term will also adjust the magnitude of the resultant d -wave OP, as will be shown below. Upon doping, the model can be solved within the slave-boson mean-field (SBMF) method [42]. The electron operator as

$$c_{i\sigma} = b_i^\dagger f_{i\sigma}, \quad (3.55)$$

where $f_{i\sigma}$ and b_i are the operators for a spinon (a neutral spin- $\frac{1}{2}$ fermion) and a holon (a spinless charged boson). These auxiliary degrees of freedom are subjected to the constraint

$$b_i^\dagger b_i + \sum_{\sigma} f_{i\sigma}^\dagger f_{i\sigma} \leq 1, \quad (3.56)$$

arising from the single occupancy of electrons $\sum_{\sigma} c_{i\sigma}^\dagger c_{i\sigma} \leq 1$. In the SBFM method, this constraint is enforced by introducing a term into the Hamiltonian

$$\sum_i \lambda_i [1 - b_i^\dagger b_i - \sum_{\sigma} f_{i\sigma}^\dagger f_{i\sigma}], \quad (3.57)$$

where λ_i is the site-dependent Lagrange multiplier in the presence of impurity scattering potential. In addition, the spin and electron density operators are given

by

$$\mathbf{S}_i = \frac{1}{2} \sum_{\sigma\sigma'} f_{i\sigma}^\dagger \boldsymbol{\sigma}_{\sigma\sigma'} f_{i\sigma'} , \quad (3.58)$$

with $\boldsymbol{\sigma}$ being the Pauli matrix, and

$$n_{i\sigma} = f_{i\sigma}^\dagger f_{i\sigma} . \quad (3.59)$$

By applying the Wick theorem to the interaction terms, we derive a mean-field Hamiltonian

$$\mathcal{H}_{\text{MF}} = \sum_{ij,\sigma} \tilde{h}_{ij} f_{i\sigma}^\dagger f_{j\sigma} + \sum_{ij} [\Delta_{ij} f_{i\uparrow}^\dagger f_{j\downarrow}^\dagger + \text{H.c.}] + \sum_i \lambda_i (1 - b_i^* b_i) \quad (3.60)$$

Here the single-particle Hamiltonian is given by

$$\tilde{h}_{ij} = -t_{ij} b_i b_j^* - \left(\frac{J}{2} + W \right) \chi_{ij} + (\varepsilon_i - \mu - \lambda_i) \delta_{ij} , \quad (3.61)$$

with the resonance valence bond order

$$\chi_{ij} = \frac{1}{4} \sum_{\sigma} [\langle f_{i\sigma}^\dagger f_{j\sigma} \rangle + \text{c.c.}] , \quad (3.62)$$

and the pair potential

$$\Delta_{ij} = \frac{J - W}{2} [\langle f_{i\uparrow} f_{i\downarrow} \rangle - \langle f_{i\downarrow} f_{j\uparrow} \rangle] . \quad (3.63)$$

Due to the holon Bose condensation, which is now treated as a c -number, at low temperatures, the quasiparticles are determined by the spinon degree of freedom only. Without loss of generality, when we take the holon operator as a real number, the application of the Hellmann-Feynman theorem gives rise to the constraints

$$b_i^2 + \sum_{\sigma} \langle f_{i\sigma}^\dagger f_{i\sigma} \rangle = 1 , \quad (3.64)$$

and

$$\lambda_i = - \sum_j t_{ij} \chi_{ij} b_j / b_i . \quad (3.65)$$

Within these mean-field approximations, the BdG equations are derived to be

$$\sum_j \begin{pmatrix} \tilde{h}_{ij} & \Delta_{ij} \\ \Delta_{ij}^\dagger & -\tilde{h}_{ij}^* \end{pmatrix} \begin{pmatrix} u_j^n \\ v_j^n \end{pmatrix} = E_n \begin{pmatrix} u_i^n \\ v_i^n \end{pmatrix} . \quad (3.66)$$

The local electronic structure around a single nonmagnetic impurity in the t - J model has been studied in the further simplification with a uniform b_i [40, 43]. The results from these studies are qualitatively consistent with those obtained from the above phenomenological BCS model for d -wave superconductors. The full self-consistent solution to the above BdG equations is left for readers to practise.

References

1. A.V. Balatsky, I. Vekhter, J.-X. Zhu, Rev. Mod. Phys. **78**, 373 (2006)
2. A.L. Fetter, Phys. Rev. A **140**, 1921 (1965)
3. K. Machida, F. Shibata, Prog. Theor. Phys. **47**, 1817 (1972)
4. H. Shiba, Prog. Theor. Phys. **50**, 50 (1973)
5. K. Machida, Prog. Theor. Phys. **51**, 1667 (1974)
6. L. Yu, Acta Phys. Sin. Ch.-Ed. **21**, 75 (1965)
7. H. Shiba, Prog. Theor. Phys. **40**, 435 (1968)
8. A.I. Rusinov, Zh. Eksp. Teor. Fiz. Pis'ma Red. **9**, 146 (1968) [JETP Lett. **9**, 85 (1969)]
9. A.I. Rusinov, Zh. Eksp. Teor. Fiz. **56**, 2047 (1969) [Sov. Phys. JETP **29**, 1101 (1969)]
10. V. Mourik et al., Science **336**, 1003 (2012)
11. A. Das et al., Nat. Phys. **8**, 887 (2012)
12. L. Rokhinson, X. Liu, J.K. Furdyna, Nat. Phys. **8**, 795 (2012)
13. C.W. J. Beenakker, Annu. Rev. Condens. Matter Phys. **4**, 113 (2013)
14. C. Nayak, S.H. Simon, A. Stern, M. Freeman, S. Das Sarma, Rev. Mod. Phys. **80**, 1083 (2008)
15. N.B. Kopnin, M.M. Salomaa, Phys. Rev. B **44**, 9667 (1991)
16. G. Volovik, JEPT Lett. **70**, 609 (1999)
17. S.R. Elliott, M. Franz, Rev. Mod. Phys. **87**, 137 (2015)
18. I. Martin, A.F. Morpurgo, Phys. Rev. B **85**, 144505 (2012)
19. S. Nadj-Perge, I.K. Drozdov, B.A. Bernevig, A. Yazdani, Phys. Rev. B **88**, 020407 (2013)
20. F. Pientka, L.I. Glazman, F. von Oppen, Phys. Rev. B **89**, 180505(R) (2014)
21. I. Reis, D.J.J. Marchand, M. Franz, Phys. Rev. B **90**, 085124 (2014)
22. A.Y. Kitaev, Phys. Usp. **44**, 131 (2001)
23. B. Braunecker, P. Simon, Phys. Rev. Lett. **111**, 147202 (2013)
24. J. Klinovaja, P. Stano, A. Yazdani, D. Loss, Phys. Rev. Lett. **111**, 186805 (2013)
25. M.M. Vazifeh, M. Franz, Phys. Rev. Lett. **111**, 206802 (2013)
26. D.J. Scalapino, Phys. Rep. **250**, 329 (1995)
27. D.J. van Harlingen, Rev. Mod. Phys. **67**, 515 (1995)
28. P.A. Lee, Phys. Rev. Lett. **71**, 1887 (1993)
29. J.M. Byers, M.E. Flatté, D.J. Scalapino, Phys. Rev. Lett. **71**, 3363 (1993)
30. C.H. Choi, Phys. Rev. B **50**, 3491 (1994)
31. A.V. Balatsky, M.I. Salkola, A. Rosengren, Phys. Rev. B **51**, 15547 (1995); A.V. Balatsky, M.I. Salkola, Phys. Rev. Lett. **76**, 2386 (1996)
32. M.I. Salkola, A.V. Balatsky, D.J. Scalapino, Phys. Rev. Lett. **77**, 1841 (1996); M.I. Salkola, A.V. Balatsky, J.R. Schrieffer, Phys. Rev. B **55**, 12648 (1997)
33. M. Franz, C. Kallin, A.J. Berlinsky, Phys. Rev. B **54**, R6897 (1996)
34. Y. Onishi et al., J. Phys. Soc. Jpn. **65**, 675 (1996)
35. M.E. Flatté, J.M. Byers, Phys. Rev. Lett. **80**, 4546 (1998)
36. A. Yazdani, C.M. Howald, C.P. Lutz, A. Kapitulnik, D.M. Eigler, Phys. Rev. Lett. **83**, 176 (1999)
37. E.W. Hudson, S.H. Pan, A.K. Gupta, K.-W. Ng, J.C. Davis, Science **258**, 88 (1999)

38. A. Shnirman, I. Adagideli, P.M. Goldbart, A. Yazdani, *Phys. Rev. B* **60**, 7517 (1999)
39. H. Tanaka, K. Kuboki, M. Sigrist, *Int. J. Mod. Phys. B* **12**, 2447 (1998)
40. H. Tsuchiura, Y. Tanaka, M. Ogata, S. Kashiwaya, *J. Phys. Soc. Jpn.* **68**, 2510 (1999)
41. S.H. Pan, E.W. Hudson, K.M. Lang, H. Eisaki, S. Uchida, J.C. Davis, *Nature (London)* **403**, 746 (2000)
42. G. Kotliar, J. Liu, *Phys. Rev. B* **38**, 5142 (1988)
43. J.-X. Zhu, T.K. Lee, C.S. Ting, C.-R. Hu, *Phys. Rev. B* **61**, 8667 (2000)

Chapter 4

Disorder Effects on Electronic and Transport Properties in Superconductors

Abstract In this chapter, we discuss the disorder effects. The disorder comprises of a distribution of nonmagnetic impurities. As such, ensemble averaged effects will be relevant. We focus on the suppression of superconductivity by considering the response of superconducting order parameter, transition temperature, and superfluid density in both *s*-wave and *d*-wave superconductors. Finally, we also discuss the localization/delocalization of gapless quasiparticles in a disordered *d*-wave superconductor within a single-parameter scaling approach.

4.1 Anderson Theorem for Disordered *s*-Wave Superconductor

A remarkable feature of the isotropic *s*-wave superconductors is the insensitivity of the superconductivity to the diluted nonmagnetic impurities. This robustness is demonstrated by the Anderson theorem [1]. The theorem states that because the superconductivity arises from the instability of the Fermi surface upon the pairing of time-reversed electronic states, any perturbation should not affect the mean-field superconducting order parameter and transition temperature as long as it does not lift the Kramers degeneracy. We first discuss this theorem within the Abrikosov-Gorkov theory [2]. For simplicity, we consider the zero-ranged interactions between the conduction electrons and nonmagnetic impurities

$$U(\mathbf{r}) = u_0 \sum_{i \in I} \delta(\mathbf{r} - \mathbf{R}_i), \quad (4.1)$$

where u_0 is the strength of the scattering potential while \mathbf{R}_i is the position of individual impurities. The Abrikosov-Gorkov equations are derived in Chap. 1 and written as in the continuum limit

$$\left[i\omega_n + \frac{\nabla^2}{2m_e} + E_F - U(\mathbf{r}) \right] \mathcal{G}(\mathbf{r}, \mathbf{r}'; i\omega_n) + \int d\mathbf{r}'' \Delta(\mathbf{r}, \mathbf{r}'') \mathcal{F}^\dagger(\mathbf{r}'', \mathbf{r}'; i\omega_n) = \delta(\mathbf{r} - \mathbf{r}'), \quad (4.2a)$$

$$\left[-i\omega_n + \frac{\nabla^2}{2m_e} + E_F - U(\mathbf{r}) \right] \mathcal{F}^\dagger(\mathbf{r}, \mathbf{r}'; i\omega_n) + \int d\mathbf{r}'' \Delta^*(\mathbf{r}, \mathbf{r}'') \mathcal{G}(\mathbf{r}'', \mathbf{r}'; i\omega_n) = 0, \quad (4.2b)$$

Here $\omega_n = (2n + 1)\pi T$ with n any integer is the Matsubara frequency for electrons, E_F is the Fermi energy, and \mathcal{G} and \mathcal{F}^\dagger are the normal and anomalous Green's functions. The pair potential is given by

$$\Delta^*(\mathbf{r}, \mathbf{r}') = V(\mathbf{r} - \mathbf{r}') T \sum_{\omega_n} \mathcal{F}^\dagger(\mathbf{r}, \mathbf{r}'; i\omega_n), \quad (4.3)$$

where $-V(\mathbf{r} - \mathbf{r}')$ is the pairing interaction. After averaging over the impurity configurations, the transitional invariance is restored so that we can write the above system of equations in the momentum space

$$[i\omega_n - \xi_{\mathbf{p}} - \mathcal{G}_{\omega_n}] \mathcal{G}(\mathbf{p}; i\omega_n) + [\Delta(\mathbf{p}) + \mathcal{F}_{\omega_n}] \mathcal{F}^\dagger(\mathbf{p}; i\omega_n) = 1, \quad (4.4a)$$

$$[i\omega_n + \xi_{\mathbf{p}} + \mathcal{G}_{-\omega_n}] \mathcal{F}^\dagger(\mathbf{p}; i\omega_n) + [\Delta^*(\mathbf{p}) + \mathcal{F}_{\omega_n}^\dagger] \mathcal{G}(\mathbf{p}; i\omega_n) = 0, \quad (4.4b)$$

where

$$\xi_{\mathbf{p}} = \frac{\mathbf{p}^2}{2m_e} - E_F, \quad (4.5)$$

and

$$\mathcal{G}_{\omega_n} = \frac{n_i u_0^2}{(2\pi)^2} \int \mathcal{G}(\mathbf{p}'; i\omega_n) d\mathbf{p}', \quad (4.6a)$$

$$\mathcal{F}_{\omega_n}^\dagger = \frac{n_i u_0^2}{(2\pi)^2} \int \mathcal{F}^\dagger(\mathbf{p}'; i\omega_n) d\mathbf{p}', \quad (4.6b)$$

with n_i as the density of nonmagnetic impurities. We note that $\mathcal{F}_{\omega_n}^\dagger = (\mathcal{F}_{\omega_n})^*$. We can solve Eq. (4.4) to obtain

$$\mathcal{G}(\mathbf{p}; i\omega_n) = -\frac{i\omega_n - \mathcal{G}_{\omega_n} + \xi_{\mathbf{p}}}{-(i\omega_n - \mathcal{G}_{\omega_n})^2 + \xi_{\mathbf{p}}^2 + |\Delta^*(\mathbf{p}) + \mathcal{F}_{\omega_n}^\dagger|^2}, \quad (4.7a)$$

$$\mathcal{F}^\dagger(\mathbf{p}; i\omega_n) = \frac{\Delta^*(\mathbf{p}) + \mathcal{F}_{\omega_n}^\dagger}{-(i\omega_n - \mathcal{G}_{\omega_n})^2 + \xi_{\mathbf{p}}^2 + |\Delta^*(\mathbf{p}) + \mathcal{F}_{\omega_n}^\dagger|^2}. \quad (4.7b)$$

On substitution of Eq.(4.7) into Eq. (4.6), we find

$$\mathcal{G}_{\omega_n} = \frac{n_i u_0^2}{(2\pi)^2} \int \frac{-(i\omega_n - \mathcal{G}_{\omega_n})}{-(i\omega_n - \mathcal{G}_{\omega_n})^2 + \xi_{\mathbf{p}'}^2 + |\Delta^*(\mathbf{p}') + \mathcal{F}_{\omega_n}^\dagger|^2} d\mathbf{p}' , \quad (4.8a)$$

$$\mathcal{F}_{\omega_n}^\dagger = \frac{n_i u_0^2}{(2\pi)^2} \int \frac{\Delta^*(\mathbf{p}') + \mathcal{F}_{\omega_n}^\dagger}{-(i\omega_n - \mathcal{G}_{\omega_n})^2 + \xi_{\mathbf{p}'}^2 + |\Delta^*(\mathbf{p}') + \mathcal{F}_{\omega_n}^\dagger|^2} d\mathbf{p}' . \quad (4.8b)$$

Here we have dropped the contribution to the integral from the term linear in $\xi_{\mathbf{p}}$ in the numerator of $\mathcal{G}(\mathbf{p}; i\omega_n)$. The pair potential is subjected to the self-consistency:

$$\Delta^*(\mathbf{k}) = T \sum_{i\omega_n} \int \frac{d\mathbf{p}}{(2\pi)^2} V(\mathbf{k} - \mathbf{p}) \mathcal{F}^\dagger(\mathbf{p}; i\omega_n) . \quad (4.9)$$

In the weak-coupling limit, the pairing interaction is limited to a small range near the Fermi surface. As we discussed in the early chapter, for the s -wave pairing symmetry, the pairing interaction is approximated as

$$V(\mathbf{k} - \mathbf{p}) = V_s . \quad (4.10)$$

From the structure of Eq. (4.8), we can write that for the s -wave pairing symmetry

$$\mathcal{G}_{\omega_n} = -i\omega_n \eta_{\omega_n} , \quad (4.11)$$

and

$$\mathcal{F}_{\omega_n} = \Delta_s \eta_{\omega_n} . \quad (4.12)$$

This gives rise to

$$\begin{aligned} \eta_{\omega_n} &= \frac{n_i u_0^2}{(2\pi)^2} \int \frac{1 + \eta_{\omega_n}}{(\omega_n^2 + \Delta_s^2)(1 + \eta_{\omega_n})^2 + \xi_{\mathbf{p}}^2} d\mathbf{p} \\ &= n_i u_0^2 N(0) \int \frac{d\phi}{2\pi} \int \frac{1 + \eta_{\omega_n}}{(\omega_n^2 + \Delta_s^2)(1 + \eta_{\omega_n})^2 + \xi^2} d\xi \end{aligned} \quad (4.13)$$

$$= n_i u_0^2 N(0) \int \frac{d\phi}{2\pi} \frac{\pi(1 + \eta_{\omega_n})}{\sqrt{(\omega_n^2 + \Delta_s^2)(1 + \eta_{\omega_n})^2}} \quad (4.14)$$

$$= \frac{1}{2\tau} \frac{1}{\sqrt{\omega_n^2 + \Delta_s^2}} \quad (4.15)$$

where $\tau^{-1} = 2\pi n_i u_0^2 N(0)$ with $N(0)$ the density of states per electron spin at the Fermi energy is the impurity scattering rate. Here we have used the integral

$$\int \frac{dx}{1+x^2} = \tan^{-1}(x) .$$

The self-consistency solution in the presence of impurity scattering can then be found as

$$\Delta_s = 2g_s \pi T \sum_{i\omega_n} \frac{\Delta_s}{\sqrt{\omega_n^2 + \Delta_s^2}} , \quad (4.16)$$

where $g_s = N(0)V_s/2$. We note that when the summation over the Matsubara frequency is performed, the cutoff frequency ω_c , which is related to the pairing mechanism, should be introduced. Equation (4.16) indicates that the s -wave superconducting order parameter does not depend on the impurity scattering rate.

The Anderson theorem can also be shown through the BdG equations [3]. As discussed in Chap. 1, the s -wave order parameter is given as

$$\Delta(\mathbf{r}) = V_s \sum_{n(E_n \geq 0)} u_n(\mathbf{r}) v_n^*(\mathbf{r}) \tanh\left(\frac{E_n}{2k_B T}\right) . \quad (4.17)$$

At zero temperature, it is further simplified as

$$\Delta(\mathbf{r}) = V_s \sum_{n(E_n \geq 0)} u_n(\mathbf{r}) v_n^*(\mathbf{r}) . \quad (4.18)$$

On the other hand, the BCS variational wave function that pairs electrons in time-reversed states is given by

$$|\Psi_{\text{BCS}}\rangle = \prod_n (a_n + b_n c_{n\uparrow}^\dagger c_{n\downarrow}^\dagger) |0\rangle . \quad (4.19)$$

Here $|0\rangle$ stands for the filling Fermi sea, and $c_{n\uparrow}^\dagger$ creates an up-spin electron with wave function $\phi_n(\mathbf{r})$, and $c_{n\downarrow}^\dagger$ creates a down-spin electron in $\phi_n(\mathbf{r})^*$, where $\phi_n(\mathbf{r})$ is an eigenfunction of the single-particle Hamiltonian. It thus restricts the trial wave function to the subspace of either doubly occupied or empty levels. The coefficients a_n and b_n are subjected to the normalization condition $|a_n|^2 + |b_n|^2 = 1$. When $\Delta(\mathbf{r})$ is independent of \mathbf{r} , we have

$$u_n(\mathbf{r}) = a_n \phi_n(\mathbf{r}) , \quad (4.20a)$$

$$v_n(\mathbf{r}) = b_n \phi_n(\mathbf{r}) , \quad (4.20b)$$

which leads to

$$\Delta(\mathbf{r}) = V_s \sum_n a_n b_n^* |\phi_n(\mathbf{r})|^2. \quad (4.21)$$

In the absence of a magnetic field, a_n , b_n , and $\phi_n(\mathbf{r})$ can be taken to be real. With the above variational wave function, the energy is given by

$$\begin{aligned} E_G &= \langle \Psi_{\text{BCS}} | \mathcal{H} | \Psi_{\text{BCS}} \rangle \\ &= \sum_n 2\xi_n - V_s \sum_{n \neq m} a_n a_m b_n b_m \int \phi_n^2(\mathbf{r}) \phi_m^2(\mathbf{r}) d\mathbf{r}, \end{aligned} \quad (4.22)$$

subject to the normalization condition for a_n and b_n , where ξ_n is the eigenvalue of the state $\phi_n(\mathbf{r})$. The a_n and b_n can be written as $a_n = \sin \theta_n$ and $b_n = \cos \theta_n$. The variational principle leads to the equation

$$\xi_n \tan(2\theta_n) = \frac{V_s}{2} \sum_{n \neq m} \sin(2\theta_m) \int \phi_n^2(\mathbf{r}) \phi_m^2(\mathbf{r}) d\mathbf{r}. \quad (4.23)$$

We now define

$$\tan(2\theta_n) = \frac{\Delta_n}{\xi_n}, \quad (4.24)$$

which implies

$$\sin(2\theta_n) = \frac{\Delta_n}{\sqrt{\xi_n^2 + \Delta_n^2}} = 2a_n b_n. \quad (4.25)$$

Equation (4.23) now becomes

$$\Delta_n = V_s \sum_{m \neq n} \frac{\Delta_m}{2\sqrt{\xi_m^2 + \Delta_m^2}} \int \phi_n^2(\mathbf{r}) \phi_m^2(\mathbf{r}) d\mathbf{r}. \quad (4.26)$$

Using Eq. (4.21), we obtain

$$\Delta_n = \int \Delta(\mathbf{r}) \phi_n^2(\mathbf{r}) d\mathbf{r}, \quad (4.27)$$

once the condition $m \neq n$ is relaxed.

For a pristine system, $\Delta_n = \Delta(\mathbf{r}) = \Delta_0$. For disordered systems, $\phi_n(\mathbf{r})$ is a complicated wave function. However, if we assume $\Delta(\mathbf{r}) = \tilde{\Delta}$, then the normalization condition $\int \phi_n(\mathbf{r})^2 d\mathbf{r} = 1$ gives rise to $\Delta_n = \tilde{\Delta}$, which is independent

of n . With this condition, the gap equation (4.26) gives

$$\tilde{\Delta} = \int V_s \frac{\tilde{\Delta} N(\epsilon, \mathbf{r})}{\sqrt{\epsilon^2 + \tilde{\Delta}^2}} \phi_n^2(\mathbf{r}) d\mathbf{r}, \quad (4.28)$$

where we introduce the normal-state single-particle density of states for the disordered system

$$N(\epsilon, \mathbf{r}) = \sum_m \phi_m^2(\mathbf{r}) \delta(\epsilon - \xi_m). \quad (4.29)$$

In weakly disordered system, $N(\epsilon, \mathbf{r}) \approx N(0)$, the gap equation (4.28) gives $\tilde{\Delta} = \Delta_0$. As such, the transition temperature is also insensitive to the disorder effect. This is the Anderson theorem.

4.2 Suppression of Superconductivity in a Disordered d -Wave Superconductor

For the $d_{x^2-y^2}$ -wave pairing symmetry, the pairing interaction can be written as

$$V(\mathbf{k} - \mathbf{p}) = V_d \cos 2\phi \cos 2\phi', \quad (4.30)$$

where the angle $\phi = \tan^{-1}(k_{F,y}/k_{F,x})$ with $k_{F,x(y)}$ the two components of the Fermi wave vector. Correspondingly, the superconducting pair potential is of the form

$$\Delta(\mathbf{k}) = \Delta_d \cos 2\phi. \quad (4.31)$$

This special form of the d -wave pairing symmetry leads to the breaking of the scaling law for \mathcal{F}_{ω_n} and in particular $\mathcal{F}_{\omega_n} = 0$. The self-consistency equation for the d -wave pair potential then becomes

$$\Delta_d = 2g_d \pi T \sum_{i\omega_n} \int \frac{d\phi'}{2\pi} \frac{\Delta_d \cos^2(2\phi')}{\sqrt{\omega_n^2(1 + \eta_{\omega_n})^2 + (\Delta_d \cos(2\phi'))^2}}, \quad (4.32)$$

where $g_d = N(0)V_s/2$ and

$$\eta_{\omega_n} = \frac{1}{2\tau} \int \frac{d\phi'}{2\pi} \frac{1 + \eta_{\omega_n}}{\sqrt{\omega_n^2(1 + \eta_{\omega_n})^2 + (\Delta_d \cos(2\phi'))^2}}. \quad (4.33)$$

Equation (4.32) suggests that the nonmagnetic impurity scattering is pairing breaking and can suppress the transition temperature of the d -wave superconductivity.

The transition temperature from the AG theory is then found [4–7] to be

$$\ln\left(\frac{T_c}{T_{c0}}\right) = \Psi\left(\frac{1}{2}\right) - \Psi\left(\frac{1}{2} + \frac{1}{4\pi\tau T_c}\right). \quad (4.34)$$

Here $\Psi(x)$ is the digamma function and T_{c0} is the transition temperature of a pure system.

The impurity scattering also influences the superfluid density and the penetration depth in a d -wave superconductor. For these quantities, one calculates the electromagnetic response tensor \mathcal{K} , relating the current density \mathbf{j} to an applied vector potential \mathbf{A} :

$$\mathbf{j} = -\mathcal{K} \mathbf{A}. \quad (4.35)$$

If the electromagnetic tensor is diagonal $\mathcal{K}_{ij} = \mathcal{K}_{ii}\delta_{ij}$, the penetration depth λ_i for the current flowing in the direction i is given by

$$\lambda_i^{-2} = (4\pi/c)\mathcal{K}_{ii}, \quad (4.36)$$

where c is the velocity of light. The AG theory for a disordered BCS d -wave superconductivity then gives the response tensor [4]:

$$\mathcal{K}_{ij} = \frac{e^2}{c} \left\langle v_i(\mathbf{k})v_j(\mathbf{k}) \int_0^\infty d\omega \tanh\left(\frac{\omega}{2k_B T}\right) \text{Re} \frac{\Delta_k^2}{(\tilde{\omega}^2 - \Delta_k^2)^{3/2}} \right\rangle. \quad (4.37)$$

Here $\langle \dots \rangle \equiv 2(2\pi)^{-2} \int dS_F / |\mathbf{v}(\mathbf{k})| \dots$ represents an angular average over an arbitrary Fermi surface in a two-dimensional metal, and $\mathbf{v}(\mathbf{k})$ is the Fermi velocity. The renormalized frequency $\tilde{\omega} = \omega - \Sigma_0$ with the impurity self-energy obtained from the T -matrix approximation [8–13]

$$\Sigma_0 = \frac{\Gamma G_0}{(u_0 N(0))^{-1} - G_0^2}, \quad (4.38)$$

where $\Gamma = n_i/\pi N(0) = 1/2\tau$ is the scattering rate with n_i being the impurity concentration, and G_0 is the integrated diagonal Green's function averaged over the impurity configuration

$$G_0 = -i \left\langle \frac{\tilde{\omega}}{(\tilde{\omega}^2 - \Delta_k^2)^{1/2}} \right\rangle. \quad (4.39)$$

Equation (4.37) can be decomposed into two parts

$$\mathcal{K}_{ij}(T) = \mathcal{K}_{ij}(T=0) + \delta\mathcal{K}_{ij}(T), \quad (4.40)$$

where

$$\mathcal{K}_{ij}(T=0) = \frac{e^2}{c} \left\langle v_i(\mathbf{k}) v_j(\mathbf{k}) \int_0^\infty d\omega \operatorname{Re} \frac{\Delta_k^2}{(\tilde{\omega}^2 - \Delta_k^2)^{3/2}} \right\rangle, \quad (4.41)$$

and

$$\delta \mathcal{K}_{ij}(T) = \frac{-2e^2}{c} \left\langle v_i(\mathbf{k}) v_j(\mathbf{k}) \int_0^\infty d\omega f_{\text{FD}}(\omega) \operatorname{Re} \frac{\Delta_k^2}{(\tilde{\omega}^2 - \Delta_k^2)^{3/2}} \right\rangle. \quad (4.42)$$

In the impurity-dominated gapless regime, the renormalized frequency takes the form [4] $\tilde{\omega} \rightarrow i\gamma + a\omega$, where γ is a constant dependent on the impurity concentration and scattering strength, while the constant $a \sim O(1)$. At low temperatures, it allows us to replace $\tilde{\omega}$ by this limiting form, which gives rise to

$$\delta \mathcal{K}_{ij}(T) = \frac{-e^2 \pi^2}{c} \frac{\gamma a T^2}{2} \left\langle v_i(\mathbf{k}) v_j(\mathbf{k}) \frac{\Delta_k^2}{(\gamma^2 + \Delta_k^2)^{5/2}} \right\rangle. \quad (4.43)$$

For the $d_{x^2-y^2}$ -wave pairing symmetry, the angular average in the above equation varies as γ^{-2} . It suggests that the coefficient of the T^2 -dependence in the penetration depth is proportional to the inverse γ but the T^2 behavior is valid in a very narrow temperature range $\sim \gamma$.

The impurity scattering also affects the zero-temperature tensor $\mathcal{K}_{ij}(T=0)$, which is given by

$$\mathcal{K}_{ij}(T=0) = \mathcal{K}_{ij}(T=0, \Gamma=0) + \frac{e^2}{c} \left\langle v_i(\mathbf{k}) v_j(\mathbf{k}) \frac{\Delta_k^2}{(\gamma^2 + \Delta_k^2)^{1/2}} \right\rangle. \quad (4.44)$$

The scaling relation between the zero-temperature superfluid density $\rho_s \propto \mathcal{K}_{ii}$ and the superconducting transition temperature based on the AG theory for a disordered d -wave superconductor is shown in Fig. 4.1. It has been found that for high-temperature cuprate superconductors, the experimentally observed T_c is much more robust than one would expect from the AG theory, when it is measured against the corresponding zero-temperature superfluid density. Originally, the failure has also been ascribed to the mean-field nature of the BCS-type theory in view of the fact that the normal state is a non-Fermi liquid in the optimally doped high-temperature cuprates [15]. It turns out [14] that the discrepancy between the theory and the experiment comes mainly from the inadequacy of the AG theory itself to determine the suppression of the superconducting transition temperature for high-temperature d -wave superconductors. In the AG theory, one crucial assumption in the derivation of the transition temperature is that the spatial dependence of the superconducting order is replaced by an averaged value, as shown in Fig. 4.2. This assumption is only valid when the superconducting coherence ξ is much larger than the average distance between impurities l_i . The superconducting coherence length is inversely proportional to the maximal amplitude of the order parameter in the momentum

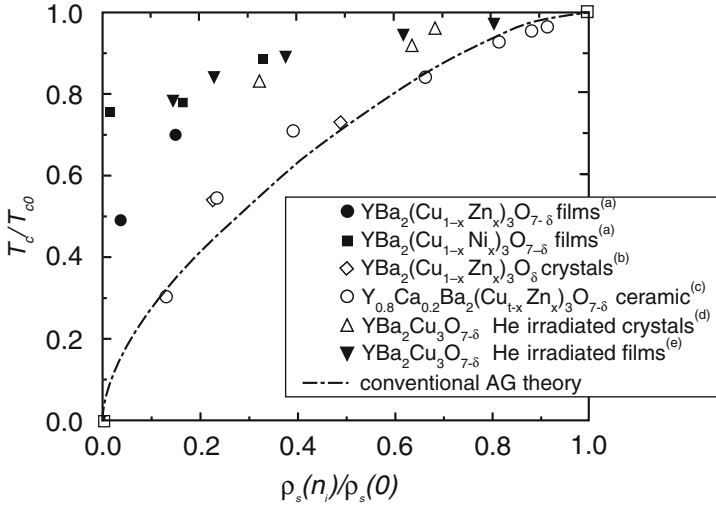


Fig. 4.1 Normalized critical temperature versus the normalized zero-temperature superfluid density. The *dashed line* denotes the results from the AG theory while the experimental data are represented by symbols. From [14]

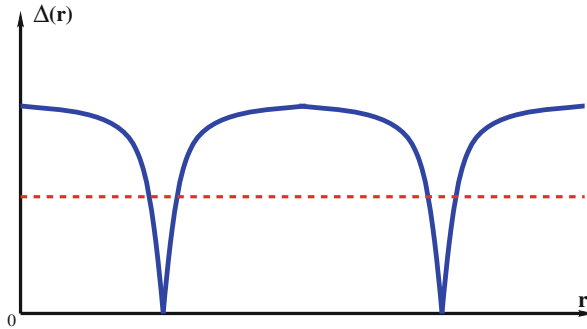


Fig. 4.2 Schematic drawing of the spatial dependence of the superconducting order parameter around impurities in a superconductor with a short coherence length (*solid blue line*). In the AG theory, it is replaced with an averaged value (*dashed red line*)

space and has the following form:

$$\xi(T) \approx \xi_0(1 - T/T_{c0})^{-1/2}. \quad (4.45)$$

For a superconductor with a short coherence length, the superconducting order parameter can be recovered to the bulk value within a distance much shorter than l_i (see solid blue line in Fig. 4.2). As such, the areas of the depressed order parameter around impurities do not overlap, and the superconducting order parameter in most areas of the system is not affected at all. Only when the depressed areas begin to

overlap ($\xi(T) \gg l_i$), the entire system can be affected as if the order parameter is suppressed everywhere. This weakness of the AG theory can be fully overcome by solving the BdG equations self-consistently, in which the inhomogeneity of the superconducting order parameter is fully taken care of.

To be complete, let us re-derive the superfluid density within the lattice model. The derivation follows closely that for the optical properties discussed in Chap. 2. Again we calculate the superfluid stiffness for a current response to a vector potential of wave vector \mathbf{q} and frequency ω along the x -direction in a two-dimensional square lattice through the Kubo formula. By expanding the Hamiltonian to include the interaction between electrons and an electromagnetic field, the time-dependent Hamiltonian is given by

$$\mathcal{H}_t = \mathcal{H}_{BCS} + \mathcal{H}'(t), \quad (4.46)$$

where the BCS Hamiltonian in the tight-binding model has already been discussed in Chap. 2, and $\mathcal{H}'(t)$ describes the coupling of electrons to the external electromagnetic field up to the second order

$$\mathcal{H}'(t) = -ea \sum_i A_x(\mathbf{r}_i, t) \left(J_x^P(\mathbf{r}_i) + \frac{ea}{2} A_x(\mathbf{r}_i, t) K_x(\mathbf{r}_i) \right), \quad (4.47)$$

where a is the lattice constant, A_x is the vector potential along the x -axis, and the particle current density operator

$$J_x^P(\mathbf{r}_i) = -i \sum_{\sigma, \delta} [t_{i, i+\delta} c_{i\sigma}^\dagger c_{i+\delta, \sigma} - \text{H.c.}], \quad (4.48)$$

and the kinetic energy density operator

$$K_x(\mathbf{r}_i) = - \sum_{\sigma, \delta} [t_{i, i+\delta} c_{i\sigma}^\dagger c_{i+\delta, \sigma} + \text{H.c.}]. \quad (4.49)$$

The variable $\delta = \hat{x}$ for the nearest-neighbor hopping model and $\delta = \hat{x}, \hat{x} \pm \hat{y}$ for next-nearest-hopping model. The charge current density operator along the x -axis is then found to be

$$J_x^Q(\mathbf{r}_i) \equiv - \frac{\delta \mathcal{H}'(t)}{\delta A_x(\mathbf{r}_i, t)} = eJ_x^P(\mathbf{r}_i) + e^2 K_x(\mathbf{r}_i) A_x(\mathbf{r}_i, t). \quad (4.50)$$

We then calculate the paramagnetic component of the electric current density to the first order in A_x :

$$\langle J_x^P(\mathbf{r}_i(t)) \rangle = -i \int_{-\infty}^t \langle [J_x^P(t), \mathcal{H}'(t')]_- \rangle_0 dt', \quad (4.51)$$

while the diamagnetic part only to the zeroth order, that is, $\langle K_x \rangle_0$. Here $\langle \dots \rangle_0$ stands for the thermodynamic average with respect to the non-perturbed \mathcal{H}_{BCS} . The current response is then obtained as

$$-\frac{J_x^Q(\mathbf{r}_i)}{e^2 A_x(\mathbf{r}_i)} = -ie^{-\mathbf{q} \cdot \mathbf{r}_i} \int_{-\infty}^t dt' \langle [J_x^P(\mathbf{q}, t), J_x^P(-\mathbf{q}, t')]_- \rangle_0 - \langle K_x(\mathbf{r}_i) \rangle_0. \quad (4.52)$$

Please keep in mind that the variables t and t' in the vector potential and the integral boundary are the time.

We then perform a lattice average over the spatial variable \mathbf{r}_i to eliminate the atomic-scale fluctuations, and define an effective ‘‘Drude weight’’ as a measure of the superfluid density

$$\rho_s \equiv \frac{D_s}{\pi e^2} = -\langle K_x \rangle_0 + \Pi_{xx}(\mathbf{q} \rightarrow 0, \omega = 0). \quad (4.53)$$

Here the first term

$$\langle K_x \rangle_0 = \frac{1}{N_L} \sum_i K_{x,i} \quad (4.54)$$

with the local kinetic energy

$$K_{x,i} = -2t \sum_{n(E_n \geq 0)} \left(f(E_n) [u_{i+\hat{x}}^{n*} u_i^n + \text{c.c.}] + f(-E_n) [v_{i+\hat{x}}^n v_i^{n*} + \text{c.c.}] \right). \quad (4.55)$$

The second term is the current-current correlation function with a double sum over lattice sites

$$\Pi_{xx}(\mathbf{q} \rightarrow 0; \omega = 0) = \frac{1}{N_L} \sum_{i,j} \Pi_{xx}^{ij}(\omega = 0), \quad (4.56)$$

where

$$\Pi_{xx}^{ij}(\omega = 0) = \sum_{n_1(E_{n_1} \geq 0), n_2(E_{n_2} \geq 0)} A_{n_1, n_2}^i [A_{n-1, n_2}^{j*} + D_{n_1, n_2}^j] \frac{f(E_{n_1}) - f(E_{n_2})}{E_{n_1} - E_{n_2}}, \quad (4.57)$$

with

$$A_{n_1, n_2}^i = 2[u_{i+\hat{x}}^{n_1*} u_i^{n_2} - u_i^{n_1*} u_{i+\hat{x}}^{n_2}], \quad (4.58a)$$

$$D_{n_1, n_2}^i = 2[v_{i+\hat{x}}^{n_1} v_i^{n_2*} - v_i^{n_1} v_{i+\hat{x}}^{n_2*}]. \quad (4.58b)$$

Typical results from the solution to the BdG equations are shown in Fig. 4.3. As the superconducting coherence length increases, the discrepancy between the

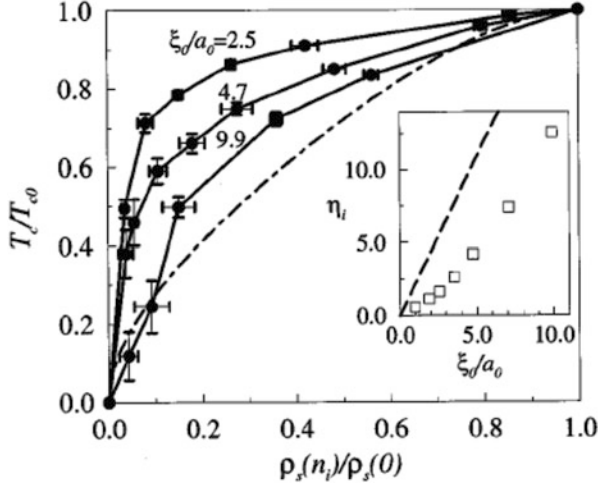


Fig. 4.3 Normalized critical temperature versus the normalized zero-temperature superfluid density obtained from a fully self-consistent solution to the BdG equations in a tight-binding model. The *dashed line* denotes the results from the AG theory. From [14]

rigorous critical temperature and that from the AG theory diminishes. However, at a very short coherence, the result from the AG theory deviates significantly from the true T_c . In addition, the typical temperature-dependence of the superfluid stiffness is shown in Fig. 4.4. The pileup of the impurity resonance states near the Fermi energy in a disordered d -wave superconductor gives rise to the T^2 -dependence of the superfluid stiffness at low temperatures. Increase of the impurity concentration expands the temperature range for the T^2 behavior of ρ_s before it turns into a T -linear behavior.

4.3 Quasiparticle Localization in a Disordered d -Wave Superconductor

In Sect. 3.4, we have shown that a single impurity in the unitary scattering limit can produce a zero-energy quasiparticle resonance states. These states have a long decay distance away from the impurity site. A natural question arises as to whether the possible overlap of these states in an ensemble of unitary impurities can create extended low-energy quasiparticle states. We consider this question by using the one-parameter scaling analysis. The one-parameter scaling analysis [17, 18] has been a popular method to study the electronic localization/delocalization in Anderson disordered metals. Our discussion is based on the transfer matrix method and follows that of MacKinnon and Kramer [19] for the disordered solids. To discuss the two-dimensional d -wave disordered superconductors, we first consider a system

Fig. 4.4 Temperature dependence of the normalized superfluid density calculated from a full self-consistent solution to the BdG equations in a two-dimensional lattice model with nearest-neighbor hopping approximation. From [16]

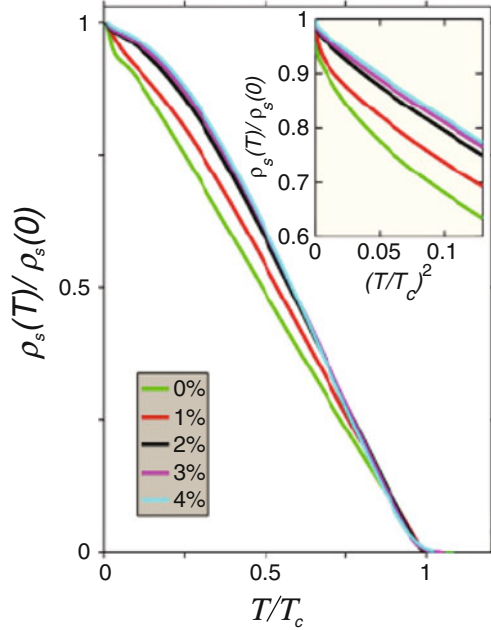
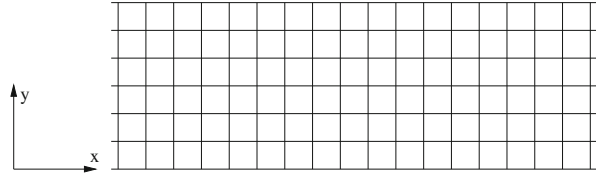


Fig. 4.5 Schematic drawing of a quasi-one-dimensional strip



of electrons defined on a quasi-one-dimensional strip. When the strip width goes to infinity, the strip is expanded into a two-dimensional lattice. The geometry is shown in Fig. 4.5.

We write down the Anderson Hamiltonian as

$$\mathcal{H} = - \sum_{ij} t_{ij} c_i^\dagger c_j + \sum_i \epsilon_i c_i^\dagger c_i . \quad (4.59)$$

Here the site index $i = (i_x, i_y)$ with the two components defined in the coordinate system shown in Fig. 4.5 and the variable ϵ_i is on-site potential for the disorder effect. For simplicity of discussion, we have neglected the spin index for electrons. By performing a canonical transformation,

$$c_i = \sum_n \phi_i^n \gamma_n , \quad (4.60)$$

with γ_n is the quasiparticle operator, the problem becomes to solve the Schrödinger equation

$$\sum_j H_{ij} \phi_j = E \phi_i . \quad (4.61)$$

In the nearest-neighbor hopping approximation, the expanded form of the above equation is

$$\phi_{i_x+1, i_y} = -E \phi_{i_x, i_y} + \epsilon_{i_x, i_y} \phi_{i_x, i_y} - \phi_{i_x, i_y+1} - \phi_{i_x, i_y-1} - \phi_{i_x-1, i_y} . \quad (4.62)$$

Here we have used the nearest-neighbor hopping parameter $t = 1$ and measured the energy in units of t . We introduce a column vector to denote the coefficients of the i_x -th one-dimensional slice (along the y -direction),

$$\hat{\phi}_{i_x} = \begin{pmatrix} \phi_{i_x, 1} \\ \phi_{i_x, 2} \\ \dots \\ \phi_{i_x, M} \end{pmatrix} , \quad (4.63)$$

where M is the width of the strip. Equation (4.62) can then be cast into a matrix form

$$\begin{pmatrix} \hat{\phi}_{i_x+1} \\ \hat{\phi}_{i_x} \end{pmatrix} = T_{i_x} \begin{pmatrix} \hat{\phi}_{i_x} \\ \hat{\phi}_{i_x-1} \end{pmatrix} . \quad (4.64)$$

Here the transfer matrix is given by

$$T_{i_x} = \begin{pmatrix} -(E\hat{1} - \hat{H}_{i_x}) - \hat{1} & \\ \hat{1} & \hat{0} \end{pmatrix} , \quad (4.65)$$

where the \hat{H}_{i_x} is the Hamiltonian for the i_x -th slice of the quasi-one-dimensional strip when it is not coupled to the rest. Equation (4.64) gives us a recursion formula for the coefficients $\hat{\phi}_{i_x}$. That is, if we are given the initial coefficients $\hat{\phi}_0$ and $\hat{\phi}_1$, the coefficient $\hat{\phi}_n$ can be obtained through the accumulated transfer matrix

$$P_n = \prod_{i_x=1}^n T_{i_x} . \quad (4.66)$$

That is,

$$\begin{pmatrix} \hat{\phi}_{n+1} \\ \hat{\phi}_n \end{pmatrix} = P_n \begin{pmatrix} \hat{\phi}_1 \\ \hat{\phi}_0 \end{pmatrix} . \quad (4.67)$$

The matrix P_n satisfies the Oseledec's multiplicative ergodic theorem [20, 21]: For any initial vector

$$\begin{pmatrix} \hat{\phi}_1 \\ \hat{\phi}_0 \end{pmatrix}, \quad (4.68)$$

there exists an orthonormal set of vectors v_i ($1 \leq i \leq 2M$) such that

$$\gamma_i = \lim_{n \rightarrow \infty} \frac{1}{n} \ln \| P_n v_i \| \quad (4.69)$$

exists. Due to the ergodicity of the system, the set of values $\{\gamma_i\}$ are independent on the initial values of the coefficients $(\hat{\phi}_1, \hat{\phi}_0)^{\text{Transpose}}$, and thus they describe the global properties of the system. The γ_i can be calculated as the log of the eigenvalues of

$$[P_n P_n^\dagger]^{\frac{1}{2n}}. \quad (4.70)$$

The vector v_i are now the eigenvectors of $P_n P_n^\dagger$ and are indecent of n for large n . In another word, the matrix $[P_n P_n^\dagger]^{\frac{1}{2n}}$ converges to a limiting matrix when $n \rightarrow \infty$, which determines the modulus of the eigenvalues of P_n and the corresponding eigenvectors. We note that the matrix P_n is not hermitian and the eigenvalues are in general complex. The eigenvectors v_i can also be called Lyapunov eigenvectors, which determine the properties of electronic states of disordered systems.

With the above introduction, let us turn to the case of disordered d -wave superconductors, where further technical details will be discussed on the calculation of the localization length. In the presence of disorder, the BdG equations (2.30) become

$$\begin{cases} E_n u_i^n = \sum_j \hat{h}_{ij} u_j^n + \sum_j \Delta_{ij} v_j^n, \\ E_n v_i^n = -\sum_j \hat{h}_{ij}^* v_j^n + \sum_j \Delta_{ji}^* u_j^n, \end{cases} \quad (4.71)$$

where the single particle Hamiltonian

$$h_{ij} = -t_{ij} + (\epsilon_i - \mu)\delta_{ij}, \quad (4.72)$$

with ϵ_i the on-site potential and μ the chemical potential. We assume the bond pair potential Δ_{ij}^* to be real and neglect the depression effect of the impurity scattering to take $\Delta_{ij} = \Delta$. The above equation in the nearest-neighbor hopping approximation is expanded as:

$$\begin{aligned} (E - (\epsilon_{ix, iy} - \mu))u_{ix, iy} &= -tu_{ix+1, iy} - tu_{ix-1, iy} - tu_{ix, iy+1} - tu_{ix, iy-1} \\ &+ \Delta v_{ix+1, iy} + \Delta v_{ix-1, iy} + \Delta v_{ix, iy+1} \\ &+ \Delta v_{ix, iy-1}, \end{aligned} \quad (4.73a)$$

$$\begin{aligned}
(E + (\epsilon_{i_x, i_y} - \mu))v_{i_x, i_y} &= tv_{i_x+1, i_y} + tv_{i_x-1, i_y} + tv_{i_x, i_y+1} + tv_{i_x, i_y-1} \\
&\quad + \Delta u_{i_x+1, i_y} + \Delta u_{i_x-1, i_y} + \Delta u_{i_x, i_y+1} \\
&\quad + \Delta u_{i_x, i_y-1} .
\end{aligned} \tag{4.73b}$$

As for the normal state case ($\Delta = 0$), we introduce a column vector

$$\hat{\phi}_{i_x} = \begin{pmatrix} u_{i_x, 1} \\ u_{i_x, 2} \\ \dots \\ u_{i_x, M} \\ v_{i_x, 1} \\ v_{i_x, 2} \\ \dots \\ v_{i_x, M} \end{pmatrix} . \tag{4.74}$$

Now this vector has a dimension of $2M$. Equations (4.73) can be recast into a matrix form:

$$\begin{pmatrix} \hat{\phi}_{i_x+1} \\ \hat{\phi}_{i_x} \end{pmatrix} = T_{i_x} \begin{pmatrix} \hat{\phi}_{i_x} \\ \hat{\phi}_{i_x-1} \end{pmatrix} , \tag{4.75}$$

Here the transfer matrix is

$$T_{i_x} = \begin{pmatrix} -(E\hat{1} - \hat{H}_{i_x}) & -\hat{1} \\ \hat{1} & 0 \end{pmatrix} , \tag{4.76}$$

where

$$\hat{H}_{i_x} = \sum_{j_y} \begin{pmatrix} -t\delta_{j_y, i_y \pm 1} + (\epsilon_{i_x, i_y} - \mu)\delta_{j_y, i_y} & \Delta\delta_{j_y, i_y \pm 1} \\ \Delta\delta_{j_y, i_y \pm 1} & t\delta_{j_y, i_y \pm 1} - (\epsilon_{i_x, i_y} - \mu)\delta_{j_y, i_y} \end{pmatrix} . \tag{4.77}$$

is the BdG Hamiltonian for the i_x -slice when it is decoupled from the rest. The transfer matrix for the entire strip is given by

$$P_n = \prod_{i_x=1}^n T_{i_x} , \tag{4.78}$$

connecting the coefficients at the left and right end of the strips

$$\begin{pmatrix} \hat{\phi}_{n+1} \\ \hat{\phi}_n \end{pmatrix} = P_n \begin{pmatrix} \hat{\phi}_1 \\ \hat{\phi}_0 \end{pmatrix} . \tag{4.79}$$

The system transfer matrix satisfies the Oseledec's multiplicative ergodic theorem. It allows to determine the localization length through the eigenvalues of $[P_n P_n^\dagger]^{1/2n}$ in the limit of $n \rightarrow \infty$. Specifically, the matrix

$$\Omega = \ln(P_n P_n^\dagger), \quad (4.80)$$

leads to $4M$ eigenvalues λ_i ($1 \leq i \leq 4M$). Lyapunov exponents can then be defined as

$$\gamma_i = \lim_{n \rightarrow \infty} \frac{\lambda_i}{2n} \quad (4.81)$$

$$= \lim_{n \rightarrow \infty} \tilde{\lambda}_i, \quad (4.82)$$

where $\tilde{\lambda}_i$ are the eigenvalues of the matrix $\ln(P_n P_n^\dagger)^{1/2n}$. Since the matrix P_n is symplectic, the eigenvalues of Ω occur in pairs, which are of opposite sign. The smallest positive Lyapunov exponent is the inverse of the quasi-one dimensional localization length

$$\lambda = \frac{1}{\gamma_{2M}}, \quad (4.83)$$

when we label the exponents in a decreasing order. In practical calculations, the eigenvalues of the matrix $e^\Omega = P_n P_n^\dagger \sim e^{2\gamma_i n}$ rises exponentially with the length of the strip. When the ratio of the eigenvalue closest to the unity from above and the largest eigenvalue becomes comparable to the machine accuracy, this closest to unity eigenvalue is lost. However, it is this eigenvalue that determines the localization length. This difficulty can be overcome by following the Gram-Schmidt orthonormalization procedure, which is carried out for each column $B_{n,i}$ of the matrix P_n in succession:

$$\bar{B}_{n,i} = (B_{n,i} - \sum_{j<i} (\bar{B}_{n,j} \cdot B_{n,i}) \bar{B}_{n,j}) / b_n^{(i)}, \quad (4.84a)$$

$$b_n^{(i)} = |B_{n,i} - \sum_{j<i} (\bar{B}_{n,j} \cdot B_{n,i}) \bar{B}_{n,j}|, \quad (4.84b)$$

for $1 \leq i \leq 4M$. Through this procedure, each column is orthonormalized to the previous columns. The first column converges to the eigenvector corresponding to the largest eigenvalue, the second column to the second largest and so on. The Gram-Schmidt transformation can be performed regularly (e.g., every fifth step) but not necessarily at every stage of iteration.

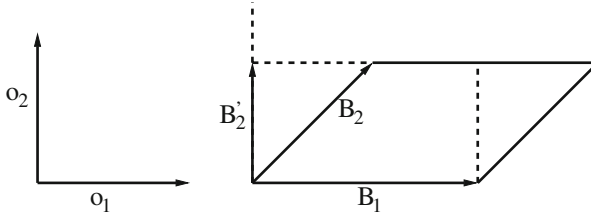


Fig. 4.6 The action of the system transfer matrix on an arbitrary set of orthonormal vectors o_1 and o_2 generates a new set of vectors of B_1 and B_2 , which are orthogonalized by the Gram-Schmidt procedure. However, the area of the parallelogram formed by B_1 and B_2 vectors is preserved

Pictorially, we can think of having P_n acting on a set of orthonormal unit vectors o_i ($1 \leq i \leq 4M$) to generate a new set of vectors

$$B_i = P_n o^i, \quad (4.85)$$

as shown in Fig. 4.6. They are just the columns of the transfer matrix itself. Notice that $B_1 \times B'_2 = B_1 \times B_2$ with $B'_2 = \bar{B}_2 * b^{(2)}$, and so on. The Gram-Schmidt orthogonalization procedure preserves the area of a parallelogram formed by two vectors B_i and B_j . This process can be iterated successively through the entire strip, and the eigenvalues are given by

$$e^{n\gamma_1} = b^{(1)}(n_1)b^{(1)}(n_2) \dots, \quad (4.86a)$$

$$e^{n\gamma_2} = b^{(2)}(n_1)b^{(2)}(n_2) \dots, \quad (4.86b)$$

$$\dots = \dots, \quad (4.86c)$$

$$e^{n\gamma_{2M}} = b^{(2M)}(n_1)b^{(2M)}(n_2) \dots, \quad (4.86d)$$

$$e^{n\gamma_{2M+1}} = b^{(2M+1)}(n_1)b^{(2M)}(n_2) \dots, \quad (4.86e)$$

$$\dots = \dots, \quad (4.86f)$$

$$e^{n\gamma_{4M-1}} = b^{(4M-1)}(n_1)b^{(4M-1)}(n_2) \dots, \quad (4.86g)$$

$$e^{n\gamma_{4M}} = b^{(4M)}(n_1)b^{(4M)}(n_2) \dots, \quad (4.86h)$$

where $n = n_1 + n_2 + \dots$. For the symplectic matrix P_n , the eigenvalues occur in pairs,

$$n\gamma_1, n\gamma_2, \dots, n\gamma_{2M}, \frac{1}{n\gamma_{2M}}, \dots, \frac{1}{n\gamma_2}, \frac{1}{n\gamma_1}, \quad (4.87)$$

where we have arranged them in descending order. As such, we have the following relation

$$n\gamma_{2M} = \frac{n}{\lambda} = \ln b_{n_1}^{(2M)} + \ln b_{n_2}^{(2M)} + \dots, \quad (4.88)$$

from which the localization length can be calculated iteratively

$$\lambda = \frac{n}{c_n^{(2M)}}, \quad (4.89)$$

with

$$c_n^{(2M)} = \ln b_n^{(2M)} + c_{n-1}^{(2M)}. \quad (4.90)$$

More generally, we can define a channel dependent localization length

$$\lambda_i = \frac{n}{c_n^{(i)}}, \quad (4.91)$$

with

$$c_n^{(i)} = \ln b_n^{(i)} + c_{n-1}^{(i)}, \quad (4.92)$$

for $1 \leq i \leq 2M$. Since the spin carried by a quasiparticle in a superconductor is conserved [23], these localization lengths can then be used to determine the spin conductance for the strip with width M [24]:

$$g_s(M, n_i) = \sum_{j=1}^{2M} \cosh^{-2} \Lambda_j, \quad (4.93)$$

where $\Lambda_j = \lambda_j/M$ is the localization length in units of the strip width. In Fig. 4.7a, g_s is shown as a function of M and it monotonically decreases with the increase of M at $E = 0$ for each selected impurity density, indicative of a localization in the large M limit. In addition, as shown in Fig. 4.7b, all the data for various values of M at different n_i can be collapsed onto a single curve:

$$g_s(M, n_i) = f\left(\frac{\xi(n_i)}{M}\right), \quad (4.94)$$

so that the one-parameter scaling law is obeyed. The quantity $\xi(n_i)$ is the thermodynamic localization length which only depends on n_i as shown in the inset of Fig. 4.7b, and remains finite for all the disorder density n_i , suggesting that all the

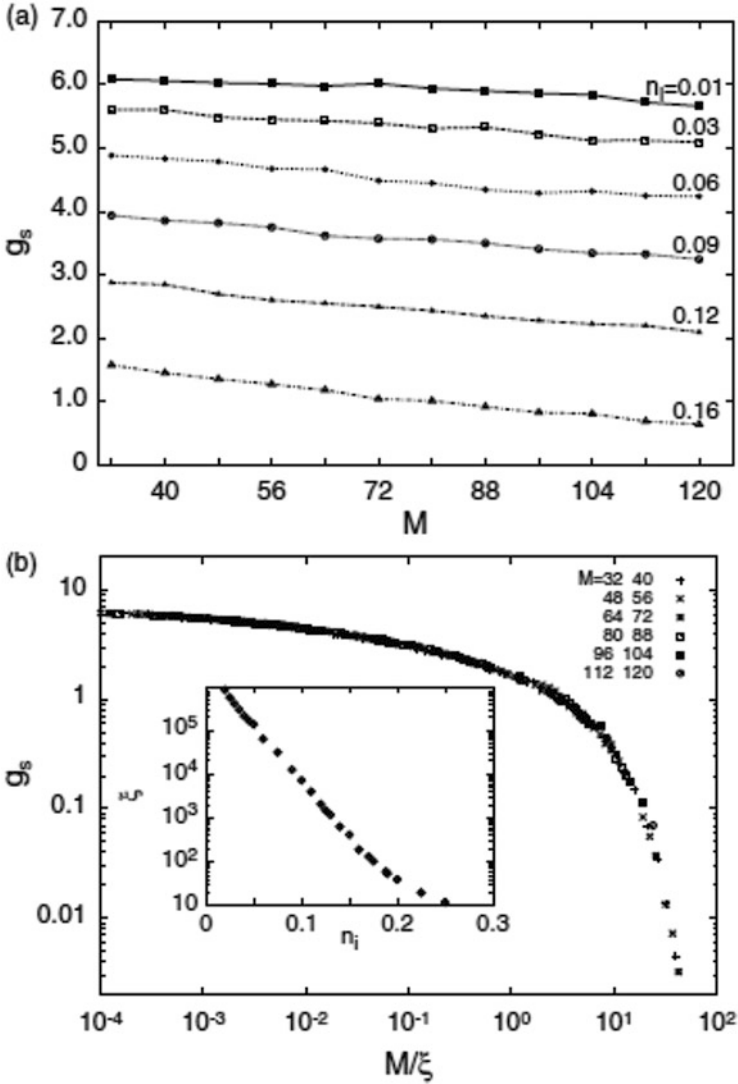


Fig. 4.7 Spin conductance as a function of the strip width M for various values of impurity concentration (a) and as a scaling function of M/ξ (b). *Inset of (b)*: The thermodynamic localization length as a function of impurity concentration n_i . The energy of the quasiparticle state is $E = 0$. From [22]

states are localized even in the unitary limit with the presence of the zero energy resonance peak.

We remark that this scaling approach can also be applied to study the localization and delocalization in disordered topological superconductors.

References

1. P.W. Anderson, Phys. Rev. Lett. **3**, 325 (1959)
2. J.-X. Zhu, W. Kim, C.S. Ting, Phys. Rev. B **57**, 13410 (1998)
3. M. Ma, P.A. Lee, Phys. Rev. B **32**, 5658 (1985)
4. P.J. Hirschfeld, N.D. Goldenfeld, Phys. Rev. B **48**, 4219 (1993)
5. H. Kim, G. Preosti, P. Muzikar, Phys. Rev. B **49**, 3544 (1994)
6. R.J. Radtke, et al., Phys. Rev. B **48**, 653 (1993)
7. P. Arberg, J.P. Carbotte, Phys. Rev. B **50**, 3250 (1994)
8. C.J. Pethick, D. Pines, Phys. Rev. Lett. **57**, 118 (1986)
9. S. Schmitt-Rink, K. Miyaki, C.M. Varma, Phys. Rev. Lett. **57**, 2575 (1986)
10. P. Hirschfeld, D. Vollhardt, P. Wölfle, Solid State Commun. **59**, 111 (1986)
11. H. Monien, et al., Solid State Commun. **61**, 581 (1987)
12. P. Hirschfeld, P. Wölfle, D. Einzel, Phys. Rev. B **37**, 83 (1988)
13. A.V. Balatsky, M.I. Salkola, A. Rosengren, Phys. Rev. B **51**, 15547 (1995)
14. M. Franz, C. Kallin, A.J. Berlinsky, M.I. Salkola, Phys. Rev. B **56**, 7882 (1997)
15. P.J. Hirschfeld, J. Phys. Chem. Solids **56**, 1605 (1995)
16. T. Das, J.-X. Zhu, M. J. Graf, Phys. Rev. B **84**, 134510 (2011)
17. E. Abrahams, P.W. Anderson, D.C. Licciardello, T.V. Ramakrishnan, Phys. Rev. Lett. **42**, 673 (1979)
18. E. Abrahams, *50 Years of Anderson Localization* (World Scientific, Singapore, 2010)
19. A. MacKinnon, B. Kramer, Z. Phys. B **53**, 1 (1983)
20. V.I. Oseledec, Trans. Mosc. Math. Soc. **19**, 197 (1968)
21. R. Carmona, J. Lacroix, *Spectral Theory of Random Schrödinger Equations* (Birkhauser, Boston, 1990)
22. J.-X. Zhu, D.N. Sheng, C.S. Ting, Phys. Rev. Lett. **85**, 4944 (2000)
23. T. Senthil, et al., Phys. Rev. Lett. **81**, 4704 (1998)
24. C.W.J. Beenakker, Rev. Mod. Phys. **69**, 731 (1997)

Chapter 5

Local Electronic Structure in Superconductors Under a Magnetic Field

Abstract In this chapter, the calculation of local electronic structure in the presence of magnetic field is discussed. It starts with the continuum theory for a single vortex and proceeds to the lattice version for the vortex lattices in both conventional *s*-wave and unconventional *d*-wave superconductors. A generalization of the BdG formulation for a topological superconductor will be briefly explored. For high- T_c cuprates, the local induction of competing order around a magnetic vortex core is examined. Finally, the Zeeman-field induced FFLO superconducting state is also analyzed in depth.

5.1 Effect of the Magnetic Field

In Chap. 1, we have addressed the non-interacting electron part of the Hamiltonian in the absence of static electric and magnetic field. Since the magnetic field effect on the superconducting properties is unique, we give it an in-depth discussion here. The second quantized Hamiltonian for electrons in the presence of a static magnetic field is

$$\mathcal{H}_0 = \int d\mathbf{r} \psi_\alpha^\dagger(\mathbf{r}) h_\alpha(\mathbf{r}) \psi_\alpha(\mathbf{r}) . \quad (5.1)$$

Here the single-particle Hamiltonian

$$h_\alpha(\mathbf{r}) = \frac{[\frac{\hbar}{i}\nabla_{\mathbf{r}} + \frac{e}{c}\mathbf{A}(\mathbf{r})]^2}{2m_e} + V(\mathbf{r}) + \alpha\mu_B H(\mathbf{r}) - E_F , \quad (5.2)$$

where $\mathbf{A}(\mathbf{r})$ is the vector potential giving rise to the magnetic field $\mathbf{H}(\mathbf{r})$ (assumed to be along the *z*-direction of the spin axis)

$$\nabla \times \mathbf{A}(\mathbf{r}) = \mathbf{H}(\mathbf{r}) , \quad (5.3)$$

$V(\mathbf{r})$ is the Coulomb potential contributed from the nuclear ions, and the third term in Eq. (5.2) describes the coupling of electron spin moment to the magnetic field.

The magnetic field has effects through both electron orbital and spin degrees of freedom. For the purpose of this chapter, we neglect the effect of spin-orbit coupling.

In wide-band systems, where $V(\mathbf{r})$ varies slowly, the free-electron gas approximation is usually made and the continuum model is a choice to study the magnetic field effect. For narrow-band systems, where the band structure effect is important, the tight-binding model is more convenient. Therefore, it is helpful to obtain the single-particle tight-binding Hamiltonian for the orbital effect of the magnetic field. The derivation follows that by Luttinger [1]. In the presence of a magnetic field, we expand the field operators as

$$\psi_{\sigma}(\mathbf{r}) = \sum_{\mathbf{R}_i} a(\mathbf{r} - \mathbf{R}_i) e^{-ie\Lambda_i/\hbar c} c_{i\sigma} . \quad (5.4)$$

Here $a(\mathbf{r} - \mathbf{R}_i)$ are either maximally localized Wannier functions or atomic orbitals. They are localized about the lattice site \mathbf{R}_i and drop off rapidly as \mathbf{r} goes away from \mathbf{R}_i . The operator $c_{i\sigma}$ annihilates one electron of spin σ at site i . The integral

$$\Lambda_i = \int_{\mathbf{R}_i}^{\mathbf{r}} \mathbf{A}(\boldsymbol{\xi}) \cdot d\boldsymbol{\xi} , \quad (5.5a)$$

$$\equiv \int_0^1 (\mathbf{r} - \mathbf{R}_i) \cdot \mathbf{A}(\mathbf{R}_i + \lambda(\mathbf{r} - \mathbf{R}_i)) d\lambda , \quad (5.5b)$$

is taken along the straight line path joining \mathbf{R}_i to \mathbf{r} . The exponential factor in Eq. (5.4) has the effect of approximately removing the troublesome $\mathbf{A} \cdot \mathbf{P}$ and $\mathbf{P} \cdot \mathbf{A}$ terms. We consider

$$\left(\mathbf{P} + \frac{e\mathbf{A}(\mathbf{r})}{c} \right) a(\mathbf{r} - \mathbf{R}_i) e^{-ie\Lambda_i/\hbar c} = e^{-ie\Lambda_i/\hbar c} \left[\mathbf{P} - \frac{e\nabla\Lambda_i}{c} + \frac{e\mathbf{A}(\mathbf{r})}{c} \right] a(\mathbf{r} - \mathbf{R}_i) , \quad (5.6)$$

which leads to

$$\left(\mathbf{P} + \frac{e\mathbf{A}(\mathbf{r})}{c} \right)^2 a(\mathbf{r} - \mathbf{R}_i) e^{-ie\Lambda_i/\hbar c} = e^{-ie\Lambda_i/\hbar c} \left[\mathbf{P} - \frac{e\nabla\Lambda_i}{c} + \frac{e\mathbf{A}(\mathbf{r})}{c} \right]^2 a(\mathbf{r} - \mathbf{R}_i) . \quad (5.7)$$

We then use the identities

$$\nabla \times \mathbf{r} = 0 , \quad (\mathbf{A} \cdot \nabla) \mathbf{r} = \mathbf{A} , \quad (5.8)$$

$$\nabla \times \mathbf{A}(\mathbf{R}_i + \lambda(\mathbf{r} - \mathbf{R}_i)) = \lambda \mathbf{H}(\mathbf{R}_i + \lambda(\mathbf{r} - \mathbf{R}_i)) , \quad (5.9)$$

while

$$\begin{aligned} \int_0^1 \mathbf{A}(\mathbf{R} + \lambda(\mathbf{r} - \mathbf{R}_i)) d\lambda &= \lambda \mathbf{A}(\mathbf{R}_i + \lambda(\mathbf{r} - \mathbf{R}_i)) \Big|_0^1 - \int_0^1 d\lambda \lambda \frac{d\mathbf{A}(\mathbf{R}_i + \lambda(\mathbf{r} - \mathbf{R}_i))}{d\lambda} , \\ &= \mathbf{A}(\mathbf{r}) - \int_0^1 d\lambda ((\mathbf{r} - \mathbf{R}_i) \cdot \nabla) \mathbf{A} , \end{aligned} \quad (5.10)$$

and prove that

$$\nabla \Lambda_i = \mathbf{A}(\mathbf{r}) + \int_0^1 d\lambda \lambda (\mathbf{r} - \mathbf{R}_i) \times \mathbf{H}(\mathbf{R}_i + \lambda(\mathbf{r} - \mathbf{R}_i)) . \quad (5.11)$$

By substituting Eq. (5.4) into Eq. (5.1), and using the expressions Eq. (5.7) and Eq. (5.11), one arrives at

$$\mathcal{H}_0 = \sum_{ij,\sigma} \tilde{h}_{ij} c_{i\sigma}^\dagger c_{j\sigma} , \quad (5.12)$$

where the field-modified one-electron Hamiltonian is given by

$$\begin{aligned} \tilde{h}_{ij} &= \int d\mathbf{r} a^*(\mathbf{r} - \mathbf{R}_i) e^{ie(\Lambda_i - \Lambda_j)/\hbar c} \left\{ \frac{1}{2m_e} \left(\mathbf{P} - \frac{e}{c} \int_0^1 d\lambda \lambda (\mathbf{r} - \mathbf{R}_i) \times \mathbf{H}(\mathbf{R}_i + \lambda(\mathbf{r} - \mathbf{R}_i)) \right)^2 \right. \\ &\quad \left. + V(\mathbf{r}) - E_F \right\} a(\mathbf{r} - \mathbf{R}_j) . \end{aligned} \quad (5.13)$$

We may now invoke the fact that the function a_i is localized, which allows us to approximate $\mathbf{r} \approx \mathbf{R}_j$ in the integral over λ in the above integral, as long as the magnetic fields are not varying too rapidly. This approximation leads to

$$\tilde{h}_{ij} = -t_{i \neq j} e^{i\varphi_{ij}} + (\epsilon_i - E_F) \delta_{ij} , \quad (5.14)$$

where

$$t_{ij} = - \int d\mathbf{r} a^*(\mathbf{r} - \mathbf{R}_i) \left(\frac{\mathbf{p}^2}{2m_e} + V(\mathbf{r}) \right) a(\mathbf{r} - \mathbf{R}_j) , \quad (5.15)$$

is the hopping integral in the absence of magnetic field, and the Peierls phase is given by

$$\begin{aligned} \varphi_{ij} &= -\frac{e}{\hbar c} \int_{\mathbf{R}_j}^{\mathbf{R}_i} \mathbf{A}(\boldsymbol{\xi}) \cdot \boldsymbol{\xi} \\ &= -\frac{2\pi}{\Phi_0} \int_{\mathbf{R}_j}^{\mathbf{R}_i} \mathbf{A}(\boldsymbol{\xi}) \cdot \boldsymbol{\xi} . \end{aligned} \quad (5.16)$$

Here the single-electron flux quantum is

$$\Phi_0 = \frac{hc}{e} \quad (5.17)$$

with h the Planck constant. The phase factor modifying the hopping integral is called as the Peierls substitution [2].

The spin Zeeman exchange interaction term can be easily found as

$$\sum_{i\sigma} \sigma \mu_B H_i c_{i\sigma}^\dagger c_{i\sigma} , \quad (5.18)$$

in the tight-binding model, where H_i is an effective magnetic field at site i .

We conclude this section by summarizing the BdG equations in the presence of magnetic field:

$$\begin{cases} \tilde{h}_\sigma(\mathbf{r}) u_\sigma^n(\mathbf{r}) + \int d\mathbf{r}' \Delta(\mathbf{r}, \mathbf{r}') v_\sigma^n(\mathbf{r}') = E_n u_\sigma^n(\mathbf{r}), \\ \int d\mathbf{r}' \Delta^*(\mathbf{r}', \mathbf{r}) u_\sigma^n(\mathbf{r}') - \tilde{h}_\sigma^*(\mathbf{r}) v_\sigma^n(\mathbf{r}) = E_n v_\sigma^n(\mathbf{r}), \end{cases} \quad (5.19)$$

in the continuum limit, and

$$\begin{cases} E_n u_{i\sigma}^n = \sum_j \tilde{h}_{ij,\sigma} u_{j\sigma}^n + \sum_j \Delta_{ij} v_{j\bar{\sigma}}^n, \\ E_n v_{i\bar{\sigma}}^n = -\sum_j \tilde{h}_{ij,\bar{\sigma}}^* v_{j\bar{\sigma}}^n + \sum_j \Delta_{ji}^* u_{j\sigma}^n, \end{cases} \quad (5.20)$$

in the tight-binding model.

5.2 Vortex Core State in an s -Wave Superconductor

5.2.1 Single Isolated Vortex

The study of the single vortex line of an s -wave superconductor based on the BdG theory has been initiated with the seminal work by Caroli, de Gennes, and Matricon [3–5] and later by Bardeen et al. [6], in which various approximations were used. Later on, Shore et al. [7] and Gygi and Schlüter [8] obtained numerical solutions for quasiparticle amplitudes in a vortex core starting with approximate forms for the pair potential. It is important to note that, in these two calculations, the pair potential used as input was modeled from the experimentally inferred coherence length. The effect of the spatial dependence of the magnetic field was neglected, which seems to be justified when the GL parameter $\kappa \equiv \lambda/\xi$ is large, where λ and ξ are the penetration depth and coherence length, respectively.

Here we consider a single vortex in a two-dimensional s -wave superconductor. When the magnetic field is applied perpendicular to the 2D plane, the orbital effect is dominant over the spin Zeeman effect. By introducing the polar coordinate system

$\mathbf{r} = (r, \theta)$, the pair potential should have the form

$$\Delta(\mathbf{r}) = \Delta(r)e^{-i\theta}. \quad (5.21)$$

It suggests that we can write the eigenfunctions as

$$\begin{pmatrix} u_n(\mathbf{r}) \\ v_n(\mathbf{r}) \end{pmatrix} = \begin{pmatrix} u_{j\mu} e^{i(\mu-1/2)\theta} \\ v_{j\mu} e^{i(\mu+1/2)\theta} \end{pmatrix},$$

which leads to the BdG equations

$$\begin{aligned} E_{j\mu} u_{j\mu}(r) &= \frac{\hbar^2}{2m_e} \left(-\frac{d^2 u_{j\mu}(r)}{dr^2} - \frac{1}{r} \frac{du_{j\mu}(r)}{dr} + \frac{(\mu-1/2)^2 u_{j\mu}(r)}{r^2} \right) - E_F u_{j\mu}(r) \\ &\quad + \Delta(r) v_{j\mu}(r), \end{aligned} \quad (5.22a)$$

$$\begin{aligned} E_{j\mu} v_{j\mu}(r) &= -\frac{\hbar^2}{2m_e} \left(-\frac{d^2 v_{j\mu}(r)}{dr^2} - \frac{1}{r} \frac{dv_{j\mu}(r)}{dr} + \frac{(\mu+1/2)^2 v_{j\mu}(r)}{r^2} \right) + E_F v_{j\mu}(r) \\ &\quad + \Delta(r) u_{j\mu}(r). \end{aligned} \quad (5.22b)$$

Here the pair potential amplitude

$$\Delta(r) = \frac{U}{2} \sum_{j\mu (|E_{j\mu}| \leq \omega_D)} u_{j\mu}(r) v_{j\mu}(r) \tanh\left(\frac{E_{j\mu}}{2k_{BT}}\right), \quad (5.23)$$

is determined self-consistently, where U is an effective pairing interaction and ω_D is the cutoff. The azimuthal quantum number $|\mu| = \frac{1}{2}, \frac{3}{2}, \frac{5}{2}, \dots$

We first focus on solutions to the BdG equations (5.22) by following the original work by Caroli, de Gennes, and Matricon [3] and that in [9] in the assumption that the pair potential is known with a shape schematically drawn in Fig. 5.1. Equations (5.22) can be rewritten as:

$$\begin{aligned} \frac{\hbar^2}{2m_e} \left(-\frac{d^2 u_{j\mu}(r)}{dr^2} - \frac{1}{r} \frac{du_{j\mu}(r)}{dr} + \frac{(\mu^2 + 1/4) u_{j\mu}(r)}{r^2} \right) - E_F u_{j\mu}(r) + \Delta(r) v_{j\mu}(r) \\ = \left(E_{j\mu} + \frac{\mu \hbar^2}{2m_e r^2} \right) u_{j\mu}(r), \end{aligned} \quad (5.24a)$$

$$\begin{aligned} -\frac{\hbar^2}{2m_e} \left(-\frac{d^2 v_{j\mu}(r)}{dr^2} - \frac{1}{r} \frac{dv_{j\mu}(r)}{dr} + \frac{(\mu^2 + 1/4) v_{j\mu}(r)}{r^2} \right) + E_F v_{j\mu}(r) + \Delta(r) u_{j\mu}(r) \\ = \left(E_{j\mu} + \frac{\mu \hbar^2}{2m_e r^2} \right) v_{j\mu}(r). \end{aligned} \quad (5.24b)$$

We now introduce a radius r_c very close to the vortex core center, that is,

$$(\mu + 1/2) k_F^{-1} \ll r_c \ll \xi.$$

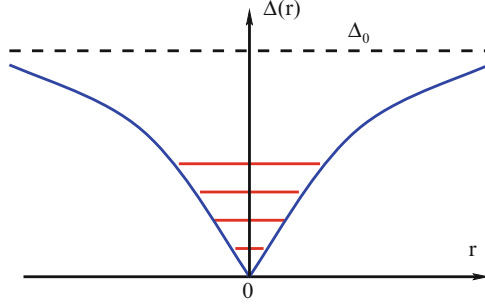


Fig. 5.1 The amplitude of superconducting order parameter $\Delta(r)$ around a single vortex core line. It vanishes at the core center $r = 0$ while rises to the bulk magnitude Δ_0 over a characteristic length ξ . The quasiparticle states with energies (red lines) smaller than the superconducting gap Δ_0 are bound near the vortex core center

For $r < r_c$, $\Delta(r)$ approaches to zero and we can neglect it in Eqs. (5.24), and obtain the solution as

$$\begin{pmatrix} u_\mu(r) \\ v_\mu(r) \end{pmatrix} = \begin{pmatrix} A_+ J_{\mu-\frac{1}{2}}[(k_F + q)r] \\ A_- J_{\mu+\frac{1}{2}}[(k_F - q)r] \end{pmatrix}, \quad (5.25)$$

where k_F is the Fermi wave number, $q = E/\hbar v_F$ with $v_F = \hbar k_F/m_e$, and J_μ is the Bessel function. Here we have used the approximation

$$\left(k_F^2 \pm \frac{2m_e E}{\hbar^2}\right)^{1/2} \approx k_F \pm q. \quad (5.26)$$

For $r > r_c$, we use the fact that the Hankel function $H_\mu(k_F r)$ satisfies the Bessel ordinary differential equation:

$$\frac{d^2 H_\mu(k_F r)}{dr^2} + \frac{1}{r} \frac{dH_\mu(k_F r)}{dr} + \left(k_F^2 - \frac{\mu^2}{r^2}\right) H_\mu(k_F r) = 0, \quad (5.27)$$

to separate this fast oscillating component out of the wave function and write in the form

$$\begin{pmatrix} u_\mu(r) \\ v_\mu(r) \end{pmatrix} = \begin{pmatrix} R_+(r) H_{\tilde{\mu}}(k_F r) + \text{c.c.} \\ R_-(r) H_{\tilde{\mu}}(k_F r) + \text{c.c.} \end{pmatrix}, \quad (5.28)$$

where the functions $R_\pm(r)$ are varying slowly in space, and the quantum number $\tilde{\mu} = \sqrt{\mu^2 + 1/4}$. Substituting Eq. (5.28) into Eq. (5.24), we obtain

$$\frac{\hbar^2}{2m_e} \left[-H_{\tilde{\mu}} \frac{d^2 R_+(r)}{dr^2} - \left(2H'_{\tilde{\mu}} + \frac{H_{\tilde{\mu}}}{r} \right) \frac{dR_+(r)}{dr} \right] + \Delta(r) H_{\tilde{\mu}} R_-(r)$$

$$= \left(E + \frac{\mu \hbar^2}{2m_e r^2} \right) H_{\tilde{\mu}} R_+(r) , \quad (5.29a)$$

$$- \frac{\hbar^2}{2m_e} \left[-H_{\tilde{\mu}} \frac{d^2 R_-(r)}{dr^2} - \left(2H'_{\tilde{\mu}} + \frac{H_{\tilde{\mu}}}{r} \right) \frac{dR_-(r)}{dr} \right] + \Delta(r) H_{\tilde{\mu}} R_+(r) \\ = \left(E + \frac{\mu \hbar^2}{2m_e r^2} \right) H_{\tilde{\mu}} R_-(r) . \quad (5.29b)$$

In the limit that $k_F r \gg 1$, we neglect the terms HR'_{\pm} and HR'_{\pm}/r , and approximate $H'(k_F r) \approx ik_F H$ from the asymptotic form of the Hankel function

$$H_{\mu}(x) = \left(\frac{2}{\pi x} \right)^{1/2} \exp \left[i \left(x + \frac{\mu^2}{2x} - \frac{\mu\pi}{2} - \frac{\pi}{4} \right) \right] , \quad (5.30)$$

for the limit $r \rightarrow \infty$. Equation (5.29) then becomes

$$-i \frac{\hbar^2 k_F}{m_e} \frac{dR_+(r)}{dr} + \Delta(r) R_-(r) = \left(E + \frac{\mu \hbar^2}{2m_e r^2} \right) R_+(r) , \quad (5.31a)$$

$$i \frac{\hbar^2 k_F}{m_e} \frac{dR_-(r)}{dr} + \Delta(r) R_+(r) = \left(E + \frac{\mu \hbar^2}{2m_e r^2} \right) R_-(r) . \quad (5.31b)$$

For $E \ll \Delta_0$ and $k_F r \gg \mu$, we can treat the right-hand-side of Eq. (5.31) perturbatively. To proceed, we write the envelope functions in the form

$$\begin{pmatrix} R_+(r) \\ R_-(r) \end{pmatrix} = \begin{pmatrix} e^{i\varphi} \\ e^{-i\varphi} \end{pmatrix} e^{-K} . \quad (5.32)$$

Substitution of Eq. (5.32) into Eq. (5.31) gives

$$\hbar v_F \left(\frac{1}{2} \frac{d\varphi}{dr} + i \frac{dK}{dr} \right) + \Delta(r) e^{-i\varphi} = E + \frac{\mu \hbar^2}{2m_e r^2} , \quad (5.33a)$$

$$\hbar v_F \left(\frac{1}{2} \frac{d\varphi}{dr} - i \frac{dK}{dr} \right) + \Delta(r) e^{i\varphi} = E + \frac{\mu \hbar^2}{2m_e r^2} . \quad (5.33b)$$

Through addition and subtraction of Eqs. (5.33a) and (5.33b), we find

$$\frac{\hbar v_F}{2} \frac{d\varphi}{dr} + \Delta(r) \cos \varphi = E + \frac{\mu \hbar^2}{2m_e r^2} , \quad (5.34a)$$

$$\hbar v_F \frac{dK}{dr} - \Delta(r) \sin \varphi = 0 . \quad (5.34b)$$

We further write the solution for φ and K up to the leading order of $E + \frac{\mu\hbar^2}{2m_e r^2}$:

$$\varphi = \varphi_0 + \varphi_1, \quad (5.35a)$$

$$K = K_0 + K_1. \quad (5.35b)$$

It can be easily found that

$$\varphi_0 = \frac{\pi}{2}, \quad (5.36a)$$

$$K_0 = (\hbar v_F)^{-1} \int_0^r \Delta(r') dr'. \quad (5.36b)$$

Upon substitution of Eq. (5.35) together with Eq. (5.36) into Eq. (5.34), we arrive at

$$\frac{\hbar v_F}{2} \frac{d\varphi_1}{dr} - \Delta(r)\varphi_1 = E + \frac{\mu\hbar^2}{2m_e r^2}, \quad (5.37a)$$

$$K_1 = 0, \quad (5.37b)$$

where we have used the approximation $\sin \varphi_1 \approx \varphi_1$. Equation (5.37a) has the solution

$$\begin{aligned} \varphi_1(r) &= - \int_r^\infty e^{\frac{2}{\hbar v_F} [\int_0^r \Delta(r') dr' - \int_0^{r'} \Delta(r'') dr'']} \left(2q + \frac{\mu}{k_F r'^2} \right) dr' \\ &= - \int_r^\infty e^{2K_0(r) - 2K_0(r')} \left(2q + \frac{\mu}{k_F r'^2} \right) dr'. \end{aligned} \quad (5.38)$$

On the other hand, for $r < r_c$, we can write

$$\varphi_1(r) = a_{-1}/r + a_0 + a_1 r + \dots,$$

and

$$\Delta(r) = \frac{d\Delta(r)}{dr} \Big|_{r=0} r + \dots,$$

and substitute them into Eq. (5.37a). By comparing the coefficients for the r^{-2} term, we have

$$a_{-1} = -\frac{\mu}{k_F},$$

so that

$$\frac{d\varphi_1}{dr} = 2q + \frac{\mu}{k_F r^2} - \frac{2\mu\Delta(r)}{\hbar k_F v_F r}, \quad (5.39)$$

for $r < r_c$. We can then obtain

$$\begin{aligned}
 \varphi_1(r_c) &= - \int_{r_c}^{\infty} e^{2K_0(r)-2K_0(r')} \left(2q + \frac{\mu}{k_F r'^2} \right) dr' \\
 &\approx - \int_0^{\infty} e^{-2K_0(r')} \left(2q + \frac{\mu}{k_F r'^2} \right) dr' - \int_0^{r_c} \frac{d\varphi_1}{dr'} dr' \\
 &\approx 2qr_c - \frac{\mu}{k_F r_c} - 2 \int_0^{\infty} e^{-2K_0(r')} \left(q - \frac{\mu \Delta(r')}{\hbar k_F v_F r'} \right) dr'. \quad (5.40)
 \end{aligned}$$

The final form of the wave function for $r > r_c$ is then

$$\begin{pmatrix} u_\mu(r) \\ v_\mu(r) \end{pmatrix} = \tilde{A} e^{-K_0(r)} \begin{pmatrix} e^{i\frac{\pi}{4} + i\frac{\varphi_1}{2}} H_{\tilde{\mu}}^-(k_F r) + \text{c.c.} \\ e^{-i\frac{\pi}{4} - i\frac{\varphi_1}{2}} H_{\tilde{\mu}}^-(k_F r) + \text{c.c.} \end{pmatrix}. \quad (5.41)$$

This wave function must be joined smoothly at $r = r_c$ with that from the region $r < r_c$ given by Eq. (5.25). Using the asymptotic form of the Bessel function

$$J_\mu(x) = \left(\frac{2}{\pi x} \right)^{1/2} \exp \left[x + \frac{\mu^2}{2x} - \frac{\mu\pi}{2} + \frac{\pi}{4} \right], \quad (5.42)$$

for $x \gg 1$ together with that of the Hankel function, Eq. (5.30), we obtain

$$\varphi_1(r_c) = 2qr_c - \frac{\mu}{k_F r_c}. \quad (5.43)$$

Comparison of Eq. (5.43) with Eq. (5.40) leads to

$$\int_0^{\infty} e^{-2K_0(r')} \left(q - \frac{\mu \Delta(r')}{\hbar k_F v_F r'} \right) dr' = 0. \quad (5.44)$$

That is,

$$\begin{aligned}
 E_\mu &= \frac{\mu}{k_F} \frac{\int_0^{\infty} e^{-2K_0(r')} \frac{\Delta(r')}{r'} dr'}{\int_0^{\infty} e^{-2K_0(r')} dr'} \\
 &= \frac{\mu}{k_F} \frac{d\Delta(r)}{dr} \Big|_{r=0} g(k_F), \quad (5.45)
 \end{aligned}$$

where the dimensionless function $g(k_F)$ depends on the shape of $\Delta(r)$ and is close to one. Using the approximation $\frac{d\Delta(r)}{dr} \Big|_{r=0} \approx \frac{\Delta_0}{\xi}$ with the coherence length $\xi = \hbar v_F / 2\Delta_0$, the energies of the vortex core bound states are given by

$$E_\mu = \mu \frac{\Delta_0^2}{E_F}. \quad (5.46)$$

These are the Caroli-de Gennes-Matricorn vortex core levels. The lowest bound state energy corresponds to $|\mu| = \frac{1}{2}$.

More rigorous solution to the BdG equations can only be obtained through numerical solution, which also determines the pair potential self-consistently [10, 11]. The radial functions are expanded in terms of the set of Bessel functions normalized in a disc of radius R :

$$\begin{pmatrix} u_{j\mu}(r) \\ v_{j\mu}(r) \end{pmatrix} = \sum_i \begin{pmatrix} c_{ji} \phi_{i\mu-\frac{1}{2}}(r) \\ d_{ji} \phi_{i\mu+\frac{1}{2}}(r) \end{pmatrix}, \quad (5.47)$$

where

$$\phi_{im}(r) = \frac{\sqrt{2}}{RJ_m(\alpha_{im})} J_m(\alpha_{im}r/R), \quad i = 1, 2, \dots, N \quad (5.48)$$

with $m = \mu \mp \frac{1}{2}$ and α_{im} is the i th zero of $J_m(x)$. The BdG equations are now solved separately in each subspace of fixed angular momentum μ , which amounts to solve a $2N \times 2N$ matrix eigenvalue problem. Once the self-consistency solution is obtained, the local density of states as derived in Chap. 1 can be computed.

Typical results are shown in Figs. 5.2 and 5.3. As the temperature decreases, the vortex core size, as defined by $\frac{d\Delta(r)}{dr}|_{r \rightarrow 0}$, shrinks, as originally predicted by Kramer and Pesch [13]. In addition, at very low-temperatures, the pair potential also exhibits Friedel-like oscillation, which is mainly contributed from the vortex core states. These vortex core states are displayed clearly in the local density of states probed near the core center. For a large zero-temperature coherence length, these core levels

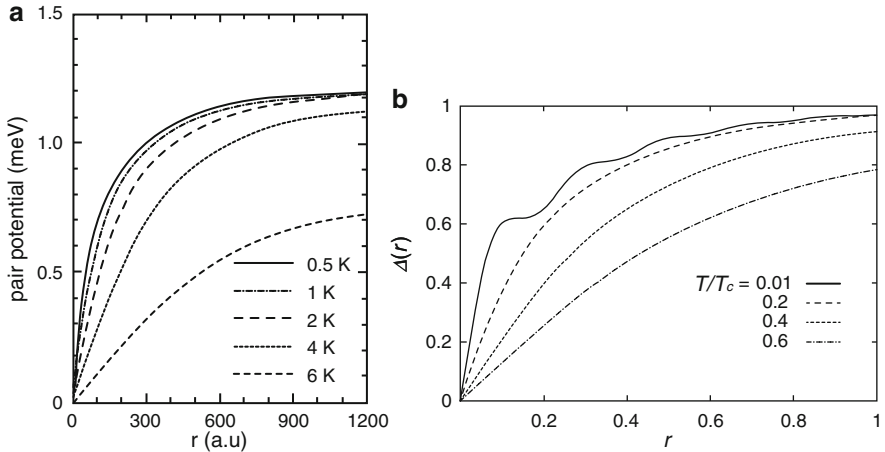


Fig. 5.2 Spatial variation of the pair potential $\Delta(r)$ as a function of distance away from the vortex core center, determined self-consistently, for $k_F \xi = 70$ (a) and 16 (b) for various temperatures. From [11] for (a) and [12] for (b)

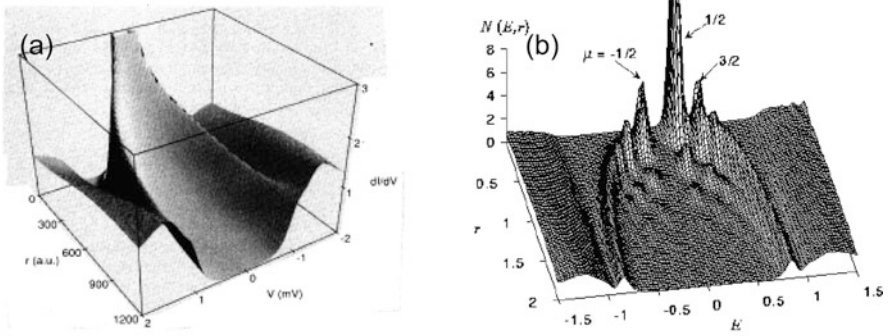


Fig. 5.3 Local density of states as a function of energy and distance from the vortex core center at $T = 0.13T_c$ and $k_F\xi = 70$ (a), and $T = 0.05T_c$ and $k_F\xi = 8$ (b). From [11] for (a) and [12] for (b)

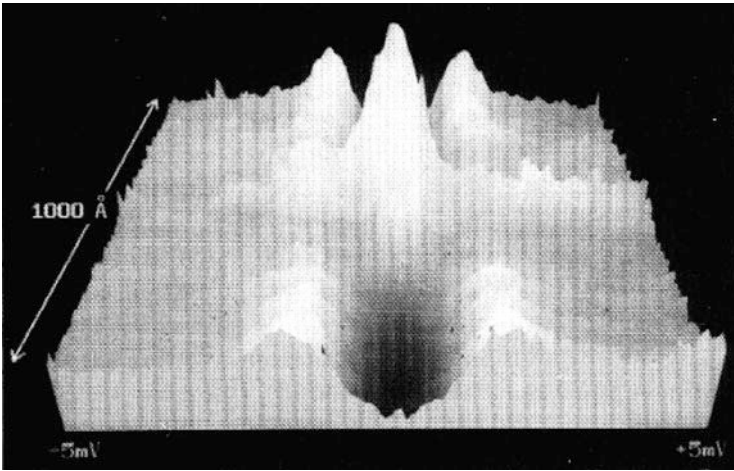


Fig. 5.4 Image of dI/dV on 2H-NbSe₂ as a function of voltage bias (horizontal axis) and position along a line that intersects a vortex (vertical axis). From [14]

are close in energy and the discretization is thermally smeared, while for a short coherence length, the discretization of the levels is evident. The first experimental evidence for the Caroli-de Gennes-Matricorn vortex core states comes from a series of scanning tunneling experiments on a layered hexagonal compound 2H-NbSe₂ at low temperatures [14–16]. A spatial image of tunneling conductance across a vortex is shown in Fig. 5.4. There a tunneling conductance peak is observed at the vortex core center.

Recently, the STM experiments have also been carried out in a vortex core of a proximity-induced s -wave superconductor in Bi₂Te₃ thin films [17, 18]. The evolution of local tunneling conductance spectra with film thickness has led to a conjecture [18] that the zero-bias conductance peak observed at the core center

reveals the existence of Majorana bound states. This conjecture has been supported by a very recent theoretical study [19] by solving a generalized set of BdG equations [20, 21]:

$$\begin{pmatrix} \hat{\mathcal{H}}_{\text{TI}}(\mathbf{r}) & \hat{\Delta}(\mathbf{r}) \\ \hat{\Delta}^\dagger(\mathbf{r}) & -\hat{\mathcal{H}}_{\text{TI}}^*(\mathbf{r}) \end{pmatrix} \begin{pmatrix} \hat{u}(\mathbf{r}) \\ \hat{v}(\mathbf{r}) \end{pmatrix} = E \begin{pmatrix} \hat{u}(\mathbf{r}) \\ \hat{v}(\mathbf{r}) \end{pmatrix}. \quad (5.49)$$

Here the normal-state effective Hamiltonian of the TI

$$\hat{\mathcal{H}}_{\text{TI}} = \epsilon \hat{\sigma}_z - iv_F \left[e^{-i\phi \hat{s}_z} \left(\partial_r \hat{s}_x + \frac{1}{r} \partial_\phi \hat{s}_y \right) + \partial_z \hat{s}_z \right] \hat{\sigma}_x - E_F, \quad (5.50)$$

with \hat{s}_i and $\hat{\sigma}_i$ the Pauli matrices for spin and orbital degrees of freedom, and the Dirac mass

$$\epsilon = -\epsilon_0 - \frac{1}{2m_e} \left(\partial_r^2 + \frac{1}{r} \partial_r + \frac{1}{r^2} \partial_\phi^2 + \partial_z^2 \right), \quad (5.51)$$

in the cylindrical coordinates with the quantity $2\epsilon_0$ describing the bulk gap of the topological insulator. The proximity-induced superconducting gap has the form

$$\hat{\Delta} = e^{i\phi} \Delta_0 \hat{s}_x, \quad (5.52)$$

where the superconducting gap Δ_0 is kept as a constant. We note that the BdG wave function $[\hat{u}(\mathbf{r}), \hat{v}(\mathbf{r})]^{\text{Transpose}}$ is a total eight-component vector spanned in a spin-orbital-Nambu space. The BdG quasiparticle wave function around an isolated vortex takes the form

$$\begin{pmatrix} u_j^{s\sigma}(\mathbf{r}) \\ v_j^{s\sigma}(\mathbf{r}) \end{pmatrix} = \begin{pmatrix} e^{i(j-s/2+1/2)} \bar{u}^{s\sigma}(\mathbf{r}) \\ e^{i(j+s/2-1/2)} \bar{v}^{s\sigma}(\mathbf{r}) \end{pmatrix}, \quad (5.53)$$

where the superscripts s (± 1) and σ ($=1, 2$) on u and v are spin and orbital indices. The coefficients ($\bar{u}^{s\sigma}(\mathbf{r})$, $\bar{v}^{s\sigma}(\mathbf{r})$) can be expanded in terms of the Bessel orthonormal functions in the radial direction [11] while the Gauss-Lobatto functions in the z -direction [22]. Numerically, the authors of [19] has used a varying Fermi energy to simulate the thickness dependence of the local density of states around the vortex core. It was found that the local density of states profile evolves from a V -shape to a Y -shape as the Fermi energy level is tuned toward the bulk gap center, in a good agreement with the experimental results.

5.2.2 High Field Limit

The quasiparticle states of a superconductor in the low field limit can be sufficiently described by considering a single isolated vortex. In the high field limit, a vortex lattice is formed as a regular array [23], in which vortices are closely packed. In this limit, the single isolated vortex description is not adequate. Quasiparticle excitations of a superconductor in the high field limit are interesting in the possibility of Landau level quantization, which plays an important role in quantum Hall effect in a semiconductor two-dimensional electron gas.

Different from the single isolated vortex case, in the high magnetic field limit, the vector potential must be treated explicitly in the BdG equations (5.19) with $h(\mathbf{r})$ given by Eq.(5.1). For the extreme type-II superconductors, we can assume the vector potential is entirely determined by the external magnetic field. In the Landau gauge with the vector potential

$$\mathbf{A} = H(-y, 0, 0) , \quad (5.54)$$

the pair potential for a triangular Abrikosov lattice has the form

$$\Delta(\mathbf{r}) = \Delta(T, H) \sum_n e^{i\pi a_{2,x} n^2 / a_\Delta} e^{i2\pi n x / a_\Delta - (y/l_B + \pi n l_B / a_\Delta)^2} , \quad (5.55)$$

where the position vector $\mathbf{r} = (x, y)$. The unit vectors in the direct space of a triangular vortex lattice are

$$\mathbf{a}_1 = (a_{1,x}, a_{1,y}) = a_\Delta (1, 0) , \quad \mathbf{a}_2 = (a_{2,x}, a_{2,y}) = a_\Delta \left(\frac{1}{2}, \frac{\sqrt{3}}{2} \right) . \quad (5.56)$$

The magnetic length $l_B = \sqrt{\hbar c / eH}$. This form of the pair potential and the explicit appearance of the vector potential in the BdG equations break the rotational symmetry existing for the single isolated vortex. The BdG wave functions can be expanded as

$$\begin{pmatrix} u(\mathbf{r}) \\ v(\mathbf{r}) \end{pmatrix} = \sum_{n,\mathbf{q}} \begin{pmatrix} u_{n\mathbf{q}} \\ v_{n\mathbf{q}} \end{pmatrix} \phi_{n,\mathbf{q}}(\mathbf{r}) . \quad (5.57)$$

Here $\phi_{n,\mathbf{q}}$ are the eigenfunctions to the single-particle Hamiltonian Eq.(5.1) in the magnetic sublattice representation for a vector potential chosen in the Landau gauge [24]:

$$\begin{aligned} \phi_{n,\mathbf{q}} = & \frac{1}{\sqrt{2^n n!} \sqrt{\pi} l_B} \sqrt{\frac{a_{2,y}}{L_x L_y}} \sum_m e^{i \frac{\pi a_{2,x}}{2a_\Delta} m - i m q_y a_{2,y}} e^{i(q_x + \pi m / a_\Delta)x - (y/l_B + q_x l_B + \pi m l_B / a_\Delta)^2 / 2} \\ & \times H_m(y/l_B + q_x l_B + \pi m l_B / a_\Delta) , \end{aligned} \quad (5.58)$$

where $\mathbf{q} = (q_x, q_y)$ is the quasimomenta in the first magnetic Brillouin zone defined by the reciprocal vectors

$$\mathbf{Q}_1 = (a_{2,y}, -a_{2,x})/l_B^2, \quad \mathbf{Q}_2 = (0, 2a_\Delta)/l_B^2, \quad (5.59)$$

L_x and L_y are the linear dimensions of the system, and $H_n(x)$ is the Hermite polynomial of order n . Substitution of Eq. (5.57) into Eq. (5.19) yields

$$\epsilon_n u_{n,\mathbf{q}} + \sum_m \Delta_{nm}(\mathbf{q}) v_{m,\mathbf{q}} = E_{n,\mathbf{q}} u_{n,\mathbf{q}}, \quad (5.60a)$$

$$-\epsilon_n v_{n,\mathbf{q}} + \sum_m \Delta_{nm}^*(\mathbf{q}) u_{m,\mathbf{q}} = E_{n,\mathbf{q}} v_{n,\mathbf{q}}. \quad (5.60b)$$

Here the normal-state Landau levels are given by

$$\epsilon_n = (n + \frac{1}{2})\hbar\omega_c - E_F, \quad (5.61)$$

with the cyclotron frequency $\omega_c = eH/m_e c$, and the matrix element for the pair potential is

$$\begin{aligned} \Delta_{nm}(\mathbf{q}) = & \frac{\Delta(T, H)}{\sqrt{2}} \frac{(-1)^m}{2^{n+m} \sqrt{n!m!}} \sum_k e^{i\pi a_{2,x} k^2 / a_\Delta + 2ikq_y a_{2,y} - (q_x l_B + \pi k l_B / a_\Delta)^2} \\ & \times H_{n+m}[\sqrt{2}(q_x + \pi k / a_\Delta) l_B]. \end{aligned} \quad (5.62)$$

Therefore, the BdG equations are now solved in a $2N_c \times 2N_c$ subspace for separate values of quasi momentum \mathbf{q} . Due to the complex structure of the pair potential matrix elements, accurate solutions can only be obtained through numerical simulations [25–30]. The numerical results show that when the magnetic field is close to the upper critical field H_{c2} , gapless quasiparticle states can occur at discrete locations of the Fermi surface. We note that the gapless quasiparticle states in the s -wave superconductors are induced from the Cooper pair motion in the high magnetic field. Their existence can be detected by the de Haas-van Alphen oscillations at high magnetic field and low temperatures [31–34].

5.3 Vortex Core States in a d -Wave Superconductor

The study of vortex cores states in a d -wave superconductor finds its immediate relevance when high-temperature cuprates are found to have a d -wave pairing symmetry. A novel feature from a d -wave pairing symmetry is that the superconducting gap function experiences a continuous sign change at some special points of the Fermi energy, showing the existence of nodal quasiparticles. Similar to the previous

section, here we first consider the quasiparticle core states in a single isolated vortex in the continuum model and for a vortex lattice in the tight-binding model.

5.3.1 Single Isolated Vortex

We begin with the BdG equations (5.19). The non-local nature of d -wave pairing introduces further complications. We introduce the center-of-mass coordinate system

$$\bar{\mathbf{R}} = \frac{\mathbf{r} + \mathbf{r}'}{2}, \quad \mathbf{s} = \mathbf{r} - \mathbf{r}', \quad (5.63)$$

to rewrite the equations as

$$h_{\mathbf{R}}u(\mathbf{R}) + \int \Delta(\mathbf{R} - \mathbf{s}/2, \mathbf{s})v(\mathbf{R} - \mathbf{s})ds = Eu(\mathbf{R}), \quad (5.64a)$$

$$-h_{\mathbf{R}}^*v(\mathbf{R}) + \int \Delta^*(\mathbf{R} - \mathbf{s}/2, \mathbf{s})u(\mathbf{R} - \mathbf{s})ds = Eu(\mathbf{R}). \quad (5.64b)$$

Here we have used a new label $\mathbf{R} = \mathbf{r}$ so that the single-particle Hamiltonian becomes

$$h_{\mathbf{R}} = \frac{\hbar^2}{2m_e} \left(\mathbf{p}_{\mathbf{R}} + \frac{e\mathbf{A}(\mathbf{R})}{c} \right) - E_F, \quad (5.65)$$

and

$$\bar{\mathbf{R}} = \mathbf{R} - \frac{\mathbf{s}}{2}, \quad \mathbf{s} = \mathbf{r} - \mathbf{r}'. \quad (5.66)$$

The pair potential in the center-of-mass coordinate system is given by

$$\Delta(\bar{\mathbf{R}}, \mathbf{s}) = V(\mathbf{s}) \sum_n [u_n(\bar{\mathbf{R}} + \mathbf{s}/2)v_n^*(\bar{\mathbf{R}} - \mathbf{s}/2) + u_n(\bar{\mathbf{R}} - \mathbf{s}/2)v_n^*(\bar{\mathbf{R}} + \mathbf{s}/2) \tanh\left(\frac{E_n}{2k_B T}\right)], \quad (5.67)$$

with the energy summation subjected to a cutoff Ω_c in the continuum limit. The pairing interaction is parametrized as

$$V(\mathbf{s}) = V_d g(\varphi) \delta(s - a) / a, \quad (5.68)$$

with $\mathbf{s} = (s, \varphi)$ in the polar coordinates and a as a length scale for nonlocal pairing interaction. For the $d_{x^2-y^2}$ -wave pairing symmetry, the angular dependent function

$$g(\varphi) = \cos^2(2\varphi). \quad (5.69)$$

This form of the pair interaction suggests that the d -wave order parameter depends on the relative coordinate \mathbf{s} only through its polar angle. Therefore, we can expand it as

$$\Delta(\bar{\mathbf{R}}, \mathbf{s}) = \Delta(\bar{\mathbf{R}}, \theta; \varphi) = \sum_{p,l} e^{ip\theta} e^{il\varphi} \Delta_{pl}(R), \quad (5.70)$$

where $\bar{\mathbf{R}} = (\bar{R}, \theta)$. In this representation, p represents the winding number of the superconducting phase around the vortex and l represents the orbital angular momentum of the relative motion of two paired electrons. For the $d_{x^2-y^2}$ -wave pairing symmetry, the order parameter near the single vortex should be contributed dominantly from a linear combination of components with $p = 1$, and $l = \pm 2$ at equal weight $\Delta(\bar{\mathbf{R}}, \theta; \varphi) = e^{i\theta} [e^{i2\varphi} \Delta_{1,2}(\bar{R}) + e^{-i2\varphi} \Delta_{1,-2}(\bar{R})]$.

For the case of single isolated d -wave vortex, we neglect the vector potential \mathbf{A} , which is reasonable for extreme type-II superconductors. We can then follow the same procedure used for the single isolated s -wave vortex to solve the BdG equations (5.64) through the expansion of the wave function as

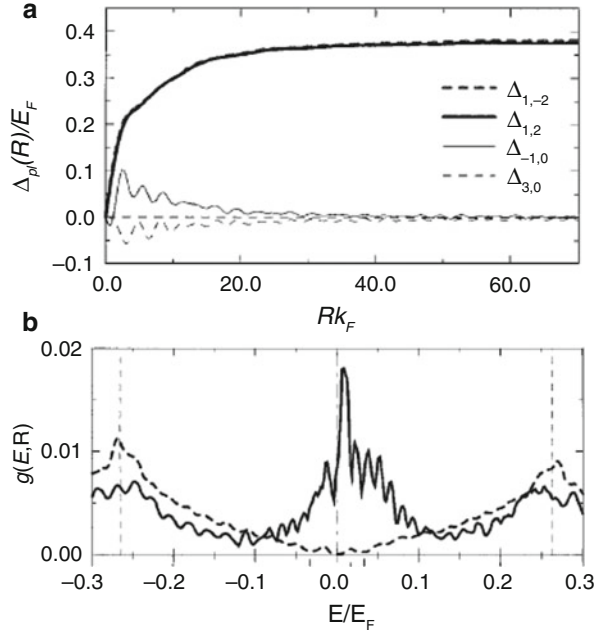
$$\begin{pmatrix} u_{j\mu}(R) \\ v_{j\mu}(R) \end{pmatrix} = \sum_i \begin{pmatrix} c_{ji} \phi_{i\mu-\frac{1}{2}}(R) \\ d_{ji} \phi_{i\mu+\frac{1}{2}}(R) \end{pmatrix}, \quad (5.71)$$

where

$$\phi_{im}(R) = \frac{\sqrt{2}}{R_0 J_m(\alpha_{im})} J_m(\alpha_{im} R/R_0), \quad i = 1, 2, \dots, N \quad (5.72)$$

with $m = \mu \mp \frac{1}{2}$ and α_{im} is the i th zero of $J_m(x)$, and R_0 is the radius of a disk. The resultant equations can be solved via exact diagonalization with the order parameter obtained through an iteration procedure. Figure 5.5 shows the variation of the dominant component of the superconducting order parameter and the local tunneling conductance at the vortex center [35]. Due to the spatial anisotropy of the dominant $d_{x^2-y^2}$ -wave component, other subdominant order parameter components are also induced near the vortex core (see Fig. 5.5a). The calculations [35] also show that for a short coherence length $k_F \xi_0$ with $\xi_0 = \hbar v_F / \pi \Delta_0$ (Δ_0 is controlled by the pairing interaction strength V_d), the profile for the $d_{x^2-y^2}$ -wave order parameter is quite universal and it follows the form $1/R^2$ instead of $\tanh(R/\xi')$ with ξ' a fitting parameter. In addition, a broad peak shows up near the Fermi energy in the local tunneling conductance at the vortex core center (see Fig. 5.5b). For the $d_{x^2-y^2}$ -wave vortex core, even for a very short coherence (e.g., $k_F \xi_0 = 2.5$ for Fig. 5.5a), no clear splitting of the core level is obtained, which is in sharp contrast with the case of the s -wave vortex core. This is a clear indication that the nodal quasiparticles pre-existing for the $d_{x^2-y^2}$ -wave pairing even at zero field play an important role in the nature of vortex core states.

Fig. 5.5 Dominant order parameter component around a d -wave vortex (a) and the theoretically obtained tunneling conductance at the vortex core center. The system size is $k_F R_0 = 120$. The other parameter values are $k_F a = 2$, $\Omega_c/E_F = 0.3$, $V_d/E_F = 1.6$, and $T = 0$. From [35]

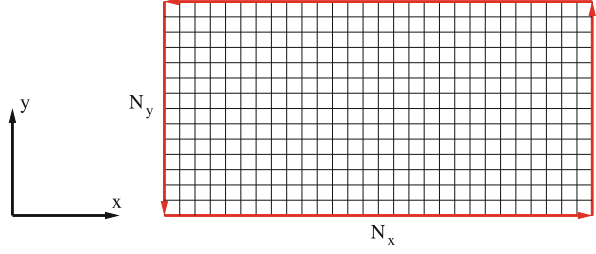


5.3.2 Quasiparticle States in a Mixed-State of d -Wave Superconductors

The order parameter profile for a single $d_{x^2-y^2}$ -wave vortex core has also been studied by solving the BdG equations within the tight-binding model [36]. The use of tight-binding model enables one to incorporate band structure of normal-state superconductors, which is especially appropriate for high- T_c cuprates. As in the case of s -wave superconductors, when the magnetic field is much larger than the lower critical field H_{c1} , a vortex lattice is formed also in the d -wave superconductors. The quasiparticle spectrum in the mixed-state within the tight-binding model has been first studied by Wang and MacDonald [37] for a pure $d_{x^2-y^2}$ -wave superconductor. It was shown that the local density of states at the d -wave vortex core exhibits a single broad peak at zero energy. The results are supported by the study of the single $d_{x^2-y^2}$ -wave vortex line discussed above in the continuum model.

In this high-field limit, we again need to treat the magnetic field effect explicitly, which is described in the BdG equations (5.20). In the mixed state, the magnetic field effect is included through the Peierls phase factor $\varphi_{ij} = -\frac{2\pi}{\Phi_0} \int_{r_j}^{r_i} \mathbf{A}(\mathbf{r}) \cdot d\mathbf{r}$, where $\Phi_0 = hc/e$ ($e > 0$) is the single-electron flux quantum. We still assume the superconductor under consideration is in the extreme type-II limit where the Ginzburg-Landau parameter $\kappa = \lambda/\xi$ goes to infinity so that the screening effect from the supercurrent is negligible. Therefore, the vector potential \mathbf{A} can be approximated by the solution

Fig. 5.6 Schematic drawing of a magnetic unit cell with linear dimensions of N_x and N_y . The red lines form a closed path around the unit cell



$\nabla \times \mathbf{A} = H\hat{z}$, where H is the magnetic field externally applied along the c axis. The enclosed flux density within each plaquette is given by $\sum_{\square} \varphi_{ij} = -\frac{2\pi Ha^2}{\Phi_0}$.

We choose a Landau gauge to write the vector potential as $\mathbf{A} = (-Hy, 0, 0)$, where y is the y -component of the position vector \mathbf{r} . By considering a rectangular lattice, we introduce the magnetic translation operator $\mathcal{T}_{mn}\mathbf{r} = \mathbf{r} + \mathbf{R}$, where the translation vector $\mathbf{R} = mN_x a \hat{\mathbf{e}}_x + nN_y a \hat{\mathbf{e}}_y$ with N_x and N_y the linear dimension of the unit cell of the vortex lattice, as shown in Fig. 5.6. Note that the original crystal lattice is a . To ensure different \mathcal{T}_{mn} to be commutable with each other, we have to take the strength of magnetic field so that the flux enclosed by each unit cell has a single-particle flux quantum, i.e., Φ_0 , which is equivalent of two superconducting flux quanta each with $hc/2e$.

Under this condition, we can decouple the translation operator \mathcal{T}_{mn} into two consecutive operations

$$\mathcal{T}_{mn} = \mathcal{T}_{0n} \mathcal{T}_{m0} . \quad (5.73)$$

As such, we have

$$\mathbf{A}(\mathcal{T}_{m0}\mathbf{r}) = \mathbf{A}(\mathbf{r}) = \mathbf{A}(\mathbf{r}) + \nabla\phi_1 , \quad (5.74)$$

which gives

$$\phi_1 = 0 , \quad (5.75)$$

and

$$\mathbf{A}(\mathcal{T}_{0n}\mathbf{r}) = -Hy\hat{\mathbf{e}}_x - H(nN_y a)\hat{\mathbf{e}}_x = \mathbf{A}(\mathbf{r}) + \nabla\phi_2 , \quad (5.76)$$

which gives

$$\phi_2 = -HnN_y a x . \quad (5.77)$$

Therefore, the transformation \mathcal{T}_{mn} leads to the transformation of the superconducting pair potential as:

$$\begin{aligned} \Delta(\mathcal{T}_{mn}\mathbf{r}) &= e^{-\frac{i4\pi}{\Phi_0}[-HnN_y a(x+mN_x a)]} e^{-\frac{i4\pi}{\Phi_0} \times 0} \Delta(\mathbf{r}) \\ &= e^{i\chi(\mathbf{r}, \mathbf{R})} \Delta(\mathbf{r}) , \end{aligned} \quad (5.78)$$

where the phase accumulated by the order parameter upon the translation is

$$\begin{aligned}\chi(\mathbf{r}, \mathbf{R}) &= -\frac{4\pi}{\Phi_0}[-HnN_y a(x + mN_x a)] \\ &= -\frac{4\pi}{\Phi_0} \mathbf{A}(\mathbf{R}) \cdot \mathbf{r} + 4mn\pi, \end{aligned} \quad (5.79)$$

when $N_x N_y a^2 H = \Phi_0$. If we perform a successive application of four transformations along a closed path around the magnetic unit cell, as shown by the red lines in Fig. 5.6,

$$(0, 0) \rightarrow (N_x a, 0) \rightarrow (N_x a, N_y a) \rightarrow (0, N_y a) \rightarrow (0, 0), \quad (5.80)$$

the accumulated phase on the superconducting order parameter is 4π , which corresponds to two superconducting flux quanta.

From this property, we can obtain the magnetic Bloch theorem for the wavefunction of the BdG equations:

$$\begin{pmatrix} u_{\mathbf{k},\sigma}(\mathcal{T}_{mm}\tilde{\mathbf{r}}) \\ v_{\mathbf{k},\sigma}(\mathcal{T}_{mm}\tilde{\mathbf{r}}) \end{pmatrix} = e^{i\mathbf{k}\cdot\mathbf{R}} \begin{pmatrix} e^{i\chi(\mathbf{r},\mathbf{R})/2} u_{\mathbf{k},\sigma}(\tilde{\mathbf{r}}) \\ e^{-i\chi(\mathbf{r},\mathbf{R})/2} v_{\mathbf{k},\sigma}(\tilde{\mathbf{r}}) \end{pmatrix}. \quad (5.81)$$

Here $\tilde{\mathbf{r}}$ is the position vector defined within a given unit cell and $\mathbf{k} = \frac{2\pi l_x}{M_x N_x} \hat{\mathbf{e}}_x + \frac{2\pi l_y}{M_y N_y} \hat{\mathbf{e}}_y$ with $m_{x,y} = 0, 1, \dots, M_{x,y} - 1$ are the wavevectors defined in the first Brillouin zone of the vortex lattice and $M_x N_x$ and $M_y N_y$ are the linear dimension of the whole system. The vortex carrying the flux quantum $hc/2e$ is the generic feature of the pairing theory for superconductivity. Comparing with the zero-field case but with the similar kind of supercell technique, we can see that the magnetic field also modifies the matching conditions between two neighboring unit cells. Similar type of the magnetic Bloch theorem can also be derived in the symmetry gauge for the vector potential. Typical numerical results are shown in Fig. 5.7 [37]: The d -wave order

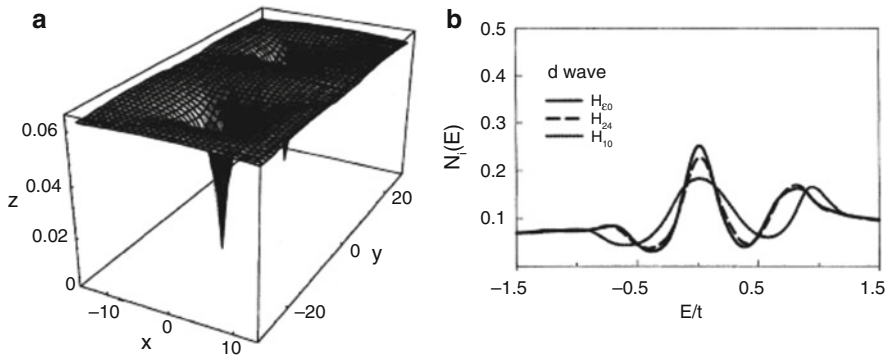


Fig. 5.7 Amplitude of a d -wave order parameter in a magnetic unit cell (a) and the local density of states at the vortex core center. From [37]

parameter as defined by

$$\Delta_d(i) = \frac{1}{4}[\Delta_{i,i+\hat{x}} + \Delta_{i,i-\hat{x}} - \Delta_{i,i+\hat{y}} - \Delta_{i,i-\hat{y}}], \quad (5.82)$$

is strongly suppressed at the vortex core. The local density of states at the vortex center exhibits a broad peak, which is clearly centered at the Fermi energy. No clear core level splitting is seen. These results are fully supported by the study of a single isolated d -wave vortex core in the continuum model discussed above.

The quasiparticle states near the vortex core can be probed by scanning tunneling microscopy. The unique feature of a pure d -wave pairing symmetry on the mix-state quasiparticles state can also be detected by nuclear magnetic resonance spectroscopy, which is essentially a site-selective probe. The correlation function between the two spin operators at equilibrium is

$$S_{ij}^{\alpha\beta}(t-t') = \langle S_i^\alpha(t) S_j^\beta(t') \rangle. \quad (5.83)$$

Its Fourier transform defines the dynamical structure factor

$$\begin{aligned} S_{ij}^{\alpha\beta} &= \int_{-\infty}^{\infty} e^{i\omega t} S_{ij}^{\alpha\beta}(t) dt \\ &= \frac{2\pi\hbar}{\mathcal{Z}} \sum_{\mu\nu} e^{-E_\mu/k_B T} \delta(E_\mu - E_\nu + \hbar\omega) \langle \mu | S_i^\alpha | \nu \rangle \langle \nu | S_j^\beta | \mu \rangle, \end{aligned} \quad (5.84)$$

where the partition function is given by

$$\mathcal{Z} = \sum_{\mu} e^{-E_\mu/k_B T}. \quad (5.85)$$

If we define the response function

$$R_{ij}^{\alpha\beta}(t-t') = -i\theta(t-t') \langle [S_i^\alpha(t), S_j^\beta(t')] \rangle, \quad (5.86)$$

where $[A, B]$ denotes a commutator. Its Fourier transform is given by

$$\begin{aligned} R_{ij}^{\alpha\beta}(\omega + i\eta) &= \int_{-\infty}^{\infty} dt e^{i(\omega+i\eta)t} R_{ij}^{\alpha\beta}(t) \\ &= \frac{1}{\mathcal{Z}} \sum_{\mu\nu} \frac{(e^{-E_\mu/k_B T} - e^{-E_\nu/k_B T}) \langle \mu | S_i^\alpha | \nu \rangle \langle \nu | S_j^\beta | \mu \rangle}{(E_\mu - E_\nu) + \hbar\omega + i\eta}, \end{aligned} \quad (5.87)$$

where η is an infinitesimal. Comparison of Eqs. (5.84) and (5.87) leads to the relation

$$S_{ij}^{\alpha\beta}(\omega) = -\frac{2}{1 - e^{-\hbar\omega/k_B T}} \text{Im} R_{ij}^{\alpha\beta}(\omega). \quad (5.88)$$

In the limit of $\omega \rightarrow 0$, we have

$$S_{ij}^{\alpha\beta}(\omega \rightarrow 0) = -\frac{2}{\hbar\omega/k_B T} \text{Im} R_{ij}^{\alpha\beta}(\omega \rightarrow 0). \quad (5.89)$$

This spin response function can be calculated conveniently in the Matsubara formalism. We are interested in the correlator between

$$S_i^+ = S_i^x + S_i^y = c_{i\uparrow}^\dagger c_{i\downarrow}$$

and

$$S_i^- = S_i^x - iS_i^y = c_{i\downarrow}^\dagger c_{i\uparrow}$$

and write down

$$\mathbf{R}_{ii}^{+-}(\tau) = -\langle T_\tau (S_i^+(\tau) S_i^-(0)) \rangle, \quad (5.90)$$

Using the Wick decoupling scheme and performing the Fourier transform, we obtain

$$\mathcal{R}_{ii}^{+-}(i\omega_n) = \sum_{mm'} u_i^n v_i^{n'} [u_i^{n*} v_i^{n'*} - v_i^{n*} u_i^{n'*}] \frac{f(E_n) - f(-E_{n'})}{i\omega_n + E_n + E_{n'}}, \quad (5.91)$$

from which we arrive at the spin-relaxation rate:

$$\begin{aligned} \frac{1}{T_1} &= \frac{J^2}{2\hbar^2} \mathcal{S}_{ii}^{+-}(\omega \rightarrow 0) \\ &= \frac{J^2 \pi k_B T}{\hbar^2} \sum_{mm'} \text{Re} \{ u_i^n v_i^{n'} [u_i^{n*} v_i^{n'*} - v_i^{n*} u_i^{n'*}] \} \\ &\quad \times \left(-\frac{\partial f(E)}{\partial E} \right) \Big|_{E=E_n} \delta(E_n + E_{n'}), \end{aligned} \quad (5.92)$$

where J is the strength of the coupling between the nuclear spin and the electron spin density on the lattice.

Figure 5.8 shows the temperature dependence of the spin relaxation rate on a few selected probing sites [38]. The results indicate that in the presence of vortices, $1/T_1$ follows $1/T_1 \sim T$ at low temperatures, which deviates from the T^3 behavior at zero field. This T -linear behavior arises from the low-energy states around the vortices. In addition, the temperature range for the T -linear behavior is expanded. This result is in sharp contrast with the $1/T_1 \propto e^{-\Delta_1/T}$ for the s -wave vortex lattice case at low temperature, where $\Delta_1 \sim \Delta_0^2/E_F$ [38]. Its magnitude of $1/T_1$ is also much larger than that for the zero-field case, suggesting a significant contribution from the gapless vortex-core states.

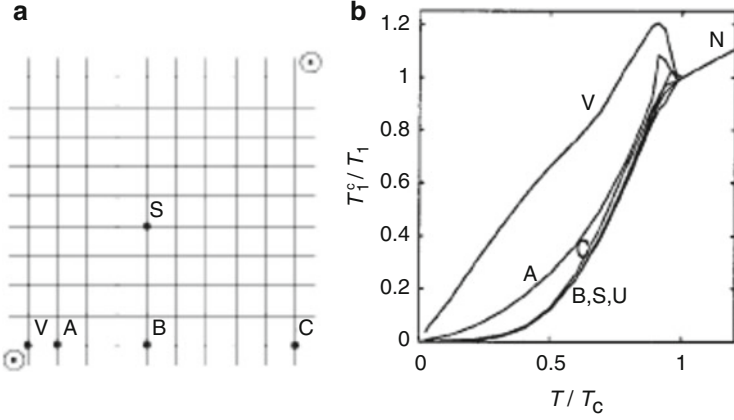


Fig. 5.8 Position of probing sites V , A , B , C , S in the square vortex lattice, where the nearest-neighbor vortex is located in the 45° direction from the x -axis (due to the choice of symmetric gauge) (a), and the temperature dependence of spin relaxation rate. Line U shows the zero-field case. The line N is for the normal state at $T > T_c$. From [38]

For high-temperature cuprates, low temperature STM experiments observed a double-peak structure around zero bias in the local differential tunneling conductance at the vortex core center [40, 41]. The discrepancy between the theory and the experiment stimulated interesting theoretical proposals on the quasiparticles in the vortex core of high- T_c cuprates, including the mixed $d_{x^2-y^2} + id_{xy}$ -wave pairing symmetry [35, 42], the Landau-level quantization [43], as well as competing order [39, 44–46]. Here we discuss the quasiparticle spectrum within a competing spin-density-wave scenario. Other competing scenarios [47] can be discussed within the same framework.

Beyond the tight-binding model with only a d -wave pairing term, we introduce a Hubbard on-site repulsion

$$H_U = U \sum_i \hat{n}_{i\uparrow} \hat{n}_{i\downarrow} , \quad (5.93)$$

where $\hat{n}_{i\sigma}$ is the local density operator and U is the strength of the on-site repulsion between two electrons with opposite spin polarization. By assuming that the on-site repulsion is solely responsible for the antiferromagnetism, we have a mean-field decoupling

$$H_{U,\text{MF}} = \sum_{\sigma} m_{i\bar{\sigma}} \hat{n}_{i\sigma} , \quad (5.94)$$

where $m_{i\sigma} = Un_{i\sigma}$ is the spin-dependent Hartree-Fock potential. The extended BdG equations can then be derived as:

$$\sum_{\mathbf{j}} \begin{pmatrix} \mathcal{H}_{\mathbf{ij},\sigma} & \Delta_{\mathbf{ij}} \\ \Delta_{\mathbf{ij}}^* & -\mathcal{H}_{\mathbf{ij},\bar{\sigma}} \end{pmatrix} \begin{pmatrix} u_{\mathbf{j}\sigma}^n \\ v_{\mathbf{j}\bar{\sigma}}^n \end{pmatrix} = E_n \begin{pmatrix} u_{\mathbf{i}\sigma}^n \\ v_{\mathbf{i}\bar{\sigma}}^n \end{pmatrix}, \quad (5.95)$$

where $(u_{i\sigma}^n, v_{i\bar{\sigma}}^n)$ is the quasiparticle wavefunction corresponding to the eigenvalue E_n , the single particle Hamiltonian $\mathcal{H}_{\mathbf{ij},\sigma} = -t_{ij}e^{i\varphi_{ij}}\delta_{\mathbf{i}+\delta_{\mathbf{j}}}\mathbf{j} + (m_{i,\bar{\sigma}} - \mu)\delta_{\mathbf{ij}}$. Notice that the quasiparticle energy is measured with respect to the Fermi energy. The self-consistent conditions read:

$$m_{i\sigma} = U \sum_n |u_{i\sigma}^n|^2 f(E_n), \quad (5.96)$$

and

$$\Delta_{\mathbf{ij}} = \frac{V}{4} \sum_n (u_{\mathbf{i}\uparrow}^n v_{\mathbf{j}\downarrow}^{n*} + v_{\mathbf{i}\downarrow}^{n*} u_{\mathbf{j}\uparrow}^n) \tanh\left(\frac{E_n}{2k_B T}\right), \quad (5.97)$$

where V is the strength of d -wave pairing interaction and the Fermi distribution function $f(E) = 1/(e^{E/k_B T} + 1)$. Here the summation is also over those eigenstates with negative eigenvalues thanks to the symmetry property of the BdG equation: If $(u_{\mathbf{i}\uparrow}^n, u_{\mathbf{i}\downarrow}^n, v_{\mathbf{i}\uparrow}^n, v_{\mathbf{i}\downarrow}^n)^{Transpose}$ is the eigenfunction of the 4×4 equation in the spin space with energy E_n , then $(v_{\mathbf{i}\uparrow}^{n*}, -v_{\mathbf{i}\downarrow}^{n*}, u_{\mathbf{i}\uparrow}^{n*}, -u_{\mathbf{i}\downarrow}^{n*})^{Transpose}$ up to a global phase factor is the eigenfunction with energy $-E_n$.

For the optimally high- T_c cuprates, since there is no static spin-density-wave (SDW) order at zero field. One can choose the relative strength of Hubbard repulsion and the d -wave pairing interaction such that the antiferromagnetic SDW order is strongly suppressed while the system is only dominated by a pure d -wave superconducting order, which is uniform in real space. As such, the competing nature of the system will be uncovered by suppressing the superconducting order in the form of vortices when a magnetic field is applied. Representative results are shown in Fig. 5.9. With an appropriately chosen strength of the Hubbard repulsion, the SDW order is nucleated at the vortex core center, where the d -wave order parameter is depressed (see the left column of Fig. 5.9). More interestingly, with the SDW order localized at the vortex core center, the near-zero-energy broad peak in the local density of states for a pure d -wave vortex is suppressed with the amplitude of the SDW order (see the left column of Fig. 5.9). The exhibited double-peak structure in the LDOS is consistent with the STM tunneling conductance measured at the vortex core center.

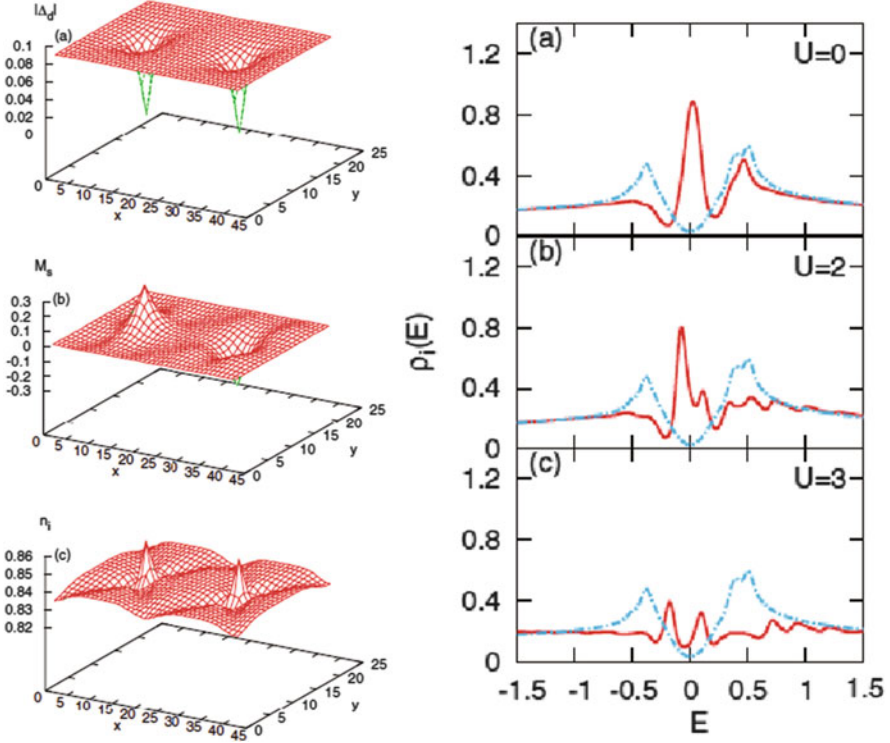


Fig. 5.9 *Left column:* Spatial variation of the d -wave order parameter (a), staggered spin-density-wave order $M_s = (-1)^i (n_{i\uparrow} - n_{i\downarrow})$ (b), and charge density $n_i = n_{i\uparrow} + n_{i\downarrow}$ (c) in a magnetic unit cell of size 42×21 for $V = 1.0$ and $U = 2$. *Right column:* The local density of states measured at the vortex core center for various values of Hubbard interaction $U = 0$ (a), 2 (b), and 3 (c). The filling factor defined as $\sum_i n_i / N_x N_y = 0.84$. From [39]

5.4 Fulde-Ferrell-Larkin-Ovchinnikov State due to a Zeeman Magnetic Field

As we mentioned at the beginning of the chapter, the magnetic field also influences the superconductivity especially with the spin-singlet pairing through the spin Zeeman interaction. This effect is especially important for a low-dimensional system, where the orbital effect of magnetic field when aligned appropriately can be completely quenched. In this section, we will focus on the spin Zeeman effect by neglecting the orbital effect of the magnetic field.

The modification of superconductivity by the external magnetic field through the Zeeman coupling was first studied by Clogston and Chandrasekhar [48, 49]. It is concerned with the bound on the paramagnetic upper critical field by considering the Zeeman interaction alone, that is the Pauli limit, and the nature of the phase boundary. The paramagnetic pair-breaking effect comes from the Zeeman splitting

of the single electron energy bands. When a magnetic field is applied in the normal state, electron band is split into spin-up and spin-down sheets to gain the magnetic energy; while in the superconducting state, this paramagnetism is eliminated by the formation of spin-singlet Cooper pairs. Qualitatively, the destruction of the superconducting state by the Pauli paramagnetic pair breaking occurs when the normal-state paramagnetic energy

$$E_P = \frac{1}{2} \chi_n H_P^2, \quad (5.98)$$

takes over the superconducting condensation energy

$$E_c = \frac{1}{2} N(0) \Delta_{\text{BCS}}^2(T). \quad (5.99)$$

Here the normal-spin susceptibility is given by

$$\chi_n = \frac{1}{2} g^2 \mu_B^2 N(0), \quad (5.100)$$

with g being the gyromagnetic ratio, μ_B being the Bohr magneton, and N_0 the density of states at the Fermi energy per spin polarization. The quantity Δ_{BCS} is the zero-field BCS energy gap. A little algebra yields

$$H_P(T) = \sqrt{2} \Delta_{\text{BCS}}(T) / |g| \mu_B. \quad (5.101)$$

On the other hand, if one assumes a second-order phase transition and the superconducting order parameter is always uniform in real space, the solution of the BdG equations (5.19) or (5.20) in the Pauli limit (that is, ignoring the orbital effect) will lead to an upper critical field, which will decrease with decreasing temperature below a critical temperature T^+ . This transition line is metastable, which suggests that the transition below T^+ (with the line defined by $H_P(T)$) becomes the first order. The phase diagram between the Zeeman field and the temperature is shown in Fig. 5.10.

A more unusual state was proposed by Fulde and Ferrell [50], and by Larkin and Ovchinnikov [51], where the pairing state is formed with a finite Cooper pair momentum at a larger Zeeman field. If the normal state is transitioned into this finite-momentum pairing (inhomogeneous in real space) state, the upper critical field can be enhanced. Specifically, the Cooper pairs are formed between electrons at (\mathbf{k}, \uparrow) and those at $(-\mathbf{k} + \mathbf{q}, \downarrow)$, as shown in Fig. 5.11. The shifted momentum q due to the Zeeman field is estimated to be $q \sim 2\mu_B H / \hbar v_F$. The state originally proposed by Fulde and Ferrell has the form

$$\Delta(\mathbf{r}) = \Delta e^{i\mathbf{q}\cdot\mathbf{r}}, \quad (5.102)$$

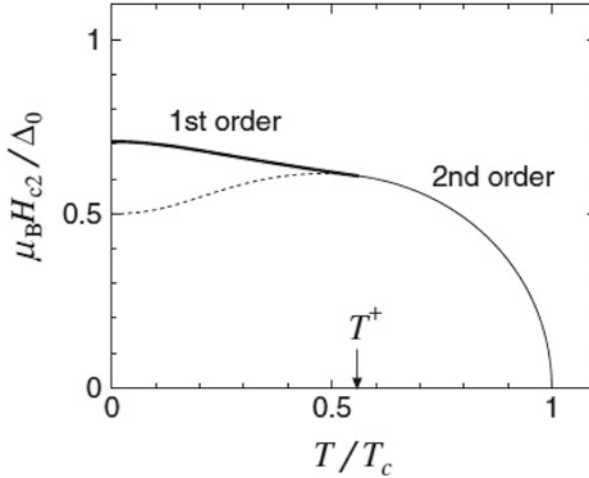


Fig. 5.10 The H - T phase diagram of a two-dimensional superconductor in the pure Pauli limit, which can be realized by applying the field parallel to the plane. Below T^+ ($\approx 0.56T_c$), the transition becomes first order. The *broken line* represents the metastable transition line. From [52]

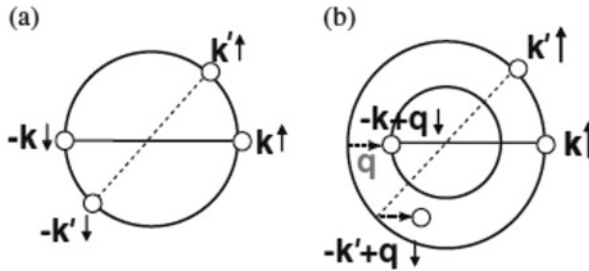


Fig. 5.11 Schematic picture of BCS pairing state ($\mathbf{q} = 0$) (a) and FFLO pairing state ($\mathbf{k} \uparrow, -\mathbf{k} + \mathbf{q} \downarrow$) (b). The *inner and outer circles* represent the Fermi surface of spin-up and spin-down electron bands. From [52]

with the amplitude of the order parameter remaining homogeneous. Note that the functionals $\Delta e^{i\mathbf{q}\cdot\mathbf{r}}$ and $\Delta e^{-i\mathbf{q}\cdot\mathbf{r}}$ are degenerate for a given \mathbf{q} , its equal weight linear combination can lift this degeneracy

$$\Delta(\mathbf{r}) = \Delta(e^{i\mathbf{q}\cdot\mathbf{r}} + e^{-i\mathbf{q}\cdot\mathbf{r}}) = 2\Delta \cos(\mathbf{q} \cdot \mathbf{r}) . \quad (5.103)$$

Larkin and Ovchinnikov suggested this form of the order parameter can lead to an even more stable superconducting state in the presence of a larger Zeeman field. Nowadays, this finite-momentum pairing state is called FFLO state [52, 53].

The interest in the FFLO state is recently revived by the observation of a so-called “Q” phase in heavy-fermion CeCoIn_5 compound [54], which has a $d_{x^2-y^2}$ -wave pairing symmetry at zero field. The problem has recently been numerically studied

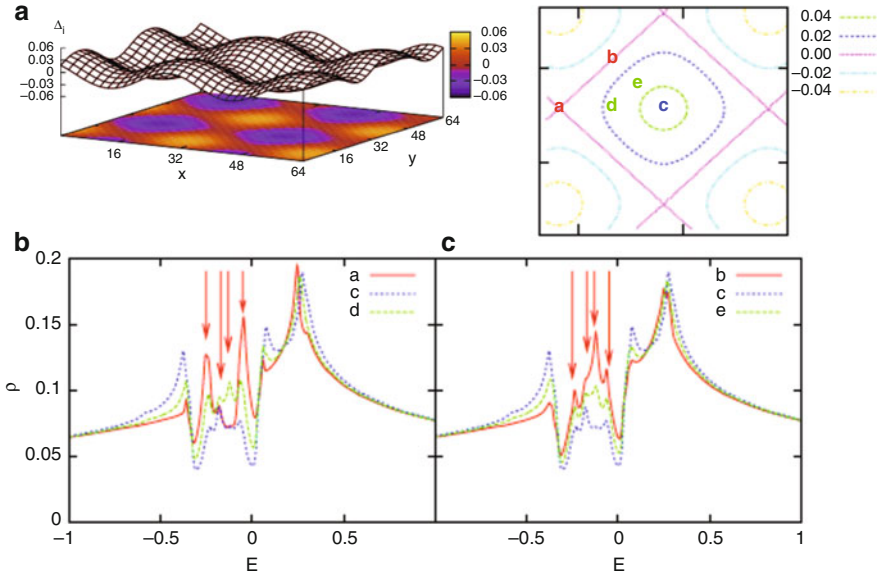


Fig. 5.12 Spatial variation of a d -wave order parameter in the Pauli limit of an external magnetic field (a) and the local density of states (b, c) at the sites marked on the contour plot (upper right panel) of equal magnitude of order parameter. The pairing interaction $V_d = 1.0$, the exchange field $h = H\mu_B = 0.15$, the chemical potential $\mu = -0.4$ in a nearest-neighbor hopping model. From [55]

by solving the BdG equations (5.20) with a d -wave pairing symmetry. Figure 5.12 shows the d -wave order parameter variation as well as the local density of states at several representative sites of the system [55]. The d -wave order parameter at low-temperatures is stabilized into a square lattice in the form of $\Delta_0[\cos q_x x + \cos q_y y]$ (see Fig. 5.12a). The spatial variation, especially the sign change of the d -wave order parameter in the real space gives rise to in-gap states exhibited in the local density of states (see Fig. 5.12b, c).

We note that just as interesting quasiparticle states in the mixed state of a superconductor arise from the vortex formation, novel quasiparticle states in the FFLO state through a large external Zeeman field are also due to the variation of order parameter, that is, the collective motion of Cooper pairs. In addition, the BdG formalism is also very powerful in studying the interplay between the Zeeman field and impurities.

References

1. J.M. Luttinger, Phys. Rev. **84**, 814 (1951)
2. R.E. Peierls, Z. Phys. **80**, 763 (1933)
3. C. Caroli, P.G. de Gennes, J. Matricon, Phys. Lett. **9**, 307 (1964)
4. C. Caroli, J. Matricon, Phys. Kondens. Mater. **3**, 380 (1965)
5. C. Caroli, Ann. Inst. Henri Poincaré **A 4**, 159 (1966)
6. J. Bardeen, R. Kümmel, A.E. Jacobs, L. Tewordt, Phys. Rev. **187**, 556 (1969)
7. J.D. Shore, M. Huang, A.T. Dorsey, J.P. Sethna, Phys. Rev. Lett. **62**, 3089 (1989)
8. F. Gygi, M. Schlüter, Phys. Rev. B **41**, 822 (1990)
9. J.B. Ketterson, S.N. Song, *Superconductivity* (Cambridge University Press, Cambridge, 1999)
10. F. Gygi, M. Schlüter, Phys. Rev. B **43**, 7609 (1990)
11. F. Gygi, M. Schlüter, Phys. Rev. B **43**, 7609 (1991)
12. N. Hayashi, T. Isoshima, M. Ichioka, K. Machida, Phys. Rev. Lett. **80**, 2921 (1998)
13. L. Kramer, W. Pesch, Z. Phys. **269**, 59 (1974)
14. H.F. Hess, et al., Phys. Rev. Lett. **62**, 814 (1989)
15. H.F. Hess, et al., Phys. Rev. Lett. **64**, 2711 (1990)
16. H.F. Hess, in *Scanning Tunneling Microscopy*, ed. by J.A. Stroscio, W.J. Kaiser (Academic Press, San Diego, 1993), p. 427
17. J.-P. Xu, et al., Phys. Rev. Lett. **112**, 217001 (2014)
18. J.-P. Xu, et al., Phys. Rev. Lett. **114**, 017001 (2015)
19. T. Kawakami, X. Hu, Phys. Rev. Lett. **115**, 177001 (2015)
20. C.K. Chiu, M.J. Gilbert, T.L. Hughes, Phys. Rev. B **84**, 144507 (2011)
21. Z.-Z. Li, F.-C. Zhang, Q.-H. Wang, Sci. Rep. **4**, 6363 (2014)
22. T. Mizushima, K. Machida, Phys. Rev. A **82**, 023624 (2010)
23. A.A. Abrikosov, Sov. Phys. JETP **35**, 1090 (1957)
24. Yu.A. Bychkov, E.I. Rashba, Sov. Phys. JETP **58**, 1062 (1983)
25. V.N. Nicopoulos, P. Kumar, Phys. Rev. B **44**, 12080 (1991)
26. S. Dukan, Z. Tešanović, Phys. Rev. B **49**, 13017 (1994)
27. M.R. Norman, A.H. MacDonald, H. Aker, Phys. Rev. B **51**, 5927 (1995)
28. P. Miller, Z. Tešanović, J. Phys. Condens. Matter **7**, 5579 (1995)
29. M.R. Norman, A.H. MacDonald, Phys. Rev. B **54**, 4239 (1996)
30. G.M. Bruun, V.N. Nicopoulos, N.F. Johnson, Phys. Rev. B **56**, 809 (1997)
31. J.E. Graebner, M. Robbins, Phys. Rev. Lett. **36**, 422 (1976)
32. F. Mueller, et al., Phys. Rev. Lett. **68**, 3928 (1992)
33. R. Corcoran, et al., Phys. Rev. Lett. **72**, 701 (1994)
34. N. Harrison, et al., Phys. Rev. B **50**, 4208 (1994)
35. M. Franz, Z. Tešanović, Phys. Rev. Lett. **80**, 4763 (1998)
36. P.I. Soininen, C. Kallin, A.J. Berlinsky, Phys. Rev. B **50**, 13883 (1994)
37. Y. Wang, A.H. MacDonald, Phys. Rev. B **52**, R3876 (1995)
38. M. Takigawa, M. Ichioka, K. Machida, Phys. Rev. Lett. **83**, 3057 (1999)
39. J.-X. Zhu, C.S. Ting, Phys. Rev. Lett. **87**, 147002 (2001)
40. I. Maggio-Aprile, et al., Phys. Rev. Lett. **75**, 2754 (1995)
41. S.H. Pan, et al., Phys. Rev. Lett. **85**, 1536 (2000)
42. R.B. Laughlin, Phys. Rev. Lett. **80**, 5188 (1998)
43. K. Yasui, T. Kita, Phys. Rev. Lett. **83**, 4168 (1999)
44. D.P. Arovas, et al., Phys. Rev. Lett. **79**, 2871 (1997)
45. J.H. Han, D.-H. Lee, Phys. Rev. Lett. **85**, 1100 (2000)
46. J.-X. Zhu, I. Martin, A.R. Bishop, Phys. Rev. Lett. **89**, 067003 (2002)
47. H.-D. Chen, O. Vafek, A. Yazdani, S.-C. Zhang, Phys. Rev. Lett. **93**, 187002 (2004)
48. A.M. Clogston, Phys. Rev. Lett. **3**, 266 (1962)
49. B.S. Chandrasekhar, Appl. Phys. Lett. **1**, 7 (1962)
50. P. Fulde, R.A. Ferrell, Phys. Rev. **135**, A550 (1964)

51. A.I. Larkin, Yu.N. Ovchinnikov, *Sov. Phys. JETP* **20**, 762 (1965)
52. Y. Matsuda, H. Shimahara, *J. Phys. Soc. Jpn.* **76**, 051005 (2007)
53. R. Casalbuoni, G. Nardulli, *Rev. Mod. Phys.* **76**, 263 (2004)
54. A. Bianchi, R. Movshovich, C. Capan, P.G. Pagliuso, J.L. Sarrao, *Phys. Rev. Lett.* **91**, 187004 (2003)
55. Q. Wang, H.-Y. Chen, C.-R. Hu, C.S. Ting, *Phys. Rev. Lett.* **96**, 11706 (2006)

Chapter 6

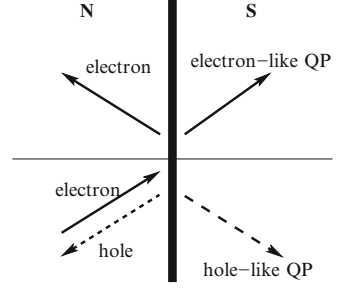
Transport Across Normal-Metal/Superconductor Junctions

Abstract In this chapter, transport properties in hybrid structures involving a superconductor are discussed. The transport quantities are expressed in terms of reflection coefficients within the framework of the Blonder-Tinkham-Klapwijk theory. These coefficients are evaluated in the scattering theory. The enhancement of conductance from Andreev reflection process is revealed, and its suppression due to the spin polarization is examined. Finally, the possible revelation of chiral Majorana modes through the tunneling differential conductance in a normal-metal-ferromagnetic insulator-*s*-wave superconductor junction is discussed.

6.1 Blonder-Tinkham-Klapwijk Scattering Formalism

In a phase-coherent normal-superconducting hybrid structure, electrons are not only intrinsically coherent in the superconducting part but also retain phase memory all through the normal conducting region. Therefore, the transport properties are determined in detail by the quasiparticle states produced by elastic scattering from inhomogeneities and boundaries. In the presence of superconductivity, a scattering process known as the Andreev reflection [1] occurs: As shown schematically in Fig. 6.1, an electron incident from the normal conductor with an energy below the superconducting quasiparticle energy gap cannot drain off individually into the superconductor. It is instead coherently reflected from the normal-metal/superconductor (NS) interface as a hole by transferring a charge $-2e$ to the superconductor. This process goes beyond the lowest-order description within the tunneling Hamiltonian model for the NS junction, which predicts that the tunneling conductance is proportional to the density of states. In 1982, Blonder, Tinkham, and Klapwijk [2] (BTK) pointed out that the contribution to the subgap conductance from the Andreev reflection can be significant, and further developed a scattering theory of transport through an NS interface with the arbitrary barrier strength.

Fig. 6.1 Schematic drawing of the scattering process for an incident electron beam impinging upon a normal-metal superconductor interface



We now discuss the derivation of the BTK formula. The time-dependent BdG equations can be directly generalized from Eq. (1.60)

$$h_{\uparrow}(\mathbf{r})f(\mathbf{r}, t) + \int d\mathbf{r}' \Delta(\mathbf{r}, \mathbf{r}')g(\mathbf{r}', t) = i\hbar \frac{\partial f(\mathbf{r}, t)}{\partial t}, \quad (6.1a)$$

$$\int d\mathbf{r}' \Delta^*(\mathbf{r}', \mathbf{r})f(\mathbf{r}', t) - h_{\downarrow}^*(\mathbf{r})g(\mathbf{r}, t) = i\hbar \frac{\partial g(\mathbf{r}, t)}{\partial t}. \quad (6.1b)$$

Now the time dependence of the potentials is included implicitly. From the above equation, we derive the continuity equation for BdG quasiparticles. We multiply Eq. (6.1a) on both sides from the left by $f^*(\mathbf{r}, t)$ while Eq. (6.1b) by $g^*(\mathbf{r}, t)$ such that

$$f^*(\mathbf{r}, t)h_{\uparrow}(\mathbf{r})f(\mathbf{r}, t) + \int d\mathbf{r}' f^*(\mathbf{r}, t)\Delta(\mathbf{r}, \mathbf{r}')g(\mathbf{r}', t) = i\hbar f^*(\mathbf{r}, t) \frac{\partial f(\mathbf{r}, t)}{\partial t},$$

$$\int d\mathbf{r}' g^*(\mathbf{r}, t)\Delta^*(\mathbf{r}', \mathbf{r})f(\mathbf{r}', t) - g^*(\mathbf{r}, t)h_{\downarrow}^*(\mathbf{r})g(\mathbf{r}, t) = i\hbar g^*(\mathbf{r}, t) \frac{\partial g(\mathbf{r}, t)}{\partial t}.$$

We then take the complex conjugation to the above two expressions

$$-f(\mathbf{r}, t)h_{\uparrow}^*(\mathbf{r})f^*(\mathbf{r}, t) - \int d\mathbf{r}' f(\mathbf{r}, t)\Delta^*(\mathbf{r}, \mathbf{r}')g^*(\mathbf{r}', t) = i\hbar f(\mathbf{r}, t) \frac{\partial f^*(\mathbf{r}, t)}{\partial t},$$

$$-\int d\mathbf{r}' g(\mathbf{r}, t)\Delta(\mathbf{r}', \mathbf{r})f^*(\mathbf{r}', t) + g(\mathbf{r}, t)h_{\downarrow}(\mathbf{r})g^*(\mathbf{r}, t) = i\hbar g(\mathbf{r}, t) \frac{\partial g^*(\mathbf{r}, t)}{\partial t}.$$

Combine the above two sets of equations together, we arrive at

$$\frac{\partial |f(\mathbf{r}, t)|^2}{\partial t} + \nabla \cdot \mathbf{J}_1 = S_1, \quad (6.4)$$

$$\frac{\partial |g(\mathbf{r}, t)|^2}{\partial t} + \nabla \cdot \mathbf{J}_2 = S_2, \quad (6.5)$$

where

$$\mathbf{J}_1 = \text{Re}[f^*(\mathbf{r}, t)\mathbf{v}_e f(\mathbf{r}, t)] , \quad (6.6)$$

$$\mathbf{J}_2 = -\text{Re}[g^*(\mathbf{r}, t)\mathbf{v}_h g(\mathbf{r}, t)] , \quad (6.7)$$

with the mechanical velocity of electron and hole as

$$\mathbf{v}_e = (\mathbf{p} + e\mathbf{A})/m_e , \quad \mathbf{v}_h = (\mathbf{p} - e\mathbf{A})/m_e . \quad (6.8)$$

The source term are respectively given by

$$S_1 = \frac{2}{\hbar} \text{Im}[f^*(\mathbf{r}, t)\Delta(\mathbf{r}, \mathbf{r}')g(\mathbf{r}', t)] , \quad (6.9)$$

and

$$S_2 = \frac{2}{\hbar} \text{Im}[g^*(\mathbf{r}, t)\Delta^*(\mathbf{r}', \mathbf{r})f(\mathbf{r}', t)] . \quad (6.10)$$

The total particle density is defined as the probability density for finding an electron or a hole at a particular time t and position \mathbf{r} ,

$$P(\mathbf{r}, t) = 2 \sum_n f(E_n) [|f^n(\mathbf{r}, t)|^2 + |g^n(\mathbf{r}, t)|^2] . \quad (6.11)$$

Correspondingly, the quasiparticle current density is given by

$$\mathbf{J}_P = 2 \sum_n f(E_n) [\mathbf{J}_1^n + \mathbf{J}_2^n] , \quad (6.12)$$

and the source term

$$S_P = 2 \sum_n f(E_n) [S_1^n + S_2^n] . \quad (6.13)$$

The charge density is defined as follows

$$Q(\mathbf{r}, t) = -2e \sum_n \{f(E_n)|f^n(\mathbf{r}, t)|^2 + [1 - f(E_n)]|g^n(\mathbf{r}, t)|^2\} . \quad (6.14)$$

Correspondingly, the electrical current density should be

$$\begin{aligned} \mathbf{J}_Q &= -2e \sum_n \{f(E_n)\mathbf{J}_1^n + [1 - f(E_n)]\mathbf{J}_2^n\} , \\ &= -2e \sum_n \{f(E_n)\text{Re}[f^{n*}(\mathbf{r}, t)\mathbf{v}_e f^n(\mathbf{r}, t)] \end{aligned}$$

$$\begin{aligned}
& -[1 - f(E_n)]\text{Re}[g^{n*}(\mathbf{r}, t)\mathbf{v}_h g^n(\mathbf{r}, t)] , \\
& = \frac{-2e\hbar}{m} \sum_n \{f(E_n)\text{Im}[f^{n*}(\mathbf{r}, t)(\nabla + ie\mathbf{A}/\hbar c)f^n(\mathbf{r}, t)] \\
& - [1 - f(E_n)]\text{Im}[g^{n*}(\mathbf{r}, t)(\nabla - ie\mathbf{A}/\hbar c)g^n(\mathbf{r}, t)]\} , \tag{6.15}
\end{aligned}$$

and the source term is

$$S_Q = -2e \sum_n \{f(E_n)S_1^n + [1 - f(E_n)]S_2^n\} . \tag{6.16}$$

The vector potential $\mathbf{A}(\mathbf{r})$ entering the BdG equations is in turn related to the electrical current distribution $\mathbf{J}_Q(\mathbf{r})$ by Maxwell's equation

$$\nabla \times (\nabla \times \mathbf{A}) = \frac{4\pi}{c} \mathbf{J}_Q . \tag{6.17}$$

It should be pointed out that the two-fold spin degeneracy has been included explicitly. At a first glance, the current are not conserved. However, if we take into account the self-consistency condition about the pair potential, we can check that the source term S_Q is zero. For this reason, in non-self-consistent theory the current is evaluated in the normal region (where the current is conserved since the pair potential is zero) and the current in the superconducting region is inferred indirectly. Obviously, the source term S_p can never become zero, which is allowed by the mother nature itself in the superconductivity. We refer to [2–4] for more discussion of these definitions. The present current expression has been used to study the transport properties through a superconducting point contact [5].

The BTK transport theory is based on the assumption that the electrons are ballistically accelerated without scattering before they hit the NS interface. In addition, one assumes that the distribution functions of all incoming particles are given by equilibrium Fermi-Dirac functions, apart from the energy shift due to the voltage bias. It is convenient to choose the electrochemical potential of the electrons in the superconductor as the reference since it remains a well-defined quantity even when the quasiparticle populations are far from equilibrium. With this convention, all incoming electrons from the superconductor side have the distribution function $f_{FD}(E)$, while those coming in from the normal-metal side have the distribution function $f_{FD}(E - eV)$. Since the current must be conserved, we can evaluate it in any plane for an actual two-dimensional or three-dimensional geometry. For a planar junction, we can always first calculate the current for a given incident direction of electron beams, with angle θ , as shown in Fig. 6.1, from which the total current can be obtained by integrating over the transverse momentum. Assuming the current flow along the x -direction, which is perpendicular the NS junction, we can write the current as

$$I(\theta, V) = 2N(0)ev_{F,x}\mathcal{A} \int_{-\infty}^{\infty} [f_{\rightarrow}(E) - f_{\leftarrow}(E)]dE . \tag{6.18}$$

Here \mathcal{A} is the cross-sectional area of the interface, $N(0)$ is the one-spin density of states at the Fermi energy at ϵ_F , and $v_{F,x} = v_F \cos \theta$. With the assumption about the incoming populations, it follows that

$$f_{\rightarrow}(E) = f_{FD}(E - eV) , \quad (6.19)$$

while

$$f_{\leftarrow}(E) = A(E)[1 - f_{\rightarrow}(E)] + B(E)f_{\rightarrow}(E) + [C(E) + D(E)]f_{FD}(E) . \quad (6.20)$$

Here the probabilities $A(E)$, $B(E)$, $C(E)$, and $D(E)$ are for normal reflection, Andreev reflection, transmission through the interface with a wave vector on the same side of the Fermi surface and that crossing the Fermi surface. We have represented the current incident from the superconducting side in terms of the summation of $C(E)$ and $D(E)$. Substituting Eqs. (6.19) and (6.20) into Eq. (6.18), we arrive at

$$I(\theta, V) = 2N(0)e v_{F,x} \mathcal{A} \int_{-\infty}^{\infty} [f_{FD}(E - eV) - f_{FD}(E)] [1 + A(E) - B(E)] dE . \quad (6.21)$$

Here we have used the symmetry that the probabilities $A(E)$, $B(E)$, $C(E)$, and $D(E)$ are even functions of E , and $f_{FD}(-E) = 1 - f_{FD}(E)$. The quantity $1 + A(E) - B(E)$ can be referred as the transmission coefficient for electrical current. It shows that while the ordinary reflection (described by $B(E)$) reduces the current, the Andreev reflection (described by $A(E)$) increases the current by giving one electron to form a Cooper pair together with the incident electron. From Eq. (6.21), we can also obtain the differential conductance for a given incident direction of electrons as:

$$G_{NS}(\theta, V) = \frac{\partial I(\theta)}{\partial V} = 2N(0)e^2 v_{F,x} \mathcal{A} \int_{-\infty}^{\infty} \left[-\frac{f_{FD}(E - eV)}{\partial E} \right] [1 + A(E) - B(E)] dE . \quad (6.22)$$

At zero temperature, we have

$$-\frac{\partial f_{FD}(E - eV)}{\partial E} = \delta(E - eV) , \quad (6.23)$$

which leads to

$$G_{NS}(\theta, V) = 2N(0)e^2 v_{F,x} \mathcal{A} [1 + A(eV) - B(eV)] . \quad (6.24)$$

Equations (6.22) and (6.24) represent the BTK scattering formalization for the transport across the NS junction, while the BdG equations provide a framework to evaluate the reflection probability quantitatively. Interestingly, the BTK formula can also be considered as the revised version of the Landauer-Büttiker formula [6, 7] for an NS junction. The latter has been extensively used to describe the quantum coherent transport in mesoscopic normal conductors. We first point out that the

original BTK theory is applicable to a junction with translational invariance along the NS interface. A more general Landauer-Büttiker-like theory has been developed [8–12] to describe the quantum phase-coherence transport through normal-metal superconductor hybrid structures. With this generalized theory, the zero-bias conductance anomaly observed in the differential conductance of a semiconductor in contact with a conventional s -wave superconductor [13–15] has been interpreted as a combined consequence of multiple impurity scattering inside the semiconductor and the Andreev reflection at the interface [11, 16]. The generalized scattering formalism can also be cast into the random matrix theory [17] to study the excess conductance of semiconductor-superconductor junctions, where the elastic impurity scattering in the normal region is important.

In this chapter, we consider no impurity scattering at the NS interface and instead focus on the consequence of superconducting pairing symmetry on the conductance. Part of the motivation comes from the observation of zero-bias conductance peak (ZBCP) when electrons are tunneling into the ab -oriented thin films of high-temperature superconductors [18–21]. This ZBCP cannot be explained by conventional tunneling theories. Although the feature was originally analyzed based on the conventional s -wave tunneling model by introducing the spin-flip scattering of the tunnel electrons from magnetic impurities speculated to exist in the insulating barrier, the mechanism is inconsistent with the experimentally observed nonlinear splitting of the ZBCP with the magnetic field and the absence of the ZBCP in the tunneling conductance of c -axis-oriented YBaCuO/Pb junctions. Now it has become clear [22–25] that the ZBCP observed in high-temperature cuprates originates instead from the d -wave pairing symmetry.

6.2 Tunneling Conductance Through a Normal-Metal/Superconductor Junction

Without loss of generality, we consider a two-dimensional normal-metal/superconductor junction. The setup is relevant to the high-temperature cuprates, where the superconductivity emerges mainly in the two-dimensional copper-oxide plane. As we have derived in Chap. 1, the motion of quasiparticles in a normal-metal superconductor junction can be described by the BdG equation (1.60)

$$\mathcal{H}_e(\mathbf{r})u(\mathbf{r}) + \int d\mathbf{r}' \Delta(\mathbf{r}, \mathbf{r}')v(\mathbf{r}') = Eu(\mathbf{r}) , \quad (6.25a)$$

$$-\mathcal{H}_e^*(\mathbf{r})v(\mathbf{r}) + \int d\mathbf{r}' \Delta^*(\mathbf{r}', \mathbf{r})u(\mathbf{r}') = Ev(\mathbf{r}) . \quad (6.25b)$$

Here $(u(\mathbf{r}), v(\mathbf{r}))$ is the quasiparticle wave function of the BdG equations. $\mathcal{H}_e(\mathbf{r}) = -\hbar^2 \nabla_{\mathbf{r}}^2 / 2m_e + V(\mathbf{r}) - E_F$ is the single-particle Hamiltonian, where $V(\mathbf{r})$ is the usual static potential, and E_F is the Fermi energy. Therefore, the excitation energy is

measured with respect to the Fermi energy E_F . Again we have dropped the spin indices to the quasiparticle wave function for the case without spin-polarization and spin-flip scattering. $\Delta(\mathbf{r}, \mathbf{r}')$ is the pair potential, the dependence of which on \mathbf{r} and \mathbf{r}' cannot be reduced to a dependence on the difference of the two coordinates, that is, $\mathbf{r} - \mathbf{r}'$, for an inhomogeneous case. By introducing the center-of-mass coordinates $\mathbf{R} = (\mathbf{r} + \mathbf{r}')/2$ and the relative coordinates $\mathbf{s} = \mathbf{r} - \mathbf{r}'$, we can write the pair potential in terms of \mathbf{R} and \mathbf{r}

$$\tilde{\Delta}(\mathbf{R}, \mathbf{s}) \equiv \Delta(\mathbf{r}, \mathbf{r}') . \quad (6.26)$$

By performing the Fourier transform with respect to the relative coordinate \mathbf{s} , we can write the pair potential in the mixed representation

$$\tilde{\Delta}(\mathbf{R}, \mathbf{k}) = \int d\mathbf{s} \tilde{\Delta}\left(\mathbf{R} + \frac{\mathbf{s}}{2}, \mathbf{R} - \frac{\mathbf{s}}{2}\right) e^{-i\mathbf{k}\cdot\mathbf{s}} . \quad (6.27)$$

This shows clearly that for an unconventional superconductor like that with d -wave pairing symmetry, the pair potential depends not only on the center-of-mass coordinate \mathbf{R} but also on the relative wave vector \mathbf{k} , which in the weak-coupling theory is fixed on the Fermi surface such that only its direction $\hat{\mathbf{k}}_F = \mathbf{k}_F/k_F$ is a variable, where k_F is the magnitude of the Fermi wave vector.

An investigation of the BdG equations shows that $u(\mathbf{r})$ and $v(\mathbf{r})$ oscillate on the scale of the superconducting coherence length $\xi_0 = \hbar v_F/2\Delta_0$, which is much larger than the inverse Fermi wave vector k_F^{-1} . Here v_F is the Fermi velocity and Δ_0 is the maximum value of the pair potential in the bulk region of the superconductor. Therefore, we can introduce a new set of wave functions

$$\begin{pmatrix} \bar{u}(\mathbf{r}) \\ \bar{v}(\mathbf{r}) \end{pmatrix} = e^{-i\mathbf{k}_F \cdot \mathbf{r}} \begin{pmatrix} u(\mathbf{r}) \\ v(\mathbf{r}) \end{pmatrix} , \quad (6.28)$$

to divide out the fast oscillation. The substitution of Eq. (6.28) into Eq. (6.25) leads to the Andreev equations [1, 26]:

$$E\bar{u}(\mathbf{r}) = -i(\hbar^2/m_e)\mathbf{k}_F \cdot \nabla\bar{u}(\mathbf{r}) + \tilde{\Delta}(\mathbf{r}, \hat{\mathbf{k}}_F)\bar{v}(\mathbf{r}) , \quad (6.29a)$$

$$E\bar{v}(\mathbf{r}) = i(\hbar^2/m_e)\mathbf{k}_F \cdot \nabla\bar{v}(\mathbf{r}) + \tilde{\Delta}^*(\mathbf{r}, \hat{\mathbf{k}}_F)\bar{u}(\mathbf{r}) . \quad (6.29b)$$

when we retain only terms of the lowest order in $(k_F\xi_0)^{-1}$. We show this by looking at

$$\int d\mathbf{r}' \Delta(\mathbf{r}, \mathbf{r}') \bar{v}(\mathbf{r}') e^{-i\mathbf{k}\cdot(\mathbf{r}-\mathbf{r}')} = \int d\mathbf{s} \tilde{\Delta}(\mathbf{r} - \mathbf{s}/2, \mathbf{s}) \bar{v}(\mathbf{r} - \mathbf{s}) e^{-i\mathbf{k}\cdot\mathbf{s}} . \quad (6.30)$$

Assuming that $\bar{v}(\mathbf{r})$ is a slowly varying function as is $\tilde{\Delta}(\mathbf{R}, \mathbf{s})$ in the first argument

$$\begin{aligned}\tilde{\Delta}(\mathbf{r} - \mathbf{s}/2, \mathbf{s}) &\approx \tilde{\Delta}(\mathbf{r}, \mathbf{s}) - \mathbf{s} \cdot \nabla_{\mathbf{r}} \tilde{\Delta}(\mathbf{r}, \mathbf{s})/2, \\ \bar{v}(\mathbf{r} - \mathbf{s}) &\approx \bar{v}(\mathbf{r}) - \mathbf{s} \cdot \nabla_{\mathbf{r}} \bar{v}(\mathbf{r}),\end{aligned}$$

we have

$$\begin{aligned}\int ds \tilde{\Delta}(\mathbf{r} - \mathbf{s}/2, \mathbf{s}) \bar{v}(\mathbf{r} - \mathbf{s}) e^{-i\mathbf{k}\cdot\mathbf{s}} &= \int ds [\tilde{\Delta}(\mathbf{r}, \mathbf{s}) - \mathbf{s} \cdot \nabla_{\mathbf{r}} \tilde{\Delta}(\mathbf{r}, \mathbf{s})/2] [\bar{v}(\mathbf{r}) - \mathbf{s} \cdot \nabla_{\mathbf{r}} \bar{v}(\mathbf{r})] \\ &\approx \int ds \tilde{\delta}(\mathbf{r}, \mathbf{s}) \bar{v}(\mathbf{r}) e^{-i\mathbf{k}\cdot\mathbf{s}} \\ &\quad - \int ds \frac{\mathbf{s}}{2} \cdot \nabla_{\mathbf{r}} \tilde{\Delta}(\mathbf{r}, \mathbf{s}) e^{-i\mathbf{k}\cdot\mathbf{s}} \\ &\quad - \int ds \tilde{\Delta}(\mathbf{r}, \mathbf{s}) \mathbf{s} \cdot \nabla_{\mathbf{r}} \bar{v}(\mathbf{r}) e^{-i\mathbf{k}\cdot\mathbf{s}} \\ &= \tilde{\Delta}(\mathbf{r}, \mathbf{k}) - i[\nabla_{\mathbf{r}} \bar{v}(\mathbf{r}) + \frac{\bar{v}(\mathbf{r})}{2} \nabla_{\mathbf{r}}] \cdot \nabla_{\mathbf{k}} \tilde{\Delta}(\mathbf{r}, \mathbf{k}).\end{aligned}\quad (6.31)$$

Here we have used the identities

$$\begin{aligned}\int ds \nabla_{\mathbf{r}} \frac{\mathbf{s}}{2} \cdot \tilde{\Delta}(\mathbf{r}, \mathbf{s}) \bar{v}(\mathbf{r}) e^{-i\mathbf{k}\cdot\mathbf{s}} &= \frac{\bar{v}(\mathbf{r})}{2} \nabla_{\mathbf{r}} \cdot \int ds \tilde{\Delta}(\mathbf{r}, \mathbf{s}) \mathbf{s} e^{-i\mathbf{k}\cdot\mathbf{s}} \\ &= \frac{\bar{v}(\mathbf{r})}{2} \nabla_{\mathbf{r}} \cdot \int ds i \nabla_{\mathbf{k}} e^{-i\mathbf{k}\cdot\mathbf{s}} \tilde{\Delta}(\mathbf{r}, \mathbf{s}) \\ &= i \frac{\bar{v}(\mathbf{r})}{2} \nabla_{\mathbf{r}} \cdot \nabla_{\mathbf{k}} \tilde{\Delta}(\mathbf{r}, \mathbf{k}),\end{aligned}$$

and similarly

$$\begin{aligned}\int ds \tilde{\Delta}(\mathbf{r}, \mathbf{s}) \mathbf{s} \cdot \nabla_{\mathbf{r}} \bar{v}(\mathbf{r}) e^{-i\mathbf{k}\cdot\mathbf{s}} &= \nabla_{\mathbf{r}} \bar{v}(\mathbf{r}) \cdot \int ds \tilde{\Delta}(\mathbf{r}, \mathbf{s}) \mathbf{s} e^{-i\mathbf{k}\cdot\mathbf{s}} \\ &= i \nabla_{\mathbf{r}} \bar{v}(\mathbf{r}) \cdot \int ds i \nabla_{\mathbf{k}} e^{-i\mathbf{k}\cdot\mathbf{s}} \tilde{\Delta}(\mathbf{r}, \mathbf{s}) \\ &= i \nabla_{\mathbf{r}} \bar{v}(\mathbf{r}) \cdot \nabla_{\mathbf{k}} \tilde{\Delta}(\mathbf{r}, \mathbf{k}).\end{aligned}$$

Therefore, it is clear that the second term of the sum in Eq. (6.31) is down by a factor of $(k_F \xi_0)^{-1}$ as compared with the first term. If we restrict ourselves to the terms in lowest order of the small parameters, we are left with Eq. (6.29), a first-order differential equation in which \mathbf{k} is treated as a parameter. Since $\tilde{\Delta}(\mathbf{r}, \mathbf{k})$ is defined only for \mathbf{k} around the Fermi wave vector, we can replace the \mathbf{k} -dependence of $\tilde{\Delta}(\mathbf{r}, \mathbf{k})$ by one on the direction $\hat{\mathbf{k}}_F$.

From now on we assume that the edge interface is specular, runs along the y -direction, and the transport direction is normal to the interface (i.e., along the x -axis) (see Fig. 6.1 for the setup). In this case, \bar{u} , \bar{v} , and $\tilde{\Delta}$ spatially depend only on the variable x since the system is translational invariant along the interface. The Andreev equations then reduce to the form:

$$E\bar{u}(x) = -i(\hbar^2/m_e)k_{Fx} \frac{d\bar{u}(x)}{dx} + \tilde{\Delta}(\hat{\mathbf{k}}_F, x)\bar{v}(x), \quad (6.32a)$$

$$E\bar{v}(x) = i(\hbar^2/m_e)k_{Fx} \frac{d\bar{v}(x)}{dx} + \tilde{\Delta}(\hat{\mathbf{k}}_F, x)\bar{u}(x). \quad (6.32b)$$

Here we have assumed the superconducting pair potential to be real. We further choose the interface at $x = 0$. The region $x < 0$ is occupied by the normal conductor while the region $x > 0$ is occupied by the superconductor. At the NS interface, quasiparticles (e.g., electron like excitations) are partially reflected as electron-like and hole-like excitations due to the non-zero pair potential in the superconductor. When the wave vectors of electron-like and hole-like excitations are different, the pair potentials experienced by electron-like and hole-like excitations should be different for an unconventional superconductor. We denote the incident and reflected wave vectors by $\mathbf{k}_+ = (k_x, k_y)$ and $\mathbf{k}_- = (-k_x, k_y)$, respectively. The pair potential then takes the form

$$\tilde{\Delta}(\mathbf{k}_{\pm}, x) = \begin{cases} 0, & x < 0 \\ \Delta_0, & 0 \leq x \end{cases} \quad (6.33)$$

for the s -wave superconductor, while

$$\tilde{\Delta}(\mathbf{k}_{\pm}, x) = \begin{cases} 0, & x < 0 \\ \Delta_0 \cos(2\theta_{\pm}), & 0 \leq x \end{cases} \quad (6.34)$$

for the $d_{x^2-y^2}$ -wave superconductor. Here $\theta_{\pm} = \theta \mp \alpha$ with θ the incident angle of electron excitations injected from the normal conductor and α the disorientation angle of the crystalline axis along which the $d_{x^2-y^2}$ -wave superconducting pair potential reaches the maximum. Both θ and α are measured relative to the positive x -axis. In addition, to capture the essential interfacial scattering at the interface, we include a δ -function potential

$$V(x) = H\delta(x). \quad (6.35)$$

The metallic contact and the tunnel junction correspond to the two limiting cases of the barrier strength $H = 0$ and $H \rightarrow \infty$.

In the condition of an electron beam incident from the normal conductor at an angle θ , the solution to the Andreev equations (6.29),

$$\Psi(x) = \begin{pmatrix} \bar{u}(x) \\ \bar{v}(x) \end{pmatrix},$$

is given by

$$\Psi_I(x) = \begin{pmatrix} 1 \\ 0 \end{pmatrix} e^{iq_e x} + a \begin{pmatrix} 0 \\ 1 \end{pmatrix} e^{iq_h x} + b \begin{pmatrix} 1 \\ 0 \end{pmatrix} e^{-iq_e x}, \quad (6.36)$$

for $x < 0$, and

$$\Psi_{II}(x) = c \begin{pmatrix} u_+ e^{i\phi_+} \\ v_+ \end{pmatrix} e^{ik_{e,+} x} + d \begin{pmatrix} v_- e^{i\phi_-} \\ u_- \end{pmatrix} e^{-ik_{h,-} x} \quad (6.37)$$

for $x \geq 0$. Here the wave vectors are determined from the energy dispersion:

$$q_{e,h} = k_{fx} \pm \frac{m_e E}{\hbar^2 k_{Fx}}, \quad (6.38)$$

$$k_{e(h),+} = k_{Fx} \pm \frac{m_e \sqrt{E^2 - |\tilde{\Delta}(\mathbf{k}_+)|^2}}{\hbar^2 k_{Fx}}, \quad (6.39)$$

$$k_{e(h),-} = k_{Fx} \pm \frac{m_e \sqrt{E^2 - |\tilde{\Delta}(\mathbf{k}_-)|^2}}{\hbar^2 k_{Fx}}. \quad (6.40)$$

For a given pair potential, these wave vectors are schematically described in Fig. 6.2. The coherence factors in the superconducting regions are

$$u_{\pm}^2 = \frac{1}{2} \left(1 + \frac{\sqrt{E^2 - |\tilde{\Delta}(\mathbf{k}_{\pm})|^2}}{E} \right), \quad (6.41)$$

$$v_{\pm}^2 = \frac{1}{2} \left(1 - \frac{\sqrt{E^2 - |\tilde{\Delta}(\mathbf{k}_{\pm})|^2}}{E} \right), \quad (6.42)$$

respectively. The characteristic phases are given by

$$\phi_{\pm} = \cos^{-1} \left(\frac{\cos 2(\theta \mp \alpha)}{|\cos 2(\theta \mp \alpha)|} \right). \quad (6.43)$$

Imposing the boundary conditions at the interface

$$\Psi_{II}(0) = \Psi_I(0), \quad (6.44a)$$

$$\Psi'_{II}(0) - \Psi'_I(0) = \left(\frac{2m_e H}{\hbar^2} \right) \Psi'_I(0), \quad (6.44b)$$

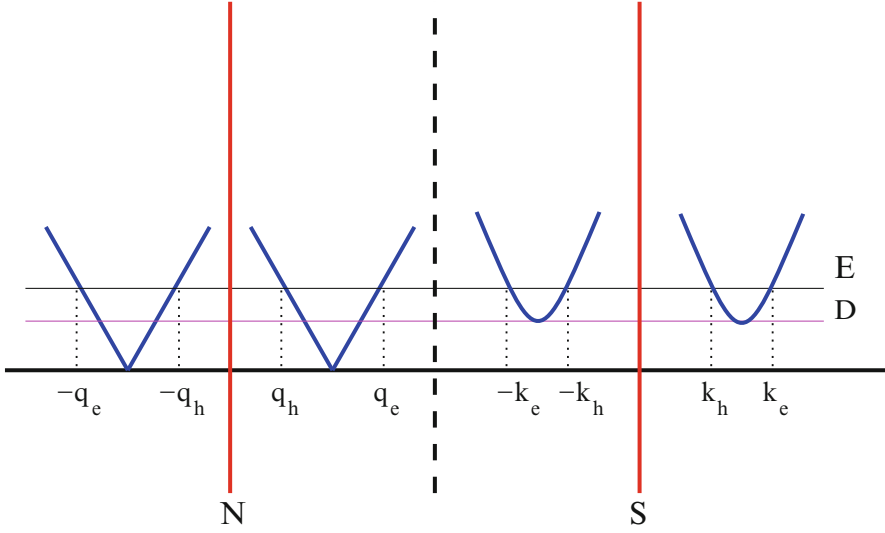


Fig. 6.2 Schematic diagram of energy versus momentum at the normal-metal/superconductor interface

and carrying out the algebraic reduction, we obtain

$$a = \frac{u_- v_+}{(1 + Z^2)u_+ u_- e^{i\phi_+} - Z^2 v_+ v_- e^{i\phi_-}} , \quad (6.45)$$

and

$$b = -\frac{(iZ + Z^2)(u_+ u_- e^{i\phi_+} - v_+ v_- e^{i\phi_-})}{(1 + Z^2)u_+ u_- e^{i\phi_+} - Z^2 v_+ v_- e^{i\phi_-}} , \quad (6.46)$$

where $Z = m_e H / \hbar^2 k_F \cos \theta = Z_0 / \cos \theta$ with $Z_0 = m_e H / \hbar^2 k_F$. The corresponding normal and Andreev reflection probabilities are then given by $B(E, \theta) = |b(E, \theta)|^2$, and $A(E, \theta) = |a(E, \theta)|^2$, respectively. Therefore, the differential conductance can be determined upon the substitution of Eqs. (6.45) and (6.46) into Eq. (6.24). For the normal-metal/normal-metal junction, that is, the superconductor in the region $x \geq 0$ replaced by the normal metal, the Andreev and normal reflection amplitudes are given by

$$a = 0 , \quad (6.47)$$

and

$$b(E, \theta) = -\frac{Z(1 + iZ)}{1 + Z^2} , \quad (6.48)$$

which leads to the differential conductance

$$G_{NN}(E, \theta) = 2N(0)e^2 \mathcal{A} \frac{v_{F,x}}{1 + Z^2}. \quad (6.49)$$

For the 2D model we are considering, we shall take an average over the incident angle

$$\begin{aligned} \bar{G}_{NS}(E) &= \frac{1}{\pi} \int_{-\pi/2}^{\pi/2} d\theta G_{NS}(E, \theta) \\ &= \frac{2N(0)e^2 \mathcal{A} v_F}{\pi} \int_{-\pi/2}^{\pi/2} d\theta \cos \theta [1 + A(E, \theta) - B(E, \theta)], \end{aligned} \quad (6.50)$$

for the NS junction, and

$$\begin{aligned} \bar{G}_{NN}(E) &= \frac{1}{\pi} \int_{-\pi/2}^{\pi/2} d\theta G_{NN}(E, \theta) \\ &= \frac{2N(0)e^2 \mathcal{A} v_F}{\pi} \int_{-\pi/2}^{\pi/2} d\theta \frac{\cos \theta}{1 + Z^2} \\ &= \frac{2N(0)e^2 \mathcal{A} v_F}{\pi} \left[2 - \frac{Z_0^2}{\sqrt{1 + Z_0^2}} \ln \frac{\sqrt{1 + Z_0^2} + 1}{\sqrt{1 + Z_0^2} - 1} \right], \end{aligned} \quad (6.51)$$

for the NN junction. Therefore, we can define a normalized differential conductance

$$\begin{aligned} g_{NS}(E) &= \frac{\bar{G}_{NS}(E)}{\bar{G}_{NN}(E)} \\ &= \frac{1}{\mathcal{N}} \int_{-\pi/2}^{\pi/2} d\theta \cos \theta [1 + A(E, \theta) - B(E, \theta)], \end{aligned} \quad (6.52)$$

where

$$\mathcal{N} = 2 - \frac{Z_0^2}{\sqrt{1 + Z_0^2}} \ln \frac{\sqrt{1 + Z_0^2} + 1}{\sqrt{1 + Z_0^2} - 1}. \quad (6.53)$$

This normalized conductance is useful to the comparison with the standard transport measurement across the NS junction. For the orifice model of the point contact spectroscopy, we can set a specific incident angle and do not perform an average. In this case, we can still define a normalized conductance but now for a given incident angle θ .

$$g_{NS.PCS}(E, \theta) = (1 + Z^2)[1 + A(E, \theta) - B(E, \theta)]. \quad (6.54)$$

In the following, we discuss a few representative cases of the transport across the NS junction.

***s*-Wave NS Junction** For the *s*-wave NS junction, the superconducting pair potential has no momentum dependence and as such is independent of the incident angle. Therefore, we have

$$u_{\pm}^2 = u_0^2 = \frac{1}{2} \left(1 + \frac{\sqrt{E^2 - |\tilde{\Delta}_0|^2}}{E} \right), \quad (6.55)$$

and

$$v_{\pm}^2 = v_0^2 = \frac{1}{2} \left(1 - \frac{\sqrt{E^2 - |\tilde{\Delta}_0|^2}}{E} \right), \quad (6.56)$$

In addition, $\phi_{\pm} = 0$. The Andreev reflection and normal reflection amplitudes are given by

$$a = \frac{u_0 v_0}{u_0^2 + (u_0^2 - v_0^2)Z^2}, \quad (6.57)$$

and

$$b = \frac{-(Z^2 + iZ)(u_0^2 - v_0^2)}{u_0^2 + (u_0^2 - v_0^2)Z^2}, \quad (6.58)$$

respectively. These expressions suggest that, for the contact case $Z_0 = 0$, when the energy E is smaller than the superconducting gap $\tilde{\Delta}_0$, $A(E) = |a|^2 = 1$ and $B(E) = |b|^2 = 0$, explaining the double of the conductance as compared with that for the NN junction. In the tunneling limit $Z_0 \rightarrow \infty$, we have $A(E) = 0$ and $B(E) = 1$ so that the conductance is zero for $E < \tilde{\Delta}_0$. The numerical results of the differential conductance for the NS junction with *s*-wave pairing symmetry are shown in Fig. 6.3. The Andreev reflection is suppressed with increased interface barrier strength in the *s*-wave NS junction and the resulting differential conductance has the profile of the *s*-wave density of states in the tunneling limit.

***d*-Wave NS Junction** As we have mentioned before, for the NS junction with an unconventional pairing symmetry, the energy experienced by electronic-like and hole-like excitations are sensitive to both the relative crystalline orientation between the normal metal and the superconductor and the incident angle. To demonstrate this, we consider the $d_{x^2-y^2}$ -wave pairing symmetry of the superconductor, choosing $\alpha = \pi/4$ and $\theta = \pi/4$.¹ This angle of the relative crystalline orientation

¹The results for $\alpha = \theta = 0$ are very similar to the *s*-wave NS junction.

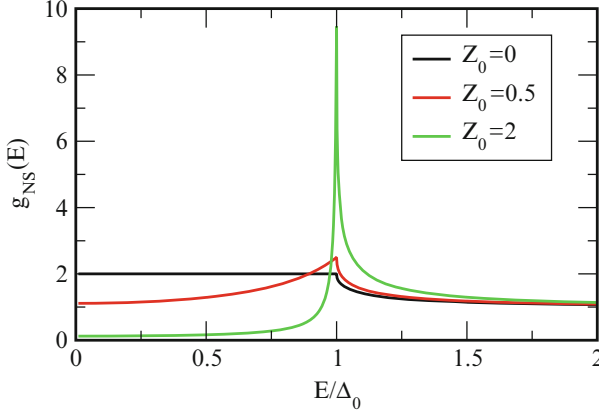


Fig. 6.3 Differential conductance for a normal-metal/*s*-wave superconductor junction for various values of interface barrier strength. The energy is measured in units of the superconducting pair potential. The incident angle is chosen to be $\theta = 0$

corresponds to the square lattice of copper-oxide plane of high-temperature cuprates interfaced with the normal metal along the $[110]$ direction. These angles determine $\tilde{\Delta}(\mathbf{k}_+) = \tilde{\Delta}_0$ while $\tilde{\Delta}(\mathbf{k}_-) = -\tilde{\Delta}_0$. The BdG wave function amplitudes u_{\pm} and v_{\pm} are still given by the formula similar to the *s*-wave case presented above. However, we have now the characteristic phase $\phi_+ = 0$ while $\phi_- = \pi$ due to the sign change of the pair potential experienced by electron-like and hole-like excitations. In this case, the Andreev and normal-state reflection amplitudes are found as

$$a = \frac{u_0 v_0}{u_0^2 + Z^2}, \quad (6.59)$$

and

$$b = -\frac{iZ + Z^2}{u_0^2 + Z^2}. \quad (6.60)$$

These expressions suggest that for the perfect contact $Z_0 = 0$, the Andreev reflection is still complete with $A(E) = 1$ and $B(E) = 0$ for $E < \Delta_0$. Even more interestingly, for the tunneling limit $Z_0 \rightarrow \infty$, as $E \rightarrow 0$, $A(E) \rightarrow 1$ while $B(E) \rightarrow 0$, indicating a conductance anomaly. The numerical results on the differential conductance for the *d*-wave NS junction are shown in Fig. 6.4 for $\alpha = \theta = \pi/4$. It shows clearly that the zero-energy conductance peak appears in the limiting case of tunneling barrier. This anomaly is solely due to the sign change of $d_{x^2-y^2}$ -wave superconducting order parameter under the above condition. This existence of the zero-bias conductance peak has been used to identify the $d_{x^2-y^2}$ -wave pairing symmetry in the high-temperature cuprates.

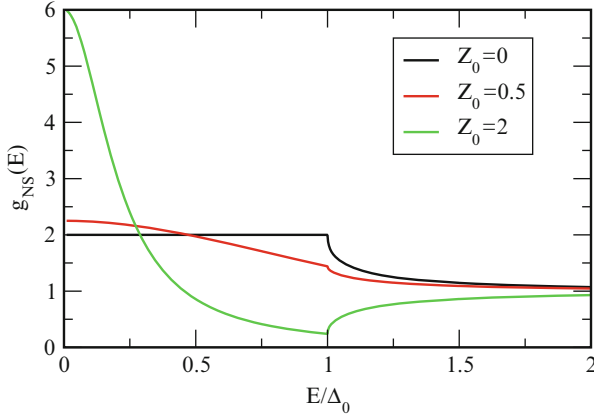


Fig. 6.4 Differential conductance for a normal-metal/*d*-wave superconductor junction for various values of interface barrier strength. The energy is measured in units of the superconducting pair potential. The crystalline orientation between the normal metal and the *d*-wave superconductor and the incident angle is chosen to be $\alpha = \pi/4$ and $\theta = \pi/4$, respectively

6.3 Suppression of Andreev Reflection in a Ferromagnet/*s*-Wave Superconductor Junction

In the Andreev reflection process, the incoming electron and the Andreev reflected hole occupy energy bands with opposite spins. For the case of normal metals, due to the spin degeneracy of the energy levels, no spin effects occur with the Andreev reflection. However, in a metallic ferromagnet, the energy band is split. The interplay of superconductivity and ferromagnetism in hybrid structures has been a very interesting topic. A lot of works have focused on the changes of the critical temperature of the superconductor in *s*-wave superconductor/ferromagnet multilayers [27–34], the Josephson critical current in superconductor/ferromagnet/superconductor junctions [35–38], and the magnetic coupling in ferromagnet/superconductor/ferromagnet multilayers [39, 40]. In tunneling regime, the Andreev reflection is unimportant [41]. However, in the contact regime, the spin splitting effect on the Andreev reflection in ferromagnet/superconductor cannot be ignored [42–44]. To model the spin splitting effect on the Andreev reflection in a ferromagnet/*s*-wave superconductor junction, we consider the Stoner model, in which the motion of conduction electrons inside the ferromagnet can be described by an effective single-particle Hamiltonian with an exchange interaction while the influence of the magnetization of the ferromagnet on the orbital motion of conduction electrons is neglected. As we have discussed in previous chapters, in the absence of spin-flip scattering, the spin-dependent (four-component) BdG equations are decoupled into two sets of (two-component) equations, one for the spin-up electron and spin-down hole quasiparticle wave functions $(u_{\uparrow}, v_{\downarrow})^T$, while the other for spin-down electron and spin-up hole quasiparticle wave functions $(u_{\downarrow}, v_{\uparrow})^T$. The

set of BdG equations for $(u_\uparrow, v_\downarrow)^T$ can be written as:

$$[\mathcal{H}_e(\mathbf{r}) - h(\mathbf{r})]u_\uparrow(\mathbf{r}) + \int d\mathbf{r}' \Delta(\mathbf{r}, \mathbf{r}')v_\downarrow(\mathbf{r}') = Eu_\uparrow(\mathbf{r}), \quad (6.61a)$$

$$-[\mathcal{H}_e^*(\mathbf{r}) + h(\mathbf{r})]v_\downarrow(\mathbf{r}) + \int d\mathbf{r}' \Delta^*(\mathbf{r}', \mathbf{r})u_\uparrow(\mathbf{r}') = Ev_\downarrow(\mathbf{r}). \quad (6.61b)$$

Compared with the case of a NS junction considered in the previous section [cf. Eq. (6.25)], an exchange field $h(\mathbf{r}) = h_0\Theta(-x)$ in the ferromagnet is now introduced. The set of BdG equations for $(u_\downarrow, v_\uparrow)^T$ is obtained by simply changing the sign before $h(\mathbf{r})$ in Eq. (6.61). Following the same procedure as given in the previous section, we have the solution to the Andreev equations as:

$$\Psi_I(x) = \begin{pmatrix} 1 \\ 0 \end{pmatrix} e^{iq_e x} + r_{\downarrow\uparrow} \begin{pmatrix} 0 \\ 1 \end{pmatrix} e^{iq_h x} + r_{\uparrow\uparrow} \begin{pmatrix} 1 \\ 0 \end{pmatrix} e^{-iq_e x}, \quad (6.62)$$

for $x < 0$, and

$$\Psi_{II}(x) = c \begin{pmatrix} u_+ e^{i\phi_+} \\ v_+ \end{pmatrix} e^{ik_e x} + \begin{pmatrix} v_- e^{i\phi_-} \\ u_- \end{pmatrix} e^{-ik_h x} \quad (6.63)$$

for $x \geq 0$. Here the wave vectors are determined from the energy dispersion:

$$q_{e\uparrow, h\downarrow} = \sqrt{k_{Fx}^2 \pm \frac{2m_e}{\hbar^2}(E + h_0)}, \quad (6.64)$$

$$k_{e(h),+} = k_{Fx} \pm \frac{m_e \sqrt{E^2 - |\tilde{\Delta}(\mathbf{k}_+)|^2}}{\hbar^2 k_{Fx}}, \quad (6.65)$$

$$k_{e(h),-} = k_{Fx} \pm \frac{m_e \sqrt{E^2 - |\tilde{\Delta}(\mathbf{k}_-)|^2}}{\hbar^2 k_{Fx}}. \quad (6.66)$$

Since the Andreev reflection for the s -wave NS junction is most pronounced in the contact case, we consider the barrier strength $H = 0$. Therefore, the boundary conditions now become:

$$\Psi_{II}(0) = \Psi_I(0), \quad (6.67a)$$

$$\Psi'_{II}(0) = \Psi'_I(0). \quad (6.67b)$$

The important difference between the NS and FS junctions are now revealed by the momentum difference in the ferromagnet. To show this, we expand the boundary

conditions:

$$\begin{pmatrix} u_+ e^{i\phi+c} + v_- e^{i\phi-d} \\ v_+ c + u_- d \end{pmatrix} = \begin{pmatrix} 1 + r_{\uparrow\uparrow} \\ r_{\downarrow\uparrow} \end{pmatrix}, \quad (6.68a)$$

and

$$\begin{pmatrix} u_+ e^{i\phi+c} - v_- e^{i\phi-d} \\ v_+ c - u_- d \end{pmatrix} = \begin{pmatrix} \frac{q_{e\uparrow}}{k_{Fx}} (1 - r_{\uparrow\uparrow}) \\ \frac{q_{h\downarrow}}{k_{Fx}} r_{\downarrow\uparrow} \end{pmatrix}, \quad (6.68b)$$

which gives

$$r_{\downarrow\uparrow} = \frac{4u_- v_+ \bar{q}_{e\uparrow}}{(1 + \bar{q}_{e\uparrow})(1 + \bar{q}_{h\downarrow})u_+ u_- e^{i\phi+c} - (1 - \bar{q}_{e\uparrow})(1 - \bar{q}_{h\downarrow})v_+ v_- e^{i\phi-d}}, \quad (6.69)$$

and

$$r_{\uparrow\uparrow} = \frac{-(1 - \bar{q}_{e\uparrow})(1 + \bar{q}_{h\downarrow})u_+ u_- e^{i\phi+c} + (1 + \bar{q}_{e\uparrow})(1 - \bar{q}_{h\downarrow})v_+ v_- e^{i\phi-d}}{(1 + \bar{q}_{e\uparrow})(1 + \bar{q}_{h\downarrow})u_+ u_- e^{i\phi+c} - (1 - \bar{q}_{e\uparrow})(1 - \bar{q}_{h\downarrow})v_+ v_- e^{i\phi-d}}. \quad (6.70)$$

Here the normalized wave vectors in the ferromagnet are given by

$$\bar{q}_{e\uparrow(h\downarrow)} = \sqrt{1 \pm \bar{h}}, \quad (6.71)$$

with $\bar{h} = 2m_e h_0 / \hbar^2 k_{Fx} = \bar{h}_0 / \cos \theta$.

We can follow the similar discussion on the NS junction and write down the differential conductance for the FS junction, for a given incident angle, as:

$$g_{FS.PCS} = \frac{1}{2} \Sigma_{\sigma} [1 + (\bar{q}_{h\bar{\sigma}} / \bar{q}_{e\sigma}) |r_{\bar{\sigma}\sigma}|^2 - |r_{\sigma\sigma}|^2], \quad (6.72)$$

which has been normalized to the conductance for the NN junction. The pre-factor $\bar{q}_{h\bar{\sigma}} / \bar{q}_{e\sigma}$ before the Andreev reflection amplitude takes care of the fact that the electron and hole have different velocity in the ferromagnet. In Fig. 6.5, the differential conductance is shown for a ferromagnet/s-wave superconductor junction for various values of the exchange interaction strength in the ferromagnet. The suppression of subgap conductance is seen clearly with the increase of exchange coupling strength. Experimental study has also been extended to ferromagnet/high- T_c superconductor junctions [45]. The corresponding theory with a $d_{x^2-y^2}$ -wave pairing symmetry has also been developed along the same line discussed above but with an emphasis on the zero-bias conductance [46] and the Fermi wave vector mismatch between the ferromagnet and superconductor [47].

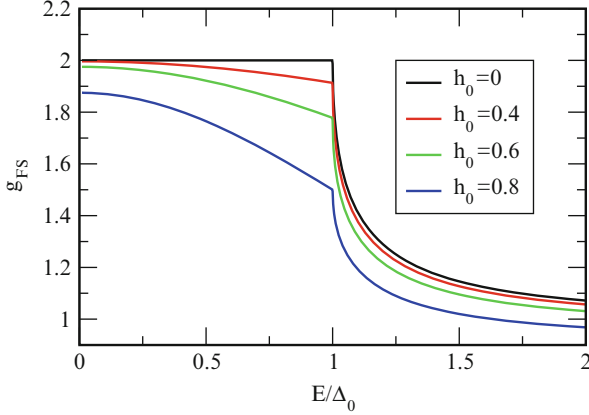


Fig. 6.5 Differential conductance for a ferromagnet/*s*-wave superconductor junction for various values of exchange interaction strength in the ferromagnet. The energy is measured in units of the superconducting pair potential. The crystalline orientation between the normal metal and the *s*-wave superconductor and the incident angle is chosen to be $\alpha = 0$ and $\theta = 0$, respectively

6.4 Transport Properties Through a Topological-Insulator/Superconductor Junction

So far, we have discussed the transport properties across the junctions involving conventional metals and ferromagnets. There is another class of quantum materials, so-called topological insulators (TI). They are insulating in bulk but host a gapless surface states with a Dirac-like linear dispersion [48, 49]. Like in graphene, the Dirac-like linear dispersion has a fundamental implication to various new phenomena. In TI, the surface states are topologically protected by time-reversal symmetry, and are robust against nonmagnetic disorder and perturbations. More interestingly, topological superconductivity can be induced in TIs through chemical doping [50] or proximately induced at the TI/superconductor interfaces [51–53]. Therefore, the transport through the topological superconductor junctions should be very interesting. Especially, the possible existence of Majorana fermions in the condensed matter systems is of significant implication to the technology like quantum computers and other electronic devices [54–58]. The property of the anti-particle of a Majorana fermion being itself holds a key to quantum coherence protection.

Here we consider a Dirac-normal-metal/ferromagnet insulator/*s*-wave topological superconductor junction. The Dirac-BdG equations can be written as:

$$\begin{pmatrix} H_{\uparrow\uparrow}(\mathbf{r}) & H_{\uparrow\downarrow} & 0 & \Delta(\mathbf{r}) \\ H_{\downarrow\uparrow}(\mathbf{r}) & H_{\downarrow\downarrow}(\mathbf{r}) & \Delta(\mathbf{r}) & 0 \\ 0 & \Delta^*(\mathbf{r}) & -H_{\uparrow\uparrow}^*(\mathbf{r}) & H_{\uparrow\downarrow}^*(\mathbf{r}) \\ \Delta^*(\mathbf{r}) & 0 & H_{\downarrow\uparrow}^*(\mathbf{r}) & -H_{\downarrow\downarrow}^*(\mathbf{r}) \end{pmatrix} \begin{pmatrix} u_{\uparrow}(\mathbf{r}) \\ u_{\downarrow}(\mathbf{r}) \\ v_{\uparrow}(\mathbf{r}) \\ v_{\downarrow}(\mathbf{r}) \end{pmatrix} = E \begin{pmatrix} u_{\uparrow}(\mathbf{r}) \\ u_{\downarrow}(\mathbf{r}) \\ v_{\uparrow}(\mathbf{r}) \\ v_{\downarrow}(\mathbf{r}) \end{pmatrix}. \quad (6.73)$$

Here the single-particle Hamiltonian matrix in the spin-space is given by

$$\hat{H} = \hat{h}(\mathbf{r}) + \hat{M}(\mathbf{r}) , \quad (6.74)$$

where the Dirac-like Hamiltonian for the topological surface state is

$$\hat{h}(\mathbf{r}) = v_F(p_x\sigma_y - p_y\sigma_x) - E_F[\Theta(-x) + \Theta(x-d)] \quad (6.75)$$

with E_F is the Fermi energy, the potential for the ferromagnetic insulator is

$$\begin{aligned} \hat{M} &= \mathbf{m} \cdot \boldsymbol{\sigma} \Theta(x)\Theta(d-x) , \\ &= \begin{pmatrix} m_z & m_x - im_y \\ m_x + im_y & -m_z \end{pmatrix} . \end{aligned} \quad (6.76)$$

with \mathbf{m} being the magnetization vector and the $\boldsymbol{\sigma}$ the Pauli matrices. The pair potential for the s -wave superconductor is given by

$$\Delta(\mathbf{r}) = \Delta\Theta(x-d) . \quad (6.77)$$

The quasiparticle energy is measured with respect to the Fermi energy $E_F = \hbar v_F k_F$ with v_F and k_F being the Fermi velocity and wave vector.

When a beam of electrons is incident from the Dirac-like normal metal with an angle θ , the wave function is given by

$$\Psi_I(x) = \begin{pmatrix} 1 \\ ie^{i\theta} \\ 0 \\ 0 \end{pmatrix} e^{ik_x x} + a \begin{pmatrix} 0 \\ 0 \\ 1 \\ -ie^{-i\theta} \end{pmatrix} e^{ik_x x} + b \begin{pmatrix} 1 \\ -ie^{-i\theta} \\ 0 \\ 0 \end{pmatrix} e^{-ik_x x} , \quad (6.78)$$

for $x < 0$;

$$\begin{aligned} \Psi_{II}(x) &= c_{e,+} \begin{pmatrix} 1 \\ \Gamma_{e,+} \\ 0 \\ 0 \end{pmatrix} e^{ik_{e,+}^+ x} + c_{e,-} \begin{pmatrix} 1 \\ \Gamma_{e,-} \\ 0 \\ 0 \end{pmatrix} e^{ik_{e,-}^- x} \\ &+ c_{h,+} \begin{pmatrix} 0 \\ 0 \\ 1 \\ \Gamma_{h,+} \end{pmatrix} e^{ik_{h,+}^+ x} + c_{h,-} \begin{pmatrix} 0 \\ 0 \\ 1 \\ \Gamma_{h,-} \end{pmatrix} e^{ik_{h,-}^- x} , \end{aligned} \quad (6.79)$$

for $0 \leq x \leq d$. Here

$$k_x = k_F \cos \theta , \quad (6.80)$$

$$k_y = k_F \sin \theta , \quad (6.81)$$

$$k_{e,\pm} = -\frac{m_y}{\hbar k_F} \pm \frac{i}{\hbar k_F} \sqrt{m_z^2 + (\hbar v_F k_y - m_x)^2} , \quad (6.82)$$

$$k_{h,\pm} = \frac{m_y}{\hbar k_F} \mp \frac{i}{\hbar k_F} \sqrt{m_z^2 + (\hbar v_F k_y + m_x)^2} , \quad (6.83)$$

$$\Gamma_{e,\pm} = -\frac{m_z}{-\hbar v_F (ik_{e,\pm} + k_y) + (m_x - im_y)} , \quad (6.84)$$

$$\Gamma_{h,\pm} = -\frac{m_z}{\hbar v_F (ik_{h,\pm} - k_y) + (m_x + im_y)} . \quad (6.85)$$

For the wave function in the topological superconducting region, we would like to give a more expanded discussion because the BdG equations become a set of 4×4 coupled matrix equations. We first write the wave function in the form

$$\begin{aligned} \Psi(x, y) &= \Psi(x) e^{ik_y y} \\ &= \begin{pmatrix} u_{0,\uparrow} \\ u_{0,\downarrow} \\ v_{0,\uparrow} \\ v_{0,\downarrow} \end{pmatrix} e^{iq_x x + ik_y y} . \end{aligned} \quad (6.86)$$

On substitution of Eq. (6.86) into Eq. (6.73), we arrive at the matrix equations

$$\begin{pmatrix} E + E_F & -\hbar v_F(-iq_x - k_y) & 0 & -\Delta \\ -\hbar v_F(iq_x - k_y) & E + E_F & -\Delta & 0 \\ 0 & -\Delta & E - E_F & \hbar v_F(iq_x - k_y) \\ -\Delta & 0 & \hbar v_F(-iq_x - k_y) & E - E_F \end{pmatrix} \begin{pmatrix} u_{0,\uparrow} \\ u_{0,\downarrow} \\ v_{0,\uparrow} \\ v_{0,\downarrow} \end{pmatrix} = 0 , \quad (6.87)$$

which leads to the eigenvalue equation

$$[(E + |\Pi| + E_F)(E - |\Pi| - E_F) - \Delta^2][(E - |\Pi| + E_F)(E + |\Pi| - E_F) - \Delta^2] = 0 . \quad (6.88)$$

In the above equation, we have denoted

$$\Pi = i\hbar v_F(q_x - ik_y) = i|\Pi|e^{-i\gamma} , \quad (6.89)$$

with $\gamma = \tan^{-1}(q_x/k_y)$. Equation (6.88) can be decoupled as

$$(E + |\Pi| + E_F)(E - |\Pi| - E_F) - \Delta^2 = 0 , \quad (6.90)$$

and

$$(E - |\Pi| + E_F)(E + |\Pi| - E_F) - \Delta^2 = 0, \quad (6.91)$$

which gives four eigenvalues

$$E_{1,2} = \pm \sqrt{(-|\Pi| - E_F)^2 + \Delta^2}, \quad (6.92)$$

$$E_{3,4} = \pm \sqrt{(|\Pi| - E_F)^2 + \Delta^2}, \quad (6.93)$$

respectively.

We now derive the eigenfunctions corresponding to the above eigenvalues. We first write Eq. (6.87) in an expanded form

$$(E + E_F)u_{0,\uparrow} + \Pi u_{0,\downarrow} - \Delta v_{0,\downarrow} = 0, \quad (6.94a)$$

$$\Pi^* u_{0,\uparrow} + (E + E_F)u_{0,\downarrow} - \Delta v_{0,\uparrow} = 0, \quad (6.94b)$$

$$-\Delta u_{0,\downarrow} + (E - E_F)v_{0,\uparrow} - \Pi^* v_{0,\downarrow} = 0, \quad (6.94c)$$

$$-\Delta u_{0,\uparrow} - \Pi v_{0,\uparrow} + (E - E_F)v_{0,\downarrow} = 0. \quad (6.94d)$$

These wavefunctions are also subjected to the normalization condition:

$$|u_{0,\uparrow}|^2 + |u_{0,\downarrow}|^2 + |v_{0,\uparrow}|^2 + |v_{0,\downarrow}|^2 = 2. \quad (6.95)$$

Here we have used an unusual normalization factor “2” to be consistent with the intensity of the incident beam. Since there are four unknowns but five equations, we use only Eqs. (6.94a)–(6.94c) together with the normalization condition. From Eqs. (6.94a) and (6.94b), we can express $u_{0,\uparrow}$ and $u_{0,\downarrow}$ in terms of $v_{0,\uparrow}$ and $v_{0,\downarrow}$. A little algebra yields:

$$u_{0,\uparrow} = \frac{\Delta}{(E + E_F)^2 - |\Pi|^2} [(E + E_F)v_{0,\downarrow} - \Pi v_{0,\uparrow}], \quad (6.96a)$$

$$u_{0,\downarrow} = \frac{\Delta}{(E + E_F)^2 - |\Pi|^2} [(E + E_F)v_{0,\uparrow} - \Pi^* v_{0,\downarrow}], \quad (6.96b)$$

Substitution of Eqs. (6.96a) and (6.96b) into Eq. (6.94c) gives

$$\begin{aligned} v_{0,\uparrow} &= -\frac{i|\Pi|e^{i\gamma}[-\Delta^2 + (E + E_F)^2 - |\Pi|^2]}{-\Delta^2(E + E_F) + (E - E_F)[(E + E_F)^2 - |\Pi|^2]} v_{0,\downarrow} \\ &= \begin{cases} ie^{i\gamma} v_{0,\downarrow}, & \text{for } E_{3,4}, \\ -ie^{i\gamma} v_{0,\downarrow}, & \text{for } E_{1,2}, \end{cases} \end{aligned} \quad (6.97)$$

which in turn gives

$$u_{0,\downarrow} = \begin{cases} ie^{iy}u_{0,\uparrow}, & \text{for } E_{3,4}, \\ -ie^{iy}u_{0,\uparrow}, & \text{for } E_{1,2}, \end{cases} \quad (6.98)$$

We can then substitute Eqs. (6.97) and (6.98) back into Eq. (6.96a) and obtain:

$$u_{0,\uparrow} = \frac{\Delta}{(E + E_F) - |\Pi|} v_{0,\downarrow}, \quad (6.99)$$

for $E_{3,4}$, while

$$u_{0,\uparrow} = \frac{\Delta}{(E + E_F) + |\Pi|} v_{0,\downarrow}, \quad (6.100)$$

for $E_{1,2}$. Substituting these relations into the normalization condition Eq. (6.95), we are able to arrive at

$$\left(u_{0,\uparrow}^{(3,4)}\right)^2 = \frac{1}{2} \left(1 + \frac{|\Pi| - E_F}{E_{3,4}}\right), \quad (6.101a)$$

$$\left(v_{0,\downarrow}^{(3,4)}\right)^2 = \frac{1}{2} \left(1 - \frac{|\Pi| - E_F}{E_{3,4}}\right), \quad (6.101b)$$

and

$$\left(u_{0,\uparrow}^{(1,2)}\right)^2 = \frac{1}{2} \left(1 - \frac{|\Pi| - E_F}{E_{1,2}}\right), \quad (6.101c)$$

$$\left(v_{0,\downarrow}^{(1,2)}\right)^2 = \frac{1}{2} \left(1 + \frac{|\Pi| - E_F}{E_{1,2}}\right). \quad (6.101d)$$

Eigenfunctions as given by Eq. (6.101) suggest that for an incident wave from the normal metal with energy E , the transmitted wave function should have the form

$$\Psi_{\text{III}}(x) = t_e \begin{pmatrix} u_0 \\ iu_0e^{i\theta} \\ iv_0e^{i\theta} \\ v_0 \end{pmatrix} e^{ik_x x} + t_h \begin{pmatrix} v_0 \\ -iv_0e^{i\theta} \\ -iu_0e^{i\theta} \\ u_0 \end{pmatrix} e^{-ik_x x} \quad (6.102)$$

for $x \geq d$, where the coherence factors

$$u_0 = \sqrt{\frac{1}{2} \left(1 + \frac{\sqrt{E^2 - \Delta^2}}{E} \right)}, \quad (6.103a)$$

$$v_0 = \sqrt{\frac{1}{2} \left(1 - \frac{\sqrt{E^2 - \Delta^2}}{E} \right)}. \quad (6.103b)$$

Here we have used the Andreev approximation to take the x -component of the wave vector to be the same as that projected from \mathbf{k}_F , that is, $q_x = k_x = k_F \cos \theta$ with $\gamma \approx \theta$.

We can now impose the boundary conditions

$$\Psi_I(x=0) = \Psi_{II}(x=0), \quad (6.104)$$

at $x=0$, and

$$\Psi_{II}(x=d) = \Psi_{III}(x=d), \quad (6.105)$$

at $x=d$. A straightforward but tedious algebra yields the reflection amplitudes

$$a = \frac{1 + e^{2i\theta}}{(\mathcal{M}_{11} - ie^{-i\theta} \mathcal{M}_{12}) - (ie^{i\theta} \mathcal{M}_{21} + \mathcal{M}_{22})}, \quad (6.106a)$$

$$b = \frac{(\mathcal{M}_{11} - ie^{-i\theta} \mathcal{M}_{12})e^{i2\theta} + (ie^{i\theta} \mathcal{M}_{21} + \mathcal{M}_{22})}{(\mathcal{M}_{11} - ie^{-i\theta} \mathcal{M}_{12}) - (ie^{i\theta} \mathcal{M}_{21} + \mathcal{M}_{22})}, \quad (6.106b)$$

where

$$\begin{aligned} \mathcal{M}_{11} = & \mathcal{D}^{-1} [-ie^{i\theta} e^{i(k_{h,+} + k_{e,+})d} (1 + \Gamma_{h,+})(\Gamma_{h,+} + \Gamma_{h,-} - \Gamma_{e,+}) \\ & + (u_0^2 - v_0^2) e^{i(k_{h,+} + k_{e,-})d} (1 + \Gamma_{h,+})(\Gamma_{h,+} + \Gamma_{h,-} - \Gamma_{e,-}) \\ & + (u_0^2 - v_0^2) e^{2i\theta} e^{i(k_{h,-} + k_{e,+})d} (1 + \Gamma_{h,-})(\Gamma_{h,+} + \Gamma_{h,-} - \Gamma_{e,+}) \\ & + ie^{i\theta} e^{i(k_{h,-} + k_{e,-})d} (1 + \Gamma_{h,-})(\Gamma_{h,+} + \Gamma_{h,-} - \Gamma_{e,-})], \end{aligned} \quad (6.107a)$$

$$\begin{aligned} \mathcal{M}_{12} = & \mathcal{D}^{-1} [ie^{i\theta} e^{i(k_{h,+} + k_{e,+})d} (1 + \Gamma_{h,+})(1 + \Gamma_{e,+}) \\ & - (u_0^2 - v_0^2) e^{i(k_{h,+} + k_{e,-})d} (1 + \Gamma_{h,+})(1 + \Gamma_{e,-}) \\ & - (u_0^2 - v_0^2) e^{2i\theta} e^{i(k_{h,-} + k_{e,+})d} (1 + \Gamma_{h,-})(1 + \Gamma_{e,+}) \\ & - ie^{i\theta} e^{i(k_{h,-} + k_{e,-})d} (1 + \Gamma_{h,-})(1 + \Gamma_{e,-})], \end{aligned} \quad (6.107b)$$

$$\begin{aligned} \mathcal{M}_{21} = & \mathcal{D}^{-1} [-ie^{i\theta} e^{i(k_{h,+} + k_{e,+})d} (\Gamma_{e,+} + \Gamma_{e,-} - \Gamma_{h,+})(\Gamma_{h,+} + \Gamma_{h,-} - \Gamma_{e,+}) \\ & + (u_0^2 - v_0^2) e^{i(k_{h,+} + k_{e,-})d} (\Gamma_{e,+} + \Gamma_{e,-} - \Gamma_{h,+})(\Gamma_{h,+} + \Gamma_{h,-} - \Gamma_{e,-}) \end{aligned}$$

$$\begin{aligned}
& +(u_0^2 - v_0^2)e^{2i\theta} e^{i(k_{h,-} + k_{e,+})d} (\Gamma_{e,+} + \Gamma_{e,-}\Gamma_{h,-})(\Gamma_{h,+} + \Gamma_{h,-}\Gamma_{e,+}) \\
& + ie^{i\theta} e^{i(k_{h,-} + k_{e,-})d} (\Gamma_{e,+} + \Gamma_{e,-}\Gamma_{h,-})(\Gamma_{h,+} + \Gamma_{h,-}\Gamma_{e,-}) , \quad (6.107c)
\end{aligned}$$

$$\begin{aligned}
\mathcal{M}_{22} = & \mathcal{D}^{-1} [ie^{i\theta} e^{i(k_{h,+} + k_{e,+})d} (\Gamma_{e,+} + \Gamma_{e,-}\Gamma_{h,+})(1 + \Gamma_{e,+}) \\
& - (u_0^2 - v_0^2)e^{i(k_{h,+} + k_{e,-})d} (\Gamma_{e,+} + \Gamma_{e,-}\Gamma_{h,+})(1 + \Gamma_{e,-}) \\
& - (u_0^2 - v_0^2)e^{2i\theta} e^{i(k_{h,-} + k_{e,-})d} (\Gamma_{e,+} + \Gamma_{e,-}\Gamma_{h,-})(1 + \Gamma_{e,+}) \\
& - ie^{i\theta} e^{i(k_{h,-} + k_{e,-})d} (\Gamma_{e,+} + \Gamma_{e,-}\Gamma_{h,-})(1 + \Gamma_{e,-})] , \quad (6.107d)
\end{aligned}$$

with

$$\mathcal{D} = \frac{2iu_0v_0e^{i\theta} e^{i(k_{e,+} + k_{e,-})d}}{(\Gamma_{e,+} - \Gamma_{e,-})(\Gamma_{h,+} - \Gamma_{h,-})} . \quad (6.108)$$

With these coefficients, the differential conductance can be calculated as $G_S(\theta) = 1 + |a|^2 - |b|^2$. Also we can evaluate the differential conductance when the superconductor is set into the normal state, which has the expression

$$G_N(\theta) = \frac{1}{\cosh^2(\kappa_e d) + \tan^2 \theta \sinh^2(\kappa_e d) (k_y - m_x/\hbar v_F)^2 / \kappa_e^2} , \quad (6.109)$$

where

$$\kappa_e = \sqrt{m_z^2 + (\hbar v_F k_y - m_x)^2 / \hbar v_F} . \quad (6.110)$$

The normalized differential conductance can be calculated according to

$$\sigma = \frac{\int_{-\pi/2}^{\pi/2} G_S(\theta) \cos \theta d\theta}{\int_{-\pi/2}^{\pi/2} G_N(\theta) \cos \theta d\theta} . \quad (6.111)$$

When $m_x = 0$, the differential conductance is reduced to [55]:

$$G_S(\theta) = \frac{G_N[1 + G_N|\Gamma|^2 - (1 - G_N)|\Gamma|^4]}{|1 + (1 - G_N)e^{i\varphi} \Gamma^2|^2} , \quad (6.112)$$

where

$$e^{i\varphi} = \frac{m_z \cos \theta + iE_F \sin \theta}{m_z \cos \theta - iE_F \sin \theta} , \quad (6.113)$$

and

$$\Gamma = \frac{\Delta}{E + \sqrt{E^2 - \Delta^2}} . \quad (6.114)$$

In the insulating limit, $G_N \rightarrow 0$, the pole of Eq. (6.112) leads to the bound state energy

$$E_b = -\frac{\Delta E_F \sin \theta \operatorname{sgn}(m_z)}{\sqrt{E_F^2 \sin^2 \theta + m_z^2 \cos^2 \theta}}. \quad (6.115)$$

These states are the manifestation of chiral Majorana mode (CMM) [51], which has a dispersion along the interface between the ferromagnetic insulator and conventional s -wave superconductor. However, these states are localized in the direction perpendicular to the interface.

Equation (6.115) suggests that the conductance is contributed mainly by these bound states in the tunneling limit. The representative results of the conductance are reported by Tanaka and co-workers [55]. As shown in Fig. 6.6, the bound state energy is dispersive as a function of the incident angle. In addition, the slope in the energy near the vertical incident angle $\theta = 0$ becomes more flat when the ferromagnetic exchange interaction increases (see Fig. 6.6a). The flatted band of bound states near $\theta = 0$ will then make dominant contribution to the integrated conductance. Therefore, the zero-bias conductance peak is enhanced with increased m_z (see Fig. 6.6b). These results are remarkable in view of the fact that the ferromagnetic exchange interaction in ferromagnet/conventional superconductor junctions suppresses the zero-bias differential conductance. Interesting results from the topological nature of the superconductor have also been found in thermal transport properties [59].

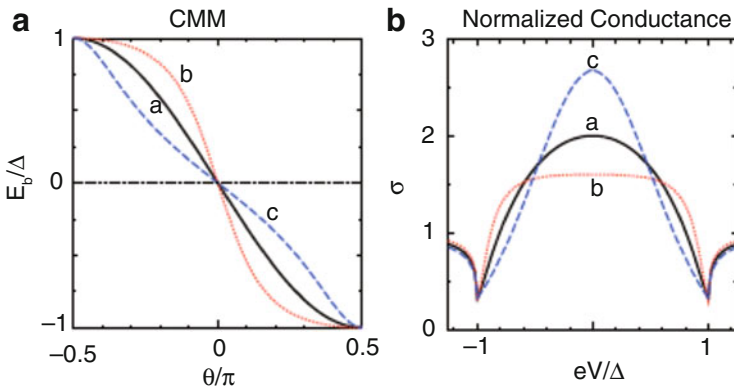


Fig. 6.6 Chiral Majorana mode energy dispersion E_b as a function of the incident angle θ (a) and integrated tunneling conductance σ in N/FI/S junctions (b). The parameter $(m_z/E_F)k_F d = 1$ is fixed and $m_x = m_y = 0$. The other variation parameter $m_z/E_F = 1, 0.5, 2$ for curves a, b, and c, respectively. From [55]

References

1. A.F. Andreev, Zh. Eksp. Teor. Fiz. **46**, 1823 (1964) [Sov. Phys. JETP **19**, 1228 (1964)]; **49**, 655 (1965) [**22**, 455 (1966)]; **51**, 1510 (1966) [**24**, 1019 (1967)]
2. G.E. Blonder, M. Tinkham, T.M. Klapwijk, Phys. Rev. B **25**, 4515 (1982)
3. W.N. Mathews, Jr., Phys. Status Solidi B **90**, 327 (1978)
4. P.F. Bagwell, Phys. Rev. B **49**, 6841 (1994)
5. C.W.J. Beenakker, H. van Houten, in *Nanostructures and Mesoscopic Systems*, ed. by W.P. Kirk, M.A. Reed (Academic Press, New York, 1992)
6. R. Landauer, Philos. Mag. **21**, 863 (1970)
7. M. Büttiker, Phys. Rev. Lett. **57**, 1761 (1986)
8. C.W.J. Beenakker, Phys. Rev. Lett. **67**, 3836 (1991); **68**, 1442(E) (1992)
9. C.W.J. Beenakker, Phys. Rev. B **46**, 12841 (1992)
10. C.J. Lambert, J. Phys.: Condens. Matter **3**, 6579 (1991)
11. B.J. van Wees, P. de Vries, P. Magn'ee, T.M. Klapwijk, Phys. Rev. Lett. **69**, 510 (1992)
12. Y. Takane, H. Ebisawa, J. Phys. Soc. Jpn. **61**, 1685 (1992); **61**, 2858 (1992); **61**, 3466 (1992); **62**, 1844 (1993)
13. A. Kastalsky, A.W. Kleinsasser, L.H. Greene, R. Bhat, F.P. Milliken, J.P. Harbison, Phys. Rev. Lett. **67**, 3026 (1991)
14. C. Nguyen, H. Kroemer, E.L. Hu, Phys. Rev. Lett. **69**, 2847 (1992)
15. S.J.M. Bakker, E. van der Drift, T.M. Klapwijk, H.M. Jaeger, S. Radelaar, Phys. Rev. B **49**, 13275 (1994)
16. I.K. Marmorosk, C.W.J. Beenakker, R.A. Jalabert, Phys. Rev. B **48**, 2811 (1993)
17. C.W.J. Beenakker, Rev. Mod. Phys. **69**, 731 (1997)
18. J. Geerk, X.X. Li, G. Linker, Z. Phys. B **73**, 329 (1988)
19. J. Lesueur, L.H. Greene, W.L. Feldmann, A. Imam, Physica C **191**, 325 (1992)
20. M. Covington, R. Scheuerer, K. Bloom, L.H. Greene, Appl. Phys. Lett. **68**, 1717 (1996)
21. M. Covington, M. Aprili, E. Paraoanu, L.H. Greene, F. Xu, J. Zhu, C.A. Mirkin, Phys. Rev. Lett. **79**, 277 (1997)
22. C.R. Hu, Phys. Rev. Lett. **72**, 1526 (1994)
23. Y. Tanaka, S. Kashiwaya, Phys. Rev. Lett. **74**, 3451 (1995).
24. S. Kashiwaya, Y. Tanaka, M. Koyanagi, H. Takashima, K. Kajimura, Phys. Rev. B **51**, 1350 (1995); J. Phys. Chem. Solids **56**, 1721 (1995)
25. S. Kashiwaya, Y. Tanaka, M. Koyanagi, K. Kajimura, Phys. Rev. B **53**, 2667 (1996)
26. J. Kurkijärvi, D. Rainer, in *Modern Problems in Condensed Matter Sciences*, ed. by W.P. Halperin, L.P. Pitaevskii (Elsevier, Amsterdam, 1989)
27. P. Koorevaar, Y. Suzuki, R. Coehoorn, J. Aarts, Phys. Rev. B **49**, 441 (1994).
28. G. Verbanck, C.D. Potter, R. Schad, P. Belien, V.V. Moschalkov, Y. Bruynseraede, Physica C **235-240**, 3295 (1994)
29. C. Struck, C. Stürgers, U. Paschen, H.V. Löhneysen, Phys. Rev. B **49**, 4053 (1994)
30. J.S. Jiang, D. Davidović, D.H. Reich, C.L. Chuen, Phys. Rev. Lett. **74**, 314 (1995)
31. Z. Radović, L. Dobrosavljević-Grujić, A.I. Buzdin, J.R. Clem, Phys. Rev. B **38**, 2388 (1988)
32. Z. Radović, M. Ledvij, L. Dobrosavljević-Grujić, A.I. Buzdin, J.R. Clem, Phys. Rev. B **44**, 759 (1991)
33. A.I. Buzdin, M.Y. Kupriyanov, Pis'ma Zh. Eksp. Teor. Fiz. **52**, 1089 (1990) [JETP Lett. **52**, 487 (1990)]; **53**, 308 (1991) [**53**, 321 (1991)]
34. A.I. Buzdin, M. Yu. Kupriyanov, B. Vujčić, Physica C **185**, 2025 (1991)
35. A.I. Buzdin, L.N. Bulaeviski, S.V. Panyukov, Pis'ma Zh. Eksp. Teor. Fiz. **35**, 147 (1982) [JETP Lett. **35**, 178 (1982)]
36. A.I. Buzdin, B. Bujčić, M.Y. Kupriyanov, Zh. Eksp. Teor. Fiz. **101**, 231 (1992) [Sov. Phys. JETP **74**, 124 (1992)]
37. E.A. Demler, G.B. Arnold, M.R. Beasley, Phys. Rev. B **55**, 15174 (1997)
38. M.O. Visscher, G.E.W. Bauer, Phys. Rev. B **54**, 2798 (1996)

39. O. Siper, B.L. Gyorffy, *J. Phys.: Condens. Matter* **7**, 5239 (1995)
40. C.A.R. Sá de Melo, *Phys. Rev. Lett.* **79**, 1933 (1997)
41. R. Meservey, P.M. Tedrow, *Phys. Rep.* **238**, 173 (1994)
42. M.J.M. de Jong, C.W.J. Beenakker, *Phys. Rev. Lett.* **74**, 1657 (1995)
43. M. Leadbeater, C.J. Lambert, K.E. Nagaev, R. Raimondi, A.F. Volkov, *Phys. Rev. B* **59**, 12264 (1999)
44. S.K. Upadhyay, A. Palanisami, R.N. Louie, R.A. Buhrman, *Phys. Rev. Lett.* **81**, 3247 (1998)
45. V.A. Vas'ko, K.R. Nikolaev, V.A. Larkin, P.A. Kraus, A.M. Goldman, *Appl. Phys. Lett.* **73**, 844 (1998)
46. J.-X. Zhu, B. Friedman, C.S. Ting, *Phys. Rev. B* **59**, 9558 (1999)
47. I. Zutic, O.T. Valls, *Phys. Rev. B* **60**, 6320 (1999)
48. M.Z. Hasan, C.L. Kane, *Rev. Mod. Phys.* **82**, 3045 (2010)
49. X.-L. Qi, S.-C. Zhang, *Rev. Mod. Phys.* **83**, 1057 (2011)
50. Y.S. Hor, A.J. Williams, J.G. Checkelsky, P. Roushan, J. Seo, Q. Xu, H.W. Zandbergen, A. Yazdani, N.P. Ong, R.J. Cava, *Phys. Rev. Lett.* **104**, 057001 (2010)
51. L. Fu, C.L. Kane, *Phys. Rev. Lett.* **100**, 096407 (2008)
52. L. Fu, C.L. Kane, *Phys. Rev. Lett.* **102**, 216403 (2009)
53. X.-L. Qi, T.L. Hughes, S.-C. Zhang, *Phys. Rev. B* **82**, 184516 (2010)
54. A.R. Akhmerov, J. Nilsson, C.W.J. Beenakker, *Phys. Rev. Lett.* **102**, 216404 (2009).
55. Y. Tanaka, T. Yokoyama, N. Nagaosa, *Phys. Rev. Lett.* **103**, 107002 (2009)
56. K.T. Law, P.A. Lee, T.K. Ng, *Phys. Rev. Lett.* **103**, 237001 (2009)
57. J. Linder, Y. Tanaka, T. Yokoyama, A. Sudbø, N. Nagaosa, *Phys. Rev. Lett.* **104**, 067001 (2010)
58. P.A. Iosevich, M.V. Feigel'man, *Phys. Rev. Lett.* **106**, 077003 (2011)
59. J. Ren, J.-X. Zhu, *Phys. Rev. B* **87**, 165121 (2013)

Chapter 7

Topological and Quantum Size Effects in Superconductors at Reduced Length Scale

Abstract The periodicity of persistent currents in multiply connected geometries arising from the Aharonov and Bohm effect is studied for both s -wave superconducting ring and d -wave superconducting cylinder. The loop geometry of a d -wave superconductor is also considered. The solutions of the BdG equations suggest that the hc/e -periodicity is a generic property in s -wave superconductor ring at the mesoscale and in unconventional superconductors. Finally, the theoretical approach to solving the BdG equations is also provided for nanoscale superconductors. The quantum size effects are showcased with the oscillation of transition temperature.

7.1 Persistent Current in a Mesoscopic s -Wave Superconducting Ring

In classical electrodynamics, the Maxwell equations determine directly the behavior of electromagnetic fields \mathbf{E} and \mathbf{B} , while the scalar and vector potentials merely play an auxiliary role through the relation

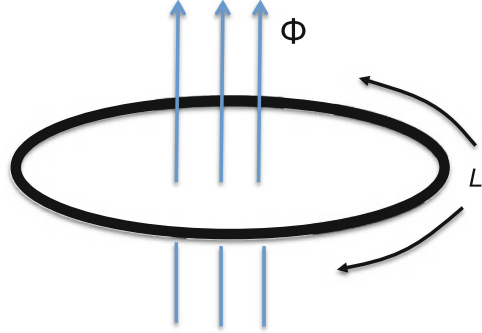
$$\mathbf{E} = -\nabla\varphi(\mathbf{r}) , \quad \mathbf{B}(\mathbf{r}) = \nabla \times \mathbf{A}(\mathbf{r}) ,$$

in the static case. Therefore, the equation of motion of an electron is determined through the Lorentz force

$$\mathbf{F} = -e \left(\mathbf{E} + \frac{\mathbf{v}}{c} \times \mathbf{B} \right) ,$$

where \mathbf{v} is the electron velocity. However, in quantum mechanics, the scalar and vector potentials enter the Schrödinger equation explicitly and have a direct consequence. In 1959, Aharonov and Bohm (AB) [1] showed that a charged particle can be deflected even when the classical force is absent. This AB effect has now been very well demonstrated by a persistent equilibrium current circulating in an isolated mesoscopic normal-metal ring pierced by an AB flux $\Phi = \oint \mathbf{A} \cdot \mathbf{l}$ [2, 3]. This current always has a periodicity of $\Phi_0 = hc/e$, where Φ_0 is the single electron flux quantum. In a superconductor, electrons form Cooper pairs from an effective pairing interaction near the Fermi surface. The flux quantization with $\Phi_0/2$ has been used

Fig. 7.1 Schematic drawing of a one-dimensional superconducting ring of circumference L threaded by a magnetic flux Φ



as a powerful proof for the formation of electron pairs in a macroscopic multiply connected geometries [4–8]. However, we must keep in mind that the Cooper pairs are well defined in momentum space rather than in real space, which makes them distinct from particles with a charge $-2e$. Therefore, there is no reason for one to expect that the persistent current in a superconducting ring should have a periodicity of $\Phi_s = \Phi_0/2$, in particular, when the system is at a mesoscale.

We study this problem by considering a one-dimensional mesoscopic s -wave superconductor ring pierced by a magnetic flux, as shown in Fig. 7.1. Since the flux is restricted to the central hollow region, no magnetic field is experienced by the electrons. The BdG equations are still given by Eq. (5.19) but with no spin Zeeman term and $\nabla \times \mathbf{A} = 0$ on the ring arm. That is, the single-particle Hamiltonian in 1D has the form

$$\tilde{h}(x) = \frac{1}{2m_e} \left(\frac{\hbar}{i} \frac{d}{dx} + \frac{eA(x)}{c} \right)^2 - E_F. \quad (7.1)$$

Here we have used the spatial coordinate $x = 2\pi\theta/L$, where θ is the azimuthal angle, varying between 0 and L . In general, the detailed shape of the ring does not matter. Before we discuss the BdG equations, we first take a look at the wave function to the single-particle Hamiltonian with the Schrödinger equation

$$\tilde{h}(x)\tilde{\varphi}(x) = \epsilon\tilde{\varphi}(x). \quad (7.2)$$

The eigenfunction $\tilde{\varphi}(x)$ satisfies a periodic boundary condition

$$\tilde{\varphi}(x + L) = \tilde{\varphi}(x). \quad (7.3)$$

We introduce a singular gauge transformation

$$\tilde{\varphi}(x) = e^{-ie\chi(x)/\hbar c} \varphi(x) \quad (7.4)$$

Using the identity

$$\left(\frac{\hbar}{i} \frac{d}{dx} + \frac{eA(x)}{c}\right) \tilde{\varphi}(x) = e^{-ie\chi(x)/\hbar c} \left(\frac{\hbar}{i} \frac{d}{dx} + \frac{e}{c}(A(x) - \chi'(x))\right) \varphi(x), \quad (7.5)$$

and

$$\left(\frac{\hbar}{i} \frac{d}{dx} + \frac{eA(x)}{c}\right)^2 \tilde{\varphi}(x) = e^{-ie\chi(x)/\hbar c} \left(\frac{\hbar}{i} \frac{d}{dx} + \frac{e}{c}(A(x) - \chi'(x))\right)^2 \varphi(x), \quad (7.6)$$

we obtain

$$\left(\frac{\hbar}{i} \frac{d}{dx} + \frac{e}{c}(A(x) - \chi'(x))\right)^2 \varphi(x) = \epsilon \varphi(x). \quad (7.7)$$

The choice of the gauge

$$\chi'(x) = A(x), \quad (7.8)$$

leads to

$$-\frac{\hbar^2}{2m_e} \frac{d^2 \varphi(x)}{dx^2} = \epsilon \varphi(x). \quad (7.9)$$

Solving Eq. (7.8) yields

$$\chi(x) = \int_0^x A(x') dx'. \quad (7.10)$$

Therefore, the boundary condition for the new wave function becomes

$$\begin{aligned} \varphi(x+L) &= e^{ie\chi(x+L)/\hbar c} \varphi(x+L) \\ &= e^{\frac{ie}{\hbar c} \int_x^{x+L} A(x') dx'} e^{\frac{ie}{\hbar c} \int_0^x A(x') dx'} \varphi(x) \\ &= e^{i2\pi \Phi / \Phi_0} \varphi(x). \end{aligned} \quad (7.11)$$

Here we have used the identity

$$\int_x^{x+L} A(x') dx' = \Phi. \quad (7.12)$$

This observation enables us to apply a singular gauge transformation also to the BdG equations and obtain

$$\begin{pmatrix} h(x) & \Delta(x) \\ \Delta^*(x) & -h^*(x) \end{pmatrix} \begin{pmatrix} u(x) \\ v(x) \end{pmatrix} = E \begin{pmatrix} u(x) \\ v(x) \end{pmatrix}, \quad (7.13)$$

with the periodic boundary condition

$$u(x+L) = e^{i2\pi\Phi/\Phi_0} u(x), \quad (7.14a)$$

$$v(x+L) = e^{-i2\pi\Phi/\Phi_0} v(x), \quad (7.14b)$$

$$\Delta(x+L) = e^{i4\pi\Phi/\Phi_0} \Delta(x). \quad (7.14c)$$

Here the single-particle Hamiltonian is

$$h(x) = -\frac{\hbar^2}{2m_e} \frac{d^2}{dx^2} - E_F. \quad (7.15)$$

If the electron wave vector is k and the wave vector for the collective drift motion (superfluid motion) of the paired electrons is q , the initial Cooper pairing ($k \uparrow, -k \downarrow$) will occur between electron states ($k+q \uparrow, -k+q \downarrow$). This allows us to write the wave function and pair potential as

$$\Delta(x) = \Delta e^{2iqx} \quad (7.16a)$$

$$u(x) = u_{k,q} e^{i(k+q)x}, \quad (7.16b)$$

$$v(x) = v_{k,q} e^{i(k-q)x}, \quad (7.16c)$$

A little algebra yields the solution to the BdG equation (7.13) [9]:

$$E_{k,q}^{\pm} = (\hbar k) \frac{\hbar q}{m_e} \pm \sqrt{E_A^2 + \Delta^2} = (\hbar k) \frac{\hbar q}{m_e} \pm E_{k,q}^{(0)}, \quad (7.17)$$

with the corresponding eigenfunctions $(u_{k,q}^+, v_{k,q}^+) = (u_{k,q}^{(0)}, v_{k,q}^0)$ while $(u_{k,q}^-, v_{k,q}^-) = (v_{k,q}^{(0)}, -u_{k,q}^0)$. Here

$$E_{k,q}^{(0)} = \sqrt{E_A^2 + \Delta^2}, \quad (7.18)$$

$$E_A = \frac{\hbar^2}{2m_e} (k^2 + q^2) - E_F, \quad (7.19)$$

and

$$\begin{pmatrix} u_{k,q}^{(0)} \\ v_{k,q}^{(0)} \end{pmatrix} = \begin{pmatrix} \sqrt{\frac{1}{2} \left(1 + \frac{E_A}{E_{k,q}^{(0)}} \right)} \\ \sqrt{\frac{1}{2} \left(1 - \frac{E_A}{E_{k,q}^{(0)}} \right)} \end{pmatrix}. \quad (7.20)$$

The order parameter is then determined by

$$\Delta = \frac{g}{4} \sum_k \frac{\Delta}{E_{k,q}^{(0)}} \left[\tanh\left(\frac{E_{k,q}^{(0)} + \hbar^2 kq/m_e}{2k_B T}\right) + \tanh\left(\frac{E_{k,q}^{(0)} - \hbar^2 kq/m_e}{2k_B T}\right) \right]. \quad (7.21)$$

Here the energy cutoff $|E_A| \leq \hbar\omega_D$ is implied in the summation. The boundary condition (7.14) on the wave functions gives

$$k = \frac{\pi}{L} n_k, \quad (7.22)$$

and

$$q = \frac{\pi}{L} \left(n_q + \frac{\Phi}{\Phi_s} \right), \quad (7.23)$$

subject to the constraint that $n_k + n_q$ is an even integer and the superconducting flux quantum $\Phi_s = \Phi_0/2$. In addition, from Eq. (6.15), the charge current is now given by

$$I_Q = \frac{2\hbar e}{m_e} \sum_k (k+q) [f(E_{k,q}^+) u_{k,q}^{(0)2} + f(E_{k,q}^-) v_{k,q}^{(0)2}], \quad (7.24)$$

where $f(E)$ is the Fermi-Dirac distribution function.

The drift momentum q defines a superfluid velocity $v_s = \hbar q/m_e$. Equation (7.17) suggests that when the superfluid velocity $v_s = v_d$ with $v_d = \Delta/\hbar v_F$ being the Landau depairing velocity, the gap in the excitation spectrum is closed. The quantity also defines a depairing flux $\Phi_d/\Phi_s = (k_F L/2\pi)(\Delta/E_F)$. This tells us that even if the superconducting gap is not depressed, a gapless quasiparticle state can be induced by the magnetic flux. The numerical results do confirm this intuitive analysis. As shown in Fig. 7.2 (left panel), for a fixed value of ring circumference, when the ration of Δ/E_F is tuned such that $\Phi_d/\Phi_s < 1$, the supercurrent is only a function of magnetic flux with a normal-state period Φ_0 . In addition, the self-consistency solution also shows that the order parameter can be suppressed by an application of the magnetic flux (see Fig. 7.2 (right panel)).

Before we turn to the discussion on the case with a d -wave pairing symmetry, we show a derivation of flux-modified boundary condition for electrons in the 1D ring

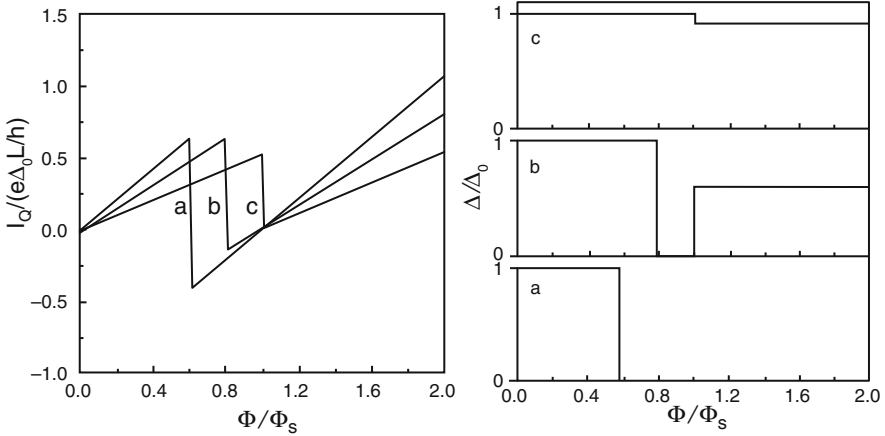


Fig. 7.2 Supercurrent at a fixed amplitude of s -wave order parameter (*left panel*) and the self-consistently obtained order parameter as a function of magnetic flux Φ/Φ_S in a mesoscopic ring at $T = 0$ K. For the *left panel*, the values of $\Delta_0/E_F = 3.0 \times 10^{-3}$ (a); 4.0×10^{-3} (b); 6×10^{-3} (c). For the *right panel*, the pairing interaction strength is first tuned to give the zero-flux gap value as used for the *left panel* before it is used for the self-consistent calculations for the flux dependence. The other parameters used are $L = 1000$ nm, and $k_F = 400\pi/L$, $\hbar\omega_D = 300$ K. Adapted from [9]

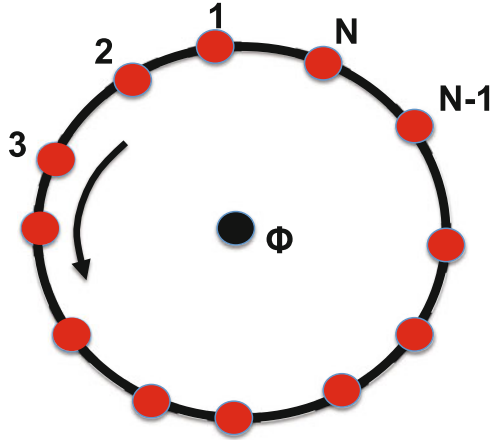


Fig. 7.3 Schematic drawing of a one-dimensional superconducting ring of circumference L threaded by a magnetic flux Φ in a tight-binding model

within a tight-binding model, as shown in Fig. 7.3. The single-particle Hamiltonian is given by:

$$H = - \sum_{i \neq j} t_{ij} e^{i\theta_{ij}} c_i^\dagger c_j + \sum_i \epsilon_i c_i^\dagger c_i, \quad (7.25)$$

where $\theta_{ij} = -\frac{2\pi}{\Phi_0} \int_j^i A(x) dx$ and ϵ is the on-site energy level. Here we have dropped the spin degrees of freedom. Introducing a canonical transformation

$$c_i = \sum_n \varphi_i^n \gamma_n, \quad (7.26)$$

with γ_n being the quasiparticle operator, and within the nearest-neighbor hopping approximation, the Hamiltonian can be diagonalized as

$$\underline{H}\underline{\varphi} = E\underline{\varphi}, \quad (7.27)$$

where

$$\underline{H} = \begin{pmatrix} \epsilon_1 & -te^{i\phi_1} & 0 & 0 & \dots & 0 & -te^{-i\phi_N} \\ -te^{-i\phi_1} & \epsilon_2 & -te^{-i\phi_2} & 0 & \dots & 0 & 0 \\ 0 & -te^{-i\phi_2} & \epsilon_3 & -te^{i\phi_3} & \dots & 0 & 0 \\ \dots & \dots & \dots & \dots & \dots & \dots & \dots \\ -te^{i\phi_N} & 0 & 0 & 0 & \dots & -t^{-i\phi_{N-1}} & \epsilon_N \end{pmatrix}, \quad (7.28)$$

and the eigenvectors $\underline{\varphi}^{\text{Transpose}} = (\varphi_1, \varphi_2, \varphi_3, \dots, \varphi_N)$. Here the accumulated phase for electrons hopping from site j to i has been abbreviated as $\theta_{i,i+1} = \phi_i$ and $\theta_{N,1} = \phi_N$. By performing a uniform transformation

$$\underline{U} = \begin{pmatrix} e^{i\sum_{i=1}^{N-1} \phi_i} & & & & & & \\ & e^{i\sum_{i=2}^{N-1} \phi_i} & & & & & \\ & & \dots & & & & \\ & & & e^{i\phi_{N-1}} & & & \\ & & & & & & 1 \end{pmatrix}, \quad (7.29)$$

the eigenequation equation becomes

$$\underline{\tilde{H}}\underline{\tilde{\varphi}} = E\underline{\tilde{\varphi}}, \quad (7.30)$$

where

$$\underline{\tilde{H}} = \begin{pmatrix} \epsilon_1 & -t & 0 & 0 & \dots & 0 & -te^{-i\sum_{i=1}^N \phi_i} \\ -t & \epsilon_2 & -t & 0 & \dots & 0 & 0 \\ 0 & -t & \epsilon_3 & -t & \dots & 0 & 0 \\ \dots & \dots & \dots & \dots & \dots & \dots & \dots \\ -te^{i\sum_{i=1}^N \phi_i} & 0 & 0 & 0 & \dots & -t & \epsilon_N \end{pmatrix}, \quad (7.31)$$

and

$$\bar{\varphi} = \underline{U}^\dagger \underline{\varphi}. \quad (7.32)$$

Note that the total phase accumulated across the entire ring is $\sum_i^N \phi_i = 2\pi \Phi / \Phi_0$. Equation (7.31) suggests that the phase factors appearing in the Hamiltonian can be removed by using a modified periodic boundary condition:

$$\bar{\varphi}_{N+1} = \bar{\varphi}_1 \rightarrow \bar{\varphi}'_{N+1} = e^{i2\pi \Phi / \Phi_0} \bar{\varphi}'_1. \quad (7.33)$$

For the BdG equations in the tight-binding model, we can perform the unitary transformation

$$\begin{pmatrix} U \\ \underline{U}^* \end{pmatrix}$$

to get the modified periodic boundary conditions for the eigenfunctions. The same procedure can also be applied to the cylindrical geometry, which can be regarded as a stacked array of rings of same radius).

7.2 Persistent Current in Multiply Connected Mesoscopic d -Wave Superconducting Geometries

7.2.1 Cylindrical Geometry

For a $d_{x^2-y^2}$ -wave pairing symmetry as appropriate to high-temperature cuprates, the pair potential experiences a sign change across the nodal directions and the gapless nodal quasiparticles exist even at zero magnetic field. The question on the periodicity of the supercurrent in a multiply connected geometry with the hollow threaded by a magnetic flux is also intriguing. We first consider the simpler case of a cylindrical geometry as shown in Fig. 7.4. We define the x - y coordinate system

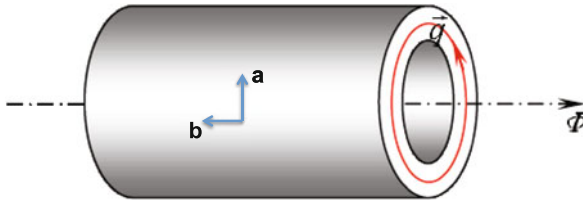


Fig. 7.4 Schematic drawing of a hollow d -wave superconducting cylinder. A magnetic flux Φ threads along the cylinder axis. The vectors \mathbf{a} and \mathbf{b} denotes the crystalline axes of an essentially two-dimensional system

to coincide with the crystalline axes, which are perpendicular and parallel to the cylinder axis, respectively. By following the same discussion as in the previous section but now in the tight-binding model, the BdG equations are given as

$$\sum_j \begin{pmatrix} \mathcal{H}_{ij} & \Delta_{ij} \\ \Delta_{ij}^* & -\mathcal{H}_{ij}^* \end{pmatrix} \begin{pmatrix} u_j^n \\ v_j^n \end{pmatrix} = E_n \begin{pmatrix} u_i^n \\ v_i^n \end{pmatrix}, \quad (7.34)$$

subject to the flux-modified boundary condition

$$\begin{pmatrix} u_{i_x+N_x, i_y}^n \\ v_{i_x+N_x, i_y}^n \end{pmatrix} = \begin{pmatrix} e^{i2\pi\Phi/\Phi_0} & 0 \\ 0 & e^{-i2\pi\Phi/\Phi_0} \end{pmatrix} \begin{pmatrix} u_{i_x, i_y}^n \\ v_{i_x, i_y}^n \end{pmatrix}. \quad (7.35)$$

Here (u_i^n, v_i^n) with i denoting the coordinates (i_x, i_y) are the eigenfunctions corresponding to eigenvalues E_n . The single particle Hamiltonian is given by

$$\mathcal{H}_{ij} = -t_{ij} - \mu\delta_{ij}, \quad (7.36)$$

where t_{ij} and μ are the hopping integral and chemical potential, respectively. We take a next-nearest-neighbor hopping approximation with t and t' representing the nearest neighbor and next-nearest neighbor hopping integrals, respectively. The BdG wave function has the form

$$\begin{pmatrix} u_i \\ v_i \end{pmatrix} = \begin{pmatrix} e^{i(\mathbf{k}+\mathbf{q})\cdot\mathbf{r}_i} & 0 \\ 0 & e^{i(\mathbf{k}-\mathbf{q})\cdot\mathbf{r}_i} \end{pmatrix} \begin{pmatrix} u_{\mathbf{k}, \mathbf{q}} \\ v_{\mathbf{k}, \mathbf{q}} \end{pmatrix}. \quad (7.37)$$

Corresponding to the energy eigenvalues

$$E_{\mathbf{k}, \mathbf{q}}^{(\pm)} = Z_{\mathbf{k}, \mathbf{q}} \pm E_{\mathbf{k}, \mathbf{q}}^{(0)}, \quad (7.38)$$

the electron and hole components of the quasiparticle amplitude are given by $(u_{\mathbf{k}, \mathbf{q}}, v_{\mathbf{k}, \mathbf{q}}) = (u_{\mathbf{k}, \mathbf{q}}^{(0)}, v_{\mathbf{k}, \mathbf{q}}^{(0)})$ and $(v_{\mathbf{k}, \mathbf{q}}^{(0)}, -u_{\mathbf{k}, \mathbf{q}}^{(0)})$ with

$$|u_{\mathbf{k}, \mathbf{q}}^{(0)}|^2 = \frac{1}{2} \left(1 + \frac{Q_{\mathbf{k}, \mathbf{q}}}{E_{\mathbf{k}, \mathbf{q}}^{(0)}} \right), \quad |v_{\mathbf{k}, \mathbf{q}}^{(0)}|^2 = \frac{1}{2} \left(1 - \frac{Q_{\mathbf{k}, \mathbf{q}}}{E_{\mathbf{k}, \mathbf{q}}^{(0)}} \right). \quad (7.39)$$

The quantities $Q_{\mathbf{k}, \mathbf{q}} = [\xi_{\mathbf{k}+\mathbf{q}} + \xi_{\mathbf{k}-\mathbf{q}}]/2$, $Z_{\mathbf{k}, \mathbf{q}} = [\xi_{\mathbf{k}+\mathbf{q}} - \xi_{\mathbf{k}-\mathbf{q}}]/2$, and $E_{\mathbf{k}, \mathbf{q}}^{(0)} = [Q_{\mathbf{k}, \mathbf{q}}^2 + |\Delta_{\mathbf{k}}|^2]^{1/2}$. In the tight-binding approximation, up to the next-nearest neighbor, the conduction electrons have the normal state dispersion,

$$\xi_{\mathbf{k}} = -2t(\cos k_x + \cos k_y) - 4t' \cos k_x \cos k_y - \mu. \quad (7.40)$$

The d -wave superconducting gap dispersion is given by

$$\Delta_{\mathbf{k}} = 2\Delta_d\phi(\mathbf{k}), \quad (7.41)$$

where $\phi(\mathbf{k}) = \cos k_x - \cos k_y$, and Δ_d is determined self-consistently:

$$\Delta_d = \frac{V_d}{4N_L} \sum_{\mathbf{k}} \frac{\phi^2(\mathbf{k})\Delta_d}{E_{\mathbf{k},\mathbf{q}}^{(0)}} \times \left[\tanh\left(\frac{E_{\mathbf{k},\mathbf{q}}^{(0)} + Z_{\mathbf{k},\mathbf{q}}}{2k_B T}\right) + \tanh\left(\frac{E_{\mathbf{k},\mathbf{q}}^{(0)} - Z_{\mathbf{k},\mathbf{q}}}{2k_B T}\right) \right], \quad (7.42)$$

where $N_L = N \times N$. Rigorously, the bond order parameters along the x and y directions do not follow the relation $\Delta_x = -\Delta_y$ in the presence of magnetic flux. Here we have imposed the restriction of $\Delta_x = -\Delta_y$ to enforce a rigorous d -wave symmetry. Notice that Δ_d is now a function of Φ/Φ_0 . From the boundary condition given by Eq. (7.35), we can find the components of wave vectors $k_x = 2\pi(n_x - m/2)/N_x$, $q_x = 2\pi(\Phi/\Phi_0 + m/2)/N_x$, while $k_y = 2\pi n_y/N_y$, and $q_y = 0$, where $n_{x(y)}$ and m are integers. In particular, m is determined by minimizing $|q_x|$ for a given value of magnetic flux Φ . The electron filling factor and the single nearest-neighbor bond current flowing around the cylinder are computed via,

$$n_e = \frac{2}{N_L} \sum_{\mathbf{k}} [f(E_{\mathbf{k},\mathbf{q}}^{(+)})|u_{\mathbf{k},\mathbf{q}}^{(0)}|^2 + f(E_{\mathbf{k},\mathbf{q}}^{(-)})|v_{\mathbf{k},\mathbf{q}}^{(0)}|^2], \quad (7.43)$$

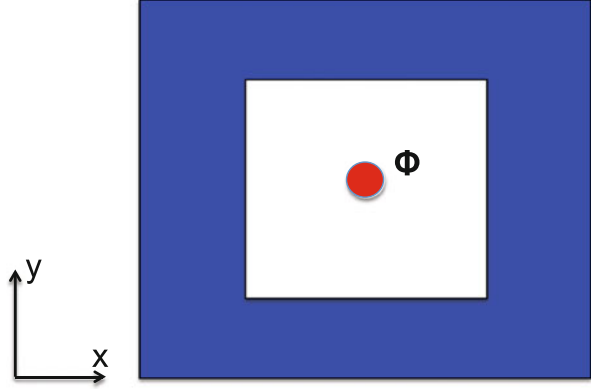
$$I = \frac{4te}{N_L} \sum_{\mathbf{k}} [f(E_{\mathbf{k},\mathbf{q}}^{(+)})|u_{\mathbf{k},\mathbf{q}}^{(0)}|^2 + f(E_{\mathbf{k},\mathbf{q}}^{(-)})|v_{\mathbf{k},\mathbf{q}}^{(0)}|^2] \times (1 + 2t' \cos k_y/t) \sin(k_x + q_x), \quad (7.44)$$

respectively. A factor of 2 has been included to account for the spin degeneracy. These physical quantities can be numerically evaluated and are reported in [10]. It is found that the order parameter and supercurrent are sensitive to both the system size and electron filling factor. We expect that the current profile should also be dependent on the crystalline orientation with respect to the magnetic flux direction. When the crystalline axes are mis-oriented by 45° away from the cylinder axis, the supercurrent flows along the quasiparticle nodal direction, the study of which is left to readers as an exercise.

7.2.2 Square Loop Geometry

For the smooth multiply geometries, the amplitude of the superconducting order parameter remains homogeneous and the breaking down of the $hc/2e$ -periodicity in the supercurrent arises mainly from the competition between the linear dimension of

Fig. 7.5 Schematic drawing of a square loop carved out of a two-dimensional superconductor. A magnetic flux threads through the hole



the system and the superconducting coherence length, which is a typical mesoscopic effect. For unconventional superconductors, the sign change of the superconducting order can have more significant consequence in systems with sharp boundaries like surfaces and interfaces. Near these boundaries, zero-energy modes can be induced. Recently, the periodicity of supercurrent in a square loop has been investigated by solving the BdG equations in real-space within a tight-binding model. The geometry is schematically shown in Fig. 7.5. In this case, it is more convenient to treat directly the Peierls phase factor from the local hopping of electrons in the geometry. Specifically, the vector potential entering Peierls phase given by Eq. (5.16)

$$\varphi_{ij} = -\frac{2\pi}{\Phi_0} \int_j^i \mathbf{A}(\boldsymbol{\xi}) \cdot \boldsymbol{\xi} \quad (7.45)$$

can take the form

$$\mathbf{A}(\mathbf{r}) = \frac{\Phi}{2\pi(x^2 + y^2)}(y, -x, 0), \quad (7.46)$$

which ensures the electrons in the arms of the square loop experience only the AB effect.

Figure 7.6 display results from a representative study [11] by solving the BdG equations within a tight-binding model. Energy spectrum is symmetric with respect to the reversal $\Phi \rightarrow -\Phi$. Due to the low-energy quasiparticles within the superconducting gap maximum, there are bands inside the gap maximum and they are dispersive with the varying magnetic flux through the AB effect. In addition, the small gap open near the Fermi energy comes from the quantum size effect of the loop. Noticeably, the spectra in the flux region $\Phi \in [0, \Phi_0/4]$ are distinct from those in the region $\Phi \in [\Phi_0/4, \Phi_0/2]$, which leads to very different energy parabolas at $\Phi = 0$ and $\Phi = \Phi_0/2$. Consequently, the $\Phi_0/2$ -periodicity is broken down in the supercurrent. Instead only the Φ_0 -periodicity is generically satisfied, and should be regarded as a fundamental property of loops formed by unconventional

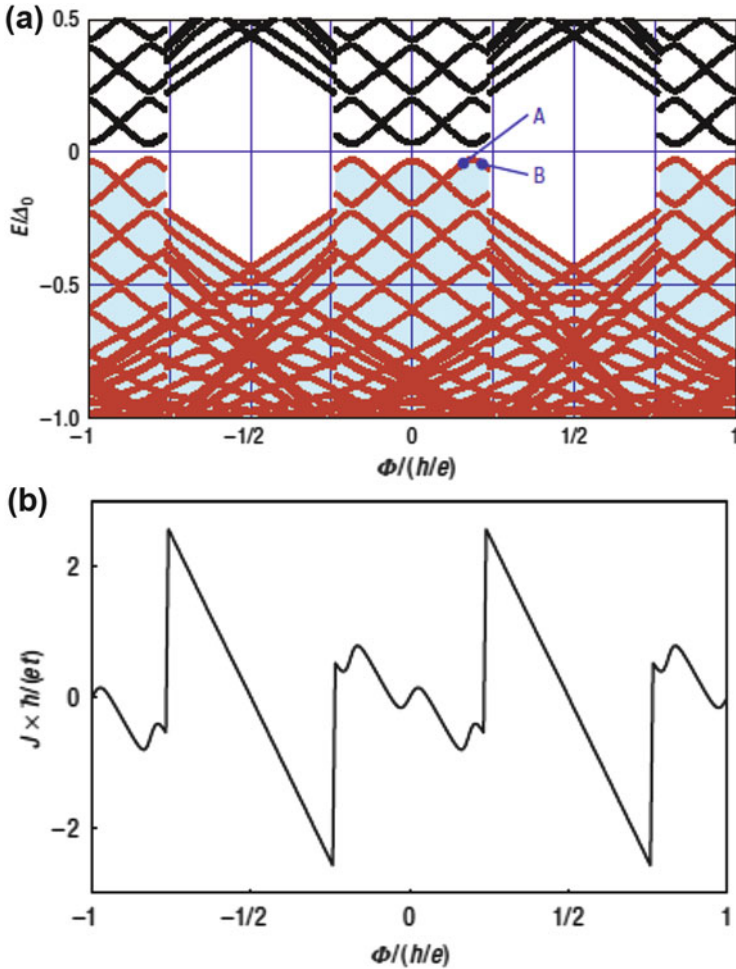


Fig. 7.6 Quasiparticle energy spectrum (a) and supercurrent (b) as a function of the magnetic flux in a square 40×40 loop with a hole of 14×14 unit cells of the original square lattice, obtained by solving the BdG equations self-consistently in a tight-binding model with a nearest-neighbor hopping approximation. The $d_{x^2-y^2}$ -wave pairing interaction $0.3t$ is chosen, where t is the nearest-neighbor hopping integral. Adapted from [11]

superconducting materials. This periodicity is also shown to survive against the impurity scattering and the change in the loop geometry. This example showcases further the power of the BdG theory when compared with the Ginzburg-Landau theory at a mesoscale.

7.3 Quantum Size Effects in Nanoscale Superconductors

Nanoscale metal and semiconductor systems like quantum dots and wires are interesting not only for their unique physical properties but also for their huge potential of technological applications. In these systems, the energy level discretization due to the quantize size effects is one of the key properties. For nanoscale superconductors, the quantum size effects not only set a quantum limit to superconductivity [12, 13], but also are responsible for many new phenomena such as shell effects [14–17], which enhance the superconducting energy gap, as well as the oscillation of superconducting transition temperature [18, 19].

Theoretically, the BdG formalism is especially powerful in addressing these quantum size effects. The key idea is to expand the BdG eigenfunctions in terms of the complete set of normal-state single-particle eigenfunctions of the nanoscale systems themselves [20–25]. This approach has also been briefly discussed for the disorder effect and high-field effects in previous chapters. As examples, we consider the continuum model of BdG formalism for s -wave superconducting quantum wires and dots, as shown in Fig. 7.7. For convenience of the discussion, we write the BdG equations for an s -wave superconductor

$$\begin{pmatrix} h(\mathbf{r}) & \Delta(\mathbf{r}) \\ \Delta^*(\mathbf{r}) & -h^*(\mathbf{r}) \end{pmatrix} \begin{pmatrix} u_n(\mathbf{r}) \\ v_n(\mathbf{r}) \end{pmatrix} = E_n \begin{pmatrix} u_n(\mathbf{r}) \\ v_n(\mathbf{r}) \end{pmatrix}, \quad (7.47)$$

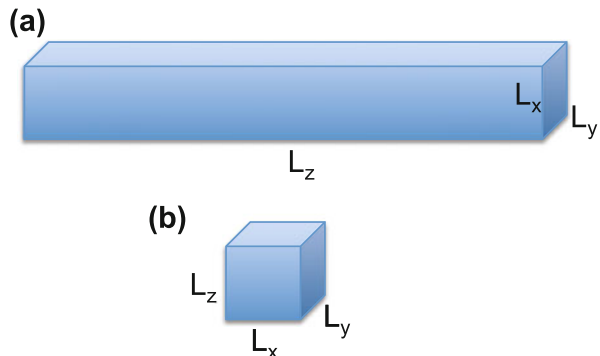
where the single-particle Hamiltonian is given by

$$h(\mathbf{r}) = -\frac{\hbar^2 \nabla^2}{2m_e} + V_c(\mathbf{r}) - E_F, \quad (7.48)$$

and the self-consistency condition is

$$\Delta(\mathbf{r}) = g \sum_{n(E_n > 0)} u_n(\mathbf{r}) v_n^*(\mathbf{r}) \tanh\left(\frac{E_n}{2k_B T}\right). \quad (7.49)$$

Fig. 7.7 Schematic drawing of a superconducting quantum wire (a) and a quantum dot (b). The variables L_x , L_y , and L_z are the linear dimension of these systems



For nanoscale superconductors, the confinement effect is described by the potential $V_c(\mathbf{r})$. For a superconducting quantum wire, the confinement is two-dimensional (e.g., in the x - y plane shown in Fig. 7.7a); while for a superconducting quantum dot, it is three-dimensional (i.e., in all three directions shown in Fig. 7.7b). In the hard-wall approximation, $V(\mathbf{r})$ is

$$V(\mathbf{r}) = \begin{cases} 0, & \text{for } 0 \leq x \leq L_x, 0 \leq |y| \leq L_y, \\ \infty, & \text{otherwise,} \end{cases} \quad (7.50)$$

for the wire; while

$$V(\mathbf{r}) = \begin{cases} 0, & \text{for } 0 \leq x \leq L_x, 0 \leq |y| \leq L_y, 0 \leq |z| \leq L_z, \\ \infty, & \text{otherwise,} \end{cases} \quad (7.51)$$

for the dot. The corresponding eigenfunctions and eigenvalues for the single-particle Hamiltonian are

$$w_\alpha(\mathbf{r}) = \frac{e^{ik_z z}}{\sqrt{2\pi}} \sqrt{\frac{2}{L_x}} \sqrt{\frac{2}{L_y}} \sin\left(\frac{n_x \pi x}{L_x}\right) \sin\left(\frac{n_y \pi y}{L_y}\right), \quad (7.52)$$

for

$$\epsilon_\alpha = \frac{\hbar^2}{2m_e} \left[\left(\frac{n_x \pi}{L_x}\right)^2 + \left(\frac{n_y \pi}{L_y}\right)^2 + k_z^2 \right], \quad (7.53)$$

with α denoting the quantum numbers (n_x, n_y, k_z) for the quantum wire; while

$$w_\alpha(\mathbf{r}) = \sqrt{\frac{2}{L_x}} \sqrt{\frac{2}{L_y}} \sqrt{\frac{2}{L_z}} \sin\left(\frac{n_x \pi x}{L_x}\right) \sin\left(\frac{n_y \pi y}{L_y}\right) \sin\left(\frac{n_z \pi z}{L_z}\right), \quad (7.54)$$

for

$$\epsilon_\alpha = \frac{\hbar^2}{2m_e} \left[\left(\frac{n_x \pi}{L_x}\right)^2 + \left(\frac{n_y \pi}{L_y}\right)^2 + \left(\frac{n_z \pi}{L_z}\right)^2 \right], \quad (7.55)$$

with α denoting the quantum numbers (n_x, n_y, n_z) for the quantum dot. We note that the eigenfunctions and eigenvalues for a harmonic potential confinement are also available analytically.

The BdG wavefunctions are then expanded as

$$u_n(\mathbf{r}) = \sum_{\alpha} u_{n,\alpha} w_{\alpha}(\mathbf{r}) , \quad (7.56a)$$

$$v_n(\mathbf{r}) = \sum_{\alpha} v_{n,\alpha} w_{\alpha}(\mathbf{r}) . \quad (7.56b)$$

Insertion of Eq. (7.56) into Eq. (7.47) leads to

$$\xi_{\alpha} u_{n,\alpha} + \sum_{\beta} \Delta_{\alpha\beta} v_{n,\beta} = E_n u_{n,\alpha} , \quad (7.57a)$$

$$\sum_{\beta} \Delta_{\alpha\beta}^* u_{n,\beta} - \xi_{\alpha} v_{n,\alpha} = E_n v_{n,\alpha} , \quad (7.57b)$$

where

$$\xi_{\alpha} = \epsilon_{\alpha} - E_F , \quad (7.58)$$

and

$$\Delta_{\alpha\beta} = \int w_{\alpha}^*(\mathbf{r}) \Delta(\mathbf{r}) w_{\beta}(\mathbf{r}) d\mathbf{r} . \quad (7.59)$$

We note that for a generally irregular wire or dot geometry, there are off-diagonal matrix elements for the single-particle Hamiltonian.

Figure 7.8 displays the numerical results on the superconducting transition temperature with the linear dimension of a square-cross-sectioned quantum wire of Pb, Sn, and Al [22]. It shows clearly the oscillation of transition temperature with the cross-section size. The pronounced resonance feature of the transition temperature is related to the tuning of the density of states in the confinement system. The relative T_c difference between the neighboring peak and valley values is increased with decreasing cross-section size. It also shows that the bulk transition temperature is approached when the linear dimension of the cross-section is several times longer than the bulk superconducting coherence. These results are qualitatively similar to those for cylindrical Al and Sn nano wires [26, 27], suggesting a robust nature of quantum confinement effects. In addition, the same method has also been applied to calculate the local electronic structure in superconducting quantum wires, from which the quasiparticle interference due to the order parameter inhomogeneity is uncovered [25]. Furthermore, the interplay between the quantum confinement and magnetic field can also be studied in the same framework, which is left for readers as an exercise.

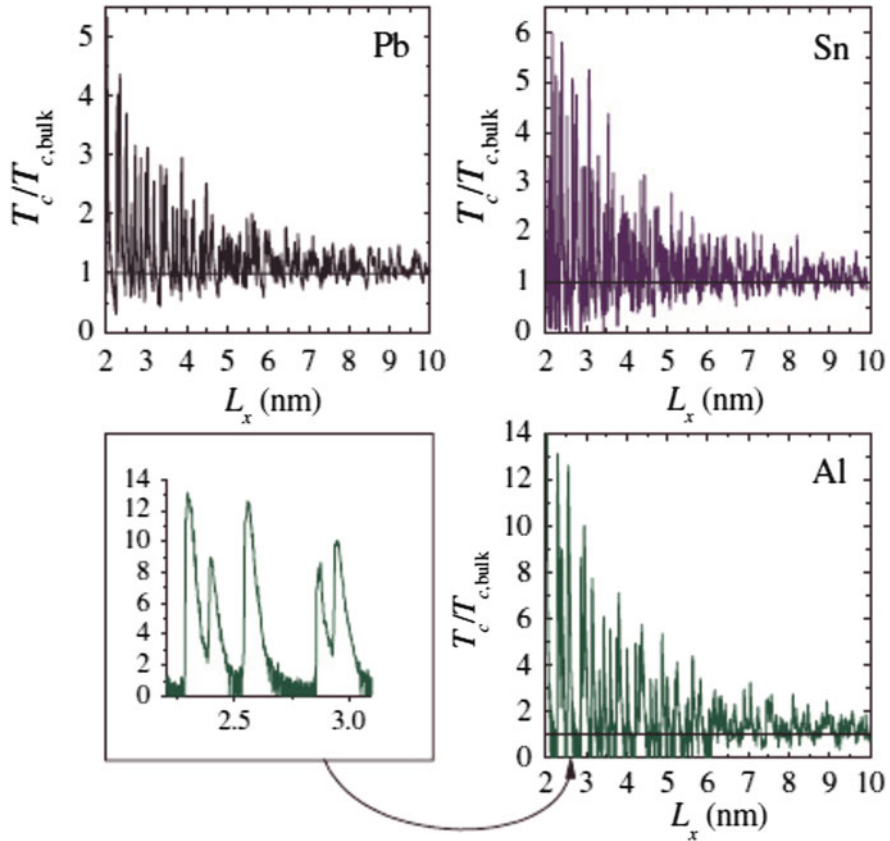


Fig. 7.8 The L_x dependent superconducting critical temperature for Pb, Sn, and Al square-cross-section nano wires. Calculations are with the Debye temperature 96, 195, 375 K and the dimensionless coupling strength $gN(0) = 0.39, 0.25, 0.18$ for Pb, Sn, and Al, respectively. The wire length $L_z = 500$ nm. From [22]

References

1. Y. Aharonov, D. Bohm, Phys. Rev. **115**, 485 (1959)
2. R. Landauer, M. Büttiker, Phys. Rev. B **54**, 2049 (1985)
3. V. Chandrasekhar, et al., Phys. Rev. Lett. **67**, 3578 (1991)
4. R. Doll, M. Näbauer, Phys. Rev. Lett. **7**, 51 (1961)
5. B.S. Deaver, W.M. Fairbank, Phys. Rev. Lett. **7**, 43 (1961)
6. N. Byers, C.N. Yang, Phys. Rev. Lett. **7**, 46 (1961)
7. W. Brenig, Phys. Rev. Lett. **7**, 337 (1961)
8. C.E. Gough, et al., Nature (London) **326**, 855 (1987)
9. J.-X. Zhu, Z.D. Wang, Phys. Rev. B **50**, 7207 (1994)
10. J.-X. Zhu, H.T. Quan, Phys. Rev. B **81**, 054521 (2010)
11. F. Loder, et al., Nat. Phys. **4**, 112 (2008)
12. D. Ralph, et al., Phys. Rev. Lett. **74**, 3241 (1995)

13. J. von Delft, *Ann. Phys.* **10**, 219 (2001)
14. V.Z. Kresin, Y.N. Ovchinnikov, *Phys. Rev. B* **74**, 024514 (2006)
15. A.M. Garca-Garca, et al., *Phys. Rev. Lett.* **100**, 187001 (2008)
16. H. Olofsson, S. Aberg, P. Leboeuf, *Phys. Rev. Lett.* **100**, 037005 (2008)
17. S. Bose, et al., *Nat. Mater.* **9**, 550 (2010)
18. Y. Guo, et al., *Science* **306**, 1915 (2004)
19. S. Qin, et al., *Science* **324**, 1314 (2009)
20. A. Shanenko, M.D. Croitou, F.M. Peeters, *Phys. Rev. B* **75**, 014519 (2007)
21. A. Shanenko, M.D. Croitou, R.G. Mints, F.M. Peeters, *Phys. Rev. Lett.* **99**, 067007 (2007)
22. M.D. Croitoru, A.A. Shanenko, F.M. Peeters, *Phys. Rev. B* **76**, 024511 (2007)
23. A. Shanenko, M. D. Croitou, F.M. Peeters, *Phys. Rev. B* **78**, 024505 (2007)
24. L.-F. Zhang, et al., *Phys. Rev. Lett.* **109**, 107001 (2012)
25. L.-F. Zhang, L. Covaci, F.M. Peeters, *Phys. Rev. B* **91**, 024508 (2015)
26. A.A. Shanenko, M.D. Croitoru, *Phys. Rev. B* **73**, 012510 (2006)
27. A.A. Shanenko et al., *Phys. Rev. B* **74**, 052502 (2006)

Additional Reading

The following list includes many references for further reading, which helps shape the treatment of several topics in the present book. Their individual features are briefly commented.

M. Tinkham: *Introduction to Superconductivity* (McGraw Hill, New York, 1975 (1st ed.) & 1996 (2nd ed.)). An excellent account of BCS and Ginzburg-Landau theory for superconductivity phenomenology.

P. G. de Gennes: *Superconductivity of Metals and Alloys* (W. A. Benjamin, New York, 1966; Addison-Wesley, New York, 1989). A pioneering work on the BdG treatment of inhomogeneous superconductivity.

J. R. Schrieffer: *Theory of Superconductivity* (W. A. Benjamin, New York, 1964). A good account of the BSC theory.

J. B. Ketterson, S. N. Song: *Superconductivity* (Cambridge University Press, Cambridge, 1999). A balanced account of phenomenological and microscopic theories for uniform and nonuniform superconductors.

G. D. Mahan: *Many-Particle Physics* (Kluwer Academic/Plenum Publishers, New York, 1981 (1st ed.), 1990 (2nd.), 2000 (3rd.)). An exhaustive book on the Green's function method, other techniques of many-body theory, and their applications to solids and liquids. It also contains the Eliashberg theory of superconductivity with retardation effects.

A. A. Abrikosov, L. P. Gorkov, I. E. Dzyaloshinski: *Methods of Quantum Field Theory in Statistical Physics* (Englewood Cliffs, New Jersey, 1963). Introductory book on the Green's function method to the theory of superconductivity.

Carlos A. R. Sá de Melo (Ed.): *The Superconducting State in Magnetic Fields* (World Scientific, Singapore, 1998). A collection of excellent review articles on the magnetic field effects on superconductivity.

R. P. Huebener, N. Schopohl, G. E. Volovik (Eds.): *Vortices in Unconventional Superconductors and Superfluids* (Springer, New York, 2002). It contains many good articles on the special topics of vortices in superconductors and superfluids.

R. D. Parks (Ed.): *Superconductivity* (Dekker, New York, 1969). The treatise contains a comprehensive account of superconductivity as it stood in 1968.